skb.se

SKB R-22-07

ISSN 1402-3091

ID 1983896

June 2025

Baseline Forsmark – Compilation of bedrock and regolith hydraulic properties data based on interpretation of single-hole hydraulic tests, regolith samples and permeameter tests

Robert Earon, Hedi Rasul, Kent Werner, Jessica Lindmark
Svensk Kärnbränslehantering AB

Keywords: Hydrogeology, Deformation zone, Fracture domain, Sheet joint, Regolith, Hydraulic properties

This report is published on www.skb.se

Abstract

Baseline Forsmark is a multidisciplinary description of datasets and site conditions prior to the start of surface contract works and underground constructions related to a deep geological repository for spent nuclear fuel (SFK) and the extension of the current geological repository for short-lived low- and intermediate-level radioactive waste (SFR) in Forsmark.

This report is part of a series of reports that present available data for the Baseline Forsmark modelling stage. Specifically, the report focuses on data that are used to describe the hydro-structural characteristics of bedrock and regolith at Forsmark. The data presented in the report are gathered from 52 core-drilled boreholes, 57 percussion-drilled boreholes and 236 regolith wells/sampling points within the area.

In this report, hydraulic test data acquired in the bedrock are categorized and presented according to geo-structural interpretations and models of the bedrock. Specifically, hydraulic test data from bedrock boreholes are linked to deformation zones, possible deformation zones, fracture domains, and/or rock domains. Moreover, data from deterministically modelled sub-horizontal structures (i.e. sheet joints) and so-called Shallow Bedrock Aquifer (SBA) structures are presented. Deterministically modelled sheet joints were not handled in the SDM-Site Forsmark modelling stage.

The main hydraulic test methods presented for the bedrock characterization in this report are high-resolution measurements of discrete flow anomalies using overlapping difference flow logging (PFL-f tests), or interval-based methods such as sequential double-packer injection tests or sequential difference flow logging (PFL-s tests). In core-drilled boreholes, overlapping PFL-f tests are assumed to best represent a heterogeneous fracture network, and, in the absence of data from PFL-s tests, short-interval injection tests.

Data from a set of field and laboratory methods are presented in this report to assess the hydraulic properties of the regolith and the regolith/bedrock interface. The geo-structural framework for the regolith is in the form of a map of the surface coverage of regolith types, and an RDM (Regolith Depth and Stratigraphy Model). Specifically, the RDM is a deterministic model of the horizontal distribution of elevations and thicknesses of individual layers consisting of different regolith types.

Hydraulic field methods related to regolith and the regolith/bedrock interface include single-hole slug tests, single-hole permeameter tests, and multi-hole interference tests. Laboratory methods related to the regolith include permeameter and CRS tests, sieve and sedimentation analyses, as well as methods to assess water storage and water retention properties of the unsaturated zone.

Sammanfattning

Baseline Forsmark är en multidisciplinär beskrivning av datamängder och platsförhållanden inför uppstart av ovan- och undermarksarbeten för ett slutförvar för använt kärnbränsle (Kärnbränsleförvaret) och utbyggnad av slutförvaret för kortlivat låg- och medelaktivt radioaktivt avfall (SFR) i Forsmark.

Denna rapport är del av en serie rapporter som presenterar tillgängliga datamängder för modelleringssteget Baseline Forsmark. Rapporten behandlar specifikt data som används för att beskriva hydrostrukturell karaktär av berg och jordlager i Forsmark. De data som beskrivs i rapporten härrör från 52 kärnborrhål, 57 hammarborrhål och 236 grundvattenrör/provtagningspunkter inom området.

I rapporten kategoriseras och presenteras hydrauliska testdata från berg utifrån geostrukturella tolkningar och modeller för berget. Hydrauliska testdata från bergborrhål kopplas till deformationszoner, möjliga deformationszoner, sprickdomäner och/eller bergdomäner. Vidare redovisas data från deterministiskt modellerade sub-horisontella strukturer och så kallade ”Shallow Bedrock Aquifers” (SBA-strukturer). Deterministiskt modellerade bankningsplanssprickor hanterades inte i modelleringssteget SDM-Site.

De huvudsakliga hydrauliska testmetoderna som presenteras för karakterisering av berg i denna rapport är högupplösta mätningar av diskreta flödesanomalier med överlappande differensflödesloggning (PFL-f-tester), eller intervallbaserade metoder såsom sekventiella injektionstester med dubbelmanschett eller sekventiell differensflödesloggning (så kallade PFL-s-tester). För kärnborrhål antas resultaten från PFL-f-tester bäst representera ett heterogent spricknätverk, och, vid frånvaro av PFL-s-tester, injektionstester med korta testintervall.

En uppsättning fält- och laboratoriemetoder presenteras i denna rapport för att uppskatta hydrauliska egenskaper för jordlager och för övergången mellan jord och berg. Det geostrukturella ramverket för jordlagren är i form av en jordartskarta, samt en RDM (eng. Regolith Depth and Stratigraphy Model). RDM är en deterministisk modell av den horisontella fördelningen av nivåer och mäktigheter för individuella lager bestående av olika typer av jordarter.

Hydrauliska fältmetoder gällande jordlager och övergången jord/berg inkluderar enhåls(slug)tester, enhåls(permeameter)tester samt flerhåls(interferens)tester. Laboratoriemetoder gällande regolit inkluderar permeameter- och CRS-tester, sil- och sedimentationsanalyser, samt metoder för att skatta magasins- och retentionsegenskaper i den omättade zonen.

Contents

1 Introduction

1.1 Background

SKB plans to construct a deep geological repository for spent nuclear fuel (SFK) at Forsmark, some 120 km NNW of Stockholm (Figure 1-1). Surface-based investigations and associated site descriptive modelling were performed 2002 through 2008 (SKB 2008), followed by assessments of post-closure safety and environmental impacts and compilation of permit applications to construct a geological disposal for spent nuclear fuel. These applications were submitted to the authorities in March 2011.

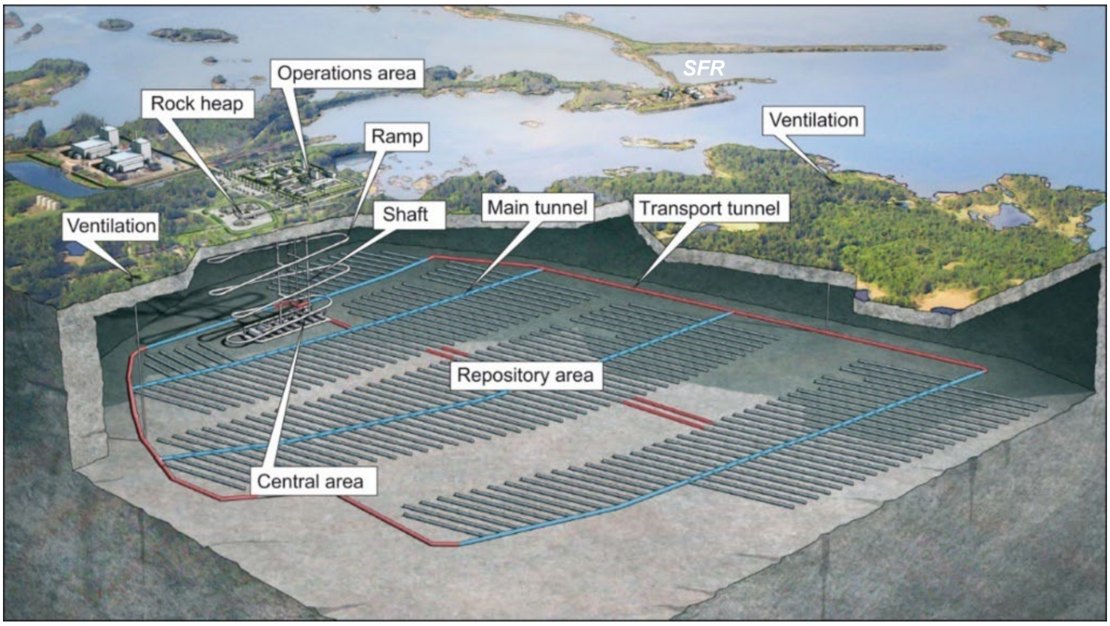

Figure 1-1. *Illustration of the proposed layout for the final repository for spent nuclear fuel, SFK, which will be built at around -470 m elevation (RH 2000 elevation system). The illustration shows the repository access ramp and shafts, the central area rock caverns, and the deposition areas. Transport and main tunnels are coloured red and blue, respectively. The location of SFR is also indicated (cf. Fig. 1-2). Modified from SKB (2010).*

In addition, SKB will construct an extension of the existing, relatively shallow (between -60 and -160 m elevation; the RH 2000 elevation system is used throughout this report), geological repository for short-lived low- and intermediate-level radioactive waste (SFR) some two kilometres north of SFK in Forsmark (Figure 1-2). For this extension, surface-based investigations and associated site descriptive modelling were performed between 2008 and 2011 (SKB 2013). This was followed by assessments of post-closure safety and environmental impacts, and compilation of permit applications, which were submitted to the authorities in December 2014. Both repositories (SFK and the SFR extension) will be nuclear facilities. This entails the need to fulfil basic requirements regarding both the stability of the facility during the construction and operational stages, as well as radiological safety during the operational stage and the post-closure period of each facility.

The demands related to the long-term radiological safety of the repositories, of which some demands implicitly also relate to environmental impacts during construction, are addressed by specified technical design requirements and associated requirements formulated by SKB together with its Finnish sister organisation Posiva (POSIVA and SKB 2017) and by the Swedish Radiation Authority (SSM 2018). A series of methodology reports support the modelling during the execution of planned underground constructions at Forsmark. Below, the acronym DFNMM refers to the methodology for discrete fracture network modelling (Selroos et al. 2022), and the acronym HGMM refers to the methodology for integrated hydrological-hydrogeological flow modelling using equivalent continuous porous media modelling tools (Odén et al. 2025).

Hydrogeological conceptual modelling of the bedrock during the previous Site Investigation Campaigns (SKB 2008; SKB 2011) included data from single and multi-well hydraulic tests and geological interpretations in e.g. core-drilled boreholes. Key deliveries from the geological modelling were deterministic geometrical model volumes for deformation zones exceeding predefined lengths, and geometrical models for fracture domains and rock domains. While the hydraulic properties outside of deterministic deformation zones were described using discrete fracture network (DFN) modelling, hydraulic parameterizations of volumes delineated as deformation zones according to the 3D volumetric deformation zone model were based on in-situ measurements and meta-analyses of hydraulic data.

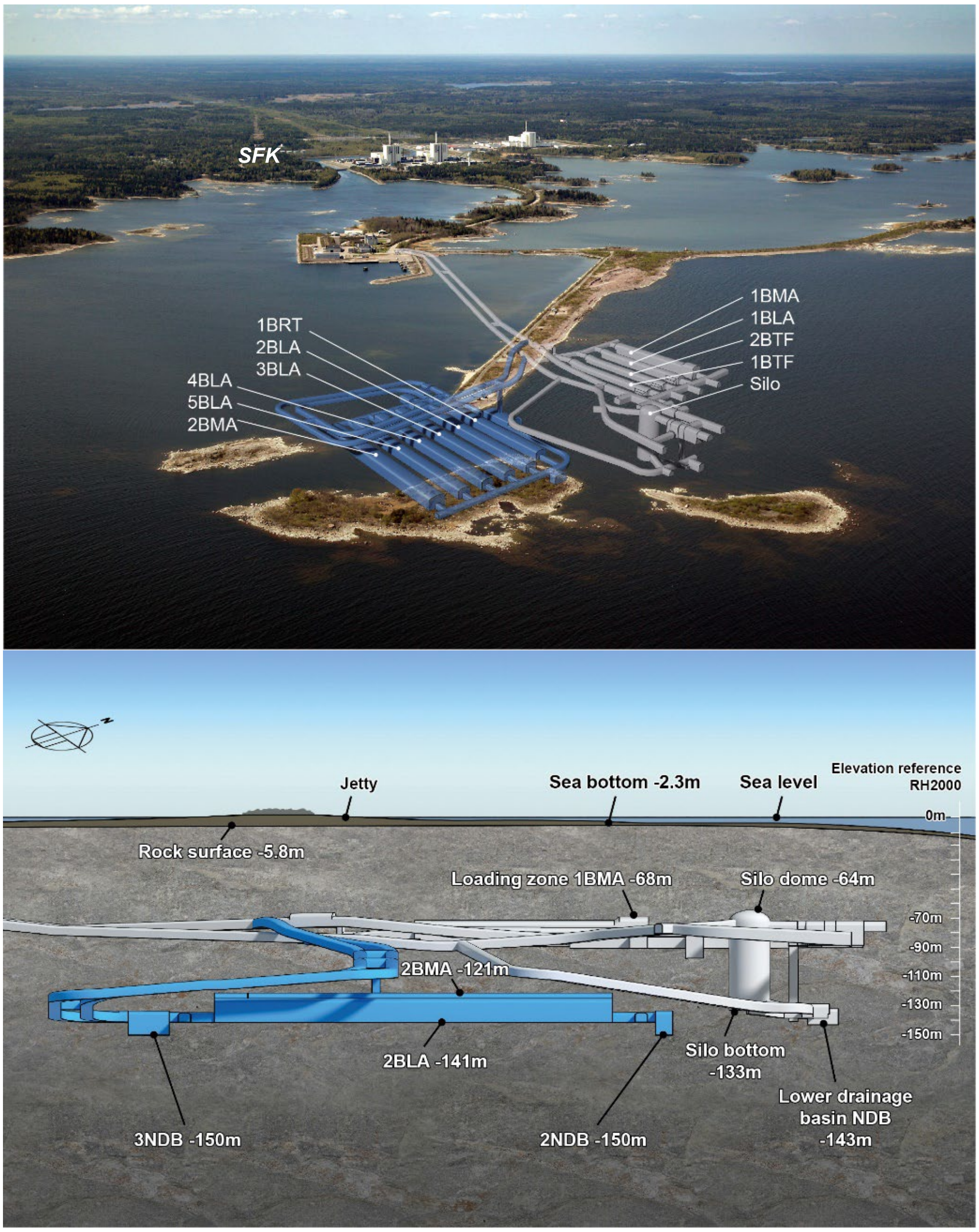

Figure 1-2. *Top: Illustration of the proposed layout of the extension (shown in blue) of the existing repository (shown in grey) for short-lived low- and intermediate-level radioactive waste (SFR). Bottom: Illustration of the elevation of different facility parts of the existing SFR (shown in grey) and its extension (shown in blue).*

1.2 Objectives and scope

Two levels of hydrological-hydrogeological reports (Figure 1-3) are planned as support for the Baseline Forsmark Main Report (Level I), which will describe the current geoscientific and ecological knowledge of the site and its state prior to start of construction of SFK and the extension of SFR (Figure 1-4).

The present report is the first of two so-called Level III reports (Figure 1-3). It collates hydraulic properties data acquired for the bedrock and the regolith in the Baseline Forsmark area. The hydraulic properties data have been interpreted from single-hole hydraulic tests, interference tests for the regolith, gradation tests (sieve and sedimentation analyses) and permeameter tests. The second Level III report (State Variables Report, see Figure 1-3) presents time series of meteorological, hydrogeological and hydrological state variables data monitored over time prior to start of constructions, as well as data pertaining to performed cross-hole (interference) tests. Together, the information gathered in the two Level III reports constitutes the basis for conceptual modelling and quantitative hydrological-hydrogeological modelling using numerical modelling tools, see HGMM (Odén et al. 2025) for details. Conceptual modelling and the setup, execution and results of the hydrological-hydrogeological numerical modelling will be presented in the two Level II reports for the bedrock and the surface system, respectively (Figure 1-3).

- Hydraulic properties of geologic media refer to physical properties; for example that describe the ease with which water can move through pore spaces or fractures.
- State variables refer to physical quantities that can be monitored and describe the condition, or state, of various elements of the hydrologic cycle, including but not limited to the atmosphere (e.g. air temperature), surface water (e.g. stream discharge) or subsurface water (e.g. groundwater level).

The objective of this report is to collate all hydraulic property data acquired for the bedrock and the regolith in support of Baseline Forsmark, which describes the site understanding of Forsmark prior to start of constructions of SFK and the extension of SFR. The collated properties data are primarily oriented towards their use in steady-state numerical modelling, i.e. transient parameters such as storativity in regolith layers will be presented in a separate report (Hydraulic State Variables Report, see Figure 1-3). It should be noted that hydraulic tests are scale-dependent and that different test methods may reflect different geological volumes. Method scale-dependencies will be presented in Section 3.

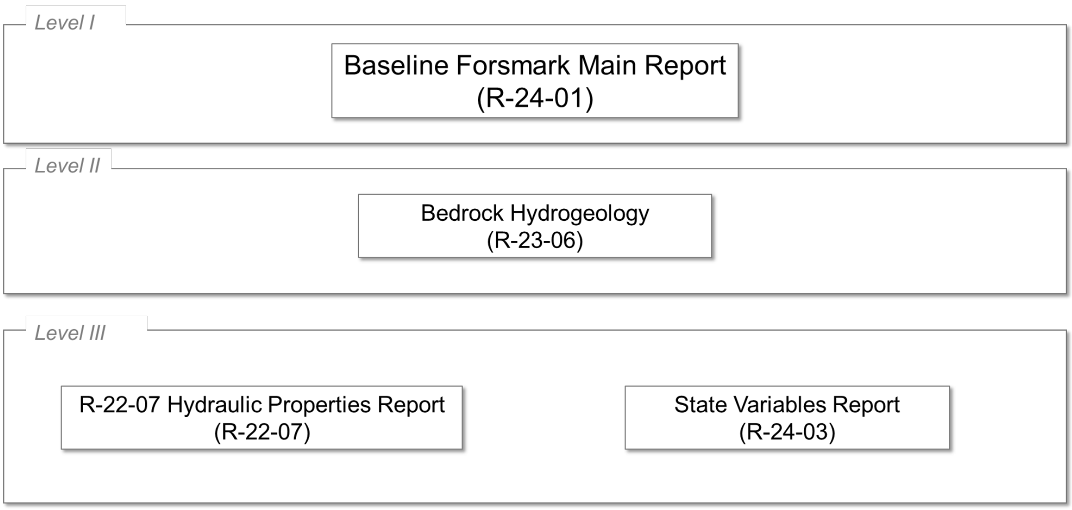

Figure 1-3. *The planned report structure for hydrological and hydrogeological modelling providing the basis for the hydrological contribution to the Baseline Forsmark main report.*

1.3 This report and supporting documents

This report relates hydrogeological test data to geological deterministic modelling. Chapter 2 gives a brief background of the Forsmark site description (SFK and SFR areas) and illustrates the integration of the two modelling areas. Chapter 3 outlines the data and methods used in compiling the hydraulic property data, in addition to outlining the geological models used in the compilation. Chapters 4 and 5 present a compilation of the available single hole hydraulic test data cross-referenced against geo-structural modelling, for core- and percussion-drilled boreholes, respectively. Section 6 presents data relevant to the near-surface hydrogeology and hydrology, including field methods and hydraulic test data primarily in the regolith. Chapter 7 gives an overview of the hydraulic datasets analysed with reference to sub-horizontal near-surface deterministic structures (i.e. sheet joints and SBA structures). Finally, Chapter 8 summarizes the report.

1.4 Organisation of work

This report has been carried out primarily by representatives of the hydrology–hydrogeology modelling group within the Site Descriptive Modelling group for the Forsmark Site. Additionally, close support has been received by representatives from the geological modelling group within the Site Descriptive Modelling group for the Forsmark Site.

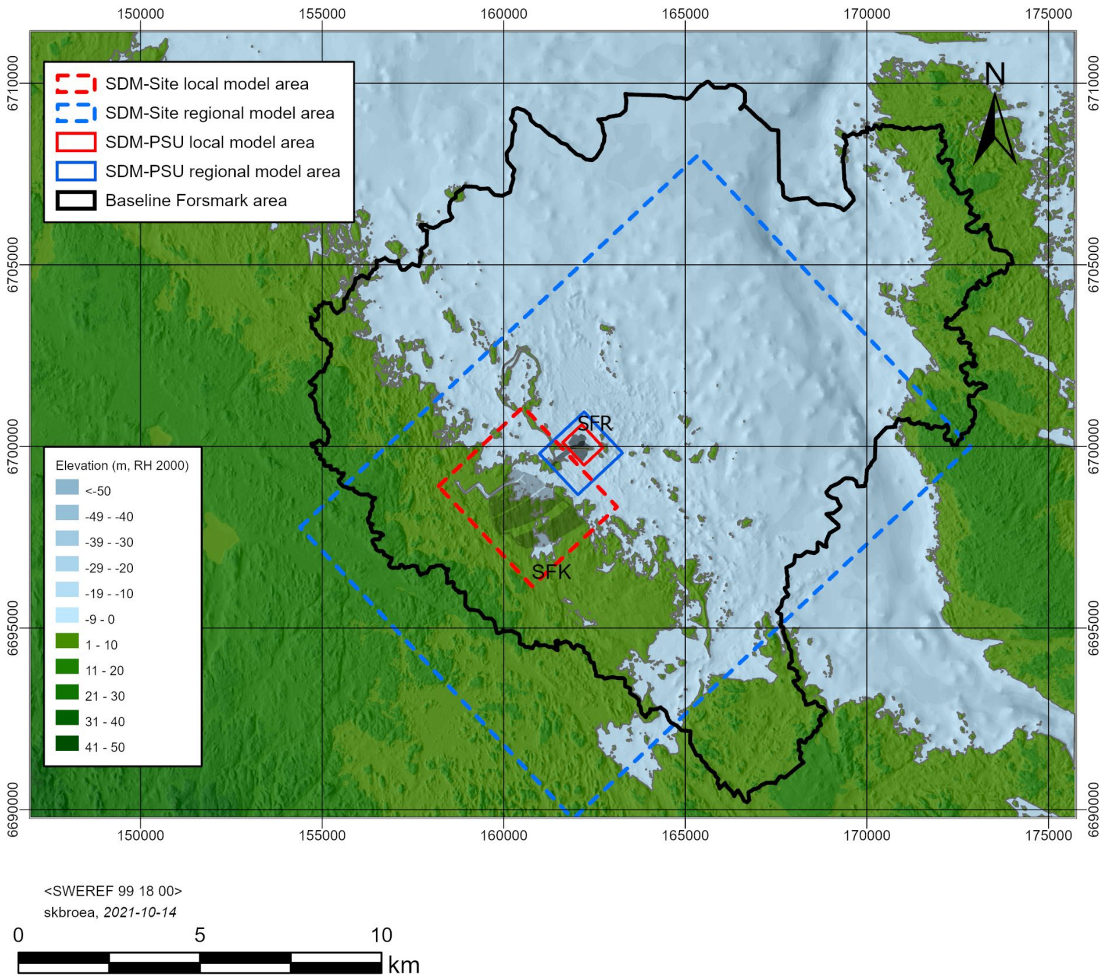

***Figure 1-4.** Topography of the Forsmark area showing the boundary of the Baseline Forsmark area (Earon et al. 2022) and the locations of SFK and SFR. The boundaries of previous model areas as applied in SDM-Site and SDM-PSU are also shown. Elevation and bathymetry data from Petrone and Strömgren (2020).*

2 Setting – the Forsmark site

2.1 SKB's systems approach to hydrogeological modelling

The term "hydrology" usually refers to components of the hydrologic cycle, i.e. water flows and storages of atmospheric, surface and subsurface waters. Here, the term hydrology is specifically related to the occurrence, flow and storage of surface water (lakes, ponds, streams and sea basins). Likewise, the term "hydrogeology" is specifically related to the occurrence, flow and storage of water below the ground surface, particularly in the saturated zones of regolith and bedrock. Differences in terms of processes, geometries and properties motivate the application of two different representations of the whole system in parallel. The Surface System Model focuses on a high level of description of surface processes on relatively short timescales including those of meteorological variability, whereas the Bedrock System Model focuses on development of the bedrock description and longer timescales including those of climatic changes (Figure 2-1).

The Surface System Modelling considers three flow domains, one hydrological and two hydrogeological. The hydrological flow domain consists of lakes, ponds, streams and sea basins. The hydrogeological flow domains consist of regolith and bedrock, respectively. The regolith is modelled as a stratified porous medium made up of several units, each having characteristic hydraulic properties (Figure 2-1). The fractured bedrock below the regolith is also treated as a porous medium, significantly more hydraulically heterogeneous and anisotropic than the regolith layers on the scale of the spatial resolution of the numerical model used for the Surface System Modelling. Porous-media equivalent hydraulic properties models (ECPMs) of the fractured bedrock are derived by means of upscaling of modelled fractures and deformation zones.

A key objective for the Surface System flow modelling is to provide support for environmental monitoring during the repository constructions, i.e. to establish a credible flow model of the conditions on a regional scale prior to start of constructions, and that can be used to clarify whether observed variations in groundwater levels, lake levels and runoff during constructions are caused by natural hydrometeorological variability and trends, or if they are due to anthropogenic changes following various engineering activities, e.g. changes in landscape morphology and water courses, bedrock excavations and grouting. To meet this requirement, the Surface System Modelling is performed on a diurnal basis.

The Bedrock System flow modelling considers two hydrogeological flow domains, the bedrock and the regolith (see the description above of the Surface System modelling), with hydrology modelled through definition of surface boundary conditions. The bedrock consists of two main classes of discrete fractures, deformation zones and fracture domains (Figure 2-1). Deformation zones are distinct individual domains of higher fracture frequency than fracture domains, although some can be single breaks of mm scale thickness. Different types of discrete stochastic structures can be modelled within the fracture domains including so-called PDZ (possible deformation zones) and sheet joints that may both be partly conditioned to data when available and modelled stochastically to maintain horizontal connectivity as presented in the conceptual model. The sheet joints are vital for the interaction between the Bedrock System and the Surface system (Follin 2008) and their recognition is a significant update of the previous modelling approach (Rhén et al. 2003). Another essential update of the previous modelling approach is that the SC (stochastic continuum) approach envisaged in Rhén et al. (2003) is replaced by the ECPM (equivalent continuous porous medium) approach as a simplified representation of the DFN (discrete fracture network) approach, see Selroos et al. (2022).

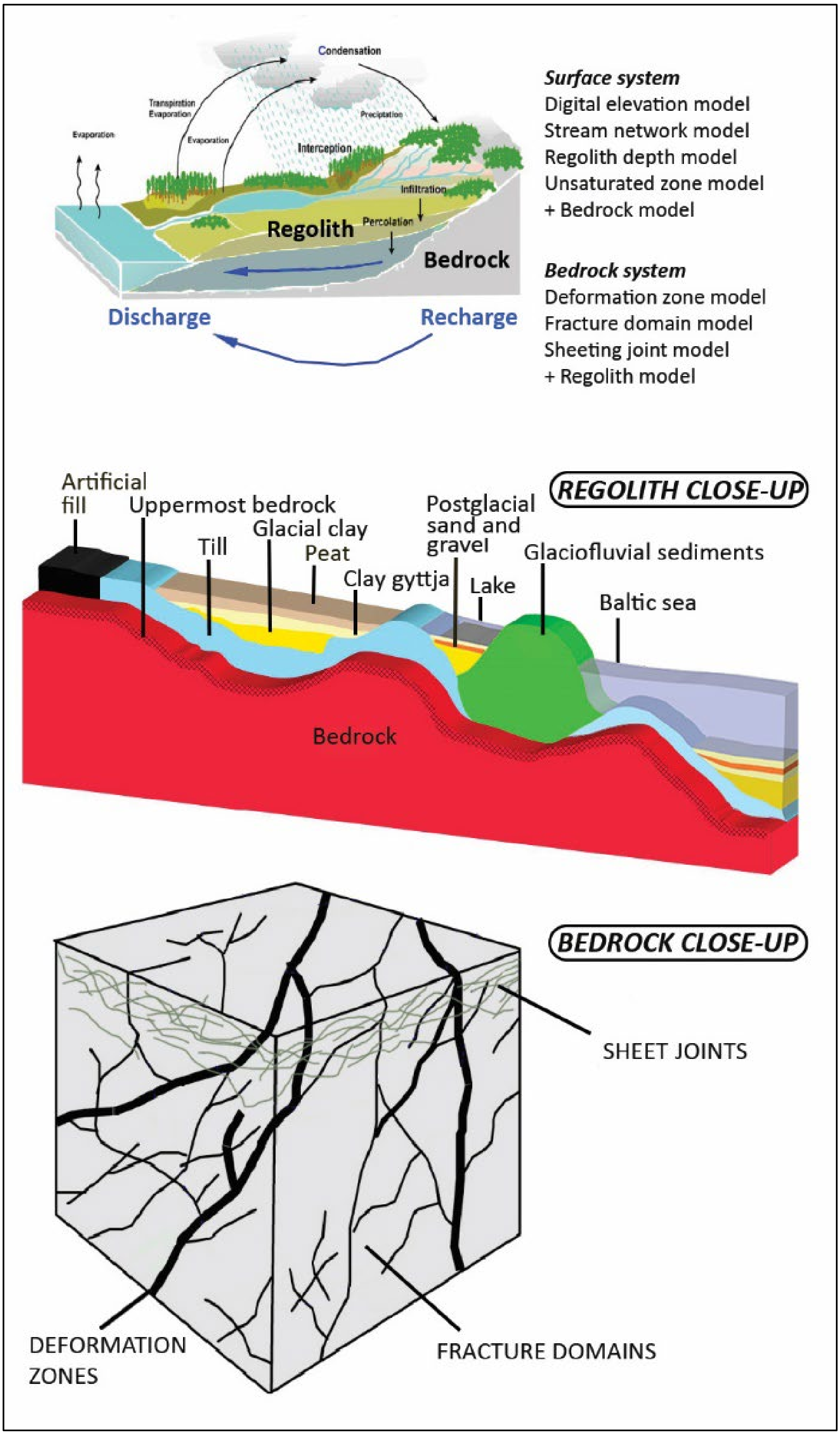

Figure 2-1. *Schematic of the hydrologic cycle, regolith layers and bedrock structures. The outlined methodology suggests that surface and subsurface flows should be represented by models of two parallel, partially overlapping systems, a Surface System and a Bedrock System.*

2.2 Geological setting at Forsmark

The Forsmark area is located in northern Uppland within the municipality of Östhammar, about 120 km north of Stockholm. The Baseline Forsmark area (Figure 1-4) is located along the shoreline of Öregrundsgrepen and extends from the Forsmark nuclear power plant and the SFR access road in the northwest to Kallrigafjärden in the southeast. The bedrock was formed between 1.89 and 1.85 million years ago and has been affected by both ductile and brittle deformation. The ductile deformation has resulted in large-scale ductile high-strain zones and the brittle deformation has given rise to large-scale fracture zones. Tectonic lenses, in which the bedrock is much less affected by ductile deformation, are enclosed between the ductile high-strain zones. The SFK area is located in the north-westernmost part of one of these tectonic lenses that extends from north-west of the nuclear power plant south-eastwards to Öregrund.

The SFR repository is located c. 1 kilometre offshore from the Forsmark nuclear power plant and two kilometres from the candidate area for SFK. The existing SFR disposal facilities are located in the bedrock approximately 60 to 140 m below the seabed of the Baltic Sea. The investigated SFR domain is part of the Forsmark site descriptive model SDM-Site (SKB 2008). Key differences between the SFR extension project and SFK include the following:

- The target depth for the SFR extension is shallower than that for SFK (the existing SFR storage facilities are located within a depth interval of -60 to -140 m). This comparatively shallow target depth shifts the attention towards factors controlling shallow hydrogeology, e.g. topography, sediments and contact to the seafloor, stress-relief structures, shoreline displacement, etc. It may be expected that deep regional flow and variable-density effects are of comparatively less importance, particularly with respect to the ongoing isostatic land upheaval.
- SFK is targeted to the tectonic lens, which is believed to be a quite different hydro-structural environment compared to the SFR area, both near the surface and at depth.

2.2.1 Overview of the deformation zone model

The term *deformation zone* has a wide range of uses. Its use here is based on the definition given in Hermanson and Petersson (2022) and is used interchangeably with the term *deterministically modelled deformation zone*. During the SDM-Site investigations the deterministic geological model version 2.2 was developed (SKB 2008). The model was later updated to version 2.3 in order to incorporate the deformation zones from the SFR deformation zone model. Subsequently, the deformation zone models Forsmark version 2.3 and SFR version 1.0 (SKB 2011) were integrated to create the Deterministically Modelled Structures (DMS) model for Baseline Forsmark, and which also includes some updated geometries in the SFR access area (Hermansson and Petersson 2022). According to SKB's latest methodology for geological modelling, deformation zones are categorized according to size into Regional (length > 10 km and thickness > 100 m), Local major (length 1–10 km and thickness 5–100 m), or Local minor deformation zones (length 100–1,000 m and thickness 0.01–5 m). Many deformation zones were identified during the SDM-Site investigations from borehole data, surface lineament mapping (primarily low magnetic lineaments for steeply dipping zones) and geophysics, particularly seismic reflectors in the case of gently dipping deformation zones. Deterministically modelled structures in Forsmark are identified by a code that begins with the prefix ZFM or JFM, often followed by a directional identifier based on their apparent strike (e.g. WNW) and a unique numerical identifier.

The updated geological modelling methodology includes methodology for geometrical modelling of sheet joints. Sheet joints differ conceptually from deformation zones as they are not the product of tectonic processes, but rather an inferred connection to unloading of the bedrock. As such, they are dilational, brittle structures roughly parallel to the surface topography and thought to develop parallel to the directions of the two greatest principal compressive stresses in the rock mass. Sheet joints are identified by the prefix JFM followed by a unique numerical identifier.

During SDM-Site deformation zone thickness was modelled as a constant taken as the mean value of individual borehole intercepts along the entire zone, including both fault damage zones and zone cores (Figure 2-2a), and which may differ from individual inferred thicknesses from individual borehole intercepts. In some cases, deformation zone thickness was inferred from representative thicknesses of individual boreholes (Figure 2-2b) and future modelling may include variable thickness of deformation zones (Figure 2-2c).

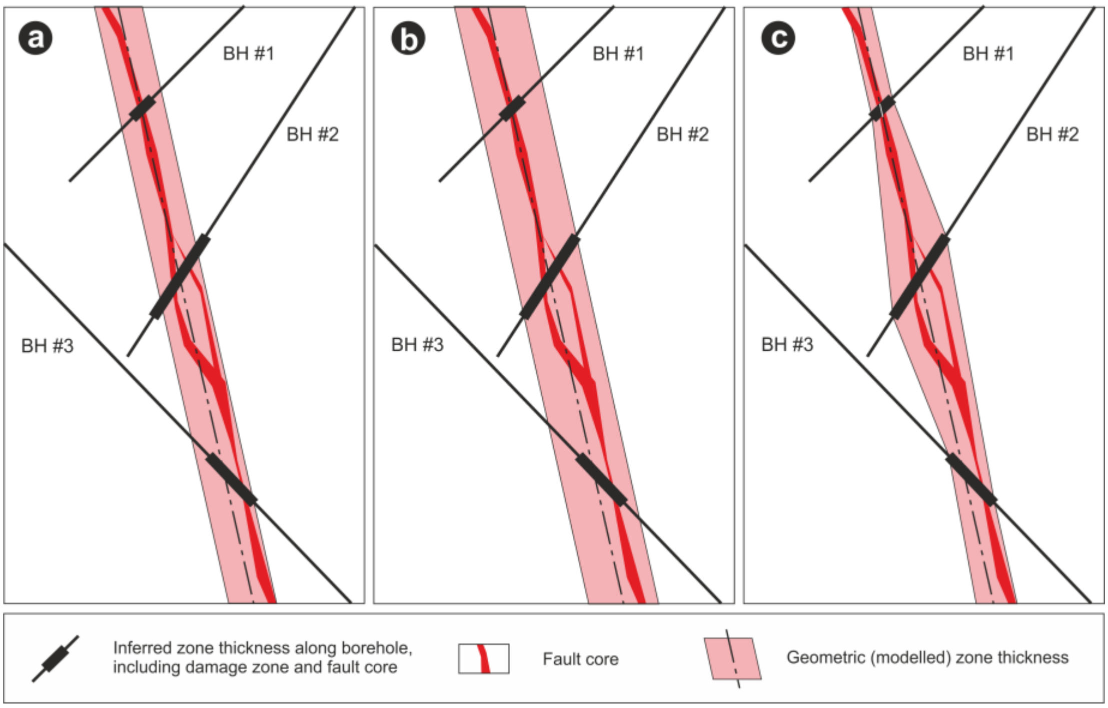

Figure 2-2. *A sketch illustrating different strategies for modelling deformation zones (from Hermansson and Petersson 2022). Zone thickness defined as (a) a mean value of the inferred thicknesses in all intersecting boreholes, and (b) the maximum inferred thickness observed in the intersecting boreholes (in this case BH #2) or (c) linear extrapolation of inferred zone thickness at each observation point.*

2.2.2 Overview of the fracture domain model

Based on a systematic assessment of the variation in the frequency (fractures/m) of fractures with depth along each borehole, the bedrock between deterministically modelled deformation zones has been divided into six fracture domains referred to as FFM01–FFM06 (Follin 2019). Fracture domains and deterministically modelled deformation zones are mutually exclusive volumes, whereas rock domains (RFM) contain both fracture domains and deterministically modelled deformation zones. The target volume for SFK lies inside FFM01, FFM02 and FFM06. Fracture domain FFM01 forms the main component in rock domain RFM029 at depth in the target volume, northwest of and in the footwall of the gently dipping zone ZFMA2 at a depth that varies from ca −40 m elevation close to drill site 8 (large distance from ZFMA2) to deeper than ca -200 m elevation close to ZFMA2. Fracture domain FFM01 shows a decreasing frequency of open and partly open fractures with depth.

Fracture domain FFM02 comprises the bedrock close to the surface, above fracture domain FFM01, predominantly in the same footwall bedrock segment. Fracture domain FFM02 is located in both rock domains RFM029 and RFM045. Whereas the bedrock in FFM01 shows a low frequency of open and partly open fractures, the bedrock in FFM02 is characterised by a complex network of sub-horizontal or gently dipping, open and partly open fractures, which locally merge into minor zones, e.g. at drill site 7. It is apparent that the transition from more fractured bedrock close to the surface (FFM02) to less fractured bedrock at depth (FFM01) takes place at larger depth closer to zone ZFMA2. FFM02 is currently separated into upper and lower subdomains (FFM02U/L) due to a marked contrast in fracture frequency distribution pattern with depth (Hermansson and Petersson 2022).

Thus, the character of fracture domain FFM02 is not solely determined by elevation. The occurrence of this domain at greater depths beneath ZFMA2 at drill sites 1, 5 and 6, and even above this zone at or close to drill sites 5 and 6, is related to an inferred higher frequency of older fractures in the vicinity of this zone, to higher rock stresses around zone ZFMA2, or to a combination of these two possibilities. The gently dipping and sub-horizontal fractures are oriented at a large angle to the present-day minimum (vertical) principal stress in the bedrock. This relationship favours the reactivation of older fractures as extensional joints, the development of new sheet joints following the glacial rebound and the development of conspicuous apertures along fractures in the present stress regime. These structural developments all contribute to a general release of the high stress in the bedrock.

Fracture domain FFM06 is defined in the target volume. In the same manner as fracture domain FFM01, FFM06 lies beneath FFM02. It comprises the largest part of the rock domain RFM045 and is distinguished from FFM01 simply on the basis of the widespread occurrence of fine-grained, altered (albitised) granitic rock, with slightly higher contents of quartz compared to unaltered granitic rock. The bedrock southeast of the target volume, in the hanging wall of zone ZFMA2, is defined as fracture domain FFM03. It is mainly situated in rock domain RFM029. Open and partly open fractures in this domain are more evenly distributed down to 1,000 m depth and the domain is spatially associated with a high frequency of gently dipping fracture zones containing both open and sealed fractures.

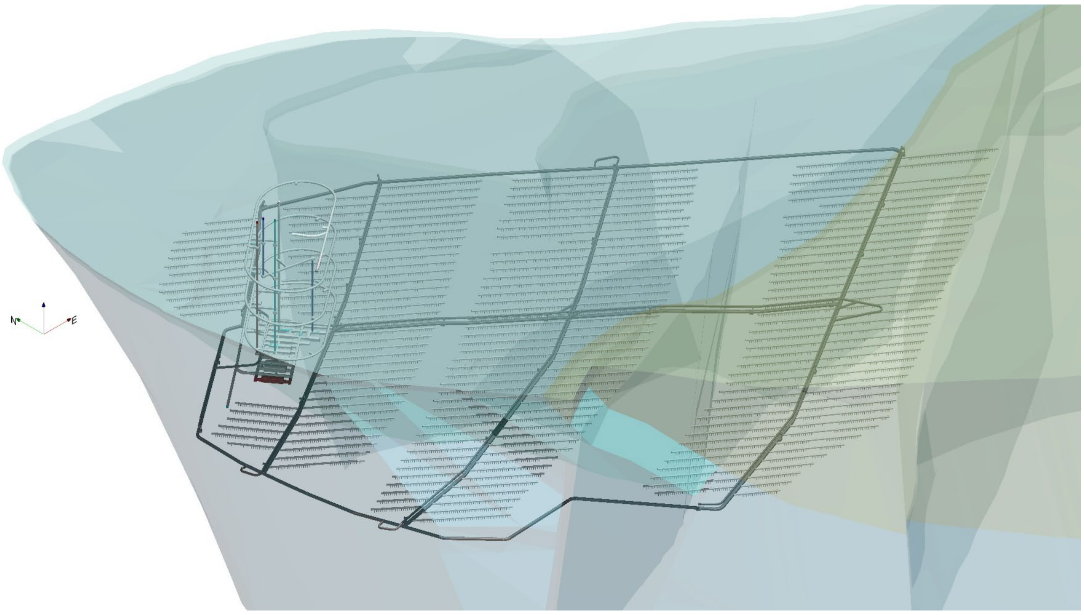

Figure 2-3. *Isometric overview of selected fracture domains (FFM01 (dark blue), FFM02U and FFM02L (light blue), FFM03(yellow)) in the Baseline Forsmark area. A potential SFK layout (SYHA 2.0) is shown for reference. View towards northeast.*

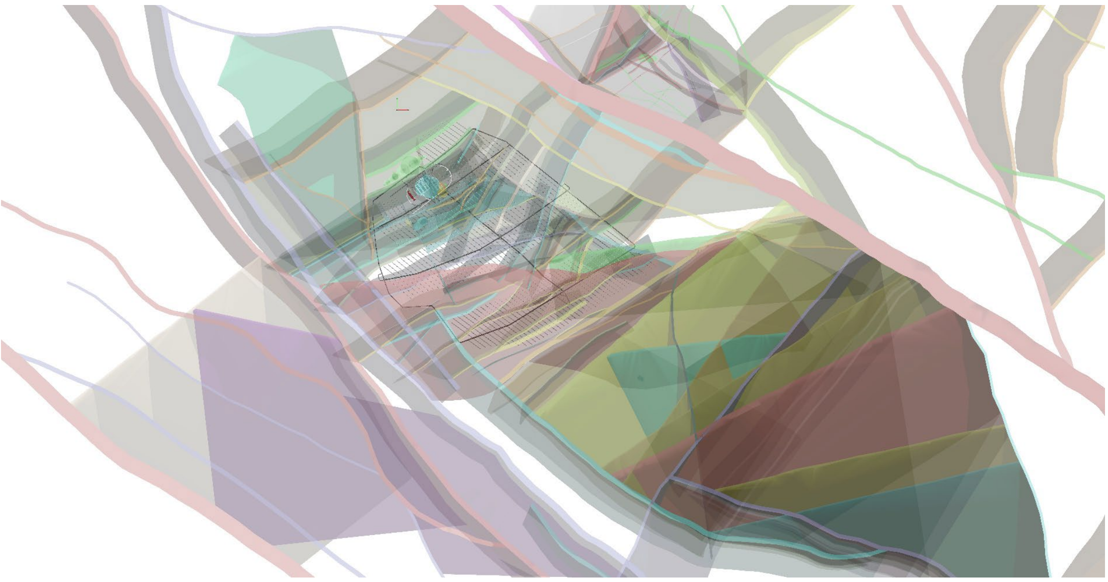

Figure 2-4. *Overhead view of the Deterministically Modelled Structures in the Baseline Forsmark area. A potential SFK layout (SYHA 2.0) is shown for reference. Top of figure faces north.*

2.2.3 Overview of models of surface distribution, depth and stratigraphy of regolith

Models of the geometrical (surface and depth) distribution of regolith constitute the conceptual-quantitative modelling framework for interpretation of field and laboratory hydraulic property data from regolith and the regolith/bedrock interface. Figure 2-5 *Figure 2-2*and Figure 2-6 show maps illustrating models of the surface distribution and the total depth, respectively, of regolith (Petrone et al. 2020). Moreover, Figure 2-1 shows a conceptual sketch of the general distribution of regolith types and associated layers ("Z-layers" of the regolith depth and stratigraphy model (Petrone et al. 2020)). Note that parts of the maps of Figure 2-5 and Figure 2-6 will be updated based on supplementary regolith data gathered in parts of the Forsmark area.

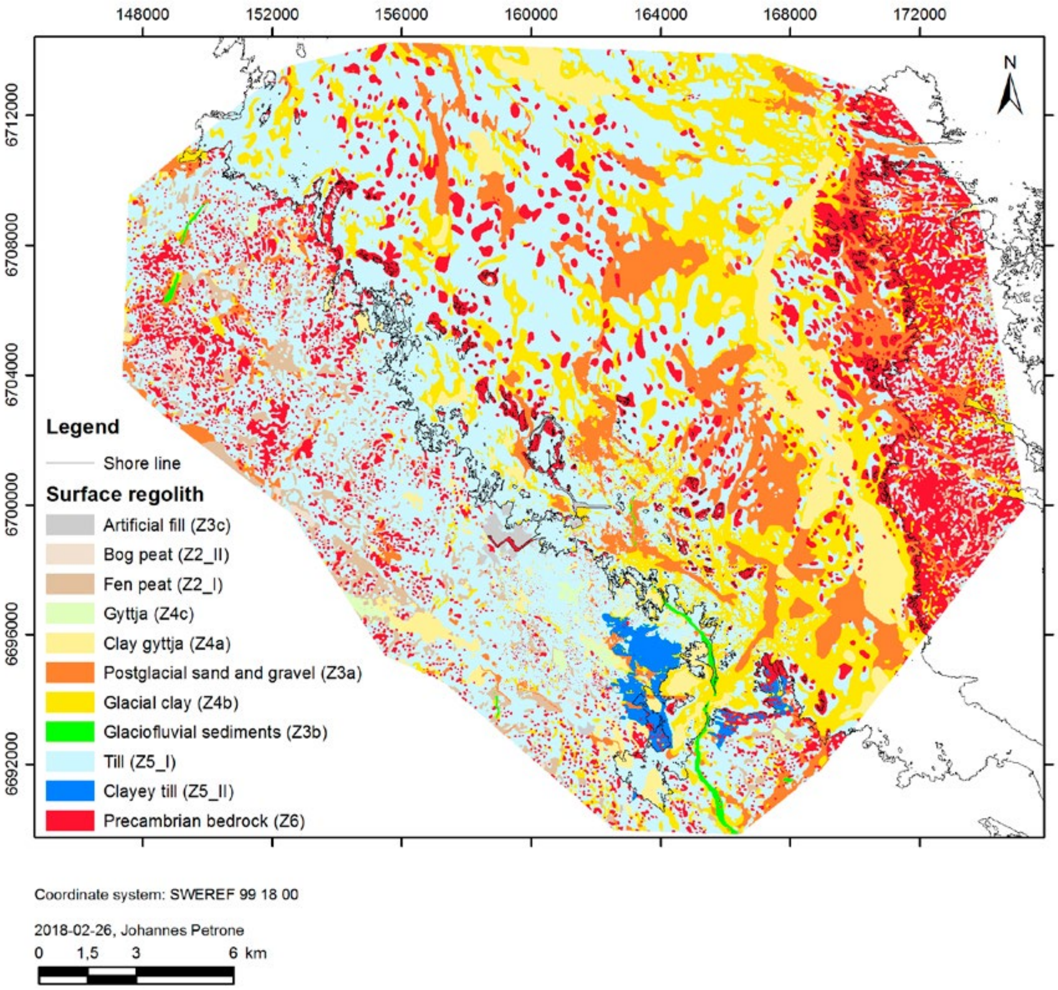

Figure 2-5. *Overview map of the model of the surface distribution of regolith in the Forsmark area, c 0.5 m below the ground surface, at which depth regolith is more or less unaffected by surface processes in the form of weathering and bioturbation (Petrone et al. 2020). The map shows the surface distribution of regolith both in terrestrial and marine areas, including regolith at the bottom of lakes and streams in terrestrial areas. Note that parts of the map will be updated based on supplementary regolith type data gathered in the SFK access area (Follin et al. (2019), in the Lake Gunnarsbotträsket catchment area (Sohlenius et al. 2019), and in wetlands (Sohlenius and Svensson 2021). The Z-designations refer to regolith types and associated layers ("Z-layers") of the regolith depth and stratigraphy model (Petrone et al. 2020).*

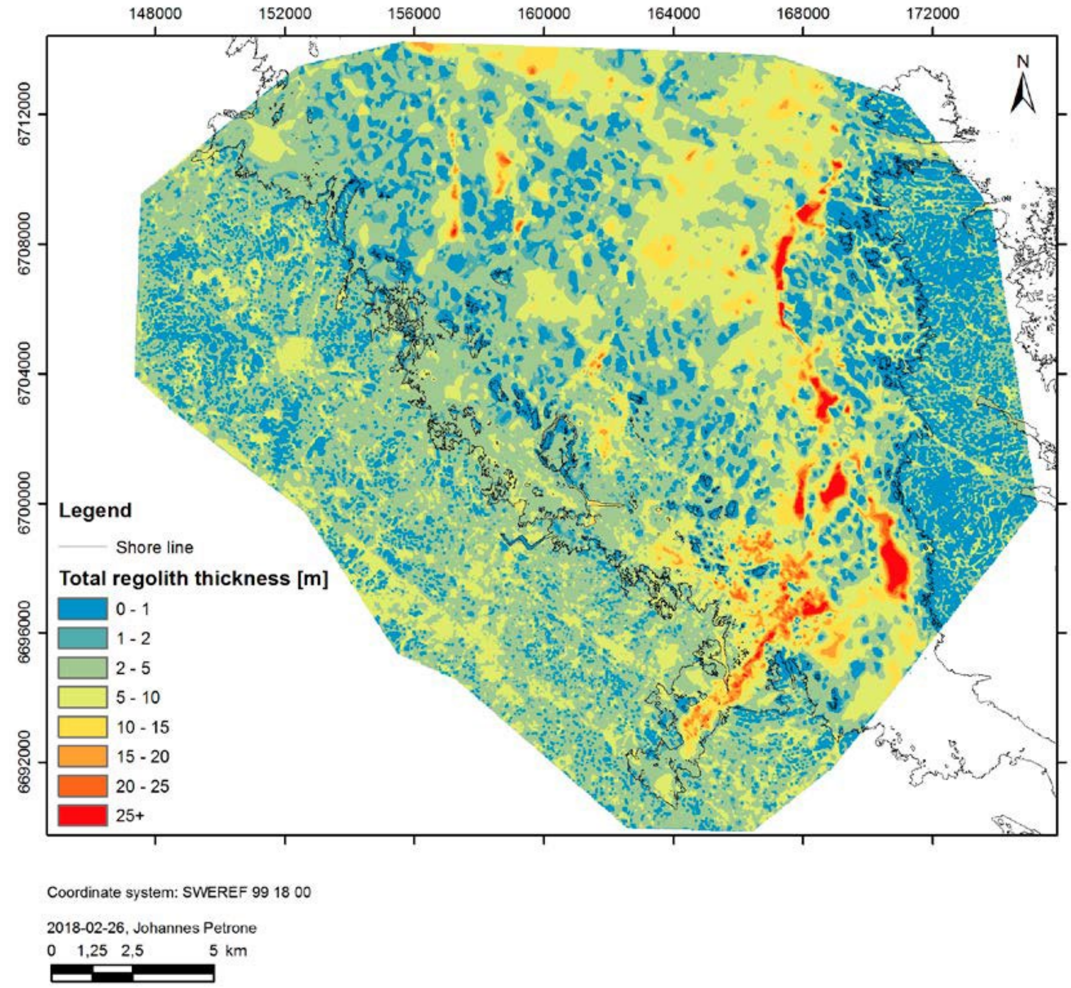

Figure 2-6. *Overview map of the model of total regolith depth in the Forsmark area (Petrone et al. 2020). The map shows the regolith surface distribution of total regolith depth both in terrestrial and marine areas, including regolith at the bottom of lakes and streams in terrestrial areas. Note that parts of the map will be updated based on supplementary regolith depth data gathered in the SFK access area (Follin et al. (2019) and in the Lake Gunnarsboträsket catchment area (Sohlenius et al. 2019), and in wetlands (Sohlenius and Svensson 2021).*

3 Boreholes, test methods and data

3.1 Boreholes, groundwater wells and sampling points

Figure 3-1, Figure 3-2 and Figure 3-3 show the locations of the core-drilled boreholes (KFM/KFR), the percussion-drilled boreholes (HFM/HFR), and the groundwater wells (SFM) for hydraulic property data are presented in this report. Regolith sampling points are shown in Chapter 6, whereas groundwater well drawings are compiled in Rasul (2022).

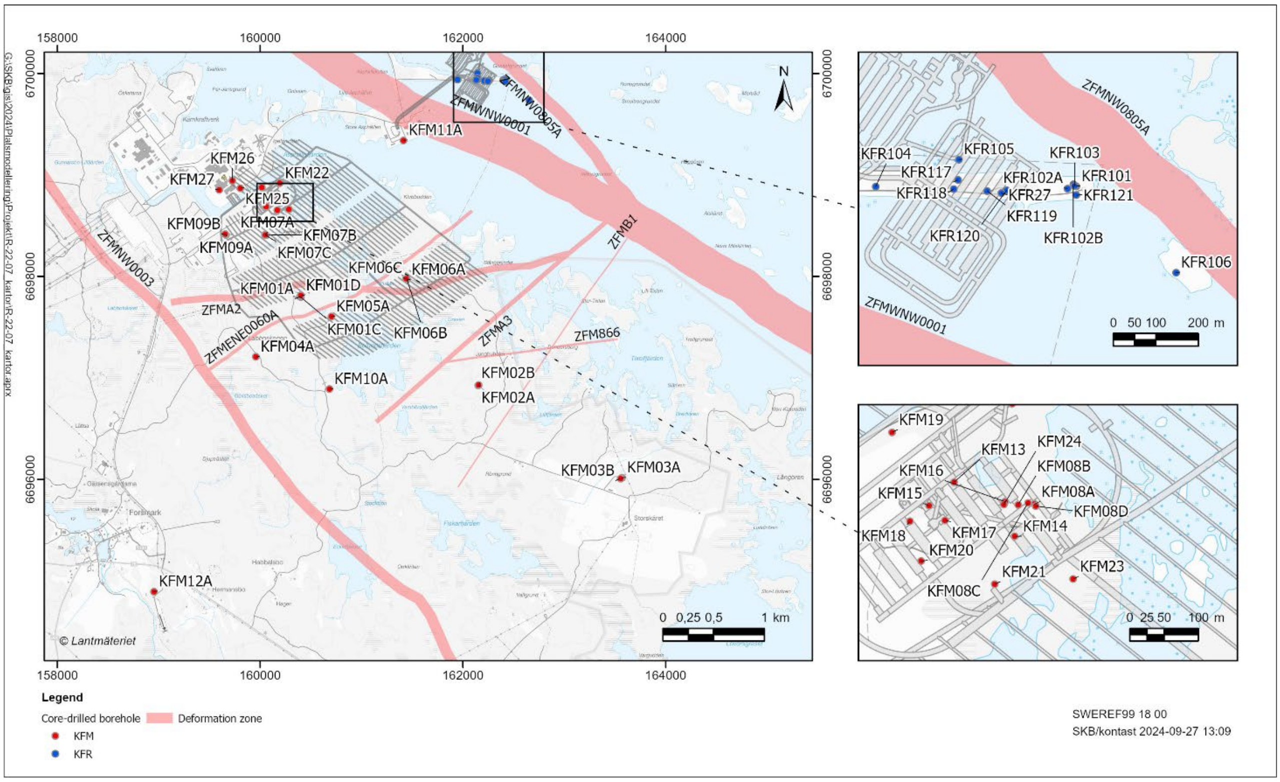

Figure 3-1. *Locations of core-drilled boreholes from which hydraulic properties data are presented in this report. Selected regional deformation zones comprising the northern and southern boundaries of the tectonic lens are shown in red for reference.*

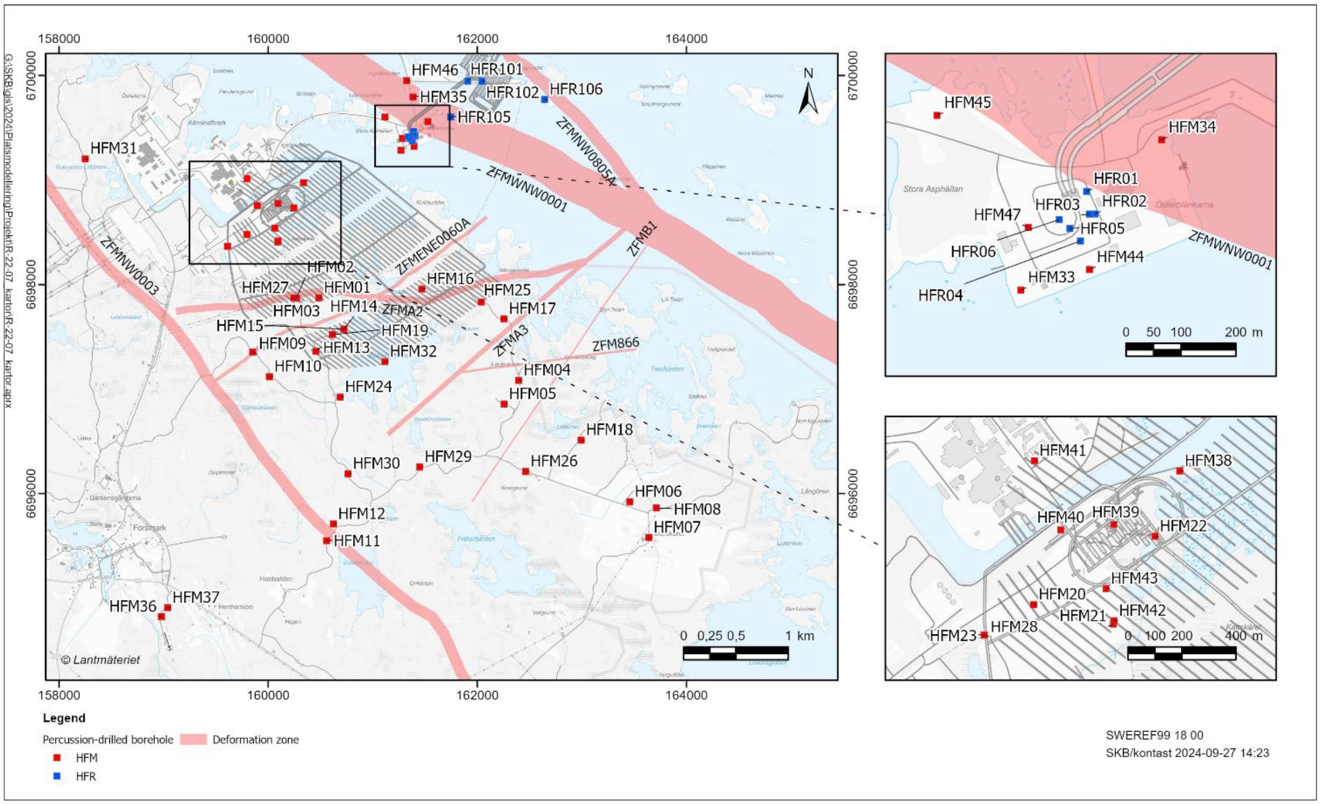

Figure 3-2. *Locations of percussion-drilled boreholes for which hydraulic properties data are presented in this report. Selected regional deformation zones comprising the northern and southern boundaries of the tectonic lens are shown in red for reference.*

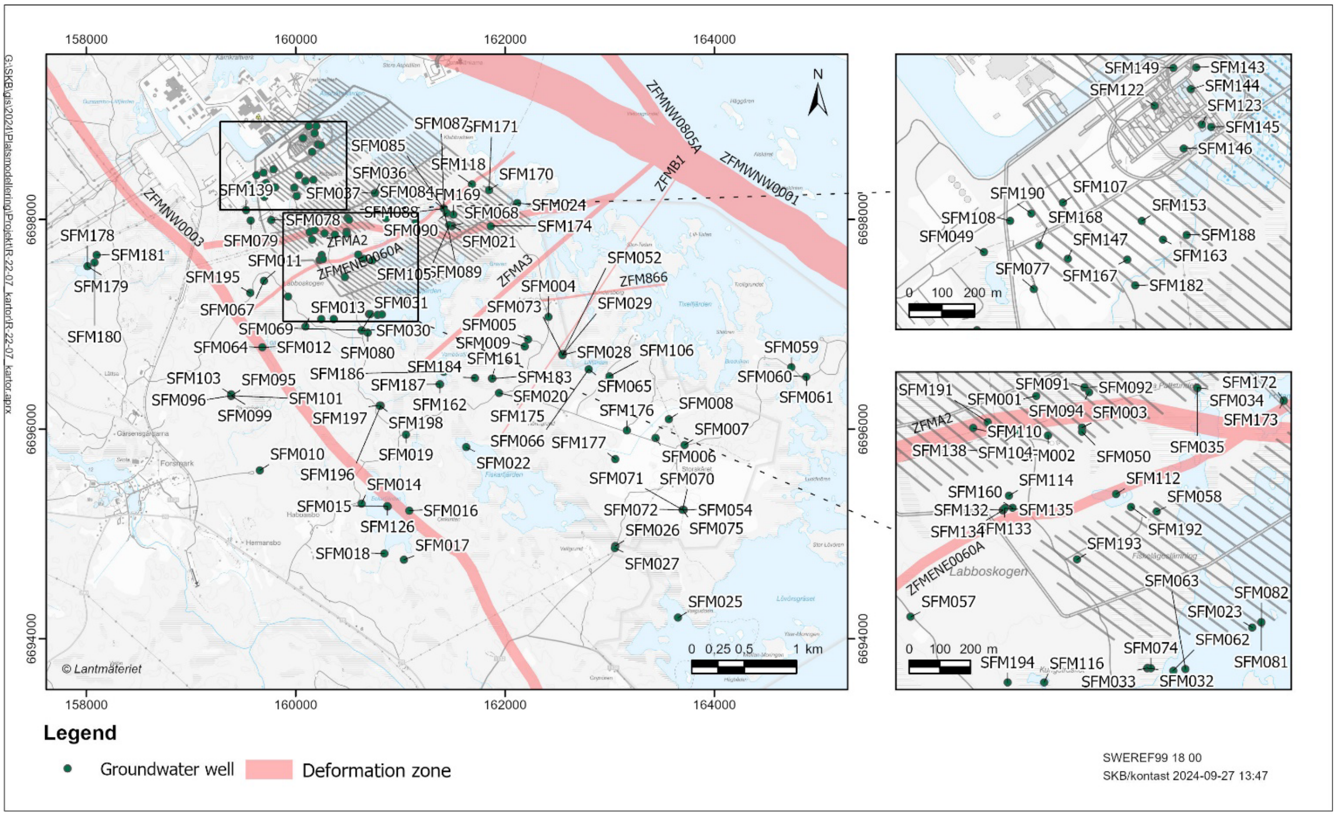

Figure 3-3. *Locations of groundwater wells for which properties data are presented in this report. Selected regional deformation zones comprising the northern and southern boundaries of the tectonic lens are shown in red for reference.*

3.2 Investigation methods

3.2.1 Single-hole hydraulic investigations in bedrock

The core-drilled boreholes presented in this report were investigated with difference flow logging using the Posiva Flow Log tool (PFL, SKB MD 322.010e) and/or by means of packer-sectioned injection tests using the Pipe String System tool (PSS, SKB MD 323.002). Some core-drilled and all percussion-drilled boreholes were investigated with the combined pumping and impeller flow logging tool (HTHB, SKB MD 322.009), except those with a very poor yield. The practical measurement ranges correspond to a transmissivity that under ideal conditions is $2 \cdot 10^{-10}$–$1 \cdot 10^{-5}$ m^2/s using the PFL method and $1 \cdot 10^{-9}$–$5 \cdot 10^{-4}$ m^2/s for the PSS method. The upper measurement limit for transmissivity using the HTHB method is roughly $1 \cdot 10^{-6}$–$1 \cdot 10^{-5}$ m^2/s, depending on borehole diameter and length of test section. Tested borehole sections that fall below the respective lower T limit are in Sicada (SKBs primary database) assigned a value corresponding to the lower measurement limit. In this report lower-limit T values are assigned to such borehole sections.

3.2.2 Quaternary deposits and surface water hydrological investigations

The main hydraulic properties of relevance for regolith and the regolith/bedrock interface are saturated-zone horizontal (K_h, m/s) and vertical hydraulic conductivity (K_v, m/s), and storage properties in terms of specific storage (S_s, m^{-1}), total and effective porosity (-) and specific yield (S_y, -). Unsaturated-zone properties of relevance include unsaturated hydraulic conductivity as function of suction head or water saturation, and the vertical hydraulic conductivity at full saturation, total porosity, field capacity, residual water content, air-entry value, and wilting point. These properties can be obtained by field and laboratory methods, with method-specific support scales that typically are smaller or much smaller than spatial resolutions associated with quantitative models on regional and local model scales.

Field-investigation methods to obtain saturated-zone properties include single-hole (slug and (in situ) permeameter) tests and interference (cross-hole) tests, with permeameter tests being more suitable than slug tests in low-conductive regolith (hydraulic conductivity $< 10^{-9}$–10^{-8} m/s). The mentioned test methods have support scales on the order of 1 m and 10–100 m, respectively, typically reflected by scale-dependent evaluated hydraulic conductivity. Moreover, methods for evaluation of regolith and regolith/bedrock interface storage properties (specific storage S_s and specific yield S_y) are usually associated with large uncertainty. In addition to evaluation of hydraulic properties, interference tests can be used to identify positive and negative boundaries and leakage conditions.

Several laboratory-investigation methods are available for evaluation of saturated-zone and unsaturated-zone properties. One major drawback with these methods is their small support scale, typically on the order of 0.1 m. These methods include empirical estimation of hydraulic conductivity based on PSD (particle-size distribution curves) and permeameter and CRS (constant rate of strain) tests on disturbed and undisturbed regolith samples, respectively. Laboratory methods are generally required to assess water-retention and water-flow properties of the unsaturated zone (e.g. Lundin et al. 2005), including model parameters associated with different empirical functions (e.g. Brooks and Corey (1964), Campbell (1974) and van Genuchten (1980)). Specifically, these methods are based on so called water-retention (or pF) curves, which provide water content as function of suction head. Important parts on such a curve include water content at full saturation (total porosity), field capacity (water content at pF 2), wilting point (water content at pF 4.2), and residual water content (water content at very high suction head, in the absence of evaporation). The drainable pore space (the part of the pF curve between full saturation and field capacity) is particularly important for the groundwater-table dynamics when the groundwater table is close to the ground surface and/or the specific yield is low.

3.3 Hydraulic test data

3.3.1 Description of available data pertaining to core-drilled boreholes

Data for core-drilled were primarily obtained from Sicada. Geometrical data were obtained from the p_borehole Sicada data table, drilling data from p_borehole_drill_info, hydraulic data from p_transmissivity_skin (SKBdocID 1925358)[1] and complemented with some missing transmissivity values using the table p_transmissivity for several boreholes not included in p_transmissivity_skin (KFR27 and KFR105) as well as for PFL flow anomaly data. Geological data was taken from the table DMS 2020_1_DZ Summary tables_delivered 2020-04-15 plus FFM and RFM.xlsx and complemented with data from parameter tables obtained in p_domain (SKBdocID 1925358). Regolith depth was taken from the parameter table p_borehole.

3.3.2 Performed tests and available data for core-drilled boreholes

Table 3-1 presents a list of available test data included in this report from core-drilled boreholes in the Forsmark area. Single-hole hydraulic data from the SFR area (Öhman et al. 2012) are also available, but investigation strategies and test methods differ from those related to data presented in this report. Older SFR data compilations are presented in Appendix C. Test methods included in this report include difference flow logging (PFL), injection tests (PSS) and combined pumping and impeller flow logging (HTHB), cf. Section 3.2.1.

Table 3-1. Available Sicada data and tests performed in core-drilled boreholes in the Forsmark area. A summary of transmissivity evaluated from the flowlogging tests is presented in Chapter 4.

I	Flowlogging-PFL-DIFF_sequential	HY680
II	Flowlogging-PFL-DIFF_overlapping	HY685
III	Flow logging-Impeller	HY690
IV	Injection test (2002-)	HY660

Borehole	I	II	III	IV	Northing (SWEREF99 18 00)	Easting (SWEREF99 18 00)	Elevation (m, RH 2000)	Borehole length (m)	Regolith depth (m)	Bearing (degrees)	Inclination (degrees)	Diameter (mm)
KFM01A	•	•		•	6697801	160394	3.3	1,001.5	9	320	-84.7	76
KFM01C				•	6697797	160401	3.1	452.1	3	167	-49.6	76
KFM01D	•	•		•	6697813	160402	3.1	800.2	7	37	-54.9	76
KFM02A	•	•	•	•	6696924	162152	7.5	1002.4	2	278	-85.4	77
KFM02B	•	•			6696931	162155	7.8	573.9	1	315	-80.3	76
KFM03A	•	•		•	6696016	163570	8.4	1,001.2	1	273	-85.7	77
KFM03B				•	6696009	163557	8.7	101.5	1	266	-85.3	77
KFM04A	•	•		•	6697207	159956	9.0	1,001.4	1	47	-60.1	77
KFM05A	•	•		•	6697605	160702	5.7	1,002.7	8	83	-59.8	77
KFM06A	•	•	•	•	6697969	161446	4.3	1,000.6	2	303	-60.2	77
KFM06B				•	6697968	161450	4.3	100.3	3	299	-83.5	77
KFM06C				•	6697977	161441	4.3	1,000.9	2	28	-60.1	76
KFM07A	•	•		•	6698410	160049	3.5	1,002.1	4	263	-59.3	77
KFM07B				•	6698406	160054	3.6	298.9	4	136	-54.7	76
KFM07C	•	•			6698408	160052	3.5	500.3	4	145	-85.3	76
KFM08A	•	•		•	6698771	160227	2.7	1,001.2	5	323	-60.8	77
KFM08B				•	6698770	160203	2.4	200.5	5	272	-58.8	76
KFM08C	•	•		•	6698773	160217	2.7	951.1	3	38	-60.5	77
KFM08D	•	•			6698768	160229	2.8	942.3	1	102	-55.2	77
KFM09A				•	6698410	159665	4.5	799.7	7	202	-59.5	77

[1] SKBdoc 1925358 ver. 1.0, Internal document.

I	Flowlogging-PFL-DIFF_sequential	HY680
II	Flowlogging-PFL-DIFF_overlapping	HY685
III	Flow logging-Impeller	HY690
IV	Injection test (2002-)	HY660

Borehole	I	II	III	IV	Northing (SWEREF99 18 00)	Easting (SWEREF99 18 00)	Elevation (m, RH 2000)	Borehole length (m)	Regolith depth (m)	Bearing (degrees)	Inclination (degrees)	Diameter (mm)
KFM09B				•	6698415	159656	4.5	616.5	7	143	-55.1	77
KFM10A	•	•		•	6696890	160683	4.7	500.2	8	12	-50.1	76
KFM11A	•	•		•	6699341	161416	3.1	851.2	7	42	-60.9	77
KFM12A				•	6694895	158952	10.9	601.0	8	38	-60.5	77
KFM13			•	•	6698803	160110	3.0	150.2	7	90	-60.6	76
KFM14	•	•	•	•	6698724	160197	2.2	60.2	5	267	-85.4	76
KFM15	•	•	•	•	6698769	160073	3.7	62.3	5	138	-83.6	76
KFM16	•	•	•	•	6698775	160184	1.7	60.4	3	323	-59.6	76
KFM17			•	•	6698748	160096	3.8	60.5	4	347	-85.9	76
KFM18			•		6698746	160045	3.7	60.5	8	157	-86.7	76
KFM19			•	•	6698876	160019	3.0	102.4	5	172	-64.8	76
KFM20	•	•	•		6698688	160061	3.0	60.5	1	339	-85.4	76
KFM21	•	•	•	•	6698654	160169	2.8	101.1	5	62	-70.9	76
KFM22	•	•	•	•	6698918	160194	2.9	60.3	7	158	-85.5	76
KFM23	•	•	•	•	6698662	160283	2.5	100.6		343	-73.0	76
KFM24	•	•		•	6698770	160182	1.2	550.2	3	314	-83.4	76
KFM25	•	•			6698869	159804	2.7	100.7	5	140	-84.3	76
KFM26	•	•			6698941	159726	3.0	100.7	5	17	-84.9	76
KFM27	•	•			6698854	159597	2.5	100.6	5	322	-75.0	76
KFR101	•	•			6699940	162421	2.6	341.8	12	31	-55.5	76
KFR102A	•	•			6699935	162399	2.9	600.8	10	304	-65.6	76
KFR102B	•	•			6699945	162413	2.7	180.1	12	347	-55.1	76
KFR103	•	•			6699941	162416	2.6	200.5	12	182	-55.1	76
KFR104	•	•			6699939	161948	3•0	454.6	7	136	-54.9	76
KFR105	•	•		•	6700003	162144	-106.6	306.8	0	176	-10.1	76
KFR106	•	•			6699737	162655	1.2	300.1	0	197	-70.3	76
KFR117				•	6699955	162142	2.4	176.0	6	34	-80.6	76
KFR118				•	6699934	162132	3.2	175.5	9	236	-85.6	76
KFR119	•	•		•	6699929	162211	3.1	176.5	7	211	-80.8	76
KFR120				•	6699931	162256	3.2	176.9	9	37	-79.9	76
KFR121	•	•			6699919	162420	2.9	362.5	9	216	-52.4	76
KFR27	•	•		•	6699924	162244	3.1	501.6		250	-87.6	76

3.3.3 Performed tests and available data for percussion-drilled boreholes

Table 3-2 presents tests performed in the percussion-drilled boreholes. Most of the percussion-drilled boreholes are investigated with combined pumping and impeller flow logging (HTHB; activity type HY690) except those with a very poor yield (HFM07, HFM25, HFM28, HFM29, HFM31, HFM41, and HFR01–06). In addition to HTHB tests, some of the percussion boreholes have also been tested using other methods, such as injection tests, instant pressure and flow measurements, pumping tests with a submersible pump, capacity tests, test and rinse pumping, air lift, wireline pumping, or an older type of steady-state injection test. This report only presents data available in the SKB database Sicada. No interpretations have been made of the presented data.

Table 3-2. Available data in Sicada from single-hole hydraulic tests performed in the percussion-drilled boreholes HFM01–47, HFR01–06, HFR101, HFR102, HFR105 and HFR106. A summary of transmissivity evaluated primarily from impeller flow logging, with a few results from pumping tests, is presented in Chapter 5. A summary of transmissivity evaluated from the impeller flow logging is presented in details in Chapter 5.

I	Flow logging-Impeller	HY690
II	Injection test (for the data after 2002-)	HY660
III	Instant pressure and flow measurements	HY115
IV	Pumping test-submersible pump	HY610
V	Misc. tests (Capacity test, Test & rinse pumping, Air lift, Wire line pumping and Old steady state injection test)	HY580, HY190, HY630, HY600, HY120

Borehole	I	II	III	IV	V	Northing (SWEREF99 18 00)	Easting (SWEREF99 18 00)	Elevation (m, RH 2000)	Borehole length (m)	Regolith depth (m)	Bearing (degrees)	Inclination (degrees)	Diameter (mm)
HFM01	•			•	•	6697873	160484	1.92	200.2	11.3	36	-77.5	140
HFM02	•			•	•	6697868	160268	3.24	100,0	12.2	8.4	-87.8	137
HFM03	•			•	•	6697868	160272	3.33	26,0	12	266.4	-87.3	136
HFM04	•		•	•	•	6697083	162395	4.06	221.7	0.8	338.8	-84.5	138
HFM05	•		•	•	•	6696856	162256	7.86	200.1	4	337.5	-84.9	134
HFM06	•			•	•	6695920	163458	6.82	110.7	2	4.3	-84.8	134
HFM07						6695578	163640	5.97	122.5	6.6	344.2	-84.5	140
HFM08	•			•	•	6695863	163711	7.32	143.5	5.1	350.6	-84.7	137
HFM09	•		•	•	•	6697353	159851	5.34	50.25	4.6	141.3	-69	141
HFM10	•			•	•	6697118	160012	5.17	150,0	2.41	94.8	-68.9	139
HFM11	•	•		•	•	6695548	160559	7.74	182.3	2.5	65.4	-49.3	139
HFM12	•	•		•	•	6695709	160623	7.21	209.5	3.64	247.1	-49.3	135
HFM13	•	•		•	•	6697362	160457	5.87	175.6	3.75	53.1	-59	135
HFM14	•			•	•	6697573	160724	4.1	150.5	0.27	333.7	-59.9	136
HFM15	•			•	•	6697572	160723	4.06	99.5	0.8	316.2	-44.2	139
HFM16	•			•	•	6697956	161469	3.4	132.5	2.3	329.9	-84.3	139
HFM17	•			•	•	6697671	162255	3.94	210.6	0.36	320.5	-84.4	136
HFM18	•	•		•	•	6696511	162993	5.22	180.6	1.37	315.2	-59.2	138
HFM19	•	•		•	•	6697521	160615	3.84	185.2	5.6	282.8	-58.3	137
HFM20	•	•		•	•	6698478	159796	3.15	301,0	2.72	356.3	-85.4	135
HFM21	•	•		•	•	6698407	160091	4.16	202,0	2.84	90.7	-58.5	137
HFM22	•			•	•	6698732	160246	1.72	222,0	3.6	92	-58.8	136
HFM23	•			•	•	6698365	159611	4.44	211.5	7.2	326.3	-58.9	134
HFM24	•			•	•	6696923	160688	3.87	151.3	11.55	49.2	-59.5	138
HFM25				•	•	6697832	162038	4.04	187.5	2.9	142.8	-57.8	139
HFM26	•			•	•	6696210	162461	2.92	202.7	5.65	114.3	-53.7	138

I	Flow logging-Impeller	HY690
II	Injection test (for the data after 2002-)	HY660
III	Instant pressure and flow measurements	HY115
IV	Pumping test-submersible pump	HY610
V	Misc. tests (Capacity test, Test & rinse pumping, Air lift, Wire line pumping and Old steady state injection test)	HY580, HY190, HY630, HY600, HY120

Borehole	I	II	III	IV	V	**Northing (SWEREF99 18 00)**	**Easting (SWEREF99 18 00)**	**Elevation (m, RH 2000)**	**Borehole length (m)**	**Regolith depth (m)**	**Bearing (degrees)**	**Inclination (degrees)**	**Diameter (mm)**
HFM27	•			•	•	6697871	160246	2.63	127.5	4.1	339.2	-67.8	139
HFM28				•	•	6698366	159613	4.45	151.2	6	148.7	-84.8	135
HFM29				•	•	6696254	161449	4.65	199.7	2.55	31.9	-58.6	138
HFM30	•			•	•	6696189	160763	3.31	200.7	13.5	30.7	-55.6	139
HFM31						6699203	158251	6.25	200.7	2.4	313.7	-69.3	139
HFM32	•			•	•	6697262	161117	1.19	202.6	1.5	118.1	-86	132
HFM33	•			•	•	6699285	161270	2.8	140.2	6.65	221.9	-59.2	139
HFM34	•			•	•	6699559	161526	2.63	200.7	7.95	32.4	-58.6	137
HFM35	•			•	•	6699794	161385	2.09	200.7	7.9	34.9	-59.3	136
HFM36	•			•	•	6694821	158979	8.6	152.5	3	258.5	-59	137
HFM37	•			•	•	6694907	159038	11.58	191.7	3.45	43.3	-59.2	139
HFM38	•			•	•	6698974	160338	2.39	200.7	5.35	95.5	-54.5	136
HFM39	•					6698776	160094	4.34	151.2	4.8	164.6	-85.8	164
HFM40	•					6698756	159897	2.54	101.7	4.9	168.2	-85.2	141
HFM41						6699012	159799	3.63	101.5	3.85	175.5	-84.8	139
HFM42	•					6698418	160094	4.21	195.3	2.05	176.2	-89.1	138
HFM43	•					6698538	160065	4.33	200,0	1.09	303.8	-85.2	137
HFM44	•					6699322	161395	2.94	199.6	3.4	255.7	-83.2	134
HFM45	•					6699603	161117	3.86	200.3	0	291.2	-85	139
HFM46	•					6699951	161325	1.7	200,0	0	108.1	-85.4	138
HFM47	•					6699399	161283	3.52	200.4	9.72	150	-84.4	138
HFR01					•	6699464	161390	0.89	13,0		232.4	-90	64
HFR02					•	6699423	161405	0.73	12.1		232.4	-90	64
HFR03					•	6699423	161395	0.64	8.4		232.4	-90	64
HFR04					•	6699374	161379	0.44	7.3		232.4	-90	64
HFR05					•	6699397	161359	0.48	7.4		232.4	-90	64
HFR06					•	6699413	161340	0.84	11.3		232.4	-90	64
HFR101	•	•		•	•	6699946	161908	2.82	209.3	6.25	135.5	-70	137
HFR102	•	•				6699945	162044	2.5	55.0	7.05	86.9	-59.1	138
HFR105	•			•	•	6699603	161745	3.46	200.5	19.42	37.3	-61.9	140

I	Flow logging-Impeller	HY690
II	Injection test (for the data after 2002-)	HY660
III	Instant pressure and flow measurements	HY115
IV	Pumping test-submersible pump	HY610
V	Misc. tests (Capacity test, Test & rinse pumping, Air lift, Wire line pumping and Old steady state injection test)	HY580, HY190, HY630, HY600, HY120

Borehole	I	II	III	IV	V	Northing (SWEREF99 18 00)	Easting (SWEREF99 18 00)	Elevation (m, RH 2000)	Borehole length (m)	Regolith depth (m)	Bearing (degrees)	Inclination (degrees)	Diameter (mm)
HFR106	•			•	•	6699771	162644	1.46	190.4	0	271.3	-59.8	139

3.3.4 Field and laboratory hydraulic investigations of regolith and the regolith/bedrock interface

The main hydraulic properties of relevance for regolith and the regolith/bedrock interface are saturated-zone horizontal (K_h, m/s) and vertical hydraulic conductivity (K_v, m/s), and storage properties in terms of specific storage (S_s, m^{-1}), total and effective porosity (-) and specific yield (S_y, -). Unsaturated-zone properties of relevance include unsaturated hydraulic conductivity as function of suction head or water saturation, and the vertical hydraulic conductivity at full saturation, total porosity, field capacity, residual water content, air-entry value, and wilting point. These properties can be obtained by field and laboratory methods, with method-specific support scales that generally are smaller or much smaller than spatial resolutions associated with quantitative models on regional and local model scales.

Field-investigation methods to obtain saturated-zone properties include single-hole (slug and (in situ) permeameter) tests and interference (cross-hole) tests, with permeameter tests being more suitable than slug tests in low-conductive regolith (hydraulic conductivity < 10^{-9}–10^{-8} m/s). The mentioned test methods have support scales on the order of 1 m and 10–100 m, respectively, typically reflected by scale-dependent evaluations of hydraulic conductivity. Moreover, methods for evaluation of regolith and regolith/bedrock interface storage properties (specific storage S_s and specific yield S_y) are usually associated with large uncertainty. In addition to evaluation of hydraulic properties, interference tests can be used to identify positive and negative boundaries and leakage conditions.

Several laboratory-investigation methods are available for evaluation of saturated-zone and unsaturated-zone properties. One major drawback with these methods is their small support scale, typically on the order of 0.1 m. These methods include empirical estimation of hydraulic conductivity based on PSD (particle-size distribution curves) and permeameter and CRS (constant rate of strain) tests on disturbed and undisturbed regolith samples, respectively. Laboratory methods are generally required to assess water-retention and water-flow properties of the unsaturated zone (e.g. Lundin et al. 2005), including model parameters associated with different empirical functions (e.g. Brooks and Corey (1964), Campbell (1974) and van Genuchten (1980)). Specifically, these methods are based on so called water-retention (or pF) curves, which provide water content as function of suction head. Important parts on such a curve include water content at full saturation (total porosity), field capacity (water content at pF 2), wilting point (water content at pF 4.2), and residual water content (water content at very high suction head, in the absence of evaporation). The drainable pore space (the part of the pF curve between full saturation and field capacity) is particularly important for the groundwater-table dynamics when the groundwater table is close to the ground surface and/or the specific yield is low.

In Table 3-3 a list of available test data presented in this report from hydraulic investigations of regolith and the regolith/bedrock interface in the Forsmark area are presented.

Table 3-3 Available data in Sicada from hydraulic investigations of regolith and the regolith/bedrock interface. ND = no data. N.A. = not applicable. 1For PFM and QFM sampling points, elevation refers to the ground surface.

I	Slug test	HY670
II	In situ (BAT) permeameter test	HY675
III	Interference test	HY610, HY640, HY645
IV	PSD	HY673, GE514
V	Lab. permeameter test	HY672
VI	CRS test	GE017
VII	pF (unsat. zone)	HY672

Well/ sampling point	I	II	III	IV	V	VI	VII	Northing (SWEREF 99 18 00)	Easting (SWEREF 99 18 00)	Elevation ToC (m, RH 2000)[1]	Depth (m b ToC)
SFM0001	•			•				6697985.95	160338.89	1.29	5.65
SFM0002	•			•				6697857.16	160376.87	2.21	6.11
SFM0003	•			•				6697882.24	160487.35	2.12	11.48
SFM0004	•			•				6697068.97	162414.83	4.33	6.02
SFM0005	•			•				6696857.22	162218.69	6.99	3.21
SFM0006	•			•				6695915.94	163437.50	6.47	4.21
SFM0007	•			•				6695848.23	163713.49	7.19	6.11
SFM0008	•			•				6696095.17	163564.57	3.95	6.14
SFM0009	•							6696788.18	162187.70	4.82	4.00
SFM0010	•			•				6695608.33	159659.01	13.72	3.00
SFM0011	•			•				6697415.58	159695.78	2.83	5.95
SFM0012	•							6696780.77	159682.35	3.13	6.42
SFM0013	•			•				6696979.03	160092.48	2.17	6.50
SFM0014	•							6695289.05	160629.27	6.80	4.27
SFM0015	•							6695263.59	160877.05	5.84	7.34
SFM0016	•			•				6695222.98	161085.66	6.37	9.57
SFM0017	•			•				6694753.20	161034.22	6.87	6.64
SFM0018	•			•				6694812.11	160847.97	6.86	6.50
SFM0019	•			•				6695948.85	161054.23	4.96	7.10
SFM0020	•			•				6696345.47	161943.03	2.43	5.00
SFM0021	•			•				6697940.47	161495.32	2.15	4.14
SFM0022	•			•				6695827.72	161628.55	1.96	5.80
SFM0023	•							6697230.89	161043.23	1.45	5.70
SFM0024	•							6698157.84	162118.57	0.65	3.21
SFM0025	•							6694200.45	163652.59	1.04	7.06
SFM0026	•			•				6694883.89	163052.94	1.77	18.49
SFM0027	•			•				6694866.64	163047.18	1.93	9.64
SFM0028	•			•				6696706.50	162550.51	1.25	9.05
SFM0029	•							6696708.76	162550.56	1.27	9.07
SFM0030	•			•				6696940.73	160631.47	2.97	6.02
SFM0031	•		•					6696944.14	160629.96	2.82	5.69
SFM0032	•		•	•				6697098.57	160699.83	1.81	5.26
SFM0033	•							6697099.25	160702.24	1.88	5.16
SFM0034	•			•				6698012.68	160863.03	1.76	4.11
SFM0035	•							6698011.42	160863.64	1.67	4.43
SFM0036	•			•				6698250.74	160758.48	1.69	4.09
SFM0037	•							6698250.74	160756.82	1.68	4.10
SFM0049	•			•				6698326.64	159547.59	4.21	6.00
SFM0050		•						6697869.16	160487.12	3.19	6.27
SFM0052		•						6696716.44	162551.63	1.22	6.27
SFM0054		•						6695228.04	163706.13	4.59	7.27
SFM0057	•			•				6697265.97	159928.72	5.00	4.55
SFM0058	•							6697608.72	160730.79	3.73	4.75
SFM0059			•					6696590.26	164735.77	4.72	6.15
SFM0060			•					6696500.78	164879.38	5.09	8.65
SFM0061	•		•					6696497.64	164879.22	5.58	8.07
SFM0062	•		•	•				6697090.74	160784.90	1.54	3.95
SFM0063	•		•					6697095.18	160825.37	1.46	3.82
SFM0064				•				6696780.05	159681.55	3.06	5.37
SFM0065	•			•				6696571.20	162798.76	1.16	4.98
SFM0067	•							6697414.37	159697.51	2.73	2.62
SFM0068	•							6697940.35	161491.88	2.25	2.36
SFM0069	•			•				6696942.77	160631.07	2.69	2.63
SFM0070	•			•				6695229.49	163696.30	3.91	3.46
SFM0071	•			•				6695229.34	163697.88	3.79	7.31
SFM0072	•			•				6695229.08	163702.10	3.88	10.00
SFM0073	•							6696711.93	162546.88	0.81	5.00
SFM0074			•					6697098.99	160712.07	1.00	12.70

I	Slug test	HY670
II	In situ (BAT) permeameter test	HY675
III	Interference test	HY610, HY640, HY645
IV	PSD	HY673, GE514
V	Lab. permeameter test	HY672
VI	CRS test	GE017
VII	pF (unsat. zone)	HY672

Well/ sampling point	I	II	III	IV	V	VI	VII	Northing (SWEREF 99 18 00)	Easting (SWEREF 99 18 00)	Elevation ToC (m, RH 2000)[1]	Depth (m b ToC)
SFM0075	•							6695229.28	163699.64	3.96	9.91
SFM0077	•							6698214.62	159700.25	5.20	8.00
SFM0078	•							6697995.32	159768.52	5.42	5.60
SFM0079	•							6697988.75	159571.18	4.38	6.70
SFM0080	•							6696919.20	160687.15	4.54	9.62
SFM0081	•			•				6697247.86	161072.62	1.48	5.25
SFM0082		•						6697248.07	161073.10	1.57	2.76
SFM0084	•		•	•				6698105.37	161413.78	1.42	4.10
SFM0085		•	•					6698105.80	161413.60	1.86	3.26
SFM0087	•		•					6698105.01	161414.15	1.49	2.35
SFM0088		•	•					6698105.05	161413.37	1.28	1.26
SFM0090			•					6698060.51	161443.87	1.82	10.43
SFM0091	•		•	•				6698013.01	160495.04	1.60	2.30
SFM0092		•	•					6698013.50	160495.14	1.60	1.81
SFM0094			•	•				6697998.54	160510.58	1.55	10.30
SFM0095	•		•	•				6696318.57	159385.23	12.28	7.10
SFM0096		•	•					6696318.42	159384.55	11.82	3.26
SFM0099		•	•					6696317.96	159385.09	11.74	2.26
SFM0101		•	•					6696318.32	159385.46	12.22	2.26
SFM0103			•	•				6696333.47	159383.35	11.98	10.26
SFM0104	•			•				6697866.52	160274.81	3.73	7.20
SFM0105	•			•				6697945.22	161467.07	3.80	4.20
SFM0106	•			•				6696504.90	162998.44	4.88	5.30
SFM0107	•			•				6698478.54	159788.86	3.33	7.05
SFM0108	•			•				6698422.93	159627.23	4.40	7.00
SFM000110	•							6697880.93	160132.03	2.53	3.05
SFM000112	•							6697665.60	160598.60	3.11	3.00
SFM000114	•							6697659.91	160248.91	3.48	3.00
SFM000116	•							6697052.29	160364.23	3.52	3.75
SFM000118	•							6698334.17	161684.12	1.83	2.25
SFM000122	•							6698774.26	160069.61	3.03	7.50
SFM000126	•							6695260.69	160877.51	6.07	7.17
SFM000132	•							6697613.73	160229.23	4.09	3.10
SFM000133	•			•		•		6697618.64	160234.76	3.75	3.10
SFM000134	•							6697613.38	160229.97	4.08	2.10
SFM000135	•							6697619.54	160235.14	3.70	2.10
SFM000138	•							6697807.69	160158.26	2.74	2.00
SFM000139	•							6698088.04	159525.68	3.85	3.00
SFM000143	•							6698891.75	160196.66	2.45	1.50
SFM000144	•							6698824.48	160180.21	2.65	2.50
SFM000145	•							6698709.18	160242.11	1.65	2.00
SFM000146	•							6698643.30	160158.07	3.29	3.10
SFM000147	•							6698307.35	159803.72	2.96	2.40
SFM000149	•							6698890.00	160127.28	1.47	2.25
SFM000153	•							6698422.33	160030.72	4.35	3.20
SFM000160	•							6697620.92	160260.99	3.25	2.50
SFM000161	•							6696481.45	161876.18	2.19	2.00
SFM000162	•							6696426.77	161377.68	2.01	1.50
SFM000163	•							6698365.45	160094.40	3.79	6.88
SFM000167	•							6698303.90	159986.18	3.17	10.91
SFM000168	•							6698348.03	159716.36	5.64	5.17
SFM000169	•							6698044.38	161506.48	2.33	4.00
SFM000170	•							6698281.06	161847.16	1.63	3.50
SFM000171	•							6698281.13	161848.15	1.74	3.50
SFM000172	•							6697970.81	161146.25	1.82	5.50
SFM000173	•							6697970.02	161145.48	1.88	5.00
SFM000174	•							6697935.95	161862.60	3.57	3.00
SFM000175	•							6696315.81	162226.80	4.33	6.00
SFM000176	•							6695987.41	163163.28	5.28	7.00
SFM000177	•							6695713.39	163054.58	4.82	6.00
SFM000178	•							6697552.63	158010.74	6.93	6.00
SFM000179	•							6697552.49	158011.86	6.89	5.00

I	Slug test	HY670
II	In situ (BAT) permeameter test	HY675
III	Interference test	HY610, HY640, HY645
IV	PSD	HY673, GE514
V	Lab. permeameter test	HY672
VI	CRS test	GE017
VII	pF (unsat. zone)	HY672

Well/ sampling point	**I**	**II**	**III**	**IV**	**V**	**VI**	**VII**	**Northing (SWEREF 99 18 00)**	**Easting (SWEREF 99 18 00)**	**Elevation ToC (m, RH 2000)[1]**	**Depth (m b ToC)**
SFM000180	•							6697589.29	158078.43	6.95	6.00
SFM000181	•							6697660.35	158098.39	9.56	4.00
SFM000182	•							6698225.22	160009.51	2.66	5.00
SFM000183	•							6696481.17	161880.08	2.50	7.10
SFM000184	•							6696488.32	161713.56	2.38	4.20
SFM000186	•							6696548.33	161413.06	1.96	5.00
SFM000187	•							6696428.88	161376.14	2.14	4.00
SFM000188	•							6698379.64	160167.73	2.29	5.10
SFM000190	•							6698445.35	159691.78	5.62	7.00
SFM000191	•			•				6697900.44	160180.13	4.49	9.20
SFM000192	•			•				6697624.66	160647.63	3.44	9.00
SFM000193	•							6697452.73	160471.64	6.05	5.10
SFM000194	•			•				6697051.76	160244.69	4.30	4.00
SFM000195	•							6697298.64	159565.60	3.77	7.00
SFM000196	•							6696224.62	160813.50	3.25	11.00
SFM000197	•							6696226.86	160803.11	2.70	8.00
SFM000198	•							6696222.97	160805.12	3.16	7.00
KFM01A				•				6697800.53	160394.46	3.31	N.A.
HFM01				•				6697872.93	160484.29	1.92	N.A.
HFM02				•				6697868.16	160268.18	3.24	N.A.
HFM03				•				6697867.63	160272.12	3.33	N.A.
HFM04				•				6697082.85	162394.81	4.06	N.A.
HFM05				•				6696855.69	162256.19	7.86	N.A.
HFM06				•				6695920.12	163457.91	6.82	N.A.
HFM07				•				6695578.17	163640.08	5.97	N.A.
HFM08				•				6695862.92	163711.40	7.32	N.A.
HFM09				•				6697353.30	159851.35	5.33	N.A.
HFM10				•				6697118.02	160011.63	5.17	N.A.
PFM002461				•				6696225.17	162380.24	2.42	N.A.
PFM002462				•				6696180.79	162518.25	2.43	N.A.
PFM002463				•				6695935.44	163305.70	2.98	N.A.
PFM002464				•				6695160.04	163695.58	3.06	N.A.
PFM002572				•				6695414.79	163470.79	4.39	N.A.
PFM002573				•				6696232.79	163381.79	3.83	N.A.
PFM002574				•				6695870.08	163469.52	6.73	N.A.
PFM002576				•				6697862.88	160330.35	N.D.	N.A.
PFM002577				•				6697697.72	162195.48	N.D.	N.A.
PFM002578				•				6696667.56	162280.21	N.D.	N.A.
PFM002581				•				6697407.61	159823.02	N.D.	N.A.
PFM002582				•				6697169.71	159366.95	N.D.	N.A.
PFM002586				•				6694798.46	159981.22	N.D.	N.A.
PFM002587				•				6695066.80	159402.96	N.D.	N.A.
PFM002588				•				6696406.88	162898.74	N.D.	N.A.
PFM002589				•				6696042.95	163493.82	N.D.	N.A.
PFM002590				•				6695885.65	163801.69	N.D.	N.A.
PFM002591				•				6695870.36	163810.18	N.D.	N.A.
PFM002592				•				6695241.71	163703.22	N.D.	N.A.
PFM002594				•				6694618.10	162874.19	N.D.	N.A.
PFM002670				•				6695758.94	163641.41	N.D.	N.A.
PFM002687				•				6696916.23	162142.45	N.D.	N.A.
PFM002760				•				6696044.64	163412.85	N.D.	N.A.
PFM002761				•				6696178.48	162608.04	N.D.	N.A.
PFM002762				•				6696281.29	162374.38	N.D.	N.A.
PFM002767				•				6695082.25	163986.00	N.D.	N.A.
PFM002768				•				6695244.87	163578.28	N.D.	N.A.
PFM002783				•				6696230.48	160746.15	N.D.	N.A.
PFM002801				•				6697581.66	160333.99	N.D.	N.A.
PFM002802				•				6697335.05	160499.84	N.D.	N.A.
PFM002890				•				6695972.08	163669.52	N.D.	N.A.
PFM002891				•				6695953.14	164028.01	N.D.	N.A.
PFM003742				•				6666220.72	125433.91	N.D.	N.A.
PFM004193				•				6695410.58	161786.20	N.D.	N.A.

I	Slug test	HY670
II	In situ (BAT) permeameter test	HY675
III	Interference test	HY610, HY640, HY645
IV	PSD	HY673, GE514
V	Lab. permeameter test	HY672
VI	CRS test	GE017
VII	pF (unsat. zone)	HY672

Well/ sampling point	**I**	**II**	**III**	**IV**	**V**	**VI**	**VII**	**Northing (SWEREF 99 18 00)**	**Easting (SWEREF 99 18 00)**	**Elevation ToC (m, RH 2000)[1]**	**Depth (m b ToC)**
PFM004204				•				6695481.71	162113.68	N.D.	N.A.
PFM004205				•				6696617.83	164494.29	N.D.	N.A.
PFM004216				•				6696808.87	164194.55	N.D.	N.A.
PFM004222				•				6697518.82	161800.39	N.D.	N.A.
PFM004294				•				6694962.00	161018.01	N.D.	N.A.
PFM004396				•				6705834.91	167373.70	N.D.	N.A.
PFM004454				•				6697724.05	162239.85	3.38	N.A.
PFM004455				•	•		•	6697723.72	162236.70	3.44	N.A.
PFM004456				•				6697723.67	162235.83	3.33	N.A.
PFM004458				•	•		•	6697728.65	162135.20	1.71	N.A.
PFM004459				•	•		•	6697742.48	162127.06	2.04	N.A.
PFM004460				•	•		•	6697753.55	162120.01	2.25	N.A.
PFM004514				•				6694551.15	162571.86	N.D.	N.A.
PFM004531				•				6695901.34	162909.91	N.D.	N.A.
PFM004752				•				6695500.58	158993.25	N.D.	N.A.
PFM004760				•				6699419.31	158801.66	N.D.	N.A.
PFM004761				•				6696867.89	160650.34	N.D.	N.A.
PFM004762				•				6697205.84	159964.35	N.D.	N.A.
PFM006073				•				6694816.60	164393.29	0.18	N.A.
PFM006094				•				6694357.72	164144.94	0.18	N.A.
PFM006095				•				6694164.09	163711.35	0.18	N.A.
PFM006097				•				6698018.28	162422.23	0.18	N.A.
PFM007784				•				6698769.43	160023.75	3.03	N.A.
PFM007785				•				6698842.08	160102.71	1.95	N.A.
PFM007787				•				6698707.97	160092.55	3.51	N.A.
PFM007788				•				6698728.61	160124.27	3.50	N.A.
PFM007789				•				6698750.94	160007.33	3.17	N.A.
PFM007790				•				6698715.54	160281.59	2.35	N.A.
PFM007791				•				6698590.04	160049.03	2.79	N.A.
PFM007792				•				6698547.33	160083.90	4.34	N.A.
PFM007855				•	•			6695064.71	162980.01	0.86	N.A.
PFM007856				•	•			6695059.95	162984.33	0.82	N.A.
PFM007857				•	•			6695069.09	162985.71	1.14	N.A.
PFM007858				•	•			6695086.27	162985.97	1.30	N.A.
PFM007860						•		6694875.87	163030.86	0.76	N.A.
PFM007861						•		6694888.70	163030.55	0.78	N.A.
PFM007862						•		6694896.09	163029.22	0.69	N.A.
PFM007863						•		6694888.60	163041.62	0.76	N.A.
PFM007864						•		6694887.40	163004.41	0.77	N.A.
PFM007866						•		6694537.31	162639.46	2.95	N.A.
PFM007867						•		6694548.21	162616.67	2.85	N.A.
PFM007868						•		6694557.50	162598.66	2.59	N.A.
PFM007869						•		6694541.58	162605.78	2.46	N.A.
QFM000099				•				6698562.43	160023.16	2.88	11.00
QFM000143				•				6698258.69	159862.32	3.03	3.78
QFM000145				•				6698312.66	159917.68	2.60	5.41
QFM000153				•				6698334.10	159780.50	2.35	7.71
QFM000156				•				6698420.77	159901.85	2.85	7.42
QFM000262				•				6698910.94	160118.61	2.03	10.41
QFM000263				•				6698853.51	159987.75	2.48	9.81
QFM000264				•				6698499.20	159898.72	2.73	9.23
QFM000265				•				6698357.40	159697.11	4.13	10.20
QFM000266				•				6698283.65	159742.82	4.61	6.57
QFM000268				•				6698372.31	160071.39	3.11	6.20

4 Compilation of transmissivity data acquired from single-hole hydraulic tests in core-drilled boreholes

This chapter presents a compilation of transmissivity data for core-drilled boreholes at the Forsmark site, updating previous work done by Follin et al. (2007b). Data presented in tables show the upper and lower vertical elevations of each unit or domain and corresponding lengths along borehole, as well as Rock Domain (RFMxxx), Fracture domain (FFMxxx) and Deformation zone (ZFM) in addition to transmissivity data. Hydraulic test data were correlated primarily against so-called Target Intercepts of domains or units from previous extended geological single-hole interpretations, subordinately solely from single-hole interpretations or when the preceding interpretations were not available from the deterministically modelled geometrical intercepts of the various geological units (i.e. KFM14–18 and KFM20–24).

A variety of single-hole hydraulic test methods have been applied in the core-drilled boreholes, such as Posiva Flow Log (PLF), constant-head injection tests with the Pipe String System (PSS), and HTHB tests (combined pumping and impeller flow logging). However, data from all test methods are not presented for each borehole in this report. For a full list of all test results see APPENDIX D with supplementary material in digital appendices. The reason for this hierarchical structure is that the different test methods are associated with different lower flow detection limits and outreach, meaning a difference in accuracy. The PFL has a lower limit of c. 30 ml/h and the pumping lasts for approximately a week. During a PSS test, water is injected during 20 minutes and the flow detection limit is c. 60 ml/h. The PFL method therefore has a higher accuracy than the PSS method, and is able to distinguish between dead end fractures/clusters whereas PSS is not. For more information on the different test methods, see Follin et.al. (2007b).

PFL data (PFL-f) from overlapping PFL measurements are shown when available. These data comprise the number of flow anomalies over a section and the summed transmissivity of those anomalies. Other hydraulic data from single-hole hydraulic testing are presented in a hierarchical form and categorized according to their Sicada denominator, with the following prioritization of data from highest to lowest priority:

i. 5 m Sequential PFL data (TD);
ii. 5 m transient evaluation of injection test transmissivity approximations based on a 2D radial flow model (5m TT);
iii. 5 m injection test transmissivity approximations based on Moye's formula (5m TM);
iv. 20 m injection test transmissivity approximations based on a 2D radial flow model (20m TT);
v. 20 m injection test transmissivity approximations based on Moye's formula (20m TM).

Table 4-1 and Table 4-2 present a colour legend, which is used in the tables of Chapter 4 and Chapter 5 where the geological interpretations of the hydraulic measurements in the tested boreholes are presented with regard to fracture domains and orientations of deformation zones.

Table 4-1. Fracture domain colour legend, used in Chapter 4 and Chapter 5.

FFM colour legend	Meaning
	Fracture domain FFM01
	Fracture domain FFM02
	Fracture domain FFM03
	Fracture domain FFM04
	Fracture domain FFM05
	Fracture domain FFM06
	Deformation Zone (DZ)
	Possible Deformation Zone (PDZ)

Table 4-2. Deformation-zone orientation colour legend, used in Chapter 4 and Chapter 5.

Orientation color legend	Meaning
WNW	West North West
NW	North West
NNW	North North West
NNE	North North East
NE	North East
ENE	East North East
EW	East West
	Gently dipping

4.1 Drill Site 1

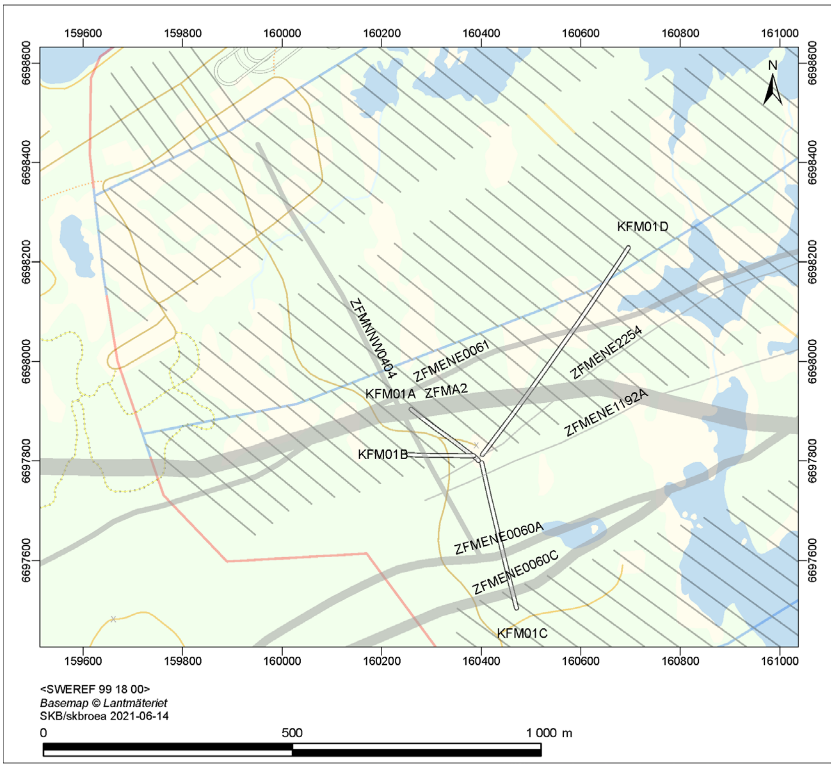

Figure 4-1. *Map of Drill Site 1 including horizontal projections of core-drilled boreholes with hydraulic test data presented in Table 4-3. A potential SFK layout (SYHA 2.0) and ground-surface intersections of deterministically modelled deformation zones (grey), which intersect with the boreholes at Drill Site 1, are shown for reference.*

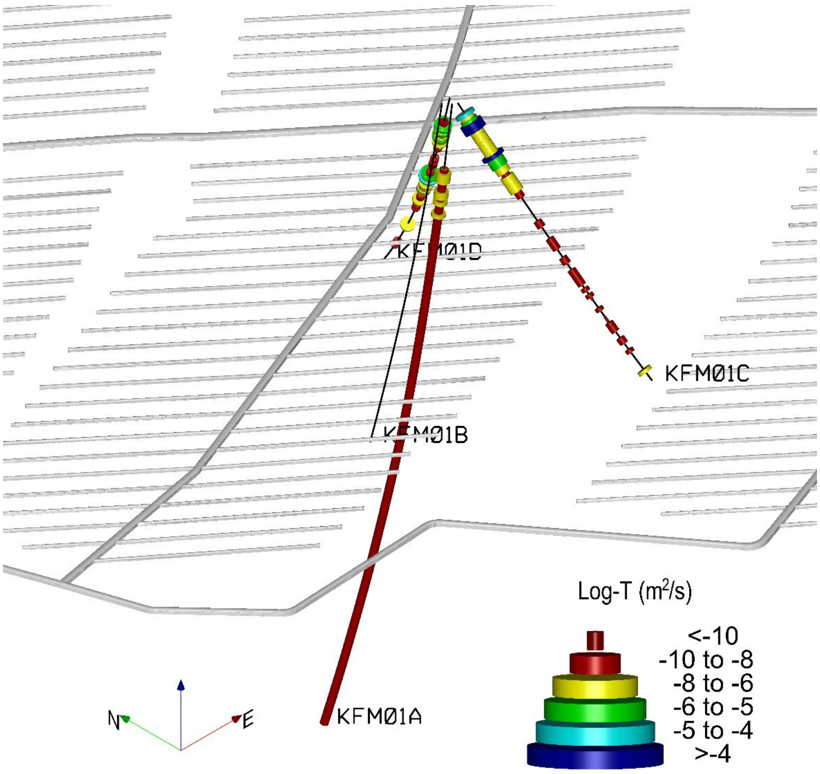

Figure 4-2. *Isometric view of core-drilled boreholes at Drill Site 1 with hydraulic test data presented in Table 4-3. A potential layout for SFK (SYHA 2.0) is shown for reference.*

Table 4-3. Compilation of transmissivity data per interpreted large-scale geological domain in core-drilled boreholes at drill site 1 (DS1, see Figure 4-1). In the table, for each borehole, the first row highlighted in grey represents the entire length of the borehole from the top of the casing to the bottom of the borehole. Dashed red line indicates casing depth (See Table E-1 in Appendix E for a more accurate and comprehensive list of casings for all boreholes.). Zup is the upper elevation of the section, Zlow is the lower elevation of the section. Secup and Seclow refer to the depth to top and bottom of the section along the borehole. ΣT PFL_f is the total transmissivity of all discrete PFL transmissivities (PFL_f) recorded between Zup and Zlow and ΣT is the total transmissivity of 5-m long sequential test section transmissivities between Zup and Zlow. n1 and n2 represent the number of discrete PFL-f anomalies and the number of 5-m long sequential test sections between Zup and Zlow, respectively. A difference between ΣT PFL_f and ΣT over a particular interval Zup and Zlow can occur; however, these differences are generally minute.

Zup (m)	Zlow (m)	Secup (m)	Seclow (m)	Rock Domain (RFMxxx)	Fracture domain (FFMxxx)	Deformation zone (ZFM / PDZ)	ΣT PFL_f (m^2/s)	n1	ΣT (m^2/s)	n2	Data type
KFM01A											
3.31	**-982**	**0**	**1,001**								
-6	-26	9	29	RFM029	FFM02U		-	-	-	-	-
-26	-47	29	51	RFM029		ZFMA2	-	-	-	-	-
-47	-97	51	102	RFM029	FFM02L		-	-	-	-	-
-97	-199	102	203	RFM029	FFM02L		1.9E-07	23	2.3E-07	20	TD
-199	-211	203	216	RFM029	FFM01				1.5E-09	2	TD
-211	-219	216	224	RFM029		PDZ4			1.5E-09	2	TD
-219	-262	224	267	RFM029	FFM01		7.1E-10	2	5.6E-09	8	TD
-262	-280	267	285	RFM029		ZFMENE1192 A	7.8E-10	2	2.4E-09	4	TD
-280	-380	285	386	RFM029	FFM01		4.8E-09	7	1.7E-08	20	TD
-380	-406	386	412	RFM029		ZFMENE1192 A			3.6E-09	5	TD
-406	-629	412	639	RFM029	FFM01				3.3E-08	46	TD
-629	-673	639	684	RFM029		ZFMENE2254			6.5E-09	9	TD
-673	-982	684	1,001	RFM029	FFM01				4.5E-08	63	TD
KFM01C											
3.09	**-333**	**0**	**450**								
1	-5	3	12	RFM029	FFM02U		-	-	-	-	-
-5	-14	12	23	RFM029	FFM01		-	-	-	-	-
-14	-33	23	48	RFM029		ZFMENE1192 A, ZFMA2			9.4E-04	5	5m TT
-33	-44	48	62	RFM029	FFM01				2.4E-07	3	5m TT
-44	-72	62	99	RFM029		ZFMA2			2.4E-04	7	5m TT
-72	-89	99	121	RFM029	FFM01				7.3E-08	3	5m TT
-89	-91	121	124	RFM029		PDZ4 (S-ENE)			4.5E-08	1	5m TT
-91	-175	124	235	RFM029	FFM01				6.1E-08	9	5m TT
-175	-187	235	252	RFM029		ZFMENE0060 A					
-187	-227	252	305	RFM029	FFM01				2.1E-09	6	5m TT
-227	-245	305	330	RFM029		ZFMENE0060 C			1.0E-09	2	5m TT
-245	-333	330	450	RFM029	FFM01				1.4E-08	9	5m TT
KFM01D											
3.13	**-612**	**0**	**800**								
-3	-52	7	68	RFM029	FFM02U		-	-	-	-	-
-52	-52	68	68	RFM029		ZFMA2	-	-	-	-	-
-52	-70	68	90	RFM029	FFM02U		-	-	-	-	-
-70	-71	90	92	RFM029	FFM02U		-	-	-	-	-
-71	-141	92	176	RFM029	FFM02L		5.3E-06	23	5.3E-06	8	TD
-141	-147	176	184	RFM029		PDZ1 (S-NNW)			3.5E-09	2	5m TT
-147	-153	184	191	RFM029	FFM02				4.4E-10	1	5m TT
-153	-326	191	411	RFM029	FFM01		4.2E-07	9	5.6E-07	9	TD
-326	-333	411	421	RFM029		PDZ2 (S-NNW)			7.5E-07	1	20m TT
-333	-384	421	488	RFM029	FFM01		6.2E-08	1	1.3E-07	1	TD
-384	-390	488	496	RFM029		PDZ3 (S-NNW)					
-390	-519	496	670	RFM029	FFM01		1.6E-08	1	1.7E-08	1	TD
-519	-541	670	700	RFM029		ZFMENE0061			6.1E-10	1	5m TT
-541	-592	700	771	RFM029	FFM01						
-592	-594	771	774	RFM029		PDZ5 (S-ENE)					
-594	-612	774	800	RFM029	FFM01						

4.2 Drill site 2

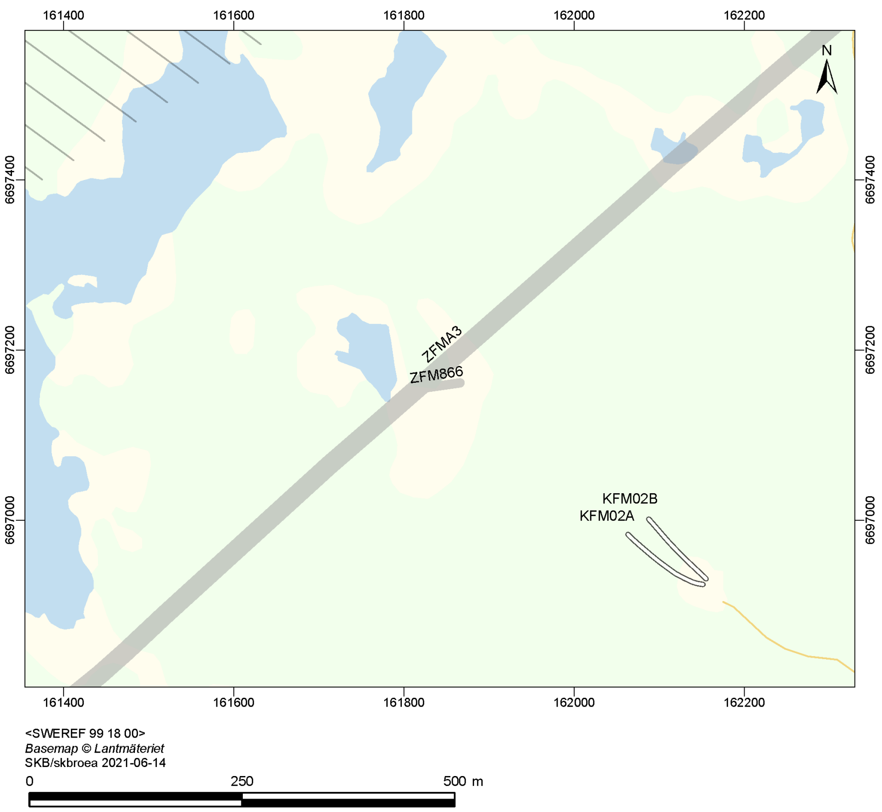

***Figure 4-3.** Map of Drill Site 2 including horizontal projections of core-drilled boreholes with hydraulic test data presented in Table 4-4. A potential SFK layout (SYHA 2.0) to the northeast and ground-surface intersections of selected deterministically modelled deformation zones (grey), which intersect with the boreholes at Drill Site 2, are shown for reference.*

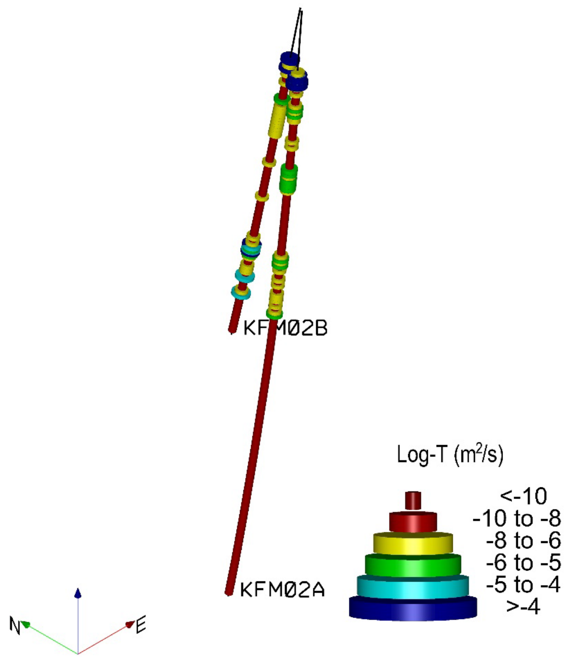

***Figure 4-4.** Isometric view of core-drilled boreholes at Drill Site 2 with hydraulic test data presented in Table 4-4. A potential layout for SFK is visualized for reference.*

Table 4-4. Hydraulic data compilation per interpreted geological domain in core-drilled boreholes at Drill Site 2 (DS2, see Figure 4-3). In the table, for each borehole, the first row highlighted in grey represents the entire length of the borehole from the top of the casing to the bottom of the borehole. Dashed red line indicates casing depth. Zup is the upper elevation of the section, Zlow is the lower elevation of the section. Secup and Seclow refer to the depth to top and bottom of the section along the borehole. ΣT PFL_f is the sum of all overlapping PFL transmissivities (PFL_f) and ΣT is the sum of sequential test section transmissivities between Zup and Zlow, n1 and n2 is number of PFL-f anomalies or flowing sections, respectively.

Zup (m)	Zlow (m)	Secup(m)	Seclow(m)	Rock Domain (RFMxxx)	Fracture domain (FFMxxx)	Deformation zone (ZFM / PDZ)	ΣT PFL_f (m^2/s)	n1	ΣT (m^2/s)	n2	Data type
KFM02A											
7.54	**-987**	**0**	**1001**								
6	-71	2	79	RFM029R			-	-	-	-	-
-71	-83	79	91	RFM029R		PDZ1	-	-	-	-	-
-83	-92	91	100	RFM029R			-	-	-	-	-
-92	-102	100	110	RFM029R	FFM03		3.3E-08	1	4.3E-05	2	TD
-102	-114	110	122	RFM029R		ZFM866	1.1E-04	14	7.1E-05	2	TD
-114	-152	122	160	RFM029R	FFM03		1.7E-07	5	3.2E-06	8	TD
-152	-176	160	184	RFM029R		ZFMA3	3.5E-06	21	3.8E-06	5	TD
-176	-232	184	240	RFM029R	FFM03		7.8E-07	3	9.4E-07	11	TD
-232	-302	240	310	RFM029R		ZFM1189	1.2E-05	31	1.1E-05	14	TD
-302	-408	310	417	RFM029R	FFM03		7.6E-08	3	5.2E-08	21	TD
-408	-433	417	442	RFM029R		ZFMA2	2.8E-06	14	3.1E-06	5	TD
-433	-467	442	476	RFM029R	FFM01		1.9E-07	10	2.0E-07	7	TD
-467	-511	476	520	RFM029R		ZFMF1	4.7E-06	22	5.6E-06	9	TD
-511	-590	520	600	RFM029R		PDZ7 (S-NNW)			2.2E-08	16	TD
-590	-881	600	893	RFM029R	FFM01				9.0E-08	58	TD
-881	-892	893	905	RFM029R		ZFMB4	2.6E-09	1	4.0E-09	3	TD
-892	-909	905	922	RFM029R	FFM01				4.3E-09	3	TD
-909	-912	922	925	RFM029R		PDZ9 (M-ENE)			2.4E-09	1	TD
-912	-963	925	976	RFM029R	FFM01				2.4E-08	10	TD
-963	-969	976	982	RFM029R		PDZ10 (M-ENE)			1.4E-09	1	TD
-969	-987	982	1001	RFM029R	FFM01				4.3E-09	3	TD
KFM02B											
7.80	**-557**	**0**	**574**								
8	-77	1	87				-	-	-	-	-
-77	-89	87	98				9.1E-06	2	1.8E-05	2	TD
-89	-106	98	115			ZFM866	1.2E-05	4	1.6E-05	4	TD
-106	-135	115	145				1.4E-08	1	7.3E-08	6	TD
-135	-193	145	204			ZFMA3	7.8E-06	4	7.6E-06	12	TD
-193	-311	204	323				9.2E-08	2	2.5E-07	23	TD
-311	-398	323	411				5.9E-07	4	9.0E-07	18	TD
-398	-417	411	431			ZFMA2	3.9E-05	14	4.5E-05	4	TD
-417	-433	431	447				2.4E-08	1	5.5E-08	3	TD
-433	-437	447	451			PDZ4			1.6E-08	1	TD
-437	-448	451	462						3.4E-08	2	TD
-448	-497	462	512			ZFMF1	6.2E-05	9	7.9E-05	10	TD
-497	-557	512	573						5.7E-08	11	TD

4.3 Drill Site 3

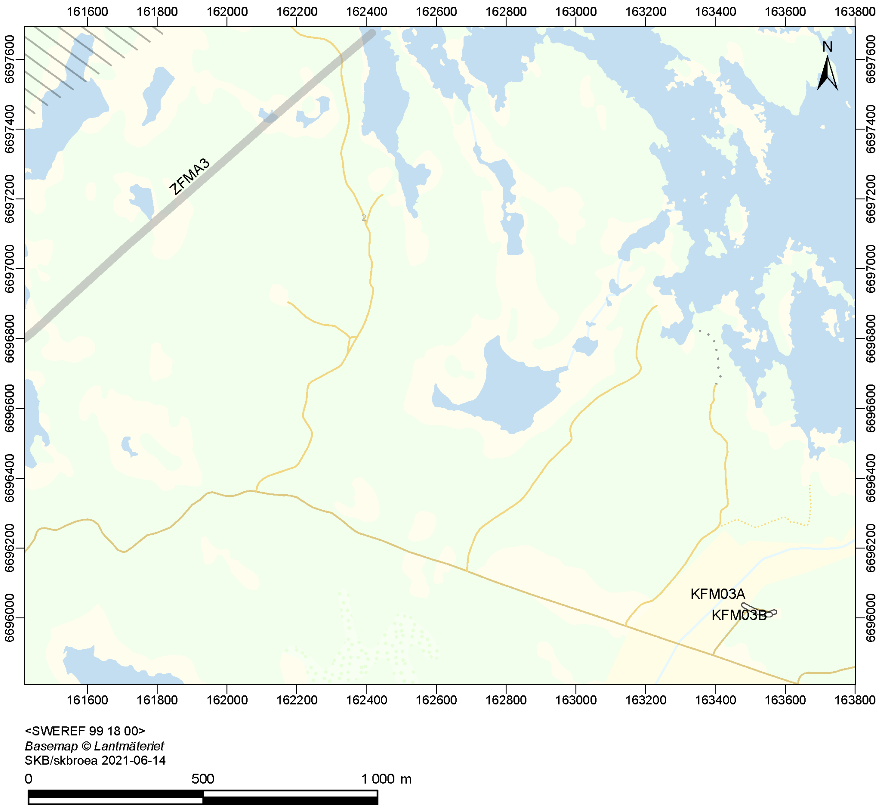

Figure 4-5. Map of Drill Site 3 including horizontal projections of core-drilled boreholes with hydraulic test data presented in Table 4-5. A potential SFK layout (SYHA 2.0) to the northeast and ground-surface intersections of selected deterministically modelled deformation zones (grey), which intersect with the boreholes at Drill Site 3, are shown for reference.

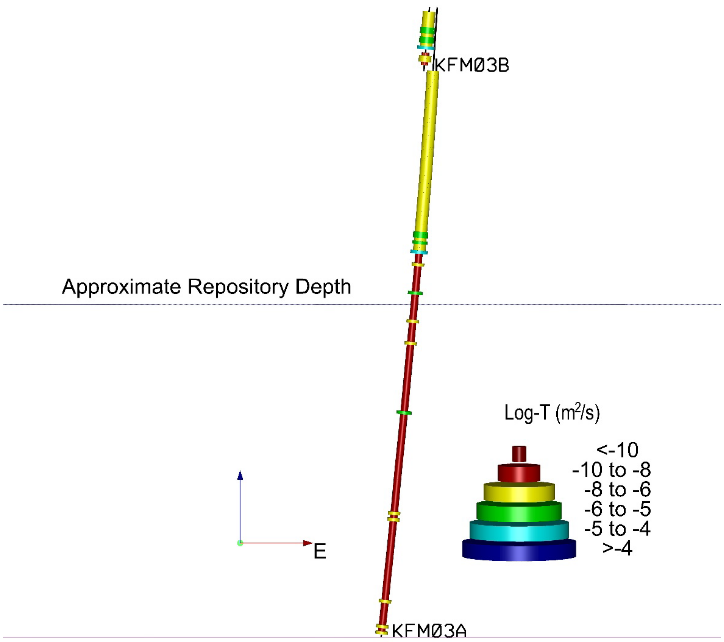

Figure 4-6. Profile view facing west of the core-drilled boreholes at Drill Site 3 with hydraulic test data presented in Table 4-5. Approximate depth of SFK is shown for reference.

Table 4-5. Hydraulic data compilation per interpreted geological domain in core-drilled boreholes at drill site 3 (DS3, see Figure 4-5). In the table, for each borehole, the first row highlighted in grey represents the entire length of the borehole from the top of the casing to the bottom of the borehole. Dashed red line indicates casing depth. Zup is the upper elevation of the section, Zlow is the lower elevation of the section. Secup and Seclow refer to the depth to top and bottom of the section along the borehole. ΣT PFL_f is the sum of all overlapping PFL transmissivities (PFL_f) and ΣT is the sum of sequential test section transmissivities between Zup and Zlow, n1 and n2 is number of PFL-f anomalies or flowing sections, respectively.

Zup (m)	Zlow (m)	Secup(m)	Seclow(m)	Rock Domain (RFMxxx)	Fracture domain (FFMxxx)	Deformation zone (ZFM / PDZ)	ΣT PFL_f (m^2/s)	n1	ΣT (m^2/s)	n2	Data type
KFM03A											
8.44	**-988**	**0**	**1001**								
7	-51	1	60	RFM029	FFM03		-	-	-	-	-
-51	-53	60	62	RFM029		ZFMA5	-	-	-	-	-
-53	-93	62	102	RFM029	FFM03		-	-	-	-	-
-93	-211	102	220	RFM029	FFM03		5.1E-07	13	1.0E-06	24	TD
-211	-284	220	293	RFM017	FFM03				6.1E-07	15	TD
-284	-347	293	356	RFM029	FFM03		4.6E-09	2	4.8E-07	12	TD
-347	-389	356	399	RFM029		ZFMA4	1.1E-04	35	6.3E-05	9	TD
-389	-438	399	448	RFM029	FFM03		2.0E-08	2	2.8E-08	9	TD
-438	-445	448	455	RFM029		ZFMA7	6.7E-06	3	6.7E-06	2	TD
-445	-627	455	638	RFM029	FFM03		6.1E-08	5	9.8E-08	36	TD
-627	-635	638	646	RFM029		ZFMB1	2.5E-06	2	2.6E-06	2	TD
-635	-791	646	803	RFM029	FFM03				1.7E-07	31	TD
-791	-804	803	816	RFM029		ZFMA3	2.9E-08	2	4.4E-08	3	TD
-804	-929	816	942	RFM029	FFM03				1.4E-07	25	TD
-929	-936	942	949	RFM029		PDZ5 (G)	3.5E-07	2	3.8E-07	2	TD
-936	-987	949	1000	RFM029	FFM03		3.1E-07	5	3.9E-07	9	TD
KFM03B											
8.65	**-92**	**0**	**102**								
8.65	4	0	5	RFM029	FFM03						
4	-15	5	24	RFM029	FFM03				5.8E-07	3	5m TT
-15	-33	24	42	RFM029		ZFMA5			1.5E-05	4	5m TT
-33	-53	42	62	RFM029	FFM03				7.4E-06	4	5m TT
-53	-58	62	67	RFM029		PDZ2 (G)			2.1E-05	1	5m TT
-58	-88	67	97	RFM029	FFM03				1.8E-07	4	5m TT

4.4 Drill Site 4

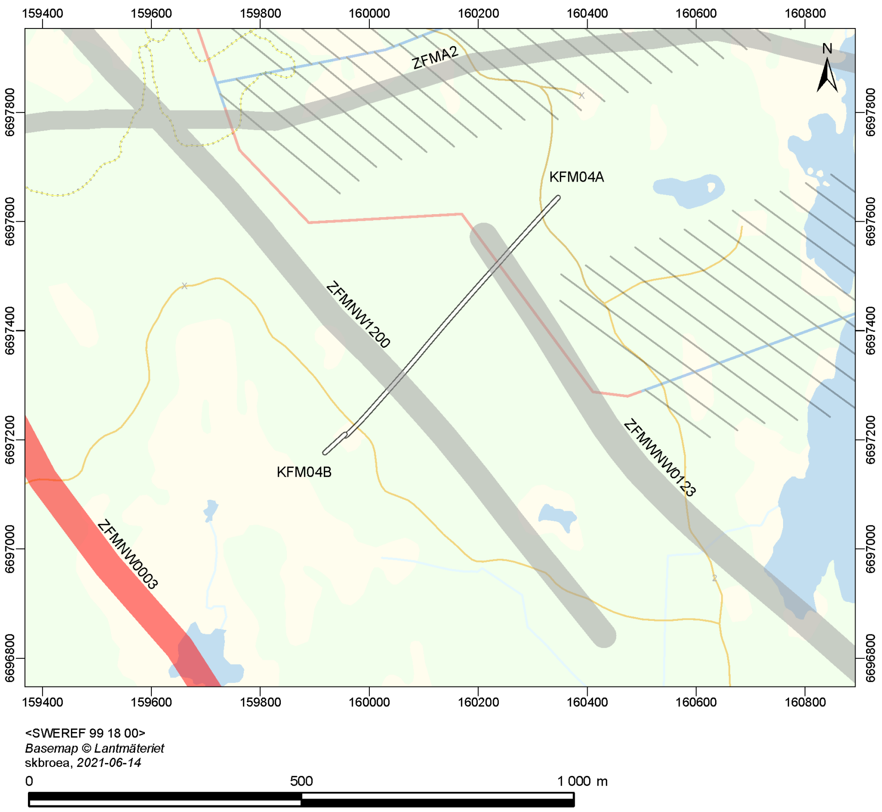

Figure 4-7. *Map of Drill Site 4 including horizontal projections of core-drilled borehole KFM04A with hydraulic test data presented in Table 4-6. A potential SFK layout (SYHA 2.0) to the northeast and ground surface intersection of selected deterministically modelled deformation zones (grey) which intersect with the boreholes at Drill Site 4 shown for reference.*

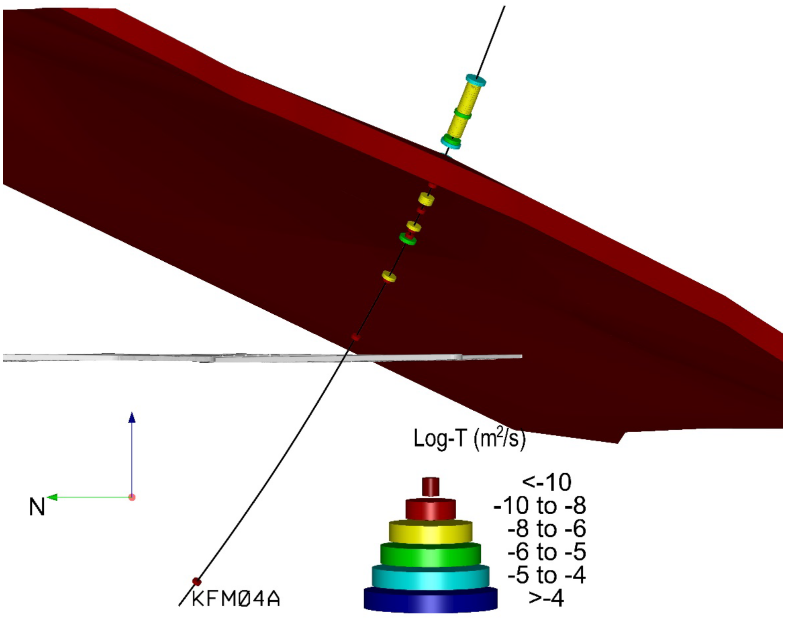

Figure 4-8. *Profile view facing west of core-drilled borehole KFM04A with hydraulic test data presented in Table 4-6. SFK SYHA 2.0 is visualized for reference in addition to the gently dipping, deterministically modelled deformation zone ZFMA2.*

Table 4-6. Hydraulic data compilation per interpreted geological domain in core-drilled boreholes at drill site 4 (DS4, see Figure 4-7). In the table, for each borehole, the first row highlighted in grey represents the entire length of the borehole from the top of the casing to the bottom of the borehole. Dashed red line indicates casing depth. Zup is the upper elevation of the section, Zlow is the lower elevation of the section. Secup and Seclow refer to the depth to top and bottom of the section along the borehole. ΣT PFL_f is the sum of all overlapping PFL transmissivities (PFL_f) and ΣT is the sum of sequential test section transmissivities between Zup and Zlow, n1 and n2 is number of PFL-f anomalies or flowing sections, respectively.

Zup (m)	Zlow (m)	Secup(m)	Seclow(m)	Rock Domain (RFMxxx)	Fracture domain (FFMxxx)	Deformation zone (ZFM / PDZ)	ΣT PFL_f (m^2/s)	n1	ΣT (m^2/s)	n2	Data type
KFM04A											
9	**-796**	**0**	**1001**								
9	-84	1	107	RFM018	FFM04		-	-	-	-	-
-84	-88	107	110	RFM018	FFM04		1.4E-07	1			
-88	-146	110	176	RFM018		ZFMNW1200	6.6E-05	35	6.6E-05	13	TD
-146	-147	176	177	RFM018	FFM04						
-147	-169	177	202	RFM012	FFM04		1.0E-06	12	1.1E-06	4	TD
-169	-204	202	242	RFM012		ZFMA2	8.8E-05	7	1.0E-04	3	TD
-204	-245	242	290	RFM012	FFM04		2.2E-08	2	2.6E-08	2	TD
-245	-313	290	370	RFM012		ZFMNE1188	1.5E-06	10	1.6E-06	7	TD
-313	-348	370	412	RFM012	FFM04				2.6E-10	2	5m TT
-348	-389	412	462	RFM012		ZFMNE1188	1.4E-08	2	1.9E-08	2	TD
-389	-420	462	500	RFM012	FFM04						
-420	-542	500	654	RFM029R	FFM04		1.4E-09	1	1.5E-09	1	TD
-542	-547	654	661	RFM029R		ZFMWNW0123					
-547	-762	661	953	RFM029R	FFM01						
-762	-764	953	956	RFM029R		PDZ7 (S-NS)	1.3E-09	1			
-764	-796	956	1001	RFM029R	FFM01				1.3E-09	1	TD

4.5 Drill Site 5

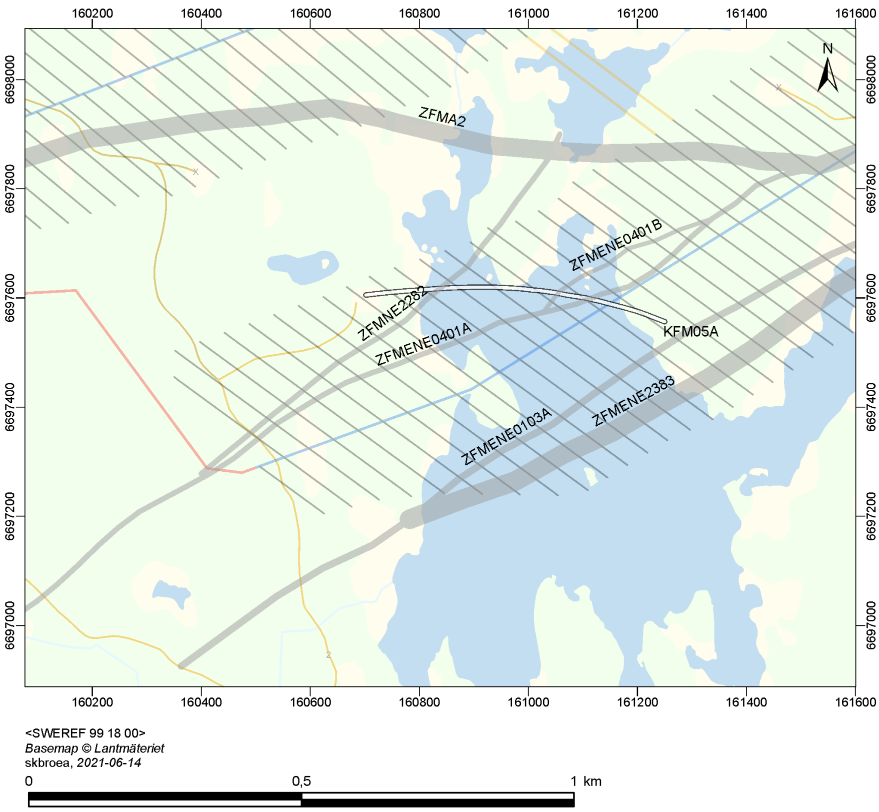

Figure 4-9. *Map of Drill Site 5 including horizontal projection of core-drilled borehole KFM05A with hydraulic test data presented in Table 4-7. A potential SFK layout SYHA 2.0 layout to the northeast and ground surface intersection of selected deterministically modelled deformation zones (grey) which intersect with the boreholes at Drill Site 5 shown for reference.*

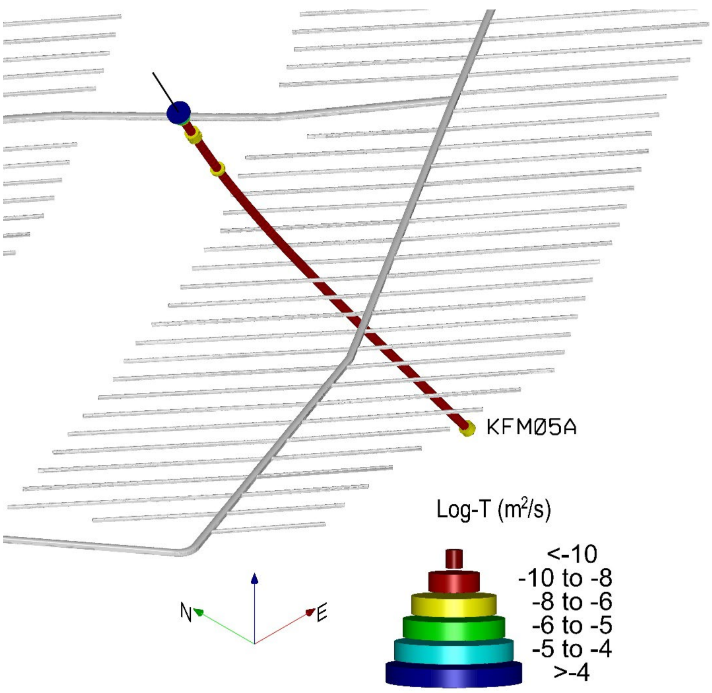

Figure 4-10. *Isometric view of core-drilled KFM05A with hydraulic test data presented in Table 4-7. A potential SFK layout SYHA 2.0 is visualized for reference.*

Table 4-7. Hydraulic data compilation per interpreted geological domain in core-drilled boreholes at drill site 5 (DS5, see Figure 4-9). In the table, for each borehole, the first row highlighted in grey represents the entire length of the borehole from the top of the casing to the bottom of the borehole. Dashed red line indicates casing depth. Zup is the upper elevation of the section, Zlow is the lower elevation of the section. Secup and Seclow refer to the depth to top and bottom of the section along the borehole. ΣT PFL_f is the sum of all overlapping PFL transmissivities (PFL_f) and ΣT is the sum of sequential test section transmissivities between Zup and Zlow, n1 and n2 is number of PFL-f anomalies or flowing sections, respectively.

Zup (m)	Zlow (m)	Secup(m)	Seclow(m)	Rock Domain (RFMxxx)	Fracture domain (FFMxxx)	Deformation zone (ZFM / PDZ)	ΣT PFL_f (m^2/s)	n1	ΣT (m^2/s)	n2	Data type
KFM05A											
5.71	**-825**	**0**	**1000**								
-1	-81	8	100	RFM029R	FFM02U		-	-	-	-	-
-81	-83	100	102	RFM029R	FFM02U		-	-	-	-	-
-83	-93	102	114	RFM029R		ZFMA2	1.2E-03	6	4.1E-04	2	TD
-93	-199	114	237	RFM029R	FFM02U		1.8E-06	18	1.9E-06	24	TD
-199	-332	237	395	RFM029R	FFM01		1.9E-08	1	5.9E-08	32	TD
-332	-366	395	436	RFM029R		ZFMNE2282			1.0E-08	8	TD
-366	-492	436	590	RFM029R	FFM01				4.1E-08	31	TD
-492	-514	590	616	RFM029R		ZFMENE0401B			6.6E-09	5	TD
-514	-570	616	685	RFM029R	FFM01				1.9E-08	14	TD
-570	-598	685	720	RFM029R		ZFMENE0401A	1.6E-09	1	1.7E-08	7	TD
-598	-738	720	892	RFM029R	FFM01		8.6E-09	1	4.6E-08	34	TD
-738	-757	892	916	RFM029R		ZFMENE0103A			6.8E-09	5	TD
-757	-773	916	936	RFM029R	FFM01				5.4E-09	4	TD
-773	-818	936	992	RFM029R		ZFMENE2383			1.1E-07	11	TD
-818	-825	992	1000	RFM029R	FFM01						

4.6 Drill Site 6

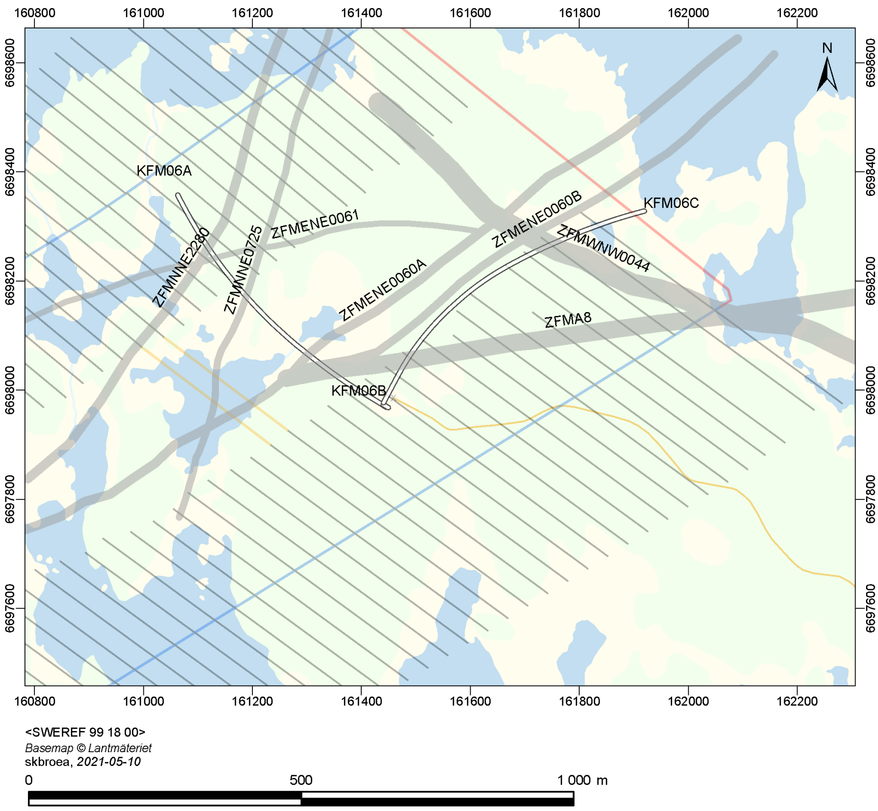

Figure 4-11. *Map of Drill Site 6 including horizontal projections of core-drilled boreholes with hydraulic test data presented in Table 4-8. A potential SFK layout SYHA 2.0 layout to the northeast and ground surface intersection of selected deterministically modelled deformation zones (grey) which intersect with the boreholes at Drill Site 6 shown for reference.*

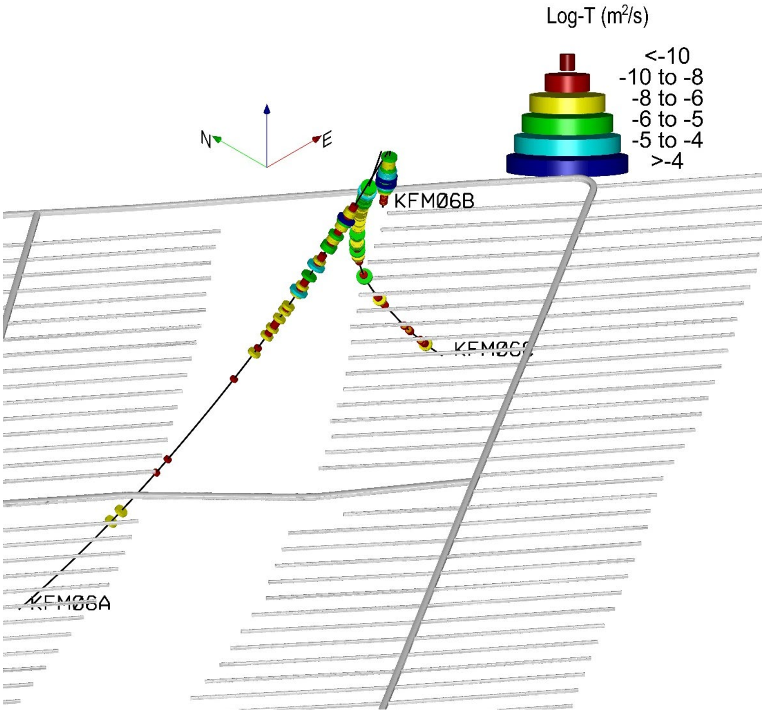

Figure 4-12. *Isometric view of core-drilled boreholes at Drill Site 6 with hydraulic test data presented in Table 4-8. A potential SFK layout SYHA 2.0 is visualized for reference.*

Table 4-8. Hydraulic data compilation per interpreted geological domain in core-drilled boreholes at drill site 6 (DS6, see Figure 4-11). In the table, for each borehole, the first row highlighted in grey represents the entire length of the borehole from the top of the casing to the bottom of the borehole. Dashed red line indicates casing depth. Zup is the upper elevation of the section, Zlow is the lower elevation of the section. Secup and Seclow refer to the depth to top and bottom of the section along the borehole. ΣT PFL_f is the sum of all overlapping PFL transmissivities (PFL_f) and ΣT is the sum of sequential test section transmissivities between Zup and Zlow, n1 and n2 is number of PFL-f anomalies or flowing sections, respectively.

Zup (m)	Zlow (m)	Secup(m)	Seclow(m)	Rock Domain (RFMxxx)	Fracture domain (FFMxxx)	Deformation zone (ZFM / PDZ)	ΣT PFL_f (m^2/s)	n1	ΣT (m^2/s)	n2	Data type
KFM06A											
4.28	**-825**	**0**	**998**								
3	-7	1	13	RFM029	FFM02U		-	-	-	-	-
-7	-40	13	51	RFM029	FFM02L		-	-	-	-	-
-40	-40	51	51	RFM029		ZFMA8	-	-	-	-	-
-40	-83	51	100	RFM029	FFM02L		-	-	-	-	-
-83	-107	100	128	RFM029	FFM02L		8.1E-06	12	6.1E-05	17	TD
-107	-122	128	146	RFM029		PDZ1 (G)	3.9E-05	17			
-122	-165	146	195	RFM029	FFM01		1.4E-05	19			
-165	-236	195	278	RFM029		ZFMENE0060B	4.5E-05	26	2.0E-05	6	TD
-236	-270	278	318	RFM029	FFM01		4.3E-08	4	3.0E-05	9	TD
-270	-304	318	358	RFM029		ZFMENE0060A ,ZFMB7	9.8E-07	13	8.3E-08	6	TD
-304	-438	358	518	RFM029	FFM01		2.7E-08	3	1.0E-06	4	TD
-438	-460	518	545	RFM029		ZFMNNE2273					
-460	-521	545	619	RFM029	FFM01				1.1E-09	1	20m TT
-521	-525	619	624	RFM029		ZFMNNE2255	4.3E-10	1	2.5E-10	1	TD
-525	-548	624	652	RFM029	FFM01						
-548	-552	652	656	RFM029		PDZ6 (S-NE)	2.7E-10	1	2.7E-10	1	TD
-552	-620	656	740	RFM029	FFM01						
-620	-649	740	775	RFM029		ZFMNNE0725	3.4E-07	3	3.6E-07	2	TD
-649	-659	775	788	RFM045	FFM06				1.8E-08	1	20m TT
-659	-677	788	810	RFM045		ZFMENE0061			6.5E-10	1	20m TT
-677	-788	810	950	RFM045	FFM06						
-734	-752	882	905	RFM045		PDZ9 (S-ENE)					
-752	-768	905	925	RFM045	FFM06						
-768	-774	925	933	RFM045		PDZ10 (S-NE)					
-774	-788	933	950	RFM045	FFM06						
-788	-819	950	990	RFM045		ZFMNNE2280					
-819	-825	990	998	RFM045	FFM06						

Table 4-8. Cont'd.

Zup (m)	Zlow (m)	Secup(m)	Seclow(m)	Rock Domain (RFMxxx)	Fracture domain (FFMxxx)	Deformation Zone (ZFM)	ΣT PFL_f (m^2/s)	n	ΣT (m^2/s)	n	Data type
KFM06B											
4	**-93**	**0**	**98**								
2	0	2	4	RFM029R	FFM02U		-	-	-	-	-
0	-18	4	22	RFM029R	FFM02U				2.8E-06	4	5m TT
-18	-50	22	55	RFM029R	FFM02L				6.1E-04	7	5m TT
-50	-88	55	93	RFM029R		ZFMA8			2.2E-05	6	5m TT
-88	-93	93	98	RFM029R	FFM02L						
KFM06C											
4.27	**-781**	**0**	**1000**								
3		1		RFM029	FFM02U		-	-	-	-	-
	-45		57	RFM029	FFM02L		-	-	-	-	-
-45	-45	57	57	RFM029		ZFMA8	-	-	-	-	-
-45	-82	57	100	RFM029	FFM02L		-	-	-	-	-
-82	-84	100	102	RFM029	FFM02L		-	-	-	-	-
-84	-140	102	169	RFM029		PDZ1 (G)			9.3E-05	7	5m TT
-140	-235	169	283	RFM029	FFM01				1.4E-05	14	5m TT
-235	-253	283	306	RFM029		ZFMNNE2008			1.4E-07	1	5m TT
-253	-296	306	359	RFM029	FFM01				3.8E-08	1	5m TT
-296	-329	359	400	RFM029		ZFMB7			8.9E-06	4	5m TT
-329	-338	400	411	RFM045	FFM01				6.9E-10	1	5m TT
-338	-341	411	415	RFM045	FFM06				1.5E-09	1	5m TT
-341	-399	415	489	RFM045		ZFMNNE2263			6.8E-08	4	5m TT
-399	-409	489	502	RFM045	FFM06						
-409	-450	502	555	RFM045		ZFMWNW0044			1.1E-06	2	5m TT
-450	-502	555	623	RFM045	FFM06				1.6E-10	1	20m TT
-502	-542	623	677	RFM045		PDZ5 (S-NE)			5.4E-08	5	5m TT
-542	-707	677	898	RFM045	FFM06				7.5E-09	4	5m TT
-707	-781	898	1000	RFM032	FFM05				1.8E-08	5	5m TT

4.7 Drill Site 7

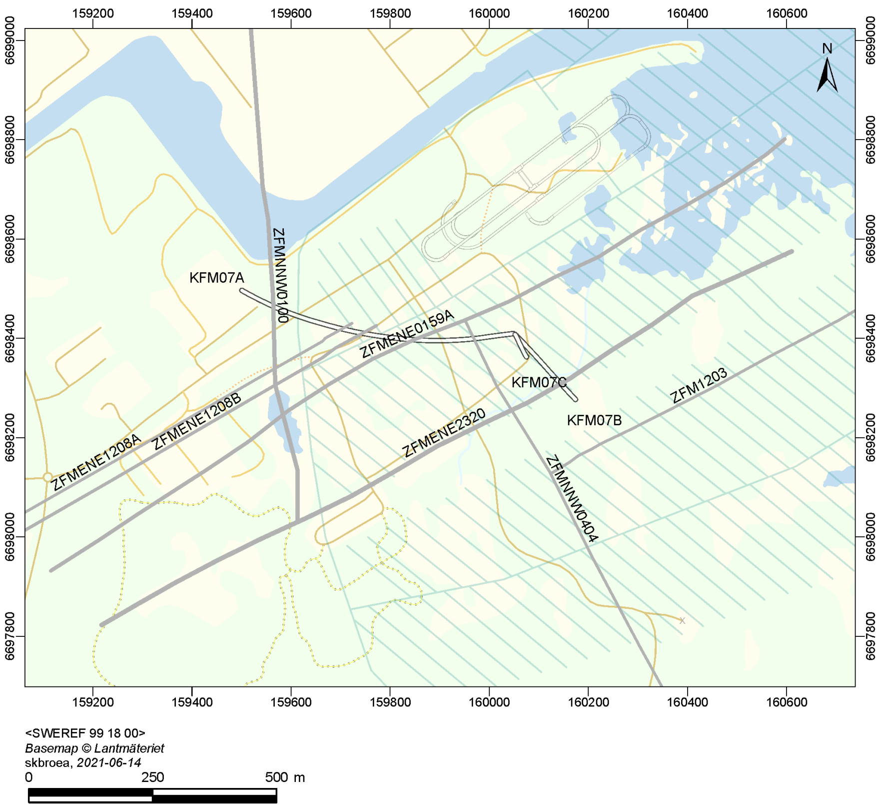

Figure 4-13. Map of Drill Site 7 including horizontal projections of core-drilled boreholes with hydraulic test data presented in Table 4-9. A potential SFK layout SYHA 2.0 layout and ground surface intersection of selected deterministically modelled deformation zones (grey) which intersect with the boreholes at Drill Site 7 shown for reference.

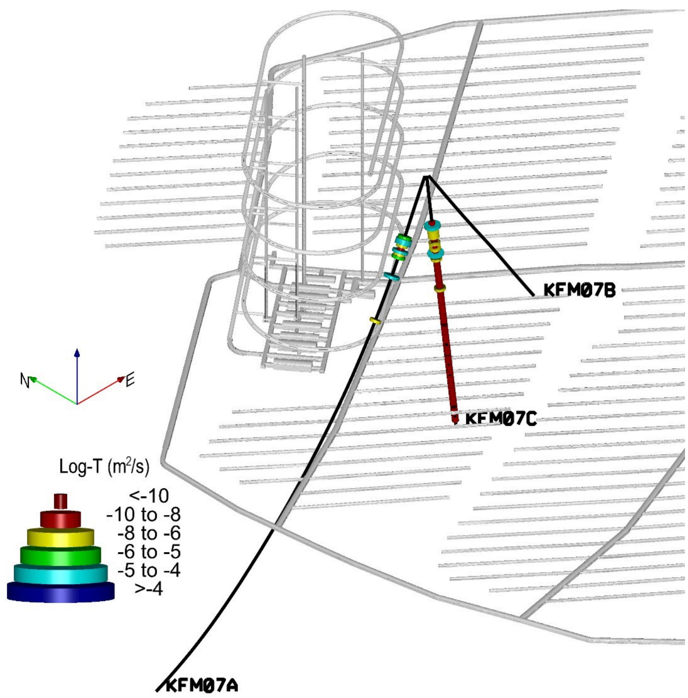

Figure 4-14. Isometric view of core-drilled boreholes at Drill Site 7 with hydraulic test data presented in Table 4-9. A potential SFK layout SYHA 2.0 is visualized for reference.

Table 4-9. Hydraulic data compilation per interpreted geological domain in core-drilled boreholes at drill site 7 (DS7, see Figure 4-13). In the table, for each borehole, the first row highlighted in grey represents the entire length of the borehole from the top of the casing to the bottom of the borehole. Dashed red line indicates casing depth. Zup is the upper elevation of the section, Zlow is the lower elevation of the section. Secup and Seclow refer to the depth to top and bottom of the section along the borehole. ΣT PFL_f is the sum of all overlapping PFL transmissivities (PFL_f) and ΣT is the sum of sequential test section transmissivities between Zup and Zlow, n1 and n2 is number of PFL-f anomalies or flowing sections, respectively.

Zup (m)	Zlow (m)	Secup(m)	Seclow(m)	Rock Domain (RFMxxx)	Fracture domain (FFMxxx)	Deformation zone (ZFM / PDZ)	ΣT PFL_f (m^2/s)	n1	ΣT (m^2/s)	n2	Data type
KFM07A											
3.51	**-819**	**0**	**999**								
1		3		RFM029R	FFM02U		-	-	-	-	-
	-83		100	RFM029R	FFM02L		-	-	-	-	-
-83	-90	100	108	RFM029R	FFM02L				7.1E-09	1	5m TT
-90	-156	108	185	RFM029R		ZFM1203, ZFMNNW0404	1.4E-04	22	1.1E-04	9	TD
-156	-166	185	196	RFM029R	FFM01				6.1E-09	2	5m TT
-166	-173	196	205	RFM029R		PDZ2 (S-ENE)			3.5E-09	1	5m TT
-173	-353	205	417	RFM029R	FFM01		9.3E-08	1	1.3E-07	1	TD
-353	-357	417	422	RFM029R		ZFMENE0159A					
-357	-661	422	793	RFM029R	FFM01						
-661	-668	793	803	RFM044	FFM05						
-668	-698	803	840	RFM044		ZFMENE1208B					
-698	-711	840	857	RFM044	FFM05						
-711	-742	857	897	RFM044		ZFMENE1208A					
-742	-760	897	920	RFM044	FFM05						
-760	-819	920	999	RFM044		ZFMNNW0100					
KFM07B											
3.55	**-237**	**0**	**299**								
1	-23	3	33	RFM029R	FFM02U		-	-	-	-	-
-23	-38	33	51	RFM029R	FFM02L		-	-	-	-	-
-38	-44	51	58	RFM029R		PDZ1 (G)	-	-	-	-	-
-38	-72	58	65	RFM029R	FFM02L		-	-	-	-	-
-44	-50	51	93	RFM029R	FFM02L						
-72	-79	93	102	RFM029R		ZFM1203					
-79	-93	102	119	RFM029R	FFM02L						
-93	-106	119	135	RFM029R		PDZ3 (S-ENE)					
-106	-154	135	195	RFM029R	FFM02L						
-154	-178	195	225	RFM029R	FFM01						
-178	-194	225	245	RFM029R		ZFMENE2320			4.8E-08	4	5m TT
-194	-237	245	299	RFM029R	FFM01						
KFM07C											
3.54	**-494**	**0**	**500**								
1	-81	3	85	RFM029R	FFM02U						
-81	-88	85	92	RFM029R	FFM02L						
-88	-99	92	103	RFM029R		ZFM1203	4.8E-05	1	4.8E-05	1	TD
-99	-119	103	123	RFM029R	FFM02L		1.1E-07	5	1.8E-07	4	TD
-119	-303	123	308	RFM029R	FFM01		4.7E-05	9	4.7E-05	37	TD
-303	-382	308	388	RFM029R		ZFMENE2320			1.3E-08	16	TD
-382	-423	388	429	RFM029R	FFM01				6.6E-09	8	TD
-423	-433	429	439	RFM029R		ZFMENE2320			1.7E-09	2	TD
-433	-494	439	500	RFM029R	FFM01				9.1E-09	11	TD

4.8 Drill Site 8

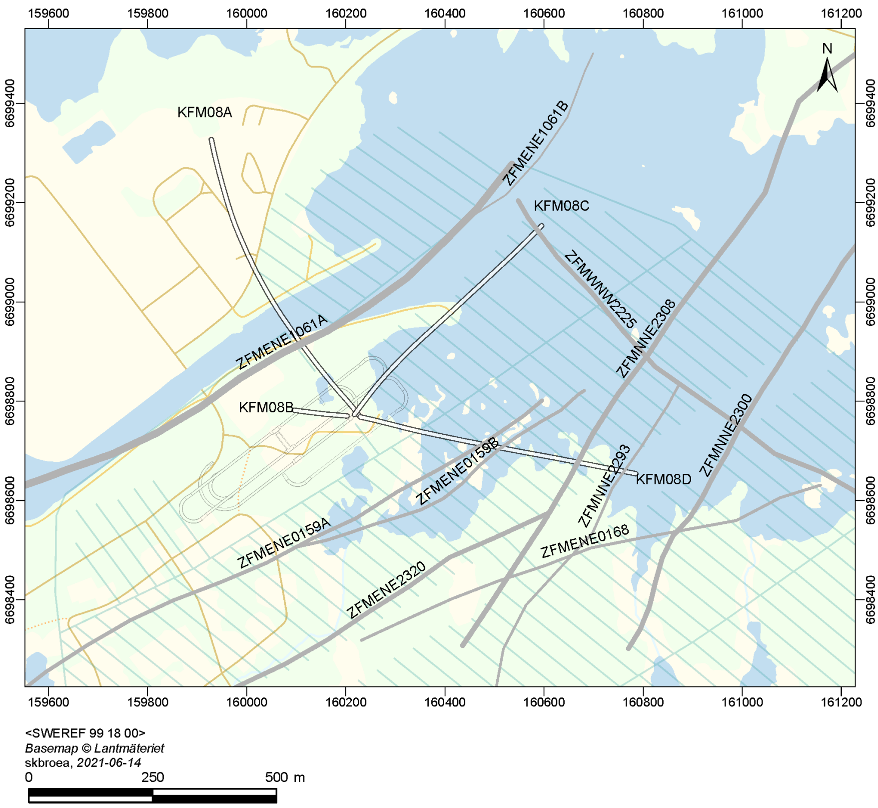

Figure 4-15. Map of Drill Site 8 including horizontal projections of core-drilled boreholes with hydraulic test data presented in Table 4-10. A potential SFK layout SYHA 2.0 layout and ground surface intersection of selected deterministically modelled deformation zones (grey) which intersect with the boreholes at Drill Site 8 shown for reference.

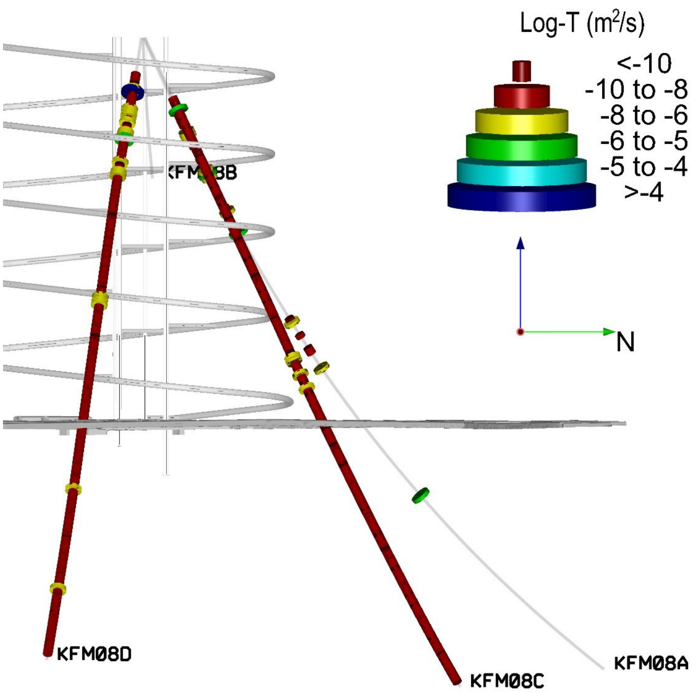

Figure 4-16. Profile view facing East of core-drilled boreholes at Drill Site 8 with hydraulic test data presented in Table 4-10. A potential layout for SFK is visualized for reference.

Table 4-10. Hydraulic data compilation per interpreted geological domain in core-drilled boreholes at drill site 8 (DS8, see Figure 4-15). In the table, for each borehole, the first row highlighted in grey represents the entire length of the borehole from the top of the casing to the bottom of the borehole. Dashed red line indicates casing depth. Zup is the upper elevation of the section, Zlow is the lower elevation of the section. Secup and Seclow refer to the depth to top and bottom of the section along the borehole. ΣT PFL_f is the sum of all overlapping PFL transmissivities (PFL_f) and ΣT is the sum of sequential test section transmissivities between Zup and Zlow, n1 and n2 is number of PFL-f anomalies or flowing sections, respectively.

Zup (m)	Zlow (m)	Secup(m)	Seclow(m)	Rock Domain (RFMxxx)	Fracture domain (FFMxxx)	Deformation zone (ZFM / PDZ)	ΣT PFL_f (m^2/s)	n1	ΣT (m^2/s)	n2	Data type
KFM08A											
2.67	**-759**	**0**	**1001**								
-2		5		RFM029R	FFM02U		-	-	-	-	-
	-83		100	RFM029R	FFM02L		-	-	-	-	-
-83	-85	100	102	RFM029R	FFM02L						
-85	-204	102	244	RFM029R	FFM01		4.1E-06	24	4.4E-06	15	TD
-204	-262	244	315	RFM029R		ZFMENE1061A	1.3E-06	6	1.5E-06	3	TD
-262	-393	315	479	RFM029R	FFM01		1.5E-08	8	1.8E-08	5	TD
-393	-406	479	496	RFM029R		ZFMNNW1204	6.9E-08	2	8.3E-08	1	TD
-406	-431	496	528	RFM029R	FFM01				1.5E-05	2	5m TM
-431	-453	528	557	RFM029R		PDZ3					
-453	-502	557	624	RFM029R	FFM01						
-502	-503	624	624	RFM029R		PDZ8 (S-NW)					
-503	-538	624	672	RFM029R	FFM01						
-538	-553	672	693	RFM029R		PDZ4 (S-EW)	1.4E-06	1	1.9E-06	1	TD
-553	-611	693	775	RFM029R	FFM01				3.7E-05	10	20m TT
-611	-658	775	843	RFM032		ZFMENE2248			9.8E-10	1	5m TT
-658	-712	843	925	RFM032	FFM05						
-705	-712	915	925	RFM032		PDZ6 (S-WNW)					
-712	-725	925	946	RFM034							
-725	-738	946	967	RFM034	RD034						
-738	-744	967	976	RFM034		PDZ7					
-744	-759	976	1001	RFM034	RD034						
KFM08B											
2.43	**-166**	**0**	**200**								
-1	-2	4	6	RFM029R	FFM02U		-	-	-	-	-
-2	-24	6	31	RFM029R	FFM02U				1.2E-05	4	5m TT
-24	-37	31	46	RFM029R	FFM02L				1.6E-05	3	5m TT
-37	-110	46	133	RFM029R	FFM01				4.7E-07	8	5m TT
-110	-116	133	140	RFM029R		ZFMNNW1205B					
-116	-139	140	167	RFM029R	FFM01				6.5E-08	3	5m TT
-139	-154	167	185	RFM029R		ZFMNNW1205A			1.2E-08	4	5m TT
-154	-166	185	200	RFM029R	FFM01				7.1E-09	1	5m TT

Table 4-10. Cont'd.

Zup (m)	Zlow (m)	Secup(m)	Seclow(m)	Rock Domain (RFMxxx)	Fracture domain (FFMxxx)	Deformation zone (ZFM / PDZ)	ΣT PFL_f (m^2/s)	n1	ΣT (m^2/s)	n2	Data type
KFM08C											
2.66	**-781**	**0**	**951**								
0	-8	3	12	RFM029	FFM02L		-	-	-	-	-
-8		12		RFM029	FFM02L						
	-86		102	RFM029	FFM02L				3.3E-06	4	TD
-86	-136	102	161	RFM045	FFM01		3.0E-06	1	1.2E-08	12	TD
-136	-162	161	191	RFM045		PDZ1 (S-ENE)	9.5E-09	3	1.1E-08	6	TD
-162	-288	191	342	RFM045	FFM01		8.8E-09	3	3.6E-08	30	TD
-288	-352	342	419	RFM045	FFM06				1.3E-08	15	TD
-352	-454	419	542	RFM045		ZFMNNE2312	1.8E-07	13	1.9E-07	25	TD
-454	-456	542	546	RFM045	FFM06				8.3E-10	1	TD
-456	-560	546	673	RFM029	FFM01				2.1E-08	25	TD
-560	-586	673	705	RFM029		ZFMWNW2225	2.6E-09	1	1.1E-08	6	TD
-586	-685	705	829	RFM029	FFM01				2.1E-08	25	TD
-685	-687	829	832	RFM029		ZFMENE1061A, ZFMENE1061B			8.4E-10	1	TD
-687	-777	832	946	RFM029	FFM01				1.9E-08	22	TD
-777	-779	946	949	RFM029		ZFMENE1061A					
-779	-781	949	951	RFM029	FFM01						
KFM08D											
2.79	**-748**	**0**	**942**								
0		1		RFM029	FFM02U		-	-	-	-	-
	-46		59	RFM029	FFM02L		-	-	-	-	-
-46	-146	59	184	RFM029	FFM01		1.8E-05	17	1.9E-05	26	TD
-146	-167	184	210	RFM029		ZFMENE2120	9.0E-08	7	1.6E-07	5	TD
-167	-256	210	318	RFM029	FFM01				3.7E-08	22	TD
-256	-261	318	324	RFM029		ZFMENE0159A			1.7E-09	1	TD
-261	-299	324	371	RFM029	FFM01				1.7E-08	10	TD
-299	-319	371	396	RFM029		ZFMENE0159B	1.3E-07	4	1.4E-07	5	TD
-319	-400	396	496	RFM045	FFM01				3.4E-08	20	TD
-400	-408	496	506	RFM045		PDZ4 (S-NE)			3.4E-09	2	TD
-408	-440	506	546	RFM045	FFM01				1.4E-08	8	TD
-440	-460	546	571	RFM045		ZFMNNE2309			2.6E-08	15	TD
-460	-468	571	582	RFM045	FFM01				3.4E-09	2	TD
-468	-510	582	634	RFM045		ZFMENE2320			1.7E-08	10	TD
-510	-517	634	644	RFM045	FFM01				3.4E-09	2	TD
-517	-553	644	689	RFM045		ZFMNNE2308	1.9E-07	3	2.3E-07	9	TD
-553	-590	689	737	RFM045	FFM01		1.3E-08	2	2.7E-08	10	TD
-590	-600	737	749	RFM045		ZFMNNE2293			3.4E-09	2	TD
-600	-616	749	770	RFM045	FFM01				8.5E-09	5	TD
-616	-621	770	777	RFM045		PDZ10 (S-NS)			1.7E-09	1	TD
-621	-654	777	819	RFM045	FFM01				1.4E-08	8	TD
-654	-672	819	842	RFM045		ZFMENE0168	2.9E-08	1	3.1E-08	5	TD
-672	-718	842	903	RFM045	FFM01				2.0E-08	12	TD
-718	-747	903	942	RFM045		ZFMNNE2300			1.1E-08	6	TD

4.9 Drill Site 9

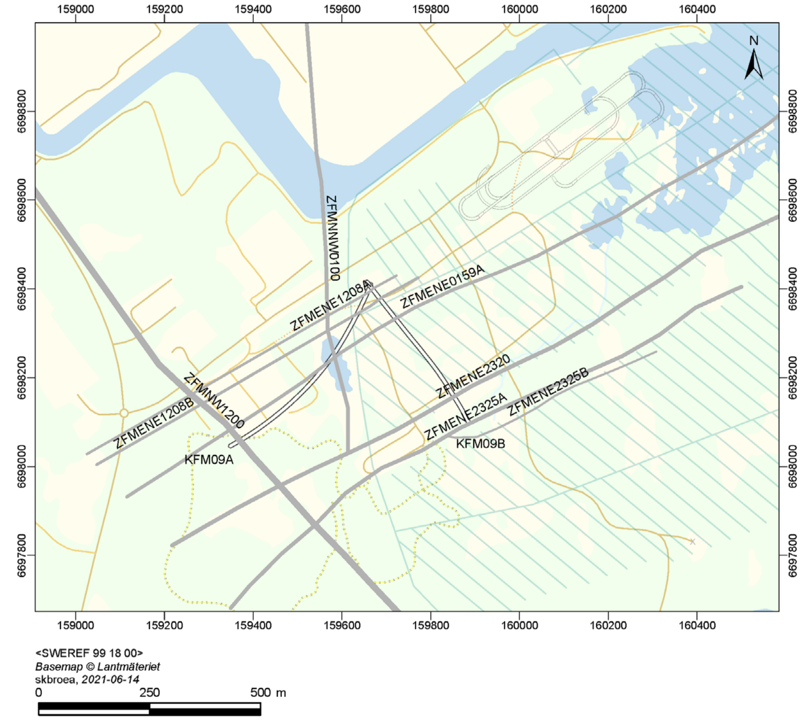

Figure 4-17. *Map of Drill Site 9 including horizontal projections of core-drilled boreholes with hydraulic test data presented in Table 4-11. A potential SFK layout SYHA 2.0 layout and ground surface intersection of selected deterministically modelled deformation zones (grey) which intersect with the boreholes at Drill Site 9 shown for reference.*

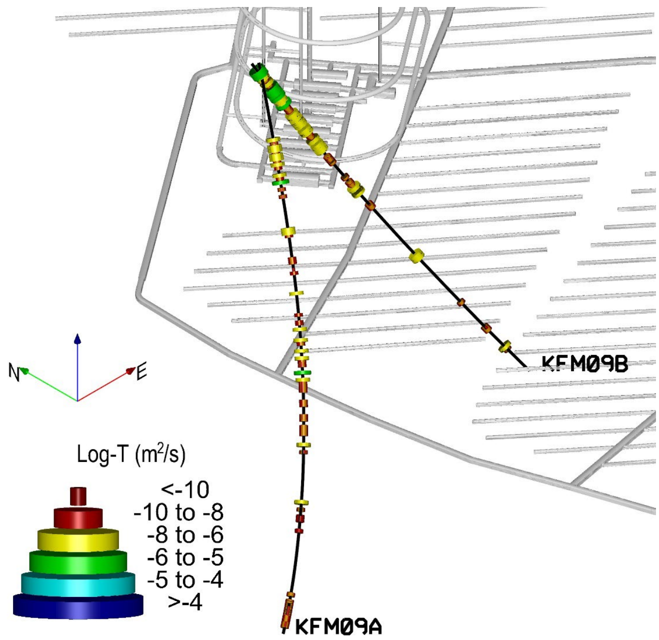

Figure 4-18. *Isometric view of core-drilled boreholes at Drill Site 9 with hydraulic test data presented in Table 4-11. A potential SFK layout SYHA 2.0 is visualized for reference.*

Table 4-11. Summary of geological data cross referenced with section transmissivities gathered through hydraulic testing in core-drilled boreholes at drill site 9 (DS9, see Figure 4-17). In the table, for each borehole, the first row highlighted in grey represents the entire length of the borehole from the top of the casing to the bottom of the borehole. Dashed red line indicates casing depth. Zup is the upper elevation of the section, Zlow is the lower elevation of the section. Secup and Seclow refer to the depth to top and bottom of the section along the borehole. ΣT PFL_f is the sum of all overlapping PFL transmissivities (PFL_f) and ΣT is the sum of sequential test section transmissivities between Zup and Zlow, n1 and n2 is number of PFL-f anomalies or flowing sections, respectively.

Zup (m)	Zlow (m)	Secup(m)	Seclow(m)	Rock Domain (RFMxxx)	Fracture domain (FFMxxx)	Deformation zone (ZFM / PDZ)	ΣT PFL_f (m^2/s)	n1	ΣT (m^2/s)	n2	Data type
KFM09A											
4.48	**-621**	**0**	**800**								
-2	-2	7	8	RFM029	FFM02U		-	-	-	-	-
-2	-8	8	15	RFM029	FFM02U						
-8	-30	15	40	RFM029		ZFMENE1208A					
-30	-69	40	86	RFM029	FFM02L						
-69	-94	86	116	RFM029		ZFMENE1208B			1.4E-08	2	5m TT
-94	-100	116	124	RFM029	FFM02L				4.3E-08	1	5m TT
-100	-179	124	217	RFM029	FFM01				1.8E-06	9	5m TT
-179	-231	217	280	RFM029		ZFMENE0159A, ZFMNNW0100			1.5E-07	5	5m TT
-231	-415	280	512	RFM044	FFM05				1.7E-06	22	5m TT
-415	-511	512	641	RFM034	RD034				4.5E-07	8	5m TT
-511	-530	641	666	RFM012	FFM04				3.8E-09	2	5m TT
-530	-531	666	667	RFM012		PDZ6 (M-SW)					
-531	-570	667	723	RFM012	FFM04				2.4E-11	1	20m TT
-570	-591	723	754	RFM012		ZFMNW1200			2.8E-09	1	5m TT
-591	-601	754	770	RFM018	FFM04				6.6E-09	3	5m TT
-601	-615	770	790	RFM018		ZFMNW1200			9.5E-09	4	5m TT
-615	-621	790	800	RFM018	FFM04						
KFM09B											
4.49	**-472**	**0**	**616**								
3	-3	7	9	RFM029	FFM02U		-	-	-	-	-
-3	-31	9	43	RFM029		ZFMENE1208A			1.4E-05	7	5m TT
-31	-44	43	59	RFM029	FFM02L				1.2E-05	3	5m TT
-44	-60	59	78	RFM029		ZFMENE1208B			6.1E-06	4	5m TT
-60	-82	78	106	RFM029	FFM02L				1.8E-07	2	5m TT
-82	-103	106	132	RFM029		ZFMENE0159A			5.5E-08	1	5m TT
-103	-224	132	284	RFM029	FFM01				1.6E-06	10	5m TT
-224	-225	284	284	RFM029		PDZ6 (S-ENE)					
-225	-244	284	308	RFM029	FFM01						
-244	-269	308	340	RFM029		PDZ2 (S-ENE)			4.2E-10	1	20m TT
-269	-287	340	363	RFM029	FFM01						
-287	-325	363	413	RFM029		ZFMENE2320			4.9E-08	2	5m TT
-325	-404	413	520	RFM029	FFM01						
-404	-426	520	550	RFM029		ZFMENE2325A			9.9E-10	2	5m TT
-426	-434	550	561	RFM029	FFM01						
-434	-443	561	574	RFM029		ZFMENE2325B			3.5E-08	1	20m TT
-443	-472	574	616	RFM029	FFM01						

4.10 Drill Site 10, Drill Site 11 and Drill Site 12

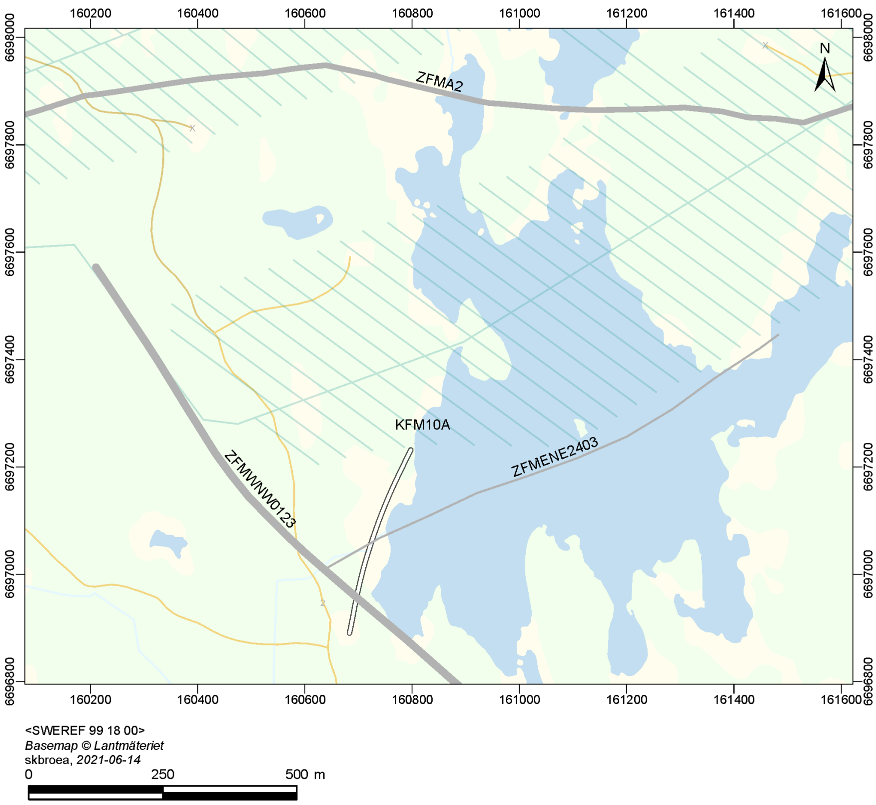

Figure 4-19. *Map of Drill Site 10 including horizontal projections of core-drilled boreholes with hydraulic test data presented in Table 4-12. A potential SFK layout SYHA 2.0 layout and ground surface intersection of selected deterministically modelled deformation zones (grey) which intersect with KFM10A shown for reference.*

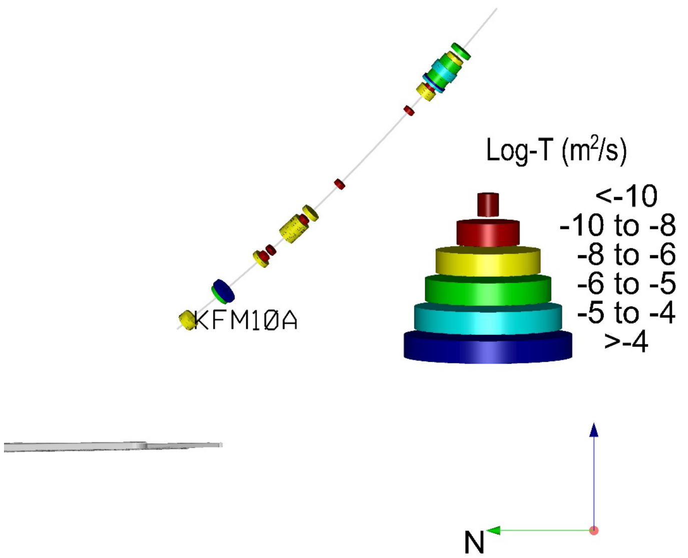

Figure 4-20. *Profile view facing East of core-drilled borehole KFM10A with hydraulic test data presented in Table 4-12. A potential SFK layout SYHA 2.0 is visualized for reference.*

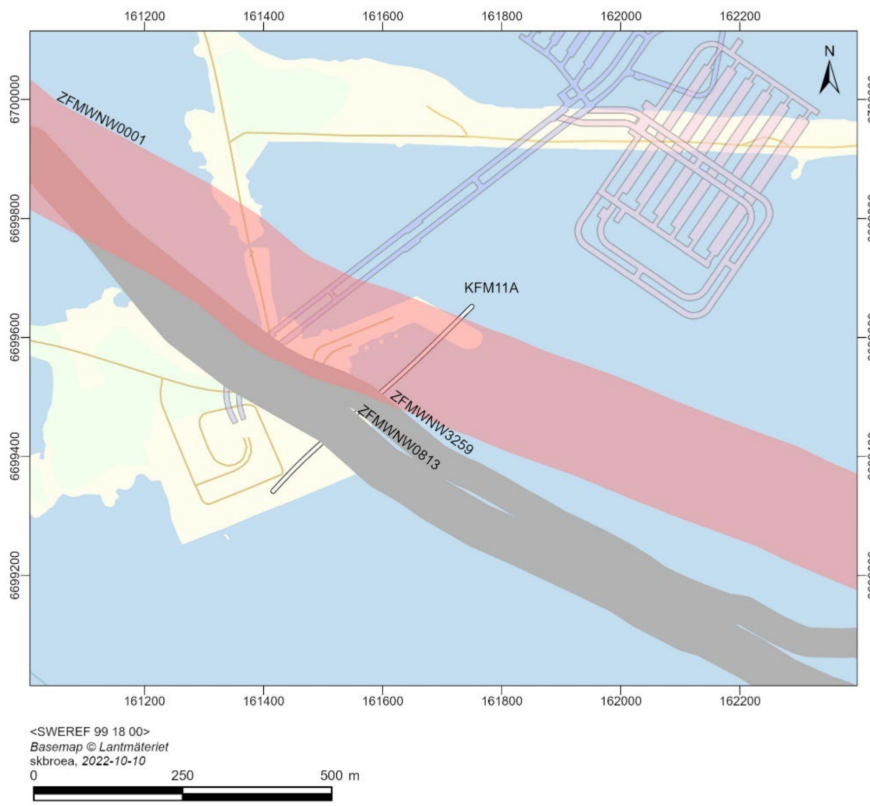

Figure 4-21. *Map of Drill Site 11 including horizontal projection of core-drilled borehole KFM11A with hydraulic test data presented in Table 4-12. A potential SFK layout SYHA 2.0 layout and ground surface intersection of selected deterministically modelled deformation zones (grey) and the Singö deformation zone (red)which intersect with KFM11A shown for reference.*

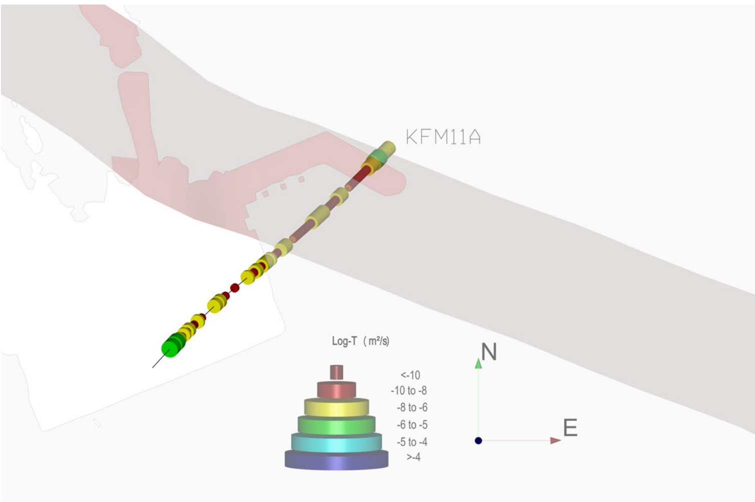

Figure 4-22. *Top-down view of core-drilled borehole KFM11A with hydraulic test data presented in Table 4-12. Current approximate shoreline and ZFMWNW0001 shown for reference.*

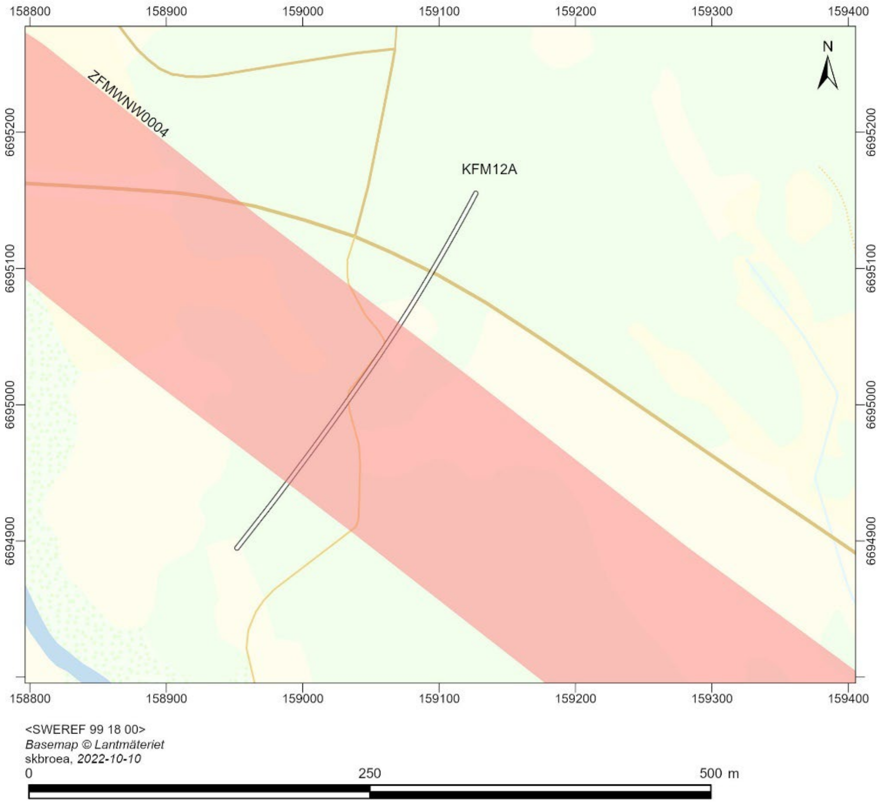

Figure 4-23. *Map of Drill Site 12 including horizontal projection of core-drilled borehole KFM12A with hydraulic test data presented in Table 4-12. Ground surface intersection of selected deterministically modelled regional deformation zones (red) which intersect with KFM10A shown for reference.*

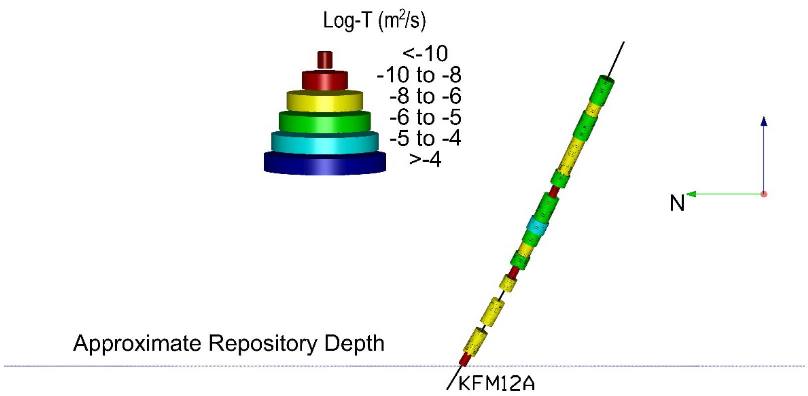

Figure 4-24. *Profile view facing East of core-drilled boreholes KFM12A with hydraulic test data presented in Table 4-12.*

Table 4-12. Hydraulic data compilation per interpreted geological domain in core-drilled boreholes KFM10A, KFM11A and KFM12A. In the table, for each borehole, the first row highlighted in grey represents the entire length of the borehole from the top of the casing to the bottom of the borehole. Dashed red line indicates casing depth. Zup is the upper elevation of the section, Zlow is the lower elevation of the section. Secup and Seclow refer to the depth to top and bottom of the section along the borehole. ΣT PFL_f is the sum of all overlapping PFL transmissivities (PFL_f) and ΣT is the sum of sequential test section transmissivities between Zup and Zlow, n1 and n2 is number of PFL-f anomalies or flowing sections, respectively.

Zup (m)	Zlow (m)	Secup(m)	Seclow(m)	Rock Domain (RFMxxx)	Fracture domain (FFMxxx)	Deformation zone (ZFM / PDZ)	ΣT PFL_f (m^2/s)	n1	ΣT (m^2/s)	n2	Data type
KFM10A											
4.69	**-338**	**0**	**500**								
4.69	-41	8	60	RFM029			-	-	-	-	-
-41	-43	60	63	RFM029			1.0E-06	2	2.6E-06	1	TD
-43	-104	63	145	RFM029		ZFMWNW0123	7.4E-05	32	6.3E-05	12	TD
-104	-197	145	275	RFM029	FFM03		2.6E-09	1	3.0E-09	1	TD
-197	-203	275	284	RFM029		ZFMENE2403			4.9E-09	1	5m TT
-203	-297	284	430	RFM029	FFM03		5.0E-07	13	4.9E-07	10	TD
-297	-308	430	449	RFM029		ZFMA2	2.9E-05	4	3.0E-05	2	TD
-308	-325	449	478	RFM029	FFM03				2.7E-09	3	5m TT
-325	-332	478	490	RFM029		ZFMA2	1.1E-06	4	1.0E-06	2	TD
-332	-338	490	500	RFM029	FFM03				3.6E-10	1	5m TT
KFM11A											
3.14	**-713**	**0**	**851**								
3.14	-59	7	71	RFM021			-	-	-	-	-
-59	-213	71	245	RFM021	FFM05		3.2E-05	50	3.1E-05	21	TD
-213	-346	245	400	RFM021		ZFMWNW0813	1.4E-07	21	2.3E-07	12	TD
-346	-429	400	498	RFM021		ZFMWNW3259	1.1E-06	21	1.3E-06	10	TD
-429	-692	498	824	RFM021		ZFMWNW0001			2.7E-06	16	20m TT
-692	-713	824	851	RFM021	FFM05				3.5E-07	1	20m TT
KFM12A											
10.92	**-501**	**0**	**601**								
10.92	-41	8	59	RFM030			-	-	-	-	-
-40	-97	59	125	RFM030					6.3E-06	3	20m TT
-97	-335	125	402	RFM030		ZFMWNW0004			2.9E-05	14	20m TT
-335	-428	402	513	RFM030					1.3E-06	4	20m TT
-428	-437	513	523	RFM030		PDZ3 (S-WNW)			2.7E-07	1	20m TT
-437	-500	523	601	RFM030					2.2E-10	1	20m TT

4.11 Boreholes KFM14 through KFM16

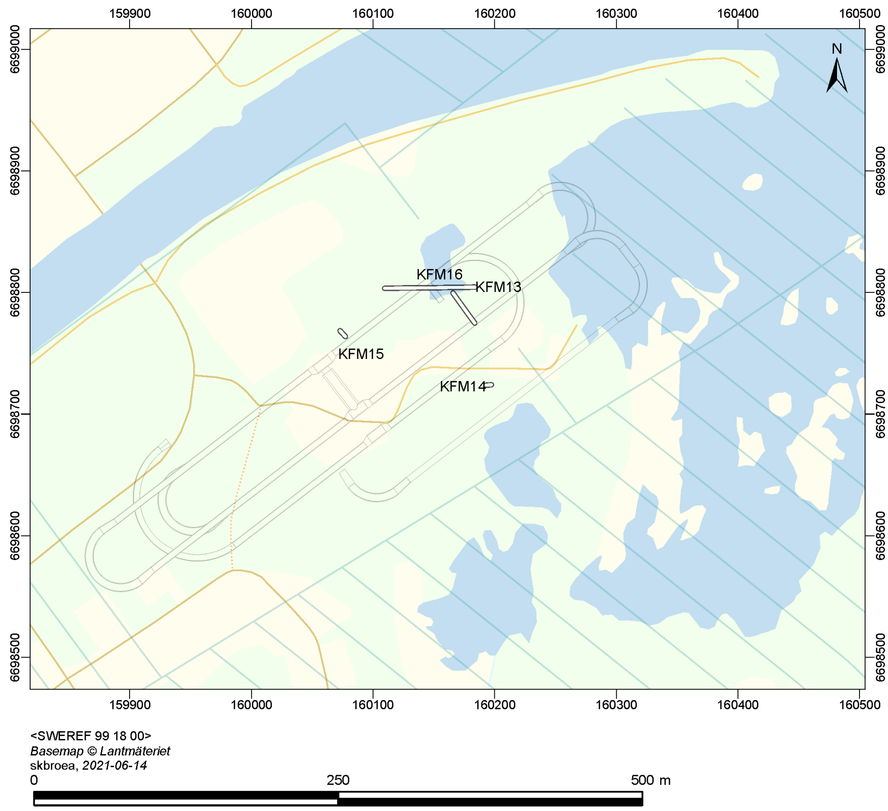

Figure 4-25. Map including horizontal projections of core-drilled boreholes KFM14-16 with hydraulic test data presented in Table 4-13. A potential SFK layout (SYHA 2.0) is shown for reference.

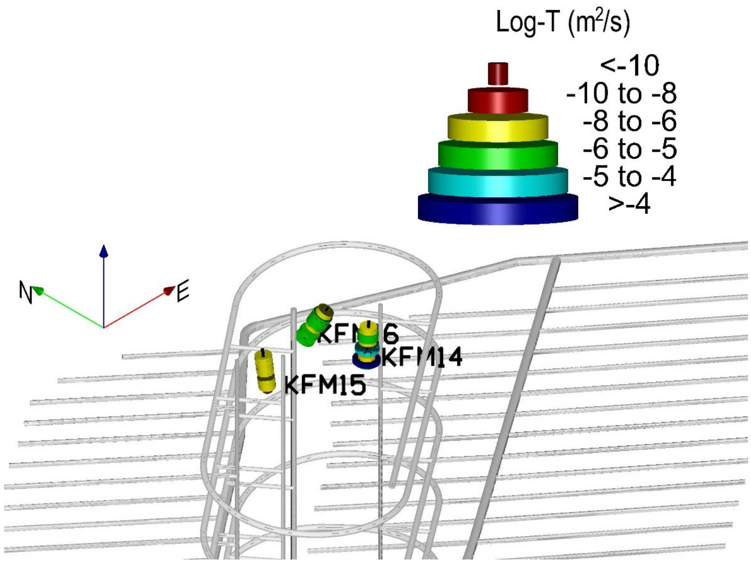

Figure 4-26. Isometric view of core-drilled boreholes KFM14, KFM15 and KFM16 with hydraulic test data presented in Table 4-13.

Table 4-13. Hydraulic data compilation per interpreted geological domain in core-drilled boreholes KFM14, KFM15 and KFM16. In the table, for each borehole, the first row highlighted in grey represents the entire length of the borehole from the top of the casing to the bottom of the borehole. Dashed red line indicates casing depth. Zup is the upper elevation of the section, Zlow is the lower elevation of the section. Secup and Seclow refer to the depth to top and bottom of the section along the borehole. ΣT PFL_f is the sum of all overlapping PFL transmissivities (PFL_f) and ΣT is the sum of sequential test section transmissivities between Zup and Zlow, n1 and n2 is number of PFL-f anomalies or flowing sections, respectively.

Zup (m)	Zlow (m)	Secup(m)	Seclow(m)	Rock Domain (RFMxxx)	Fracture domain (FFMxxx)	Deformation zone (ZFM / PDZ)	ΣT PFL_f (m^2/s)	n1	ΣT (m^2/s)	n2	Data type
KFM14											
2.15	**-58**	**0**	**60**								
-3	-4	5	6		FFM02U		-	-	-	-	-
-4	-23	6	25		FFM02U		1.3E-05	8	1.2E-05	4	TD
-23	-47	25	50		FFM02L		2.5E-05	7	1.4E-04	5	TD
-47	-58	50	60		FFM01		4.2E-05	2	2.1E-06	1	TD
KFM15											
3.65	**-58**	**0**	**62**								
-1	-4	5	7		FFM02U		-	-	-	-	-
-4	-11	7	15		FFM02U		3.8E-08	5	2.3E-08	1	TD
-11	-13	15	17			PDZ1 (G)	2.4E-07	4	2.2E-07	1	TD
-13	-18	17	22		FFM02U		2.9E-07	4	2.5E-07	1	TD
-18	-19	22	23		FFM02L						
-19	-58	23	62		FFM01		8.4E-07	10	8.6E-07	6	TD
KFM16											
1.69	**-50**	**0**	**60**								
-1	-2	3	4		FFM02U		-	-	-	-	-
-2	-23	4	29		FFM02U		1.5E-05	16	1.5E-05	6	TD
-23	-36	29	45		FFM02L		2.4E-06	4	2.5E-06	2	TD
-36	-50	45	60		FFM01		8.9E-06	5	8.0E-06	1	TD

4.12 Boreholes KFM20 through KFM27

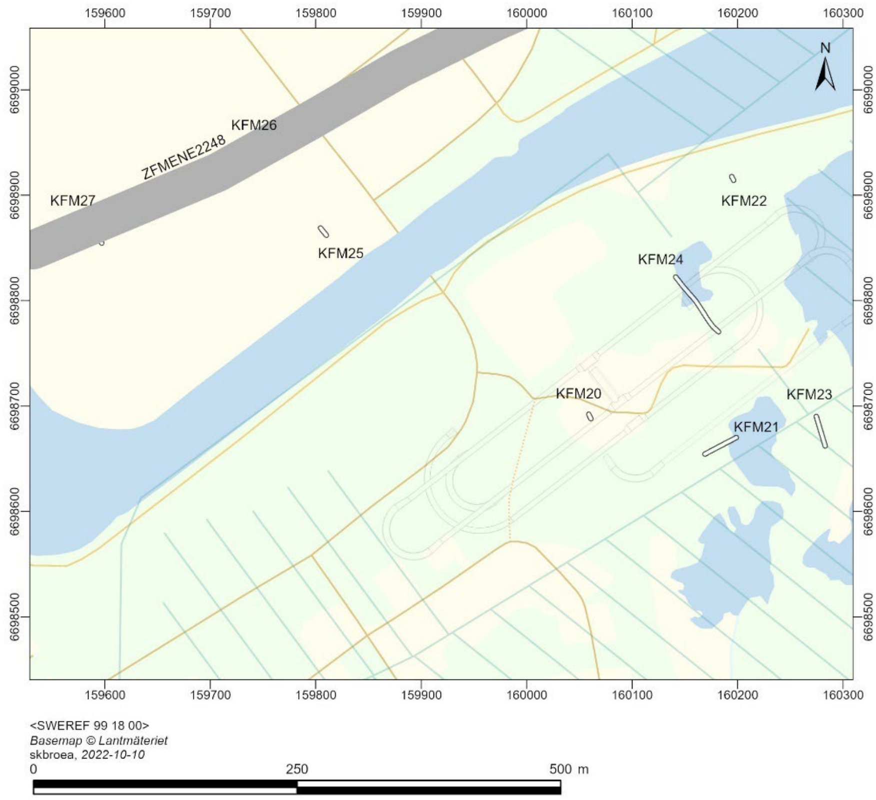

Figure 4-27. *Map including horizontal projections of core-drilled boreholes KFM20-27 with hydraulic test data presented in Table 4 14. A potential SFK layout (SYHA 2.0) and ground surface intersection of selected deterministically modelled deformation zones (grey) which intersect with the boreholes is shown for reference.*

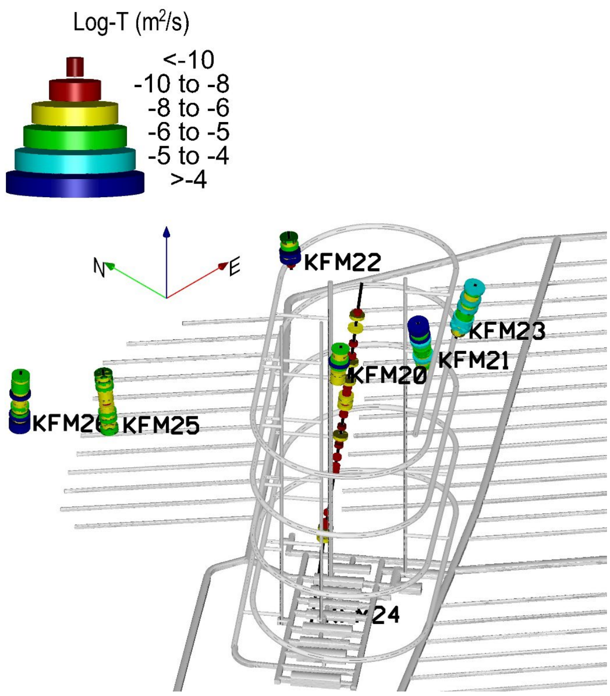

Figure 4-28*. Isometric view of core-drilled boreholes KMF20, KFM21, KFM22, KFM23, KFM24, KFM25, KFM26 and KFM27 with hydraulic test data presented in Table 4 14. A potential SFK layout (SYHA 2.0) and ground surface intersection of selected deterministically modelled deformation zones (grey) which intersect with the boreholes is shown for reference.*

Table 4-14. Hydraulic data compilation per interpreted geological domain in core-drilled boreholes KFM20, KFM21, KFM22, KFM23, KFM24, KFM25, KFM26 and KFM27. In the table, for each borehole, the first row highlighted in grey represents the entire length of the borehole from the top of the casing to the bottom of the borehole. Dashed red line indicates casing depth. Zup is the upper elevation of the section, Zlow is the lower elevation of the section. Secup and Seclow refer to the depth to top and bottom of the section along the borehole. ΣT PFL_f is the sum of all overlapping PFL transmissivities (PFL_f) and ΣT is the sum of sequential test section transmissivities between Zup and Zlow, n1 and n2 is number of PFL-f anomalies or flowing sections, respectively.

Zup (m)	Zlow (m)	Secup(m)	Seclow(m)	Rock Domain (RFMxxx)	Fracture domain (FFMxxx)	Deformation zone (ZFM / PDZ)	ΣT PFL_f (m^2/s)	n1	ΣT (m^2/s)	n 2	Data type
KFM20											
2.99	**-57**	**0**	**61**								
2	1	1	2		FFM02U		-	-	-	-	-
1	-24	2	27		FFM02U		3.1E-05	14	3.4E-05	5	TD
-24	-30	27	33		FFM02L		3.4E-06	6	2.9E-06	1	TD
-30	-43	33	47		FFM01		1.9E-07	2	2.2E-07	2	TD
-43	-44	47	48			PDZ1 (M-SSE)					
-44	-57	48	61		FFM01		1.7E-07	4	2.0E-07	2	TD
KFM21											
2.80	**-92**	**0**	**101**								
-2	-3	5	6		FFM02U		-	-	-	-	-
-2	-14	6	18		FFM02U		8.9E-05	10	5.0E-05	4	TD
-14	-23	18	28			ZFMNNW1205A	2.0E-05	9	1.8E-05	2	TD
-23	-57	28	64		FFM02L		5.9E-05	22	5.0E-05	7	TD
-57	-63	64	70			PDZ2 (G)	8.6E-07	4	8.1E-07	1	TD
-63	-78	70	86		FFM01		1.2E-05	8	1.3E-05	4	TD
-78	-86	86	95			ZFMNNW1205B	2.6E-06	7	2.4E-06	2	TD
-86	-92	95	101		FFM01						
KFM22											
2.94	**-57**	**0**	**60**								
-3	-5	7	8		FFM02U		-	-	-	-	-
-5	-25	8	28		FFM02U		7.2E-06	10	6.7E-06	4	TD
-25	-39	28	42		FFM02L		5.9E-05	13	7.6E-05	3	TD
-39	-57	42	60		FFM01		7.0E-09	1	6.4E-09	1	TD
KFM23											
2.45	**-93**	**0**	**101**								
2	-2	0	5		FFM02U		-	-	-	-	-
-2	-18	5	22		FFM02U		5.2E-05	12	5.8E-05	3	TD
-18	-31	22	35			ZFMENE2120	3.0E-05	8	2.3E-05	3	TD
-31	-56	35	61		FFM02L		4.6E-05	18	4.6E-05	6	TD
-56	-93	61	101		FFM01		8.3E-05	16	7.9E-05	5	TD
KFM24											
1.21	**-545**	**0**	**550**								
-2	-24	3	25	RFM029	FFM02U		-	-	-	-	-
-24	-34	25	35	RFM029	FFM02L		-	-	-	-	-
-34	-36	35	37	RFM029	FFM02L						
-36	-545	37	550	RFM029	FFM01		8.1E-07	34	8.3E-07	24	TD
KFM25											
2.66	**-98**	**0**	**101**								
				RFM029	FFM02U		-	-	-	-	-
-2	-3	5	6	RFM029	FFM02L		-	-	-	-	-
-3	-98	6	101	RFM029	FFM01		2.7E-05	42	2.5E-05	19	TD
KFM26											
3.00	**-97**	**0**	**101**								
-2	-3	5	6	RFM029	FFM02U		-	-	-	-	-
-3	-51	6	54	RFM029	FFM02U		3.2E-05	23	3.4E-05	9	TD
-51	-97	54	101	RFM029	FFM01		7.7E-05	26	7.5E-05	9	TD

Table 4-14. Cont'd.

Zup (m)	Zlow (m)	Secup(m)	Seclow(m)	Rock Domain (RFMxxx)	Fracture domain (FFMxxx)	Deformation zone (ZFM / PDZ)	ΣT PFL_f (m^2/s)	n1	ΣT (m^2/s)	n 2	Data type
KFM27											
2.54	**-94**	**0**	**101**								
-2	-6	5	9	RFM029	FFM02U		-	-	-	-	-
-6	-26	9	30	RFM029	FFM02U		1.8E-05	16	1.4E-05	5	TD
-26	-86	30	92	RFM029		ZFMENE2248	9.3E-05	50	6.7E-05	12	TD
-86	-94	92	101	RFM029	FFM01		1.7E-07	3	1.6E-07	2	TD

4.13 KFR boreholes

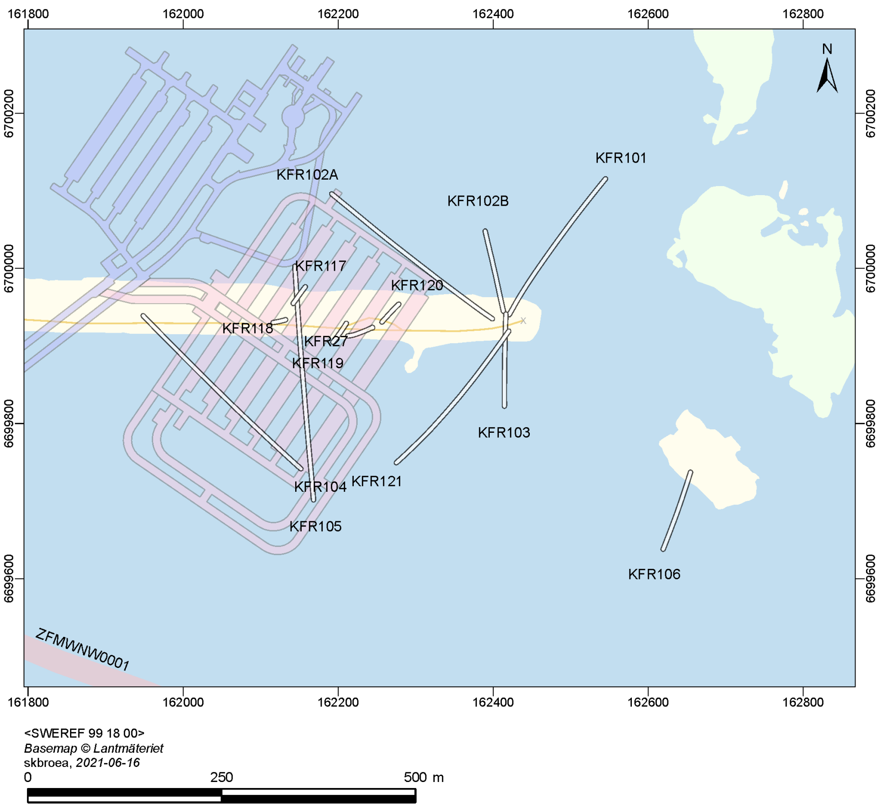

Figure 4-29. *Map including horizontal projections of KFR boreholes with hydraulic test data presented in Table 4-15. SFR1 and SFR3 layouts are shown for reference. KFR105 is drilled sub-horizontally from the SFR1 NBT tunnel section.*

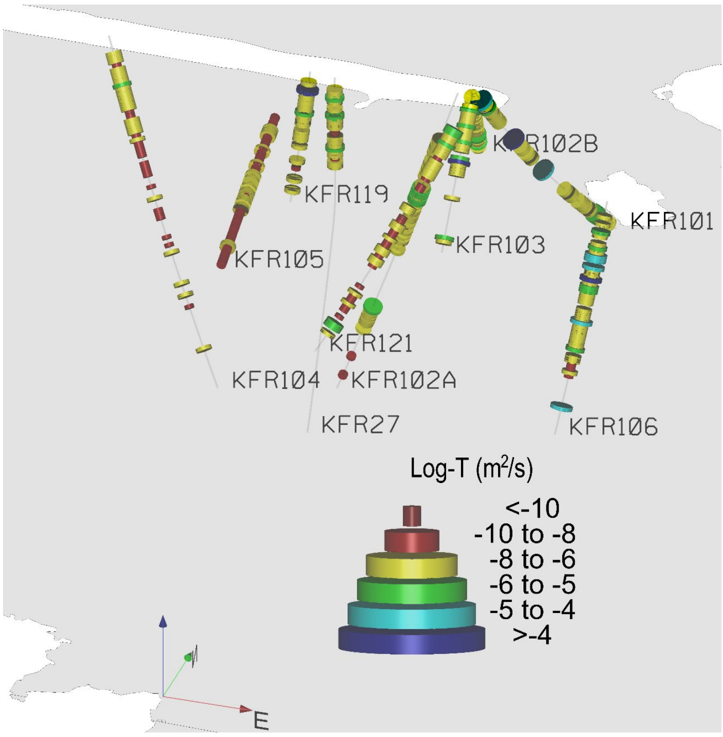

Figure 4-30. *Visualization of sequential PFL data (Table 4-15 to Table 4-22) from core-drilled boreholes with KFR prefix. The current shoreline is shown for reference.*

Table 4-15. Hydraulic data compilation per interpreted geological domain in core-drilled borehole KFR101. In the table, the first row highlighted in grey represents the entire length of the borehole from the top of the casing to the bottom of the borehole. Dashed red line indicates casing depth. Zup is the upper elevation of the section, Zlow is the lower elevation of the section. Secup and Seclow refer to the depth to top and bottom of the section along the borehole. ΣT PFL_f is the sum of all overlapping PFL transmissivities (PFL_f) and ΣT is the sum of sequential test section transmissivities between Zup and Zlow, n1 and n2 is number of PFL-f anomalies or flowing sections, respectively.

Zup (m)	Zlow (m)	Secup(m)	Seclow(m)	Rock Domain (RFMxxx)	Fracture domain (FFMxxx)	Deformation zone (ZFM / PDZ)	ΣT PFL_f (m^2/s)	n1	ΣT (m^2/s)	n2	Data type
KFR101											
2.62	**-262**	**0**	**342**								
-7	-9	12	14	RFM021			-	-	-	-	-
-9	-69	14	88	RFM021		ZFMNNW1034	1.6E-05	19	1.6E-05	11	TD
-69	-77	88	97	RFM021							
-77	-92	97	116	RFM021		ZFMNW0805B	8.3E-06	1	1.2E-05	1	TD
-92	-142	116	179	RFM021			5.1E-07	5	8.5E-07	4	TD
-142	-147	179	186	RFM021		PDZ3 (S-WNW)	1.3E-05	1	1.8E-05	1	TD
-147	-156	186	197	RFM021							
-156	-168	197	213	RFM021		PDZ4 (S-NW)					
-168	-190	213	242	RFM021			1.8E-08	1	9.7E-08	2	TD
-190	-262	242	342	RFM021		ZFMNW0805A	6.1E-06	25	8.9E-06	12	TD

Table 4-16. Hydraulic data compilation per interpreted geological domain in core-drilled boreholes KFR102A and KFR102B. In the table, for each borehole, the first row highlighted in grey represents the entire length of the borehole from the top of the casing to the bottom of the borehole. Dashed red line indicates casing depth. Zup is the upper elevation of the section, Zlow is the lower elevation of the section. Secup and Seclow refer to the depth to top and bottom of the section along the borehole. ΣT PFL_f is the sum of all overlapping PFL transmissivities (PFL_f) and ΣT is the sum of sequential test section transmissivities between Zup and Zlow, n1 and n2 is number of PFL-f anomalies or flowing sections, respectively.

Zup (m)	Zlow (m)	Secup(m)	Seclow(m)	Rock Domain (RFMxxx)	Fracture domain (FFMxxx)	Deformation zone (ZFM / PDZ)	ΣT PFL_f (m^2/s)	n1	ΣT (m^2/s)	n2	Data type
KFR102A											
2.85	**-537**	**0**	**601**								
0	-61	10	70	RFM021			-	-	-	-	-
-61	-133	70	149	RFM021			1.2E-06	28	1.0E-06	10	TD
-133	-144	149	161	RFM021		ZFMNE3137	9.5E-09	2	2.6E-08	2	TD
-144	-272	161	302	RFM021			1.3E-05	50	1.3E-05	20	TD
-272	-292	302	325	RFM021		ZFMNE3112	1.9E-08	1	1.6E-08	1	TD
-292	-379	325	422	RFM021							
-379	-451	422	503	RFM021		ZFMENE3115	1.7E-06	21	2.2E-06	7	TD
-451	-537	503	601	RFM021			9.6E-09	2	1.5E-08	2	TD
KFR102B											
2.70	**-143**	**0**	**180**								
2.70	-9	12	14	RFM021			-	-	-	-	-
-9	-52	14	67	RFM021			3.9E-06	37	3.6E-06	9	TD
-52	-54	67	70	RFM021		PDZ1 (S-WNW)	8.8E-07	3	8.9E-07	1	TD
-54	-86	70	109	RFM021			4.3E-07	23	5.6E-07	8	TD
-86	-90	109	114	RFM021		ZFMNE3137	1.4E-07	5	1.9E-08	1	TD
-90	-118	114	150	RFM021			2.5E-06	10	8.2E-06	6	TD
-118	-119	150	151	RFM021		PDZ3 (G)	5.0E-06	1			
-119	-137	151	173	RFM021			1.1E-06	8	3.6E-08	3	TD
-137	-143	173	180	RFM021		ZFMNE3112	5.9E-07	2			

Table 4-17. Hydraulic data compilation per interpreted geological domain in core-drilled borehole KFR103. In the table, the first row highlighted in grey represents the entire length of the borehole from the top of the casing to the bottom of the borehole. Dashed red line indicates casing depth. Zup is the upper elevation of the section, Zlow is the lower elevation of the section. Secup and Seclow refer to the depth to top and bottom of the section along the borehole. ΣT PFL_f is the sum of all overlapping PFL transmissivities (PFL_f) and ΣT is the sum of sequential test section transmissivities between Zup and Zlow, n1 and n2 is number of PFL-f anomalies or flowing sections, respectively.

Zup (m)	Zlow (m)	Secup(m)	Seclow(m)	Rock Domain (RFMxxx)	Fracture domain (FFMxxx)	Deformation zone (ZFM / PDZ)	ΣT PFL_f (m^2/s)	n1	ΣT (m^2/s)	n2	Data type
KFR103											
2.61	**-159**	**0**	**201**								
-7	-8	12	13	RFM021			-	-	-	-	-
-8	-17	13	25	RFM021			1.0E-04	5	5.3E-06	2	TD
-17	-19	25	27	RFM021		PDZ1 (S-EW)	2.5E-07	1	3.6E-07	1	TD
-19	-65	27	84	RFM021			5.2E-06	24	6.5E-06	10	TD
-65	-71	84	91	RFM021		PDZ2 (G)	1.6E-05	5	1.5E-05	1	TD
-71	-142	91	180	RFM021			1.9E-07	5	3.7E-07	4	TD
-142	-144	180	183	RFM021		ZFMWNW3262	5.1E-06	3	1.0E-05	1	TD
-144	-159	183	201	RFM021			2.2E-08	1	4.5E-08	1	TD

Table 4-18. Hydraulic data compilation per interpreted geological domain in core-drilled boreholes KFR104. In the table, for each borehole, the first row highlighted in grey represents the entire length of the borehole from the top of the casing to the bottom of the borehole. Dashed red line indicates casing depth. Zup is the upper elevation of the section, Zlow is the lower elevation of the section. Secup and Seclow refer to the depth to top and bottom of the section along the borehole. ΣT PFL_f is the sum of all overlapping PFL transmissivities (PFL_f) and ΣT is the sum of sequential test section transmissivities between Zup and Zlow, n1 and n2 is number of PFL-f anomalies or flowing sections, respectively.

Zup (m)	Zlow (m)	Secup(m)	Seclow(m)	Rock Domain (RFMxxx)	Fracture domain (FFMxxx)	Deformation zone (ZFM / PDZ)	ΣT PFL_f (m^2/s)	n1	ΣT (m^2/s)	n2	Data type
KFR104											
3.01	**-352**	**0**	**455**								
3.01	-4	7	9	RFM021							
-4	-22	9	30	RFM021			1.6E-07	4	9.0E-08	2	TD
-22	-34	30	46	RFM021		ZFMNE3118	1.8E-07	9	1.6E-07	3	TD
-34	-117	46	149	RFM021			4.6E-06	55	4.6E-06	21	TD
-117	-121	149	154	RFM021		ZFMENE3115	3.9E-09	1	3.9E-09	1	TD
-121	-211	154	268	RFM021			4.6E-07	16	4.4E-07	11	TD
-211	-222	268	283	RFM021		ZFMNE3112	1.1E-07	2	1.1E-07	1	TD
-222	-297	283	382	RFM021			6.9E-08	3	6.9E-08	3	TD
-297	-301	382	387	RFM021		ZFMNE3137					
-301	-308	387	396	RFM021							
-308	-352	396	455	RFM021		ZFMWNW3267	1.1E-08	1	1.5E-08	1	TD

Table 4-19. Hydraulic data compilation per interpreted geological domain in core-drilled boreholes KFR105. In the table, for each borehole, the first row highlighted in grey represents the entire length of the borehole from the top of the casing to the bottom of the borehole. Dashed red line indicates casing depth. Zup is the upper elevation of the section, Zlow is the lower elevation of the section. Secup and Seclow refer to the depth to top and bottom of the section along the borehole. ΣT PFL_f is the sum of all overlapping PFL transmissivities (PFL_f) and ΣT is the sum of sequential test section transmissivities between Zup and Zlow, n1 and n2 is number of PFL-f anomalies or flowing sections, respectively.

Zup (m)	Zlow (m)	Secup(m)	Seclow(m)	Rock Domain (RFMxxx)	Fracture domain (FFMxxx)	Deformation zone (ZFM / PDZ)	ΣT PFL_f (m^2/s)	n1	ΣT (m^2/s)	n2	Data type
KFR105											
-106.63	**-156**	**0**	**307**								
-106.63	-107	0	3	RFM021			-	-	-	-	-
-107	-114	3	45	RFM021			1.5E-07	15	1.6E-07	6	TD
-114	-116	45	52	RFM021		ZFMENE3115	6.1E-09	2	1.3E-08	2	TD
-116	-122	52	89	RFM021			3.8E-08	18	3.9E-08	7	TD
-122	-123	89	97	RFM021		ZFMNE3112	2.3E-09	3	2.6E-09	2	TD
-123	-135	97	171	RFM021			8.8E-07	40	1.1E-06	14	TD
-135	-136	171	176	RFM021		ZFMWNW8042	2.7E-07	5	1.1E-07	1	TD
-136	-139	176	191	RFM021			5.1E-08	13	6.1E-08	3	TD
-139	-141	191	205	RFM021		ZFMNE3137	5.4E-09	7	1.1E-08	3	TD
-141	-149	205	258	RFM021			2.2E-08	22	1.5E-08	9	TD
-149	-153	258	283	RFM021		ZFMWNW3267	4.1E-08	11	4.4E-08	4	TD
-153	-154	283	294	RFM021			5.7E-09	5	5.8E-09	2	TD
-154	-156	294	304	RFM021		PDZ5 (S-NW)	1.4E-08	9	1.2E-08	2	TD
-156	-156	304	307	RFM021							

Table 4-20. Hydraulic data compilation per interpreted geological domain in core-drilled boreholes KFR106. In the table, for each borehole, the first row highlighted in grey represents the entire length of the borehole from the top of the casing to the bottom of the borehole. Dashed red line indicates casing depth. Zup is the upper elevation of the section, Zlow is the lower elevation of the section. Secup and Seclow refer to the depth to top and bottom of the section along the borehole. ΣT PFL_f is the sum of all overlapping PFL transmissivities (PFL_f) and ΣT is the sum of sequential test section transmissivities between Zup and Zlow, n1 and n2 is number of PFL-f anomalies or flowing sections, respectively.

Zup (m)	Zlow (m)	Secup(m)	Seclow(m)	Rock Domain (RFMxxx)	Fracture domain (FFMxxx)	Deformation zone (ZFM / PDZ)	ΣT PFL_f (m^2/s)	n1	ΣT (m^2/s)	n2	Data type
KFR106											
1.24	**-279**	**0**	**300**								
1.24	-7	0	9	RFM021							
-7	-62	9	15	RFM021			-	-	-	-	-
-13	-18	15	20	RFM021		PDZ1 (S-NNE)	4.9E-07	1	5.0E-07	1	TD
-18	-33	20	37	RFM021			6.4E-08	1	8.2E-08	1	TD
-33	-48	37	52	RFM021		PDZ2	2.9E-06	5	3.4E-06	2	TD
-48	-62	52	67	RFM021			1.9E-06	6	2.2E-06	3	TD
-62	-67	67	73	RFM021		ZFMWNW3262	2.0E-05	4	1.7E-05	1	TD
-67	-78	73	85	RFM021			4.7E-06	3	1.4E-05	1	TD
-78	-80	85	86	RFM021		PDZ4 (G)	1.5E-05	2	1.8E-05	1	TD
-80	-93	86	101	RFM021			3.0E-07	5	3.2E-07	2	TD
-93	-94	101	101	RFM021		PFZ5 (G)	1.5E-05	1	1.7E-05	1	TD
-94	-142	101	153	RFM021			5.2E-06	17	5.8E-06	9	TD
-142	-146	153	157	RFM021		PDZ6 (G)	2.4E-05	3	2.5E-05	1	TD
-146	-238	157	256	RFM021			3.0E-06	19	4.2E-06	13	TD
-238	-248	256	266	RFM021		ZFMNNW1034	7.6E-06	1	1.1E-05	1	TD
-248	-280	266	300	RFM021							

Table 4-21. Hydraulic data compilation per interpreted geological domain in core-drilled boreholes KFR27. In the table, for each borehole, the first row highlighted in grey represents the entire length of the borehole from the top of the casing to the bottom of the borehole. Dashed red line indicates casing depth. Zup is the upper elevation of the section, Zlow is the lower elevation of the section. Secup and Seclow refer to the depth to top and bottom of the section along the borehole. ΣT PFL_f is the sum of all overlapping PFL transmissivities (PFL_f) and ΣT is the sum of sequential test section transmissivities between Zup and Zlow, n1 and n2 is number of PFL-f anomalies or flowing sections, respectively.

Zup (m)	Zlow (m)	Secup(m)	Seclow(m)	Rock Domain (RFMxxx)	Fracture domain (FFMxxx)	Deformation zone (ZFM / PDZ)	ΣT PFL_f (m^2/s)	n1	ΣT (m^2/s)	n2	Data type
KFR27											
3.06	**-497**	**0**	**502**								
3.06	-9	5	12	RFM021			-	-	-	-	-
-9	-105	12	108	RFM021					9.1E-06	16	TD
-105	-117	108	120	RFM021		PDZ1 (M-EW)			2.3E-08	2	TD
-117	-319	120	323	RFM021			7.2E-06	20	6.8E-06	14	TD
-319	-464	323	469	RFM021		ZFMWNW0835	3.2E-06	44	6.1E-06	17	TD
-464	-496	469	502	RFM021			1.1E-07	1	2.1E-07	1	TD

Table 4-22. Hydraulic data compilation per interpreted geological domain in core-drilled boreholes KFR117-121. In the table, for each borehole, the first row highlighted in grey represents the entire length of the borehole from the top of the casing to the bottom of the borehole. Dashed red line indicates casing depth. Zup is the upper elevation of the section, Zlow is the lower elevation of the section. Secup and Seclow refer to the depth to top and bottom of the section along the borehole. ΣT PFL_f is the sum of all overlapping PFL transmissivities (PFL_f) and ΣT is the sum of sequential test section transmissivities between Zup and Zlow, n1 and n2 is number of PFL-f anomalies or flowing sections, respectively.

Zup (m)	Zlow (m)	Secup(m)	Seclow(m)	Rock Domain (RFMxxx)	Fracture domain (FFMxxx)	Deformation zone (ZFM / PDZ)	ΣT PFL_f (m^2/s)	n1	ΣT (m^2/s)	n2	Data type
KFR117											
2.44	**-172**	**0**	**176**								
-3	-6	6	9	RFM021			-	-	-	-	-
-6	-60	9	63	RFM021					1.1E-04	9	5m TM
-60	-171	63	176	RFM021					2.3E-06	19	5m TM
KFR118											
3.16	**-171**	**0**	**175**								
-6	-9	9	12	RFM021			-	-	-	-	-
-9	-19	12	23	RFM021					6.5E-06	1	5m TM
-19	-33	23	36	RFM021		ZFMENE3115			1.3E-06	3	5m TM
-33	-143	36	147	RFM021					1.2E-05	18	5m TM
-143	-171	147	175	RFM021		PDZ2 (S-NW)			5.1E-09	5	5m TM
KFR119											
3.10		**0**	**176**								
-4	-6	7	9	RFM021			-	-	-	-	-
-6	-90	9	94	RFM021			3.9E-05	29	2.3E-05	14	TD
-90	-102	94	107	RFM021		PDZ1	8.0E-08	2	9.5E-08	1	TD
-102	-159	107	164	RFM021			8.5E-07	4	9.9E-07	4	TD
-159	-170	164	176	RFM021		PDZ2			1.3E-09	2	5m TM
KFR120											
3.19	**-171**	**0**	**177**								
-6	-9	9	12	RFM021			-	-	-	-	-
-9	-57	12	61	RFM021					2.0E-05	8	5m TM
-57	-70	61	74	RFM021		PDZ1 (M-NE)			3.7E-07	2	5m TM
-70	-124	74	130	RFM021					6.4E-07	10	5m TM
-124	-167	130	173	RFM021		PDZ2 (S-NS)			7.8E-08	8	5m TM
-167	-171	173	177	RFM021							
KFR121											
2.87	**-282**	**0**	**363**								
-5	-29	9	41	RFM021			-	-	-	-	-
-29	-67	41	89	RFM021			6.3E-06	32	7.5E-06	10	TD
-67	-76	89	100	RFM021		ZFMWNW3262	2.4E-07	10	4.6E-07	3	TD
-76	-100	100	131	RFM021			1.9E-07	10	5.8E-08	4	TD
-100	-115	131	149	RFM021		PDZ2 (S-NNE)	3.2E-08	1	4.2E-08	1	TD
-115	-174	149	225	RFM021			4.0E-07	29	4.5E-07	14	TD
-174	-181	225	233	RFM021		ZFMWNW0835	5.2E-08	5	1.6E-08	1	TD
-181	-225	233	290	RFM021			3.8E-08	12	9.9E-08	6	TD
-225	-236	290	303	RFM021		ZFMWNW8042	6.4E-08	3	9.6E-09	2	TD
-236	-282	303	363	RFM021			7.5E-06	5	7.5E-06	4	TD

4.14 Core-drilled boreholes with impeller flow logging data

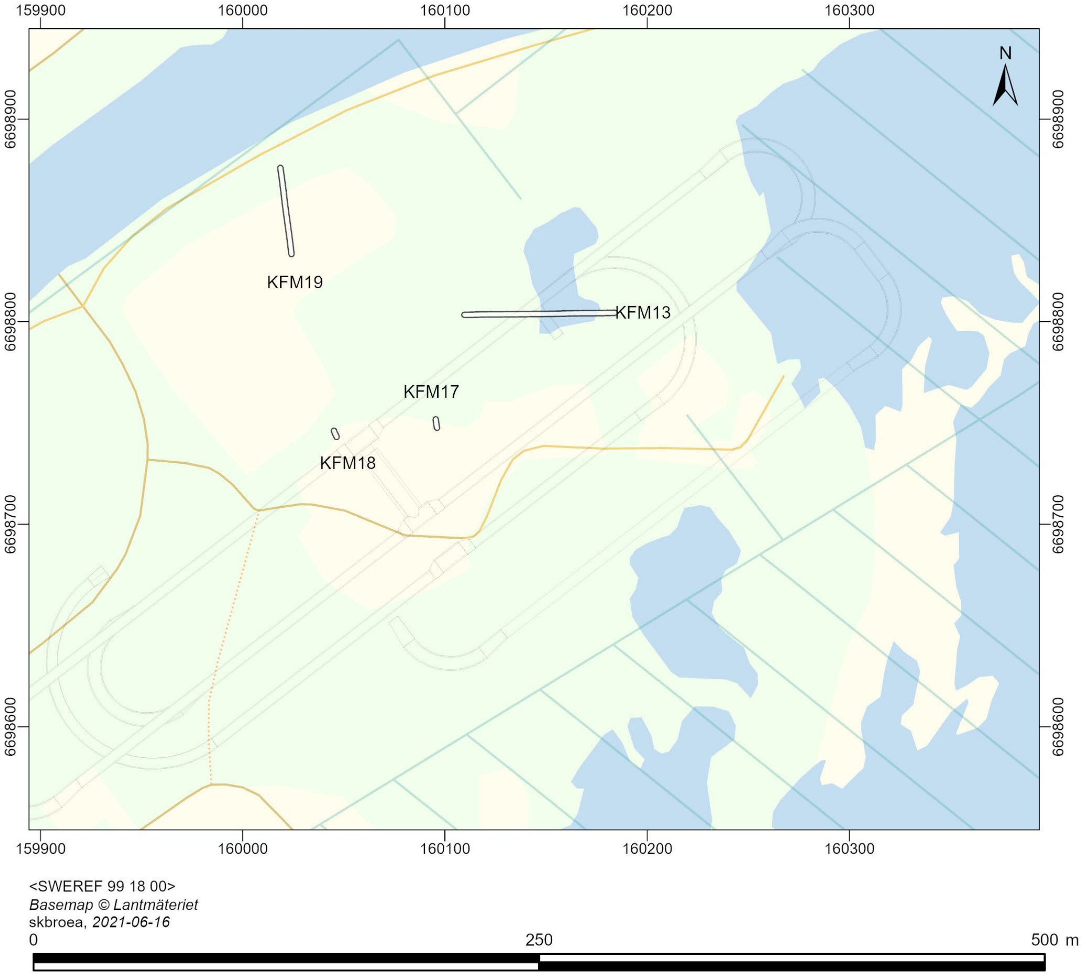

Figure 4-31. *Map of core-drilled boreholes with impeller flow logging data presented in Table 4-23. A potential SFK layout (SYHA 2.0) is shown for reference.*

Table 4-23. Summary of geological data cross referenced with impeller flow logging data (TFa) gathered through hydraulic testing in core-drilled boreholes KFM13, KFM17, KFM18 and KFM19 (Jönsson 2013) In the table, for each borehole, the first row highlighted in grey represents the entire length of the borehole from the top of the casing to the bottom of the borehole. Dashed red line indicates casing depth. Zup is the upper elevation of the section, Zlow is the lower elevation of the section. Secup and Seclow refer to the depth to top and bottom of the section along the borehole. ΣT PFL_f is the sum of all overlapping PFL transmissivities (PFL_f) and ΣT is the sum of sequential test section transmissivities between Zup and Zlow, n1 and n2 is the number of PFL-f anomalies or flowing sections, respectively.

Zup (m)	Zlow (m)	Secup (m)	Seclow (m)	Rock Domain (RFMxxx)	Fracture domain (FFMxxx)	Deformation zone (ZFM / PDZ)	ΣT PFL_f (m^2/s)	n1	ΣT (m^2/s)	n2	Data type
KFM13											
2.98	**-127**	**0**	**150**								
-3	-4	7	8				-	-	-	-	-
-4	-21	8	28		FFM02U				1.1E-04	2	Tfa
-21	-29	28	37		FFM02L						
-29	-40	37	49			ZFMNNW1205A, ZFMNNW1205B					
-40	-127	49	150		FFM01						
KFM17											
4	**-56**	**0**	**60**								
0	-2	4	6		FFM02U		-	-	-	-	-
-2	-20	6	24		FFM02U						
-20	-32	24	36		FFM02L				1.6E-06	2	TFa
-32	-56	36	60		FFM01						
KFM18											
3.65		**0**	**60**								
-4	-5	8	9		FFM02U		-	-	-	-	-
-5	-21	9	25		FFM02U				2.0E-06	4	TFa
-21	-22	25	26		FFM02L				3.6E-07	1	TFa
-22	-56	26	60		FFM01				1.7E-07	2	TFa
KFM19											
2.96	**-90**	**0**	**102**								
-2	-4	5	7		FFM02U		-	-	-	-	-
-3	-90	7	102			ZFMENE1061A			1.2E-04	5	TFa

5 Compilation of transmissivity data acquired from single-hole hydraulic tests in percussion-drilled boreholes

5.1 Overview

Figure 5-1 shows locations of percussion-drilled boreholes at Forsmark, colour coded based on the total transmissivity (T) of each borehole. Table 5-1 compiles T data acquired with the HTHB tests (combined pumping and impeller flow logging) method in 57 percussion-drilled boreholes (47 HFM boreholes and 10 HFR boreholes). For each borehole the first row in Table 5-1, highlighted in grey, shows the top and bottom elevations (Zup/Z_low) and borehole lengths (SECUP/SECLOW); Zup and SECUP start at the borehole casing. Each such row is followed by rows that summarise rock domains (RFMxxx), deformation zones (ZFMxxxx) and fracture domains (FFMxxx) associated with T data from single-hole hydraulic tests.

The geo-structural interpretations in terms of fracture domains (FFMxxx) and deformation zones (ZFMxxx) uses the colour legends of Table 4-1 and Table 4-2, respectively. Possible deformation zones (DZ1, DZ2 and DZ3) are also assigned to the "Deformation zone (ZFMxxx)" column.

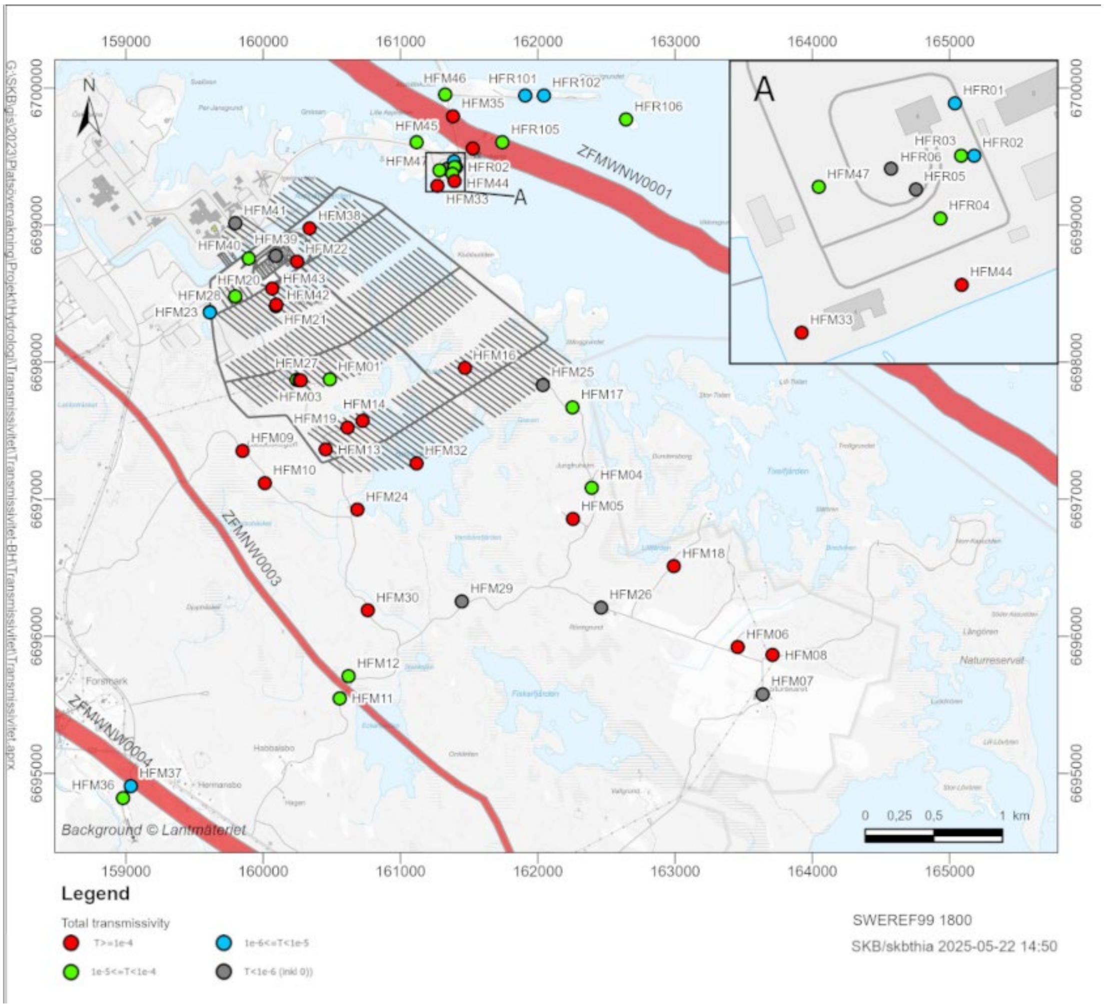

***Figure 5-1.** Locations of percussion-drilled boreholes in Forsmark. The grey dots are boreholes with total T ≤ 1·10^{-6} m^2/s, or boreholes without T data. Blue dots are boreholes with 1·10^{-6} m^2/s < total T < 1·10^{-5} m^2/s, green dots are boreholes with 1·10^{-5} m^2/s < total T < 1·10^{-4} m^2/s, and red dots are boreholes with total T ≥ 1·10^{-4} m^2/s.*

Table 5-1. Compilation of HTHB T data gathered in HFM01–47, HFR01–06, HFR101, HFR102, HFR105 and HFR106.[2]

BOREHOLE ID	Zup (m)	Zlow (m)	Secup (m)	Seclow (m)	Rock domain (RFMxxx)	Fracture domain (FFMxxx)	Deformation zone (ZFMxxxx)	ΣT HTHB[1] (m^2/s)
HFM01	**2**	**-195**	**0**	**200**				-
HFM01	-28	-32	31	35	RFM029R	FFM02		Low yield
HFM01	-32	-41	35	44	RFM029R		ZFMA2	4.5E-05
HFM01	-41	-192	44	197	RFM029R	FFM02		1.9E-05
HFM02	**3**	**-97**	**0**	**100**				-
HFM02	-22	-39	25	42	RFM029R	FFM02		Low yield
HFM02	-39	-44	42	47	RFM029R		ZFMA2	5.9E-04
HFM02	-44	-96	47	99	RFM029R	FFM02		Low yield
HFM03	**3**	**-23**	**0**	**26**				-
HFM03	3	-10	0	13	RFM029R			Low yield
HFM03	-10	-20*	13	23	RFM029R	FFM02U		4.2E-04
HFM03	-20	-23	23	26	RFM029R	FFM02L		Low yield
HFM04	**4**	**-214**	**0**	**222**				-
HFM04	-8	-57	12	61	RFM029R	FFM03		Low yield
HFM04	-57	-60	61	64	RFM029R		ZFM866	7.9E-05
HFM04	-60	-177	64	183	RFM029R	FFM03		Low yield
HFM04	-177	-181	183	187	RFM029R		ZFMA3	Low yield
HFM04	-181	-214	187	222	RFM029R	FFM03		Low yield
HFM05	**8**	**-190***	**0**	**200**				-
HFM05	-4	-144	12	153	RFM029R	FFM03		Low yield
HFM05	-144	-145	153	154	RFM029R		ZFM866	4.0E-04
HFM05	-145	-189	154	199	RFM029R	FFM03		Low yield
HFM06	**7**	**-103***	**0**	**111**				-
HFM06	-4	-54	11	61	RFM029R	FFM03		1.0E-04
HFM06	-54	-64	61	71	RFM029R		ZFMA5	2.3E-04
HFM06	-64	-100	71	108	RFM029R	FFM03		Low yield
HFM07	**6**	**-116***	**0**	**123**				Low yield
HFM07	-5	-48	11	54	RFM029R	FFM03		Low yield
HFM07	-48	-60	54	66	RFM029R		ZFMA6	Low yield
HFM07	-60	-102	66	109	RFM029R	FFM03		Low yield
HFM08	**7**	**-135***	**0**	**144**				-
HFM08	-10	-128	17	136	RFM029R	FFM03		5.7E-05
HFM08	-128	-133	136	141	RFM029R		ZFMA5	1.2E-03
HFM08	-133	-134	141	142	RFM029R	FFM03		Low yield
HFM09	**5**	**-41***	**0**	**50**				-
HFM09	-11	-11	17	18	RFM018	FFM04		Low yield
HFM09	-11	-21	18	28	RFM018		ZFMENE0060A	3.3E-04

[2]Low yield means that the borehole was too dry to be tested. A zero transmissivity means that the impeller logging could not detect any flow above the measurement limit.
*Zup or Zlow values are predicted from nearest points along the borehole.
**Sections are taken from the model version 2.2 (Follin et. al. 2007b).
*** No SHI and/or no HTHB data are available.

BOREHOLE ID	Zup (m)	Zlow (m)	Secup (m)	Seclow (m)	Rock domain (RFMxxx)	Fracture domain (FFMxxx)	Deformation zone (ZFMxxxx)	ΣT HTHB[1] (m^2/s)
HFM09	-21	-41	28	50	RFM018	FFM04		4.7E-05
HFM10	**5**	**-134**	**0**	**150**				-
HFM10	-6	-55	12	65	RFM018	FFM04		
HFM10	-55	-59	65	69	RFM018		DZ2	
HFM10	-59	-96	69	108	RFM018	FFM04		
HFM10	-96	-104	108	117	RFM018		DZ1	3.1E-04
HFM10	-104	-133	117	149	RFM018	FFM04		
HFM11	**8**	**-118**	**0**	**182**				-
HFM11	-1	-53	12	83	RFM026	FFM04		2.3E-05
HFM11	-53	-104	83	160	RFM026		ZFMNW0003	2.8E-05
HFM11	-104	-118*	160	182	RFM026	FFM04		Low yield
HFM12	**7**	**-137***	**0**	**210**				-
HFM12**	-4	-60	15	91	RFM026	FFM04		6.4E-6
HFM12**	-60	-118	91	179	RFM026		ZFMNW0003	7.9E-6
HFM12**	-118	-136	179	209	RFM026	FFM04		Low yield
HFM13	**6**	**-147**	**0**	**176**				-
HFM13	-7	-135	15	162	RFM029R	FFM03		2.1E-05
HFM13	-135	-146*	162	175	RFM029R		ZFMENE0401A	2.9E-04
HFM14	**4**	**-127**	**0**	**151**				-
HFM14	1*	-18*	3	25	RFM029R	FFM02U		2.5E-04
HFM14	-18	-56	25	68	RFM029R	FFM02L		1.8E-04
HFM14	-56	-63	68	76	RFM029R		ZFMA2	1.7E-04
HFM14	-63	-77	76	92	RFM029R	FFM02L		Low yield
HFM14	-77	-87	92	104	RFM029R		ZFMA2	2.6E-04
HFM14	-87	-126	104	149	RFM029R	FFM02L		0.0
HFM15	**4**	**-65**	**0**	**100**				-
HFM15	1	-15*	4	27	RFM029R	FFM02U		6.9E-05
HFM15	-15*	-56	27	86	RFM029R	FFM02L		1.5E-04
HFM15	-56	-63	86	96	RFM029R		ZFMA2	1.0E-04
HFM15	-63	-65	96	99	RFM029R	FFM02L		Low yield
HFM16	**3**	**-128**	**0**	**133**				-
HFM16	-9	-67	12	71	RFM029R		ZFMA8	5.3E-04
HFM16	-67	-126	71	130	RFM029R	FFM02		Low yield
HFM17	**4**	**-204**	**0**	**211**				-
HFM17**	-4	-202	8	209	RFM029R	FFM03		3.9E-05
HFM18	**5**	**-143**	**0**	**181**				-
HFM18	-2	-4	9	11	RFM017		DZ1	Low yield
HFM18	-4	-20	11	30	RFM017	FFM03		Low yield
HFM18	-20	-25	30	36	RFM029R	FFM03		Low yield
HFM18	-25	-36	36	49	RFM029R		ZFMA4	1.6E-04
HFM18	-36	-94	49	119	RFM029R	FFM03		Low yield
HFM18	-94	-117	119	148	RFM029R		ZFMNE0065, ZFMA7	Low yield
HFM18	-117	-142	148	180	RFM029R	FFM03		Low yield

Table 5-1. Cont'd.

BOREHOLE ID	Zup (m)	Zlow (m)	Secup (m)	Seclow (m)	Rock domain (RFMxxx)	Fracture domain (FFMxxx)	Deformation zone (ZFMxxxx)	ΣT HTHB (m^2/s)
HFM19	**4**	**-144**	**0**	**185**				-
HFM19	-6	-94	11	121	RFM029R	FFM03		4.0E-05
HFM19	-94	-115	121	148	RFM029R		ZFMA2	1.6E-05
HFM19**	-115	-131	148	168	RFM029R	FFM02		6.2E-06
HFM19	-131	-144	168	185	RFM029R		ZFMA2	2.8E-04
HFM20	**3**	**-297**	**0**	**301**				-
HFM20	-9	-24*	12	27	RFM029R	FFM02U		5.7E-05
HFM20	-24*	-133*	27	136	RFM029R	FFM02L		1.2E-05
HFM20	-133	-297	136	301	RFM029R	FFM01		Low yield
HFM21	**4**	**-153**	**0**	**202**				-
HFM21	-6	-20*	12	28	RFM029R	FFM02U		1.0E-04
HFM21	-20*	-74	28	94	RFM029R	FFM02L		7.0E-05
HFM21	-74	-80	94	102	RFM029R		ZFM1203	3.0E-04
HFM21	-80	-124	102	160	RFM029R	FFM02L		
HFM21	-124	-136	160	177	RFM029R		DZ2	
HFM21	-136	-153	102	202	RFM029R	FFM02L		2.1E-04
HFM22	**2**	**-155**	**0**	**222**				-
HFM22	-9	-86	12	110	RFM029R	FFM01		1.6E-04
HFM22	-86	-99	110	129	RFM029R		ZFMENE2120	Low yield
HFM22	-99	-152	129	216	RFM029R	FFM01		Low yield
HFM23	**4**	**-73**	**0**	**212**				-
HFM23	-13	-17	21	26	RFM029R	FFM02		Low yield
HFM23	-17	-30	26	42	RFM029R		ZFMENE1208A	4.3E-06
HFM23	-30	-55	42	82	RFM029R	FFM02		Low yield
HFM23	-55	-62	82	95	RFM029R		ZFMNNW0100	Low yield
HFM23	-62	-75	95	146	RFM029R	FFM02		Low yield
HFM23	-75	-76	146	166	RFM044	FFM05		Low yield
HFM23	-76	-76	166	169	RFM044		DZ3	Low yield
HFM23	-76	-76	169	181	RFM044	FFM05		Low yield
HFM24	**4**	**-129**	**0**	**151**				-
HFM24	-12	-23	18	32	RFM029R		ZFMWNW0123	3.0E-05
HFM24**	-23	-32	32	42	RFM029R	FFM04		Low yield
HFM24	-32	-50	42	63	RFM029R		ZFMWNW0123	8.0E-05
HFM24**	-50	-54	63	67	RFM029R	FFM04		Low yield
HFM24	-54	-85	67	103	RFM029R		ZFMWNW0123	Low yield
HFM24	-85	-129	103	151	RFM029R	FFM03		Low yield
HFM25	**4**	**-134***	**0**	**188**				-
HFM25	-4	-26	9	36	RFM029R		DZ1	Low yield
HFM25	-26	-31	36	42	RFM029R	FFM03		Low yield
HFM25	-31	-41	42	54	RFM029R		DZ2	Low yield
HFM25	-41	-61	54	80	RFM029R	FFM03		Low yield
HFM25	-61	-70	80	92	RFM029R		DZ3	Low yield
HFM25	-70	-105	92	143	RFM029R	FFM03		Low yield
HFM25	-105	-113	143	155	RFM029R		ZFMENE0062A	Low yield
HFM25	-113	-122	155	169	RFM029R	FFM03		Low yield
HFM25	-122	-134	169	187	RFM029R		ZFMENE0062A	Low yield
HFM26	3	-144	0	203				-
HFM26	-7	-33	12	46	RFM029R		ZFMA4	Low yield

Table 5-1. Cont'd.

BOREHOLE ID	Zup (m)	Zlow (m)	Secup (m)	Seclow (m)	Rock domain (RFMxxx)	Fracture domain (FFMxxx)	Deformation zone (ZFMxxxx)	ΣT HTHB (m^2/s)
HFM26**	-33	-44	46	60	RFM029R	FFM03		Low yield
HFM26	-44	-70	60	95	RFM029R		ZFMA4	Low yield
HFM26**	-70	-116	95	161	RFM029R	FFM03		Low yield
HFM26	-116	-144	161	203	RFM029R		ZFMNE0065	Low yield
HFM27	**3**	**-115***	**0**	**128**				-
HFM27	-9	-21	12	26	RFM029R	FFM02U		1.3E-05
HFM27	-21	-25	26	30	RFM029R		ZFMA2	2.3E-05
HFM27	-25	-39	30	45	RFM029R	FFM02L		
HFM27	-39	-55	45	63	RFM029R		DZ2	4.0E-05
HFM27	-55	-105	63	117	RFM029R	FFM02L		
HFM27	-105	-111	117	123	RFM029R		ZFMNNW0404	6.7E-06
HFM27	-111	-115	123	127	RFM029R	FFM02L		Low yield
HFM28	**4**	**-144**	**0**	**151**				-
HFM28	-8	-60	12	65	RFM029R		ZFMENE1208A	Low yield
HFM28	-60	-141	65	148	RFM029R	FFM02		Low yield
HFM29	**5**	**-178**	**0**	**200**				-
HFM29**	-3	-12	9	19	RFM029R	FFM03		Low yield
HFM29	-12	-17	19	25	RFM029R		ZFMWNW0123	Low yield
HFM29**	-17	-49	25	62	RFM029R	FFM03		Low yield
HFM29	-49	-67	62	81	RFM029R		ZFMWNW0123	Low yield
HFM29**	-67	-127	81	146	RFM029R	FFM03		Low yield
HFM29	-127	-131	146	150	RFM029R		ZFMWNW0123	Low yield
HFM29**	-131	-178	150	200	RFM029R	FFM03		Low yield
HFM30	**3**	**-170**	**0**	**201**				-
HFM30	-12	-63	18	79	RFM018	FFM04		6.9E-06
HFM30	-63	-170	79	201	RFM018		ZFMNW0017	1.3E-04
HFM31	**6**	**-177***	**0**	**201**				-
HFM31**	-2	-176	9	200	RFM025	FFM04		Low yield
HFM32	**1**	**-198***	**0**	**203**				-
HFM32	-7	-129	8	132	RFM029R			9.4E-04
HFM32	-5	-198	6	203	RFM029R	FFM03		9.5E-04
HFM33	**3**	**-110**	**0**	**140**				-
HFM33	-8*	-110*	12	140	RFM032	FFM05		4.7E-04
HFM34	**3**	**-161**	**0**	**201**				-
HFM34	-8	-29	12	37	RFM021	FFM05		8.9E-04
HFM34	-29	-110*	37	133	RFM021		ZFMWNW0001	2.1E-04
HFM34	-110*	-146	133	180	RFM021	FFM05		Low yield
HFM34	-146	-149*	180	184	RFM021		ZFMWNW0001, ZFMNW0002	Low yield
HFM34	-149*	-151,79*	184	188	RFM021	FFM05		Low yield
HFM34	-152*	-155	188	192	RFM021		ZFMWNW0001, ZFMNW0002	Low yield

Table 5-1. Cont'd.

BOREHOLE ID	Zup (m)	Zlow (m)	Secup (m)	Seclow (m)	Rock domain (RFMxxx)	Fracture domain (FFMxxx)	Deformation zone (ZFMxxxx)	Σ T HTHB (m^2/s)
HFM35	**2**	**-150**	**0**	**201**				-
HFM35	-8	-18	12	24	RFM021	FFM05		Low yield
HFM35	-18	-26*	24	33	RFM021		ZFMWNW0001, ZFMNW0002	Low yield
HFM35	-26*	-37*	33	47	RFM021	FFM05		Low yield
HFM35	-37*	-41	47	53	RFM021		ZFMWNW0001, ZFMNW0002	Low yield
HFM35	-41	-81	53	104	RFM021	FFM05		Low yield
HFM35	-81	-150	104	200	RFM021		ZFMWNW1035	1.2E-04
HFM35	-150	-150	200	201	RFM021	FFM05		Low yield
HFM36	**9**	**-110**	**0**	**153**				-
HFM36	-2*	-26	12	42	RFM030			2.4E-05
HFM36	-26	-106	42	147	RFM030		DZ1	
HFM36	-106	-110*	147	152	RFM030			
HFM37	**12**	**-159**	**0**	**192**				-
HFM37	-2	-154	16	186				9.4E-06
HFM37	4*	-1*	9	15	RFM030			-
HFM37	-1*	-8*	15	23	RFM030		ZFMWNW0004	-
HFM37	-8*	-52*	23	72	RFM030			-
HFM37	-52*	-80*	72	104	RFM030		ZFMWNW0004	-
HFM37	-80*	-103*	104	130	RFM030			-
HFM37	-103*	-159*	130	191	RFM030		ZFMWNW0004	-
HFM38	**2**	**-141**	**0**	**201**				-
HFM38	-5	-28*	9	38	RFM029R	FFM02U-above FFM06		8.2E-05
HFM38	-28*	-40	38	54	RFM029R	FFM02L-above FFM06		Low yield
HFM38	-40	-108	54	149	RFM029R	FFM06		Low yield
HFM38	-108	-118	149	164	RFM029R		ZFMNNE2312	Low yield
HFM38	-118	-137	164	195	RFM029R	FFM06		4.8E-05
HFM39	**4**	**-145**	**0**	**151**				-
HFM39***	-2	-145	6	151	RFM029R			3.3E-07
HFM40	**3**	**-98**	**0**	**102**				-
HFM40***	-4	-98	6	102	RFM029R			5.7E-05
HFM41***	**4**	**-97**	**0**	**102**				-
HFM42	**4**	**-191**	**0**	**195**				-
HFM42	-2*	-84*	6	89	RFM029R	FFM01		Low yield
HFM42	-84*	-92*	89	96	RFM029R		ZFM1203	1.5E-04
HFM42	-92*	-191	96	195	RFM029R	FFM01		5.3E-04
HFM43	**4**	**-195**	**0**	**200**				-
HFM43	-2*	-195*	6	200	RFM029R	FFM01		8.7E-04
HFM44	**3**	**-196**	**0**	**200**				-
HFM44	-6*	-158*	9	162	RFM043	FFM05		
HFM44	-158	-164	162	168	RFM043		DZ1	4.2E-04
HFM44	-164	-169	168	200	RFM043	FFM05		

Table 5-1. Cont'd.

BOREHOLE ID	Zup (m)	Zlow (m)	Secup (m)	Seclow (m)	Rock domain (RFMxxx)	Fracture domain (FFMxxx)	Deformation zone (ZFMxxxx)	ΣT HTHB (m^2/s)
HFM45	**4**	**-196**	**0**	**200**				**-**
HFM45	-2*	-162*	6	166	RFM021	FFM05		2.4E-05
HFM45	-162*	-196*	166	200	RFM043	FFM05		4.6E-06
HFM46	**2**	**-197**	**0**	**200**				
HFM46	-4*	-79	6	81	RFM021	FFM05		6.0E-05
HFM46	-79	-85	81	87	RFM021		DZ1	
HFM46	-85	-135	87	137	RFM021	FFM05		2.0E-05
HFM46	-135	-141	137	144	RFM021		DZ2	
HFM46	-141	-161	144	164	RFM021	FFM05		
HFM46	-161	-183	164	187	RFM021		DZ3	
HFM46	-183	-197	187	200	RFM021	FFM05		9.0E-06
HFM47***	**4**	**-173**	**0**	**200**				-
HFM47	-9	-173	12	200	RFM043	FFM05		-
HFR01***	**1**	**-12**	**0**	**13**	**RFM021**	FFM05		-
HFR01	-	-12	2	13	RFM021	FFM05		6.1E-05
HFR02***	1	-11	0	12	RFM021	FFM05		-
HFR02	-	-11	7	12	RFM021	FFM05		5.0E-06
HFR03***	1	-8	0	8	RFM021	FFM05		
HFR03	-	-8	5	8	RFM021	FFM05		1.0E-06
HFR04***	0	-7	0	7	RFM021	FFM05		-
HFR04	-	-	4	7	RFM021	FFM05		6.6E-05
HFR05***	0	-7	0	7	RFM021	FFM05		-
HFR05	-	-7	4	7	RFM021	FFM05		5.7E-05
HFR06***	1	-10	0	11	RFM021	FFM05		-
HFR06	-	-10	6	11	RFM021	FFM05		7.8E-06
HFR101	**3**	**-187**	**0**	**209**				-
HFR101	-5	-51*	8	58	RFM021		ZFMNE0870	Low yield
HFR101	-51*	-90	58	101	RFM021			2.6E-06
HFR101	-90	-103	101	115	RFM021		DZ2	
HFR101	-103	-170	115	190	RFM021			
HFR101	-170	-180	190	202	RFM021		ZFMNE3118	2.5E-07
HFR101	-180	-186	202	208	RFM021			0.0
HFR102	**3**	**-44**	**0**	**55**				-
HFR102	-5	-44	9	55	RFM021			2.8E-06
HFR105	**3**	**-178**	**0**	**201**				-
HFR105	-15	-24*	21	31	RFM021		ZFMWNW0001	Low yield
HFR105	-24*	-75*	31	88	RFM021	FFM05		5.7E-06
HFR105	-75*	-79	88	92	RFM021		ZFMWNW0001	6.0E-06
HFR105	-79	-104	92	119	RFM021	FFM05		Low yield
HFR105	-104	-129	119	147	RFM021		ZFMWNW1035	1.1E-05
HFR105	-129	-177	147	200	RFM021	FFM05		Low yield
HFR106	**1**	**-153***	**0**	**190**				-
HFR106	-6	-30	9	38	RFM021			3.1E-05
HFR106	-30	-32	38	40	RFM021		DZ1	
HFR106	-32	-127	40	158	RFM021			
HFR106	-127	-130*	158	162	RFM021		ZFMNNW1034	Low yield
HFR106	-130*	-142	162	177	RFM021			Low yield
HFR106	-142	-146	177	182	RFM021		ZFMNNW1034	2.1E-05
HFR106	-146	-153	182	190	RFM021			Low yield

5.2 Summary of HTHB transmissivity data

Figure 5-2 (HFM boreholes) and Figure 5-3 (HFR boreholes) are histograms that shows borehole lengths for the percussion-drilled boreholes in Forsmark. In the Figure 5-4 to Figure 5-27, data of HTHB flow anomalies and transmissivity, pumping test data, and injection test data are shown together with total borehole length, regolith length and casing length. The blue line in each plot represents the borehole length. Its assigned position on the x-axis, "1E-6", is arbitrarily chosen. Each transmissivity value is presented with the length along the borehole of the measured section. Figure 5-28 shows all the "low yield" boreholes without HTHB flow anomalies, or in which total $T < 10^{-6}$ m^2/s where the 10^{-6} m^2/s is an approximate lower measurement limit for the method.

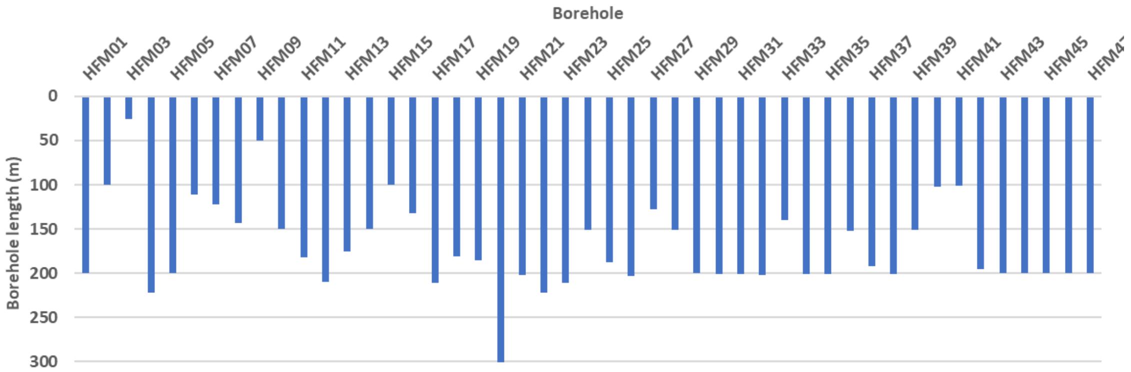

Figure 5-2. Borehole lengths of HFM percussion-drilled boreholes in Forsmark (for visibility, only odd borehole ID's are shown).

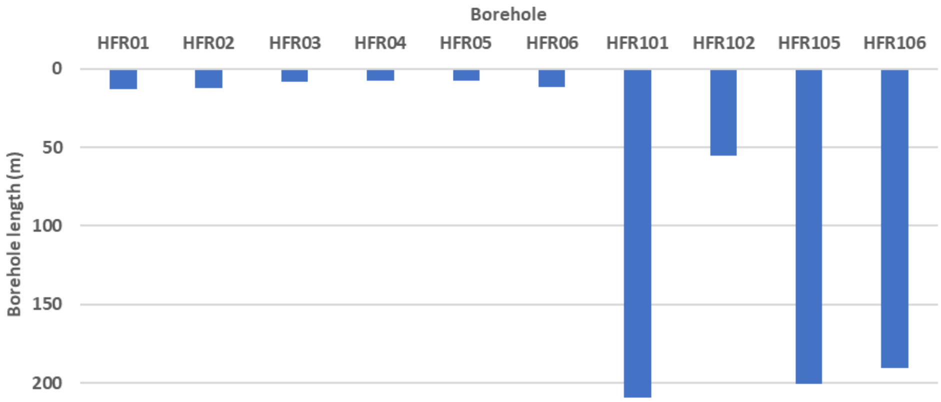

Figure 5-3. Borehole lengths of the HFR percussion-drilled boreholes in Forsmark.

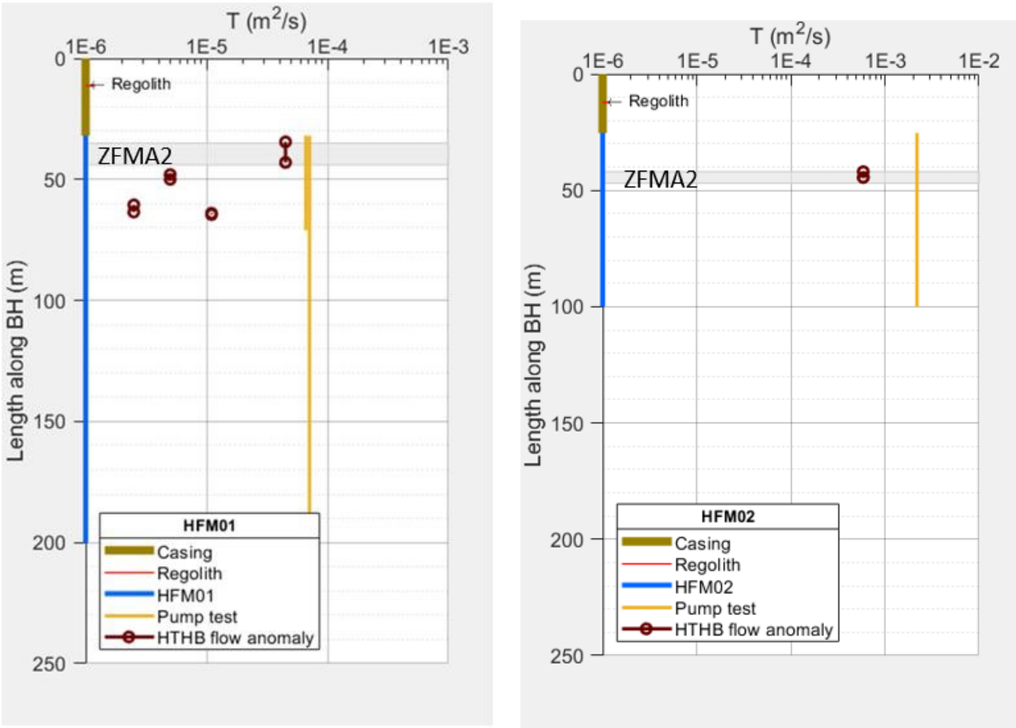

Figure 5-4. *HTHB T acquired in HFM01 (left) and HFM02 (right). Shaded areas indicate modelled deformation zone ZFMA2 (35–44 m in HFM01 and 42–47 m in HFM02).*

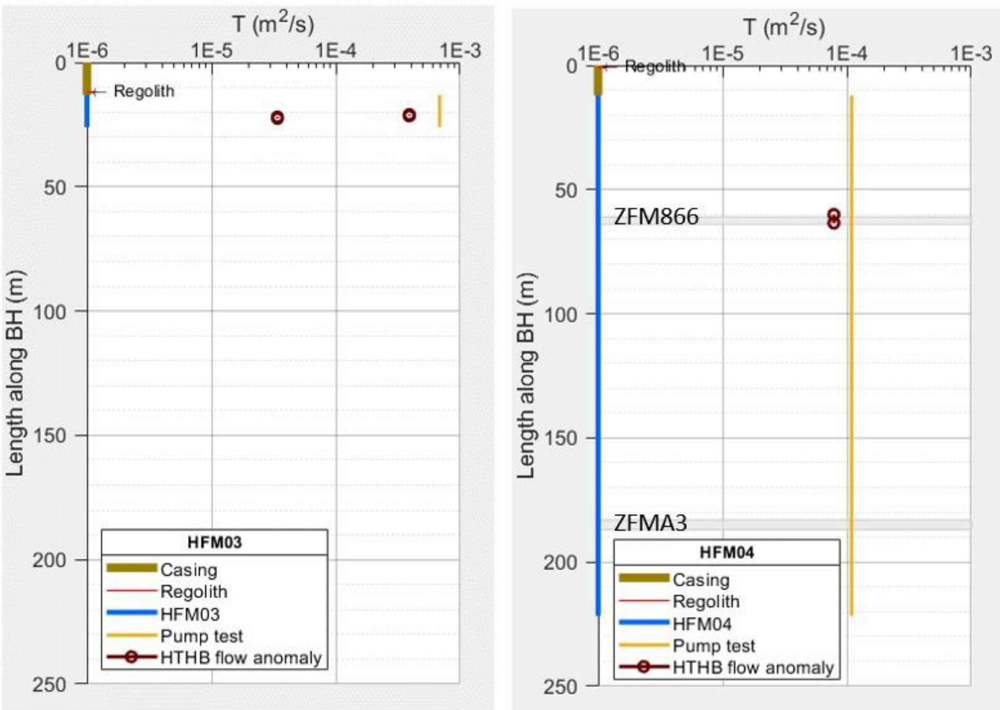

Figure 5-5. *HTHB T acquired in HFM03 (left) and HFM04 (right). Shaded areas indicate modelled deformation zones ZFM866 (61–64 m) and ZFMA3 (183–187 m).*

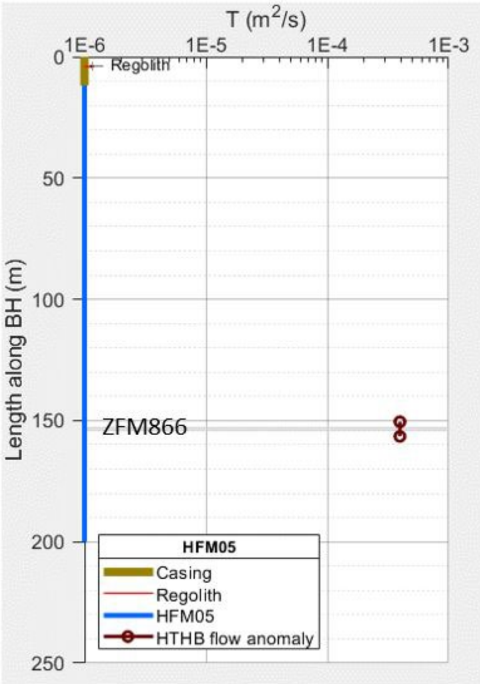

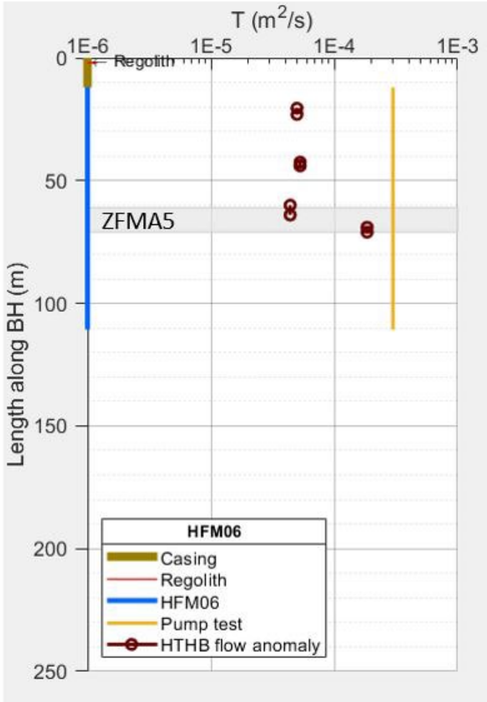

Figure 5-6. *HTHB T acquired in HFM05 (left) and HFM06 (right). Shaded areas indicate modelled deformation zones ZFM866 (153–154 m) and ZFMA5 (61–71 m).*

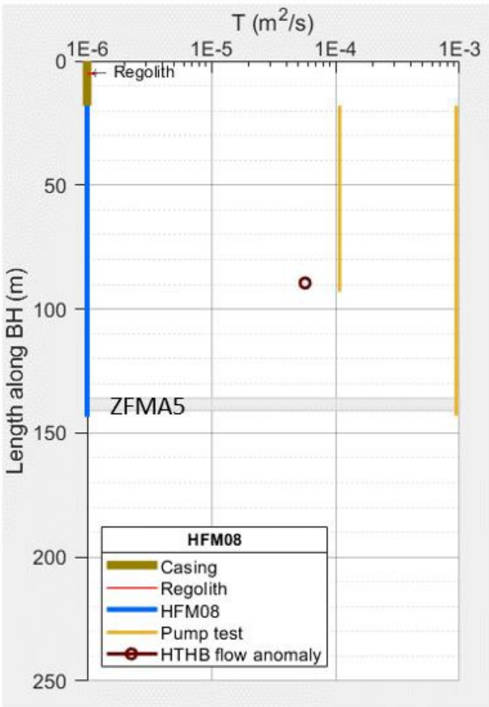

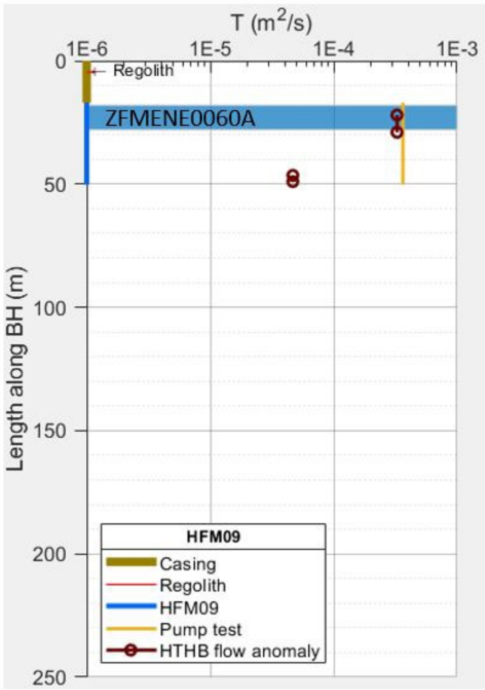

Figure 5-7. *HTHB T acquired in HFM08 (left) and HFM09 (right). Shaded areas indicate modelled deformation zones ZFMA5 (136–141 m) and ZFMENE0060A (18–28 m).*

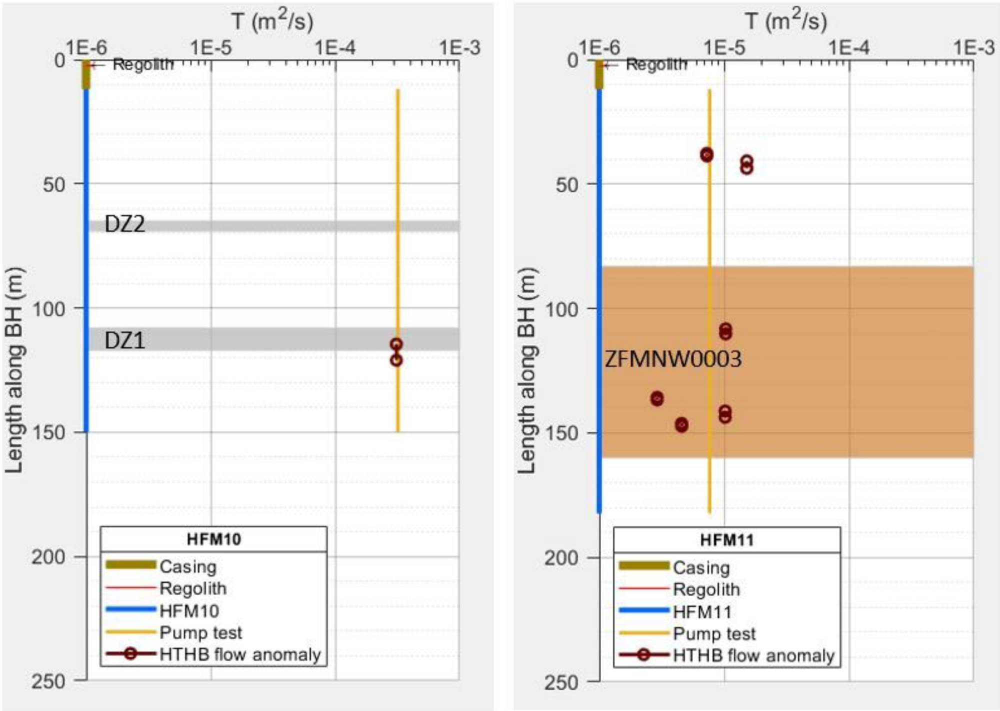

Figure 5-8. *HTHB T acquired in HFM10 (left) and HFM11 (right). Shaded areas indicate possible deformation zones DZ2 (65–69 m), DZ1 (108–117 m), and modelled deformation zone ZFMNW0003 (83–160 m).*

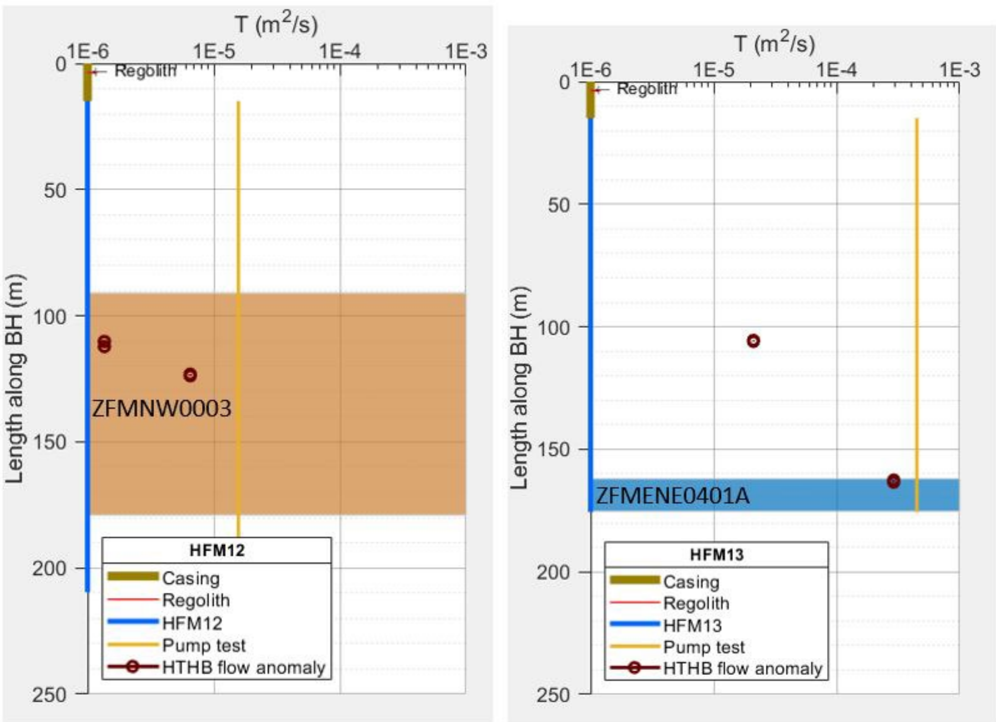

Figure 5-9*. HTHB T acquired in HFM12 (left) and HFM13 (right). Shaded areas indicate modelled deformation zones ZFMNW0003 (91–179 m) and ZFMENE0401A (162–175 m).*

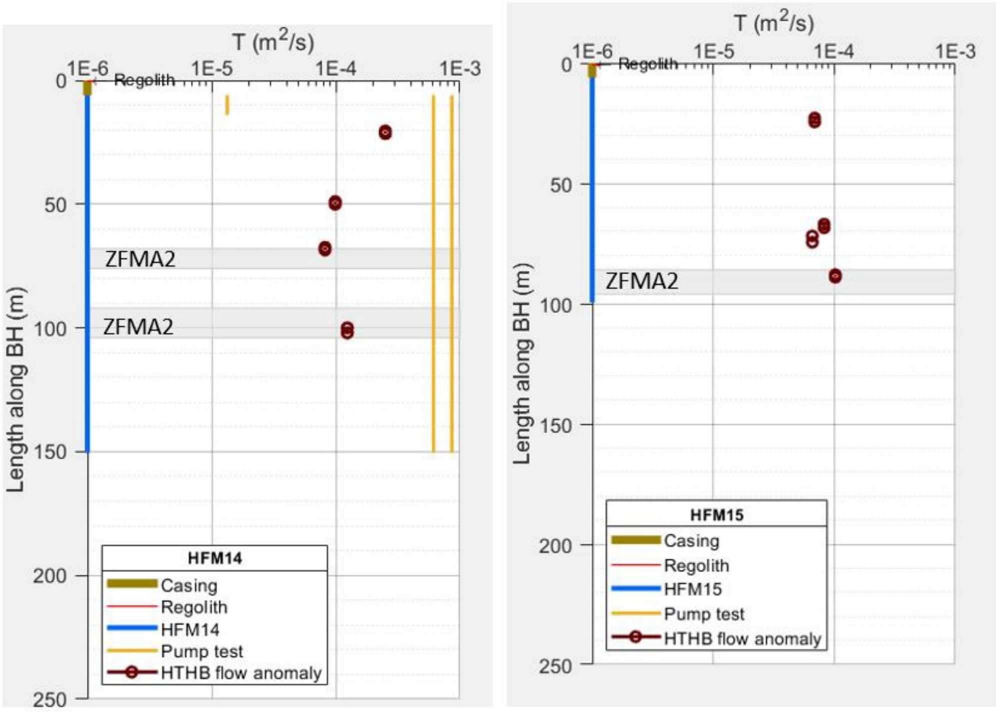

Figure 5-10. *HTHB T acquired in HFM14 (left) and HFM15 (right). Shaded areas indicate modelled deformation zone ZFMA2 (68–76 m and 92–104 m in HFM14 and 86–96 m in HFM15).*

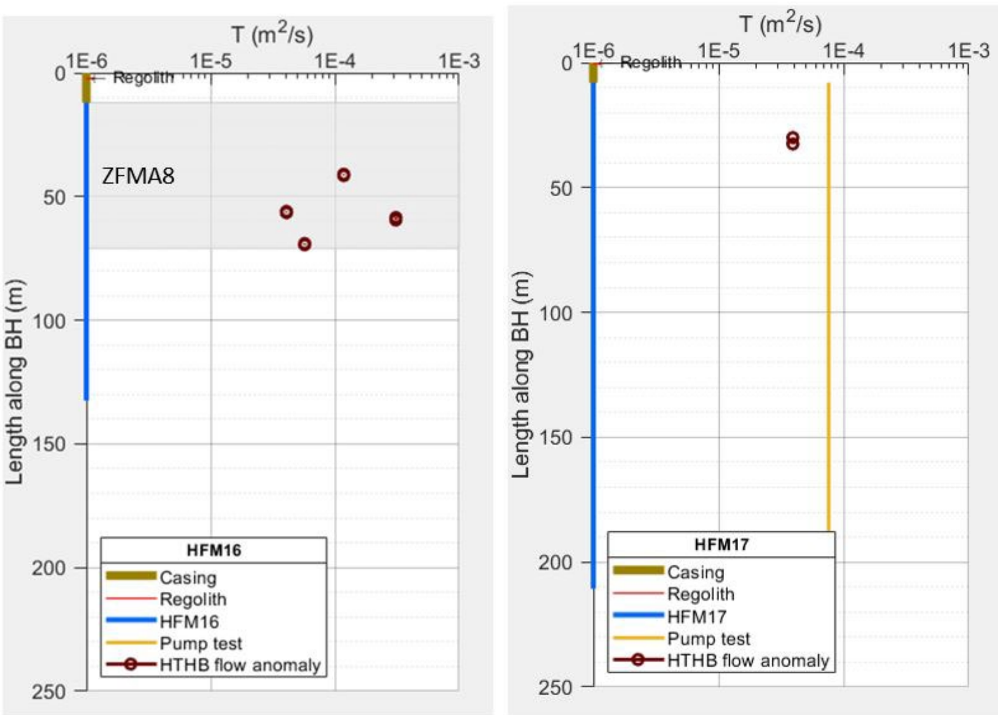

Figure 5-11. *HTHB T acquired in HFM16 (left) and HFM17 (right). Shaded area indicates modelled deformation zone ZFMA8 (12–71 m).*

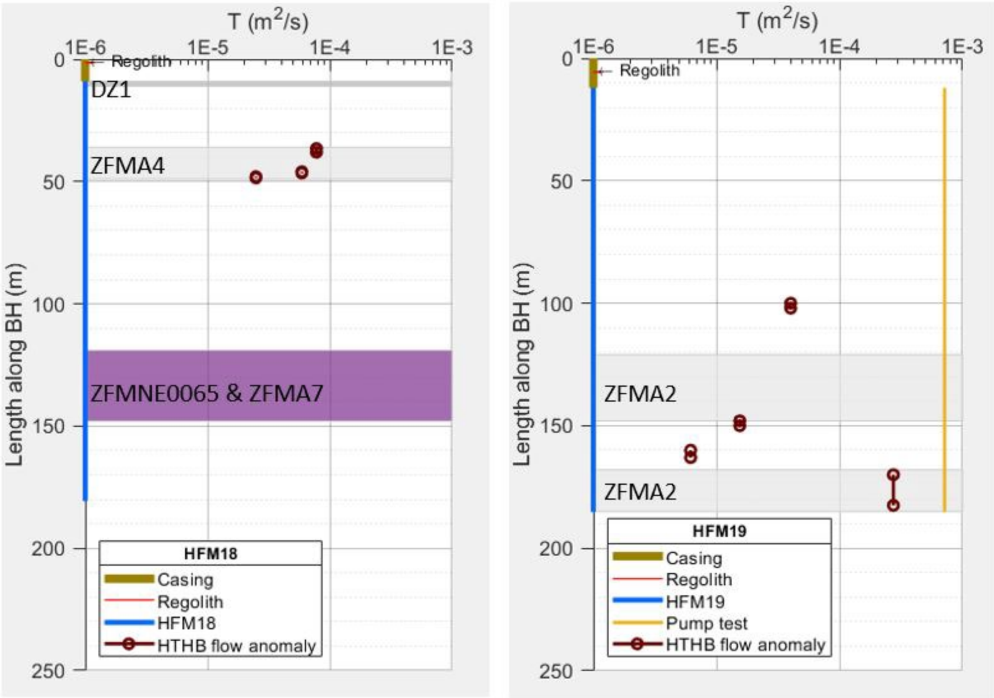

Figure 5-12. *HTHB T acquired in HFM18 (left) and HFM19 (right). Shaded areas indicate possible deformation zone DZ1 (9–11 m), and modelled deformation zones ZFMA4 (36–49 m), ZFMNE0065 and ZFMA7 (119-148 m) in HFM18 and ZFMA2 (121-148 m and 168-185 m) in HFM19.*

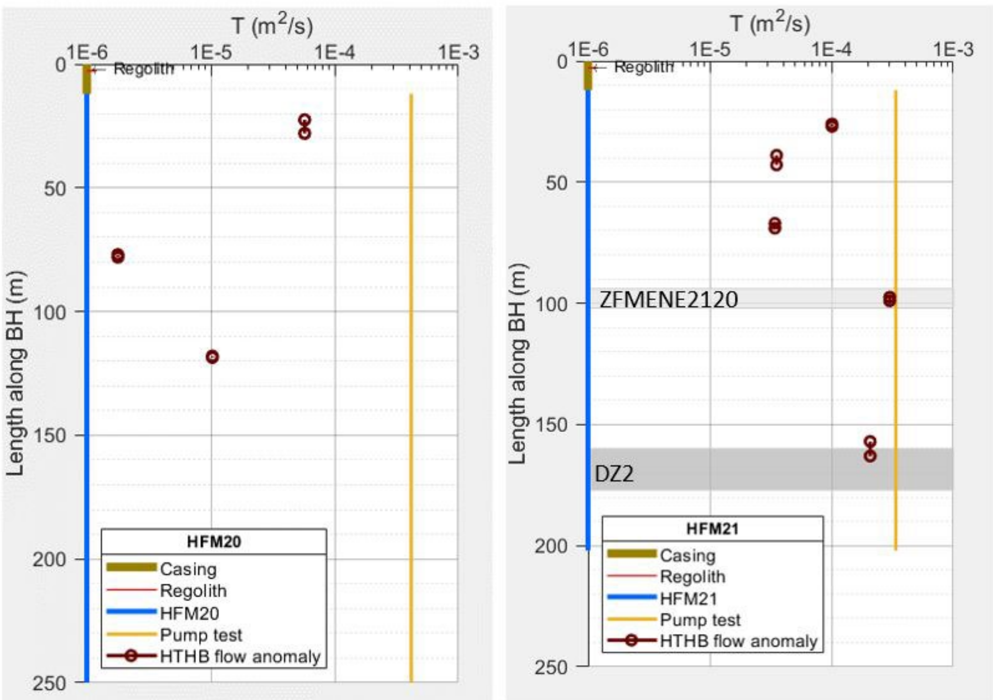

Figure 5-13*. HTHB T acquired in HFM20 (left) and HFM21 (right). Shaded areas indicate modelled deformation zone ZFMENE2120 (110–129 m) and possible deformation zone DZ2 (160–177 m).*

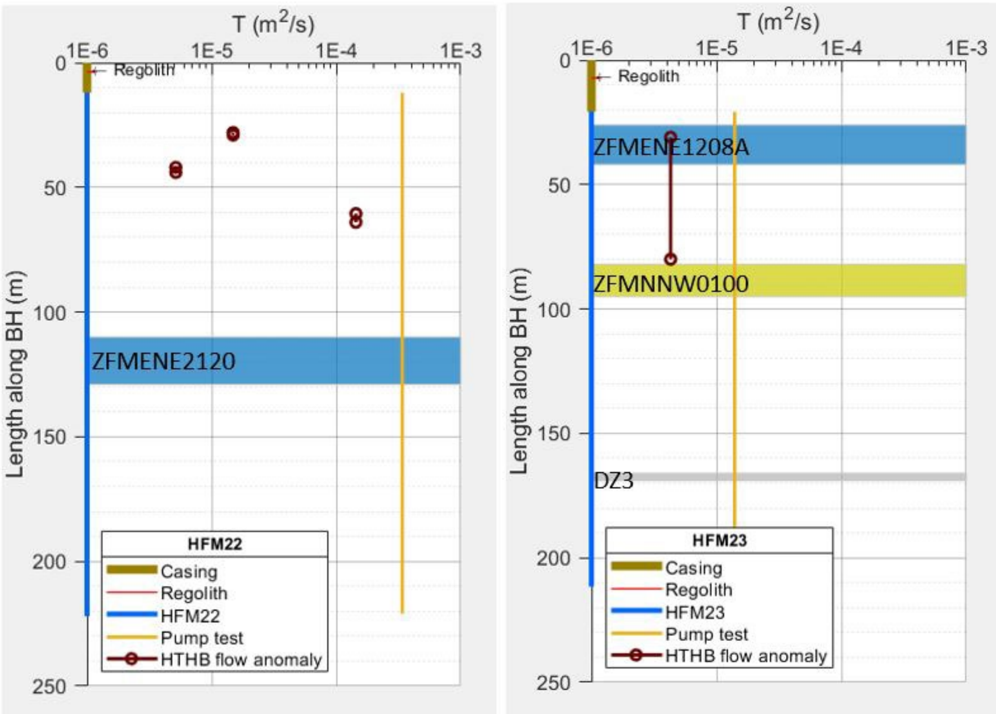

Figure 5-14. *HTHB T acquired in HFM22 (left) and HFM23 (right). Shaded areas indicate modelled deformation zones and possible deformation zones; ZFM2120 (110-129 m) in HFM22, and ZFMENE1208A (26-42 m), ZFMNNW0100 (82-95 m) and DZ3 (166-169 m) in HFM23.*

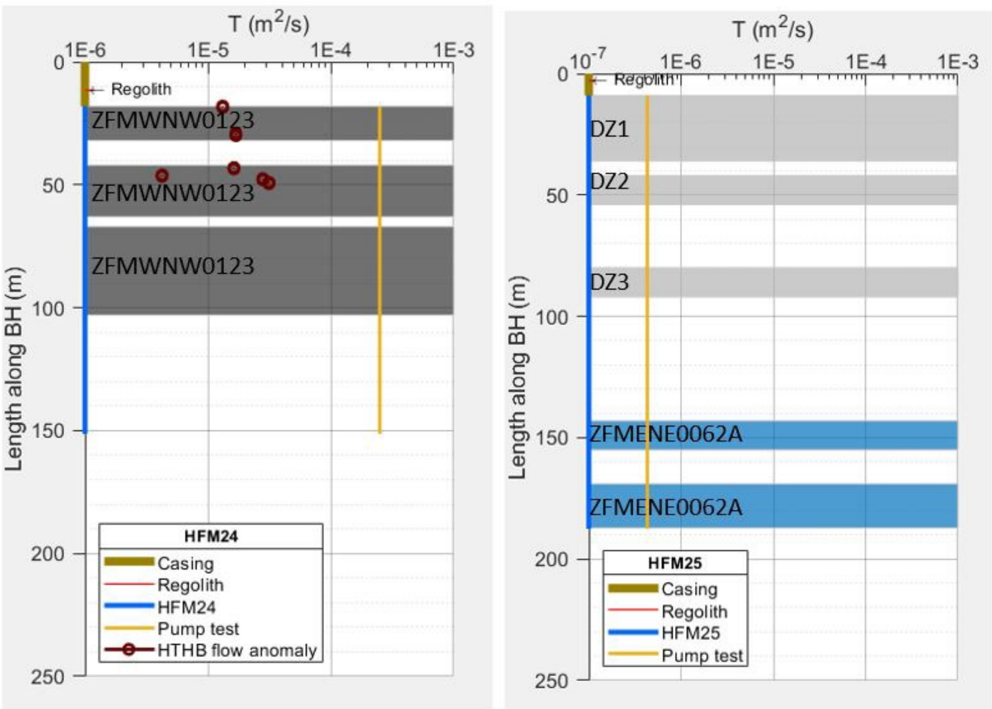

Figure 5-15. *HTHB T acquired in HFM24 (left) and HFM25 (right). Shaded areas indicate modelled deformation zones ZFMWNW0123 (18–32 m, 42–63 and 67–103 m), possible deformation zones (DZ1(9–36 m), DZ2(42–54 m) and DZ3(80–92 m)) and ZFMENE0062A (143–155 m and 169–187 m).*

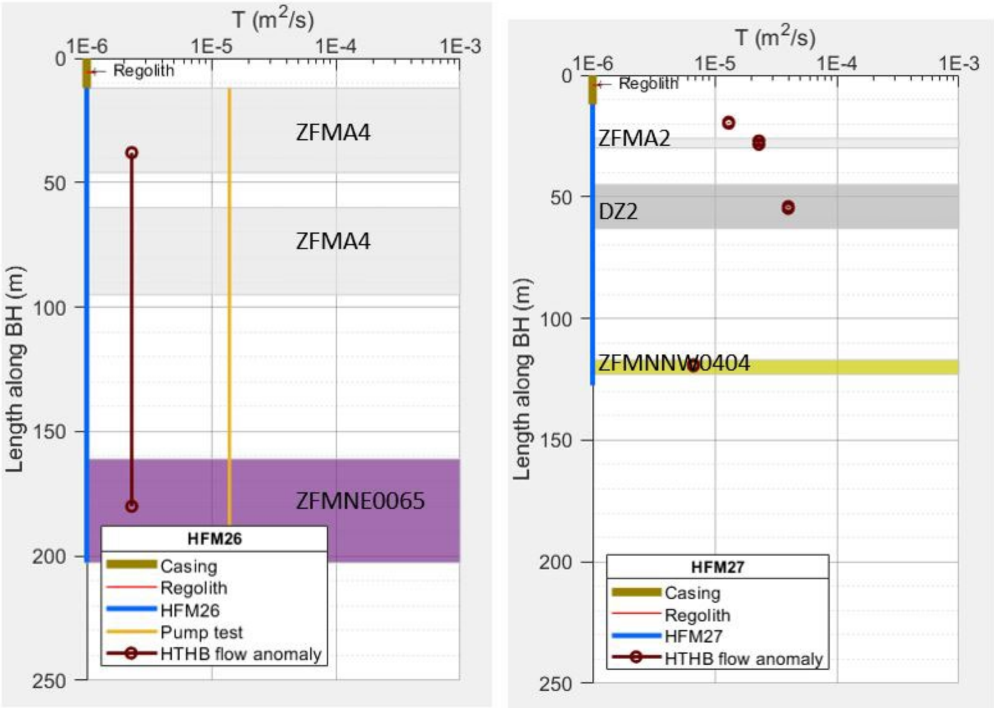

Figure 5-16. *HTHB T acquired in HFM26 (left) and HFM27 (right). Shaded areas indicate modelled deformation zones and possible deformation zones, ZFMA4 (12-46 m and 60-95 m) and ZFMNE0065 (161-203). ZFMA2 (26-30 m), DZ2 (45-63 m) and ZFMNNW0404 (117-123 m).*

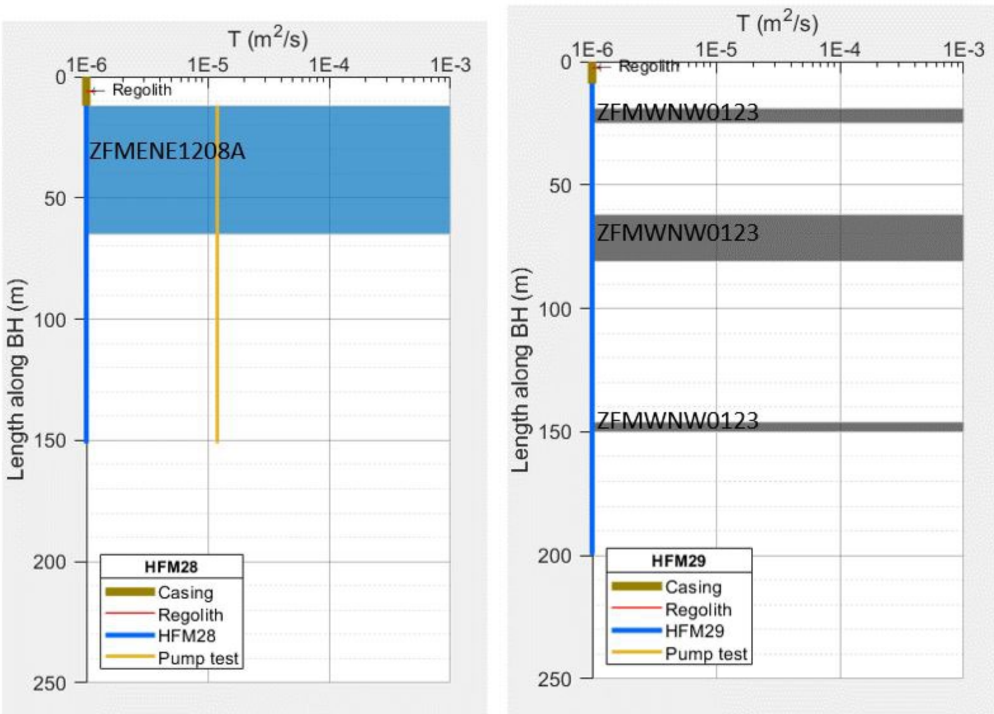

Figure 5-17. *HTHB T acquired in HFM28 (left) and HFM29 (right). Shaded areas indicate modelled deformation zones ZFMENE1208A (12–65 m) and ZFMWNW0123 (19–25 m, 62–81 m, and 146–150 m).*

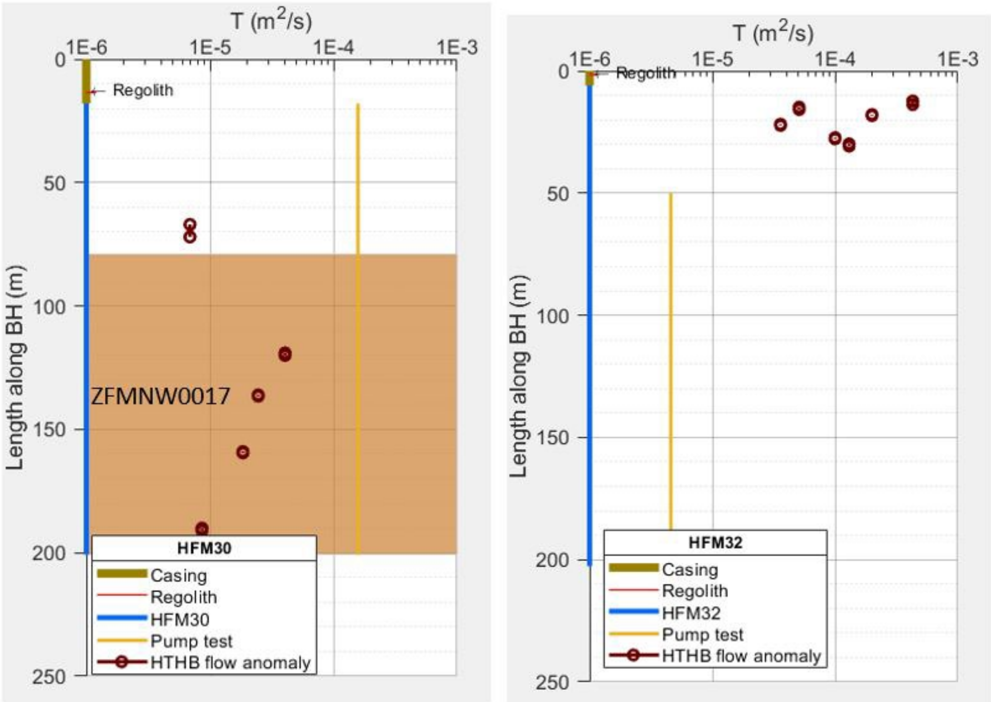

Figure 5-18. *HTHB T acquired in HFM30 (left) and HFM32 (right). Shaded area indicates modelled deformation zone ZFMNW0017 (79–201 m).*

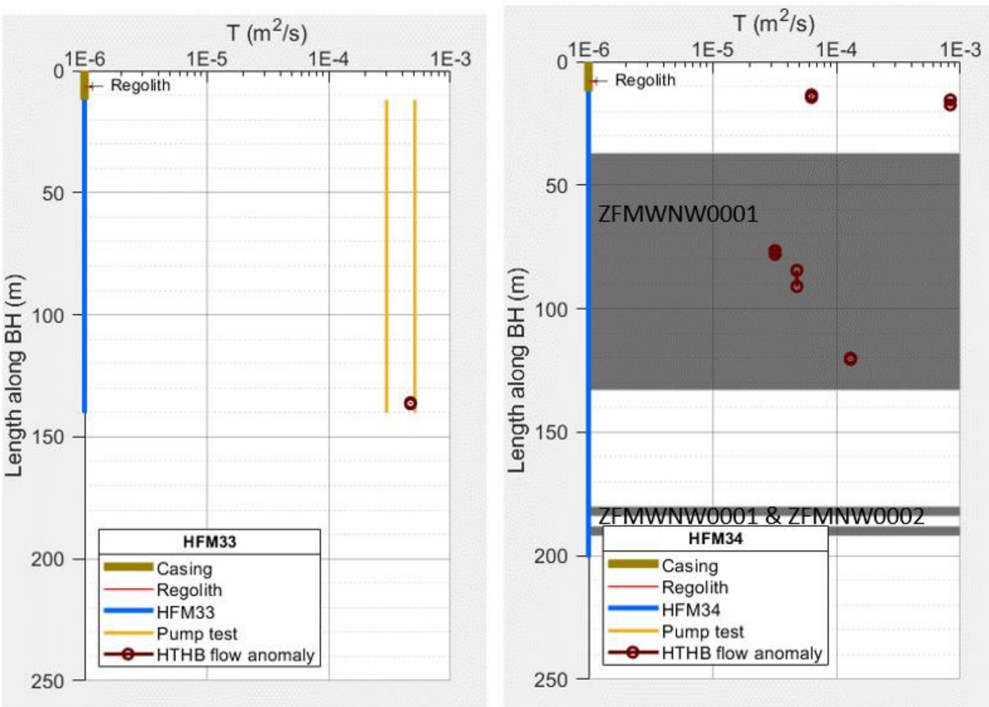

Figure 5-19. *HTHB T acquired in HFM33 (left) and HFM34 (right). Shaded areas indicate modelled deformation zones ZFMWNW0001(37–133 m and 180–184 m) , ZFMNW0002 (188–192 m).*

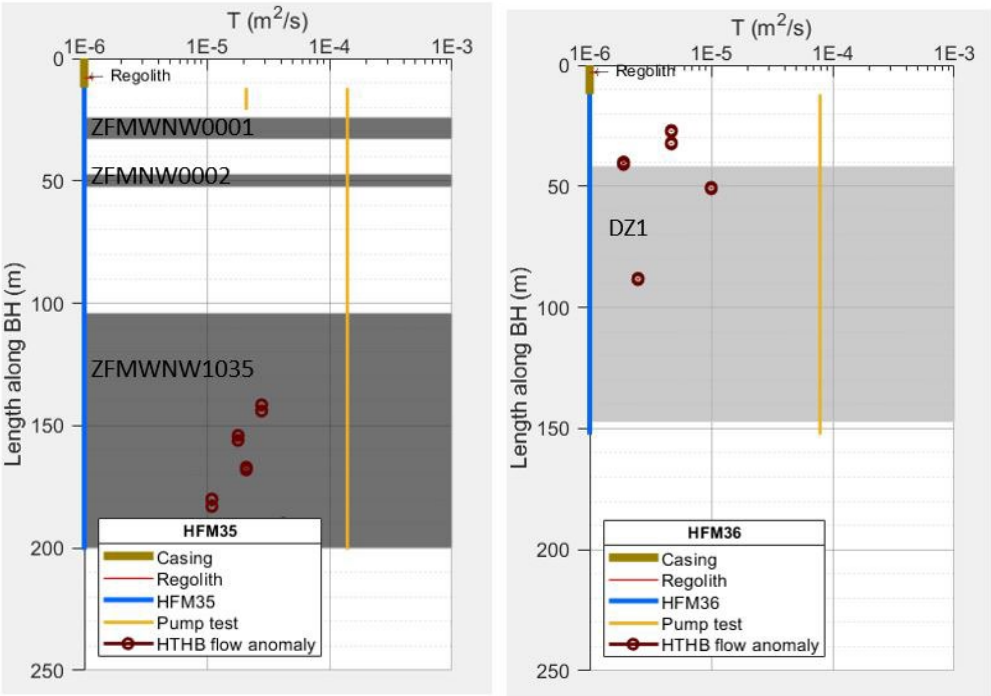

Figure 5-20. *HTHB T acquired in HFM35 (left) and HFM36 (right). Shaded areas indicate modelled deformation zones ZFMWNW0001(24–33 m), ZFMNW0002(47–53 m), ZFMWNW1035(104–200 m) in HFM35 and possible deformation zone DZ1(42–177 m) in HFM36.*

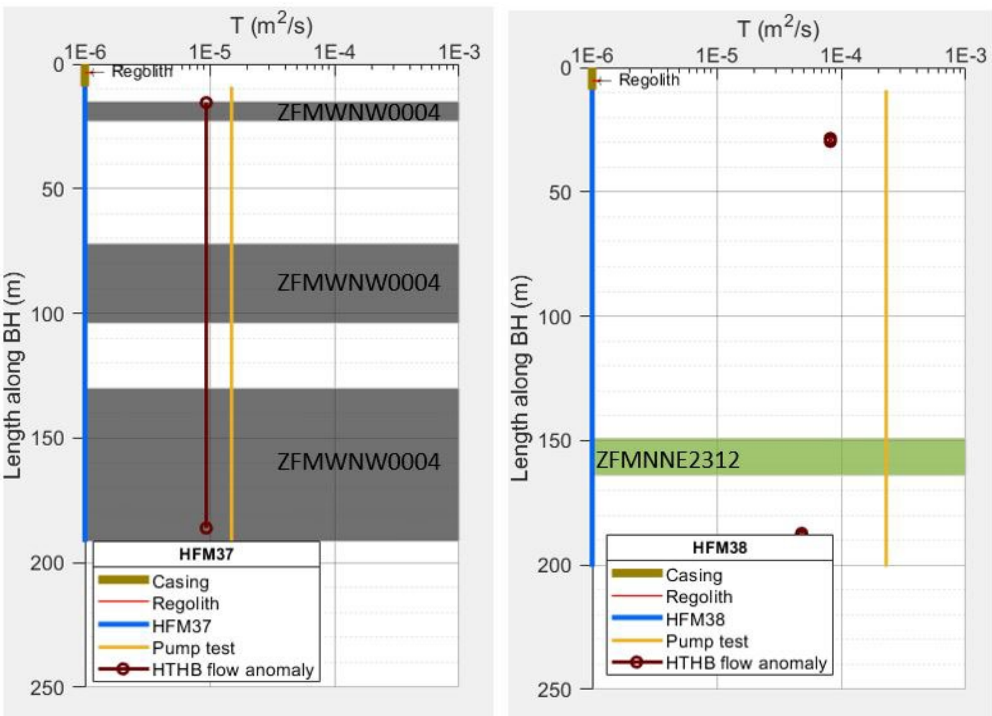

Figure 5-21. *HTHB T acquired in HFM37 (left) and HFM38 (right). Shaded areas indicate modelled deformation ZFMWNW0004 (15–23 m, 72–104 m and 130–191 m) in HFM37 and ZFMNNE2312(149–164 m) in HFM38.*

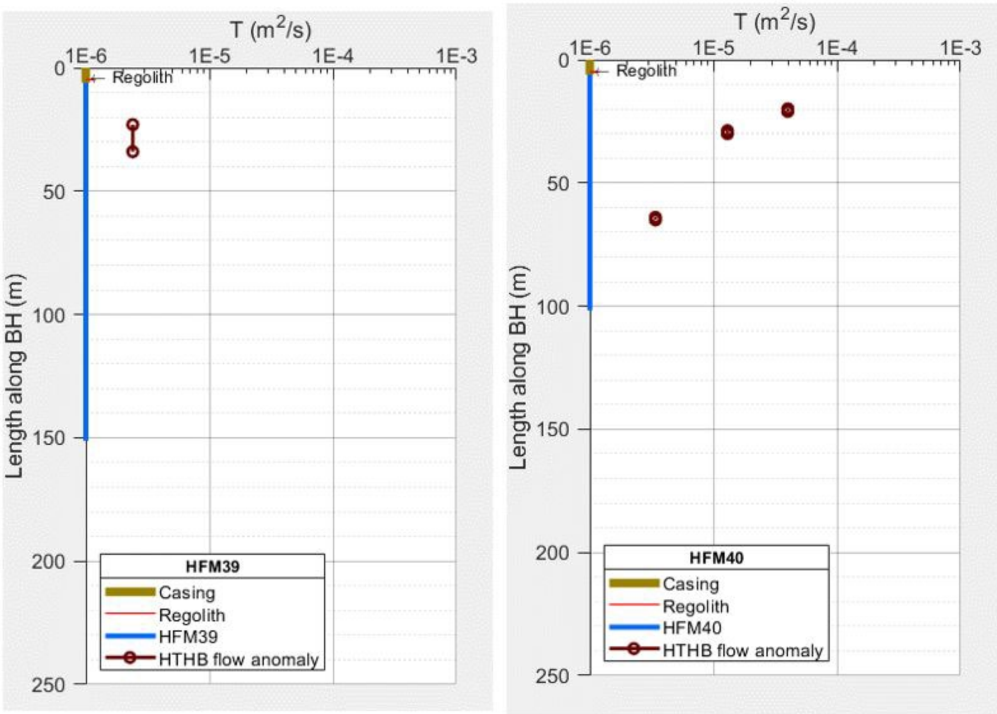

Figure 5-22. *HTHB T acquired in HFM39 (left) and HFM40 (right).*

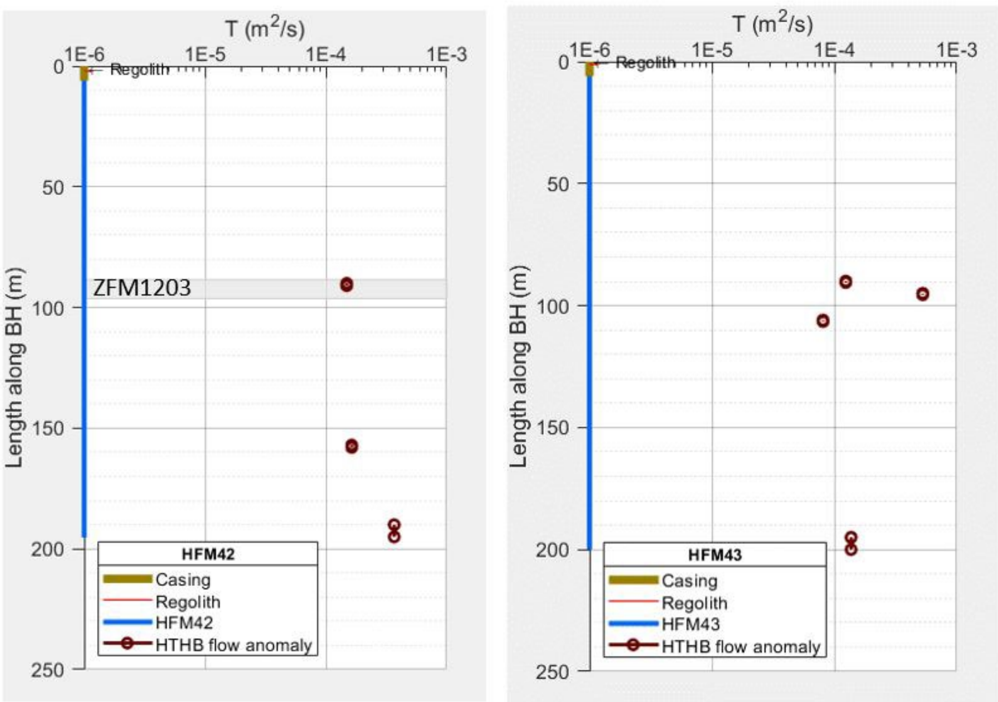

Figure 5-23. *HTHB T acquired in HFM42 (left) and HFM43 (right). Shaded areas indicate modelled deformation zone ZFM1203 (88–96 m).*

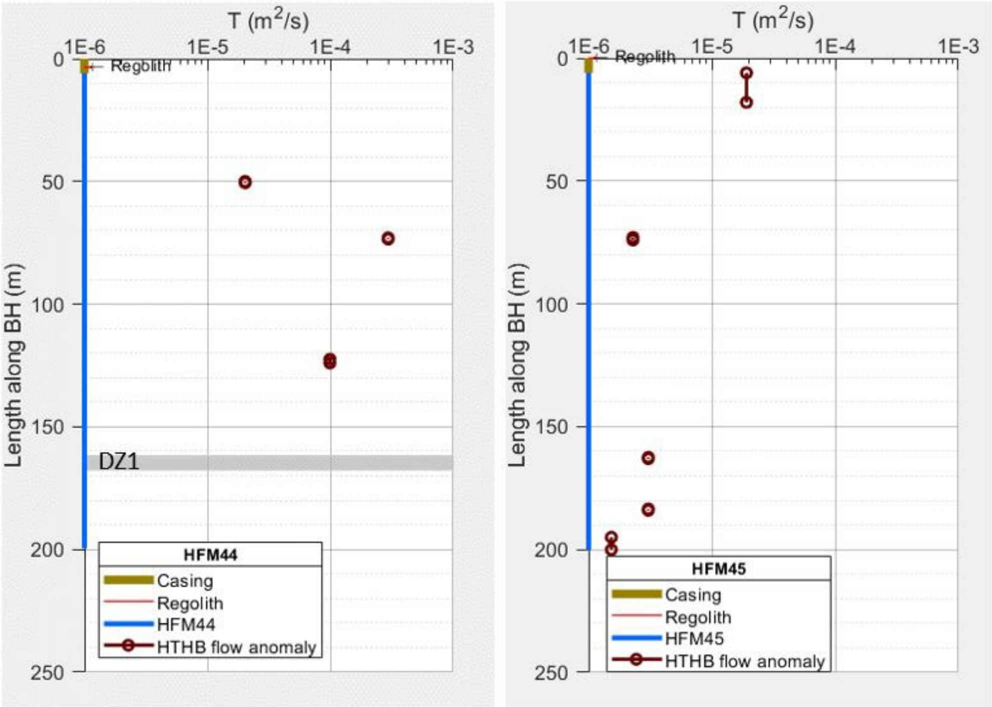

Figure 5-24. *HTHB T acquired in HFM44 (left) and HFM45 (right). Shaded area indicates possible deformation zone DZ1 (162–168 m).*

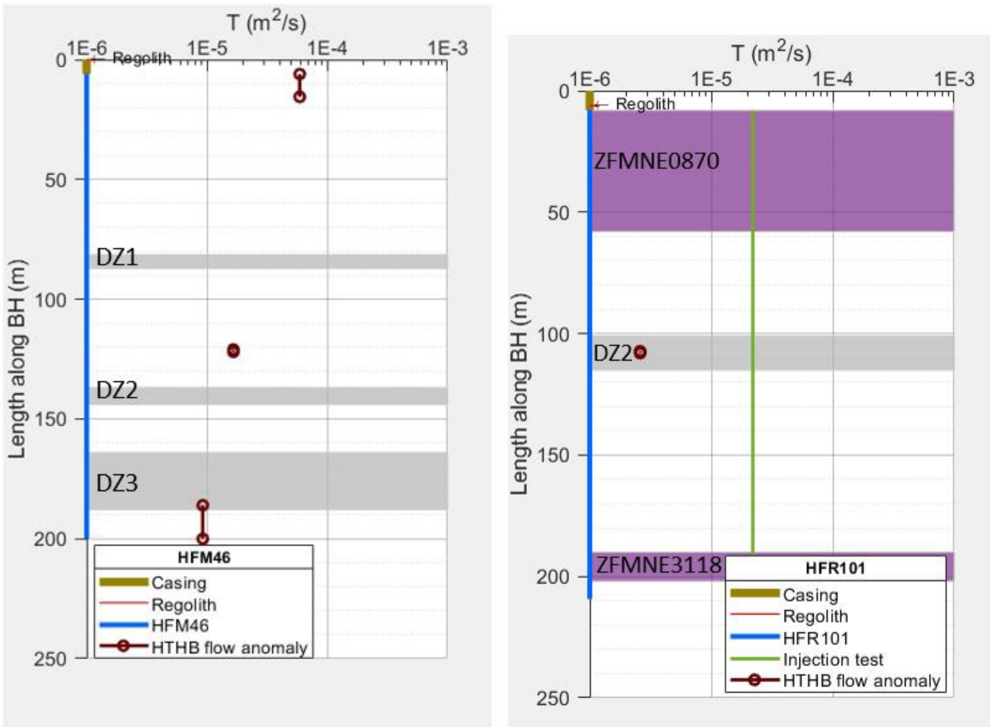

Figure 5-25. *HTHB T acquired in HFM46 (left) and HFR101 (right). Shaded areas indicate possible deformation zones (DZ1(81–87 m), DZ2(137–144 m) & DZ3(164–187 m)) in HFM46 and modelled deformation zones ZFMNE0870(8–58 m), ZFMNE3118(190–202 m) and a possible deformation zone DZ2(101–115 m) in the HFR101.*

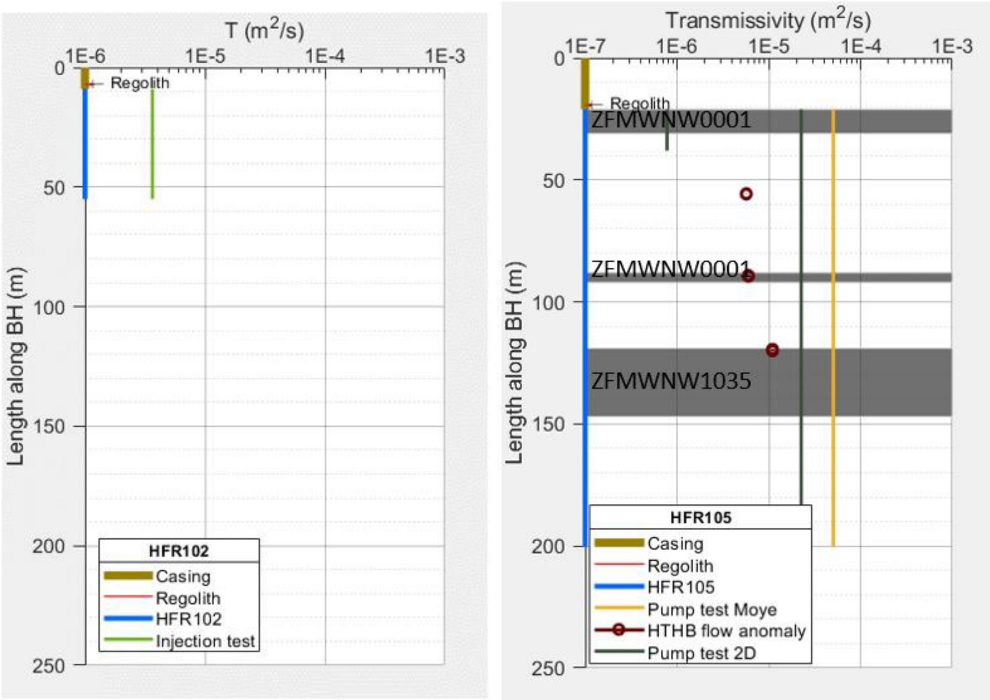

Figure 5-26. *HTHB T acquired in HFR102 (left) and HFR105 (right). Shaded areas indicate modelled deformation zones ZFMWNW0001(21–31 m and 88–92 m) and ZFMWNW1035(119–147 m).*

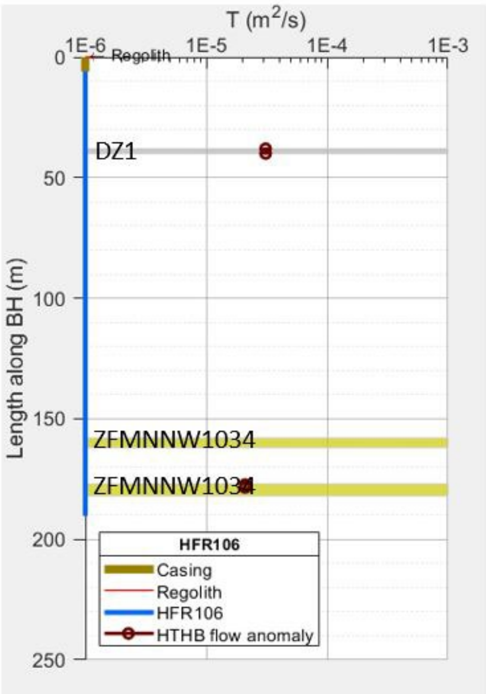

Figure 5-27. *HTHB T acquired in HFR106. Shaded areas indicate modelled deformation zone ZFMNNW1034(158–162 m and 177–182 m) and possible deformation zone DZ1(38–40 m).*

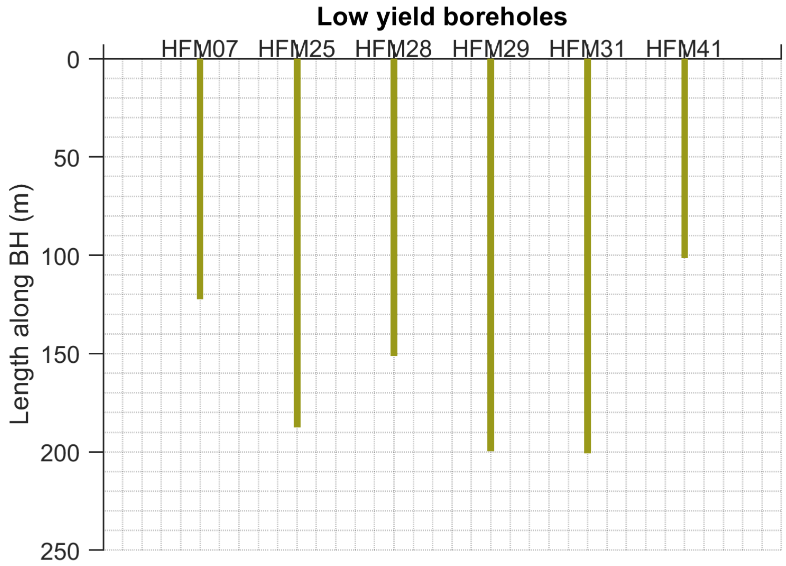

Figure 5-28. *Total borehole lengths of percussion-drilled boreholes with low yield ($T < 1{\cdot}10^{-6}$ m^2/s).*

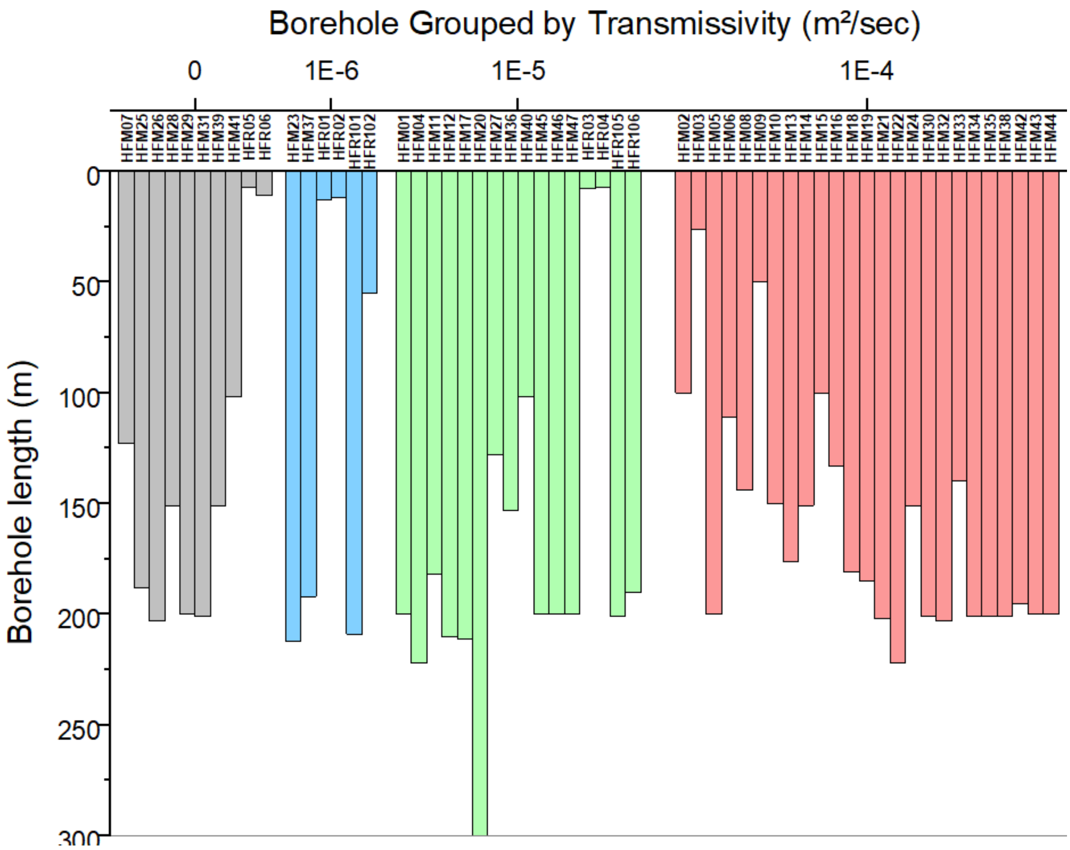

Figure 5-29. *All percussion boreholes grouped by total T. Grey bars are boreholes with $T \le 1{\cdot}10^{-6}$ m^2/s or no T data, blue bars are boreholes with $1{\cdot}10^{-6}$ $m^2/s < T < 1{\cdot}10^{-5}$ m^2/s, green bars are boreholes with $1{\cdot}10^{-5}$ $m^2/s < T < 1{\cdot}10^{-4}$ m^2/s, and red bars are boreholes with $T \ge 1{\cdot}10^{-4}$ m^2/s.*

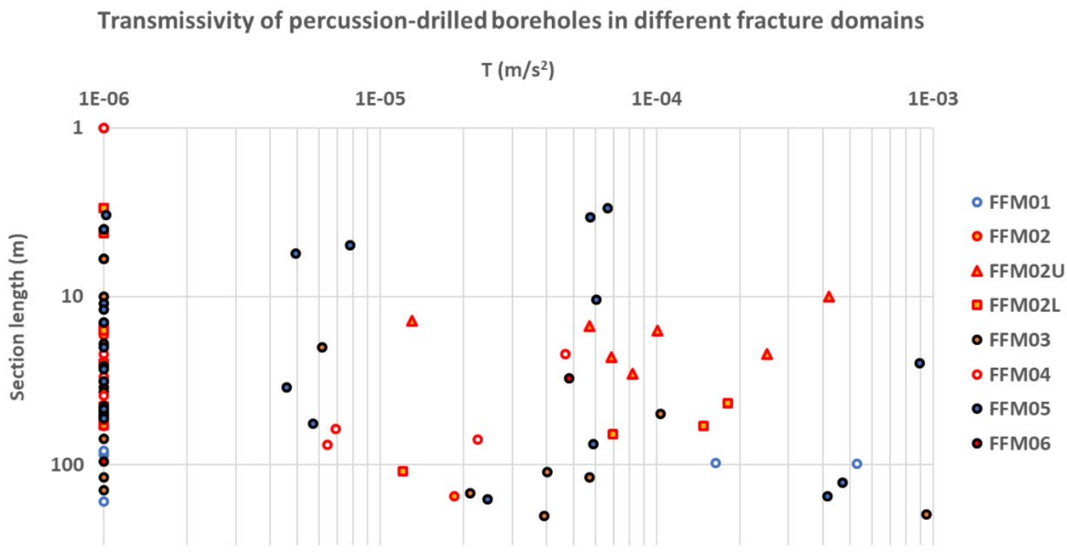

Figure 5-30. *Total HTHB T of each percussion-drilled borehole categorized by fracture domain.*

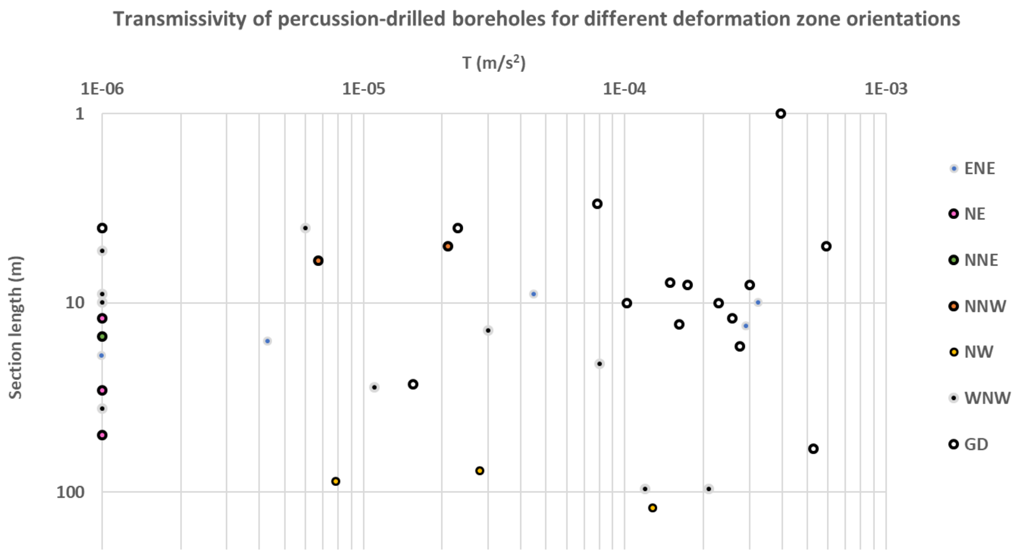

Figure 5-31. *Total HTHB T associated with different deformation-zone orientations (ENE = east-northeast, NE = northeast, NNE = north-northeast, NNW = north-northwest, NW = northwest, WNW = west-northwest, GD = gently dipping).*

6 Compilation of hydraulic properties data – regolith and the regolith/bedrock interface

6.1 Background

This chapter summarises field and laboratory data available at the Forsmark Baseline stage in terms of hydraulic properties of regolith and the regolith/bedrock interface. Johansson (2008) summarises regolith and regolith/bedrock interface hydraulic properties data available for conceptual and quantitative water flow modelling at the SDM-Site stage (Bosson et al. 2008), and which were also used in the water flow modelling of SR-Site (Bosson et al. 2010) and SR-PSU (Werner et al. 2013).

The present summary is intended to provide support to and act as reference for conceptual and quantitative modelling of hydrology and near-surface hydrogeology, and ultimately for the interdisciplinary site understanding at the Forsmark Baseline stage. The geometrical framework for interpretation of the compiled hydraulic properties data is presented in Section 2.1 (Figure 2-1) and Section 2.2.3.

Specifically, the chapter presents hydraulic properties data in terms of horizontal and vertical saturated hydraulic conductivity of regolith and the regolith/bedrock interface, and total porosity, specific yield, and field capacity of regolith. These data are available from field (single hole (slug and permeameter) tests and pumping (interference) tests), and laboratory investigations (CRS and permeameter tests and particle size distribution (PSD) analyses). These methods and associated spatial support scales are described in Section 3.2.2.

6.2 Field tests

6.2.1 Single hole (slug) tests: Groundwater wells (HY670)

This section summarizes results of single hole (slug) tests performed in groundwater wells installed with their screens in regolith or across the regolith/bedrock interface in the Forsmark area. Slug test results available for the Baseline Forsmark stage are reported in Werner and Johansson (2003), Werner (2004), Alm et al. (2006), Smith (2017), Werner (2018a, b), Söderqvist and Svensson (2018)[3], and Rasul et al. (2023). All available regolith well drawings are presented and stored in SKBdoc (Rasul 2022).

Table 6-1 lists all slug test results available in the Sicada database, whereas Figure 6-1 shows the locations of the tested wells and corresponding evaluated Kh-values plotted as log10 (Kh). It should be noted that different methods are available for slug test evaluation (e.g. Butler 1998), and each slug test involves two test phases (falling and rising head, respectively) that are evaluated separately. Moreover, for some wells slug tests have also been repeated at one or several occasions as part of well function control.

Table 6-1 and Figure 6-1 are based on the value of transmissivity T (here recalculated to Kh) or Kh chosen to be reported to Sicada from the first slug test performed subsequent to well installation. Full ranges of evaluation results, and results from repeated slug tests, are available in the reports mentioned above.

Figure 6-2 summarises the results of the slug tests in wells installed in regolith or at the regolith/bedrock interface, in terms of a cumulative frequency distribution curve for horizontal hydraulic conductivity Kh (m/s). As can be seen in the figure, evaluated Kh values are in the approximate interval 2E-08–6E-03 m/s, i.e. spanning five orders of magnitude, with a cumulative frequency of 50 % at Kh ≈ 5E-06 m/s.

[3] SKBdoc 1700798 ver. 1.0, Internal document (in Swedish).

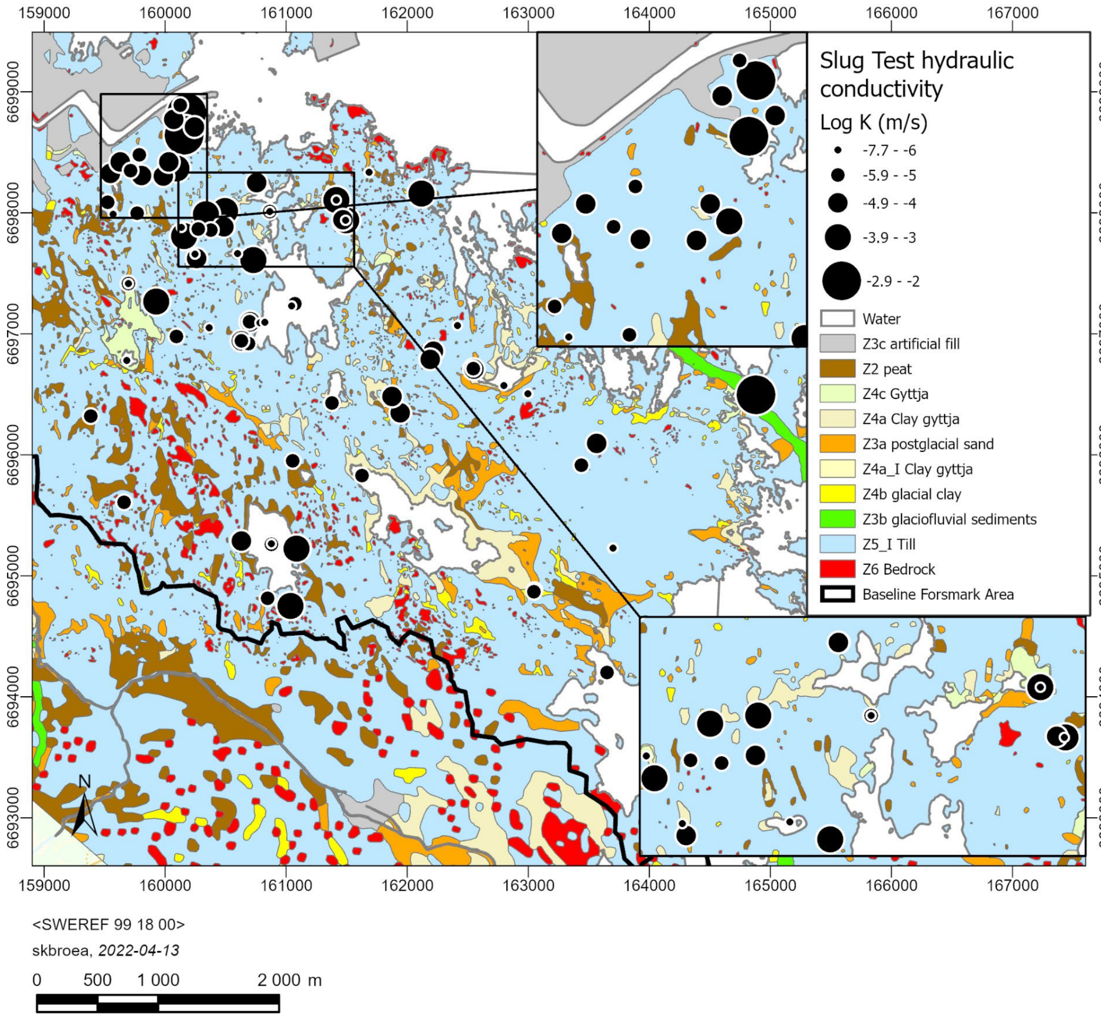

Figure 6-1. *Locations of slug-tested groundwater wells, displayed on the map of surface distribution of regolith. The Z notations in the legend refer to regolith types implemented in the RDM (Regolith Depth and Stratigraphy Model) of Forsmark.*

Table 6-1 Summary of Kh (m/s) evaluated from slug tests in groundwater wells (cf. Figure 6-1). GSE = ground surface elevation. m b gs = metres below ground surface.

Well	GSE (m, RH 2000)	Secup (m b gs)	Seclow (m b gs)	Regolith type at well screen depth	K_h (m/s)	Comment
SFM0001	1.14	3.80	4.80	Clayey sandy-silty till	1.41E-04	
SFM0002	1.80	3.80	4.80	Sandy till	7.68E-06	
SFM0003	1.64	8.50	10.50	Sand	8.85E-06	
SFM0004	3.71	4.40	5.40	No data	1.59E-07	
SFM0005	6.18	1.40	2.40	Sandy till	8.07E-05	
SFM0006	5.96	2.70	3.70	Clayey sandy-silty till	2.97E-06	
SFM0008	3.54	4.73	5.73	Clayey sandy till	2.27E-05	
SFM0009	4.52	1.70	2.70	Clayey till/Bedrock	1.50E-05	
SFM0010	13.42	0.70	1.70	Clayey sandy-silty till	9.92E-06	
SFM0011	2.19	2.85	3.85	Sandy till	8.71E-06	
SFM0012	2.12	3.73	4.73	Till	7.66E-07	
SFM0013	1.47	3.78	4.78	Till/Bedrock	4.42E-06	
SFM0014	5.78	0.98	1.98	Till	2.30E-05	
SFM0015	5.25	3.15	4.15	Till	5.95E-07	
SFM0016	5.40	6.53	7.53	Clayey-sandy till	1.01E-04	

Well	GSE (m, RH 2000)	Secup (m b gs)	Seclow (m b gs)	Regolith type at well screen depth	K_h (m/s)	Comment
SFM0017	5.83	2.96	3.96	Clayey sandy-silty till	2.80E-04	
SFM0018	5.96	3.60	4.60	Clayey-gravelly till	4.56E-06	
SFM0019	3.86	3.40	4.40	Sandy till	3.46E-06	
SFM0020	1.85	2.42	3.42	Clayey-sandy till	9.88E-05	
SFM0021	1.61	1.46	2.46	Clayey-sandy till	3.91E-04	
SFM0022	1.16	3.90	4.40	Sandy till	1.56E-06	
SFM0023	0.34	1.42	2.42	Till	3.01E-07	
SFM0024	-0.15	-1.30	1.91	Till	6.98E-04	
SFM0025	-0.27	4.25	5.25	Till	9.75E-06	
SFM0026	0.88	15.11	16.11	Till	5.74E-06	
SFM0027	1.09	6.16	7.16	Silty till/Bedrock	1.02E-06	
SFM0028	0.40	6.15	7.15	Clayey-sandy till	3.90E-05	
SFM0029	0.40	6.13	7.13	Till	4.36E-05	
SFM0030	1.85	2.88	3.88	Clayey-sandy till	1.86E-06	
SFM0031	1.93	2.61	3.61	Clayey-sandy till	1.09E-06	
SFM0032	0.75	1.94	2.94	Till	7.68E-05	
SFM0033	0.72	1.84	2.84	Till/Bedrock	5.50E-04	
SFM0034	0.85	1.09	2.09	Sandy till	2.69E-06	
SFM0035	0.84	1.17	2.17	Sandy till	5.62E-08	
SFM0036	0.80	1.10	2.10	Sandy till	7.17E-05	
SFM0037	0.78	1.10	2.10	Sandy till	2.39E-05	
SFM0049	3.11	2.90	3.90	Till/bedrock	9.82E-05	
SFM0057	4.45	2.90	4.00	Bedrock	1.88E-04	
SFM0058	3.38	2.50	3.50	No data	6.67E-04	
SFM0061	4.51	4.95	6.99	Gravel, stone/Bedrock	1.16E-03	
SFM0062	0.86	1.90	2.30	Sandy till	1.89E-07	
SFM0063	0.02	1.75	2.25	Sandy till	1.23E-07	
SFM0065	0.21	3.10	3.50	Clayey-sandy till	3.23E-07	
SFM0067	2.30	0.47	1.47	Till	2.58E-7	
SFM0068	1.80	0.34	1.34	Till	5.78E-07	
SFM0069	2.06	0.37	1.37	Sandy gravel	4.20E-05	
SFM0070	3.45	1.22	2.22	Clayey sandy-silty till	6.20E-07	
SFM0071	3.48	4.69	5.69	Clayey till/Silty till	8.95E-07	
SFM0072	3.46	8.08	9.08	Clayey sandy-silty till	4.29E-07	
SFM0073	0.42	3.10	4.10	Till	9.50E-06	
SFM0075	3.46	7.15	8.15	Silty till	2.83E-07	
SFM0077	4.93	5.73	6.73	Till/Bedrock	No data	
SFM0078	5.02	3.10	4.10	Till/Bedrock	1.95E-06	
SFM0079	3.78	4.10	5.10	Till/Bedrock	1.76E-07	
SFM0080	3.77	7.85	8.85	Unknown	7.76E-06	
SFM0081	0.63	2.30	2.70	Till	2.30E-06	
SFM0084	0.86	3.15	3.55	Till	3.25E-07	
SFM0087	0.84	1.35	1.55	Sand	3.88E-04	
SFM0090	1.19	2.44	4.94	Till/Bedrock	2.47E-06	
SFM0091	0.80	1.10	1.50	Sand/Clay/Till	2.25E-04	
SFM0095	11.28	4.00	5.00	Till	6.72E-06	
SFM0104	3.13	3.40	4.40	Till	4.50E-06	
SFM0105	3.10	1.30	2.30	Till/Bedrock	2.87E-05	
SFM0106	4.48	2.60	3.60	Till	1.95E-08	
SFM0107	2.68	4.35	5.35	Till/Bedrock	2.30E-06	

Well	GSE (m, RH 2000)	Secup (m b gs)	Seclow (m b gs)	Regolith type at well screen depth	K_h (m/s)	Comment
SFM0108	3.60	4.20	5.20	Till/Bedrock	7.50E-05	
SFM0109	7.59	3.35	4.40	Gravelly clay/Silty clay	4.24E-04	
SFM000110	1.75	1.25	1.75	Stone/Gravel	9.30E-07	
SFM000112	2.19	1.10	1.60	Sandy-silty till	4.44E-07	
SFM000114	2.73	1.30	1.80	Silty sand	5.42E-07	
SFM000116	2.76	1.85	2.35	Silty sand/till	2.64E-08	
SFM000118	1.08	0.65	1.15	Silty-sandy till	8.26E-07	
SFM000122	2.63	6.60	7.10	Till	1.69E-05	
SFM000126	5.60	3.23	3.83	Till	4.62E-06	
SFM000132	3.11	1.12	2.02	Sandy-silty gravel/Sandy-silty gravelly till	No data in Sicada	
SFM000133	2.73	1.08	1.98	Sandy-silty till	No data in Sicada	
SFM000134	3.06	0.08	0.98	Silty clay/Sandy-silty till	No data in Sicada	
SFM000135	2.71	0.11	1.01	Silty clay/Sandy-silty till	No data in Sicada	
SFM000138	1.58	-0.16	0.84	Peat/Till	1.66E-04	
SFM000139	3.06	1.20	2.20	Peat/Clay/Till	8.21E-06	
SFM000143	0.95	0.50	1.50	Sandy-silty-gravel till/Sandy-gravelly silty till	No data	
SFM000144	1.15	1.50	2.50	Gravelly-sandy silty till	5.58E-03	
SFM000145	0.65	0.00	1.00	Sandy-silty till	1.04E-05	
SFM000146	2.39	1.10	2.10	Till	3.21E-03	
SFM000147	2.36	0.80	1.80	Sandy-silty till	3.39E-05	
SFM000149	0.67	0.45	1.45	Sandy-gravelly silty till	3.82E-06	
SFM000153	3.55	1.40	2.40	Sandy-silty till	2.40E-05	
SFM000160	2.66	0.92	1.92	Peat/Mud/Till	8.56E-05	
SFM000161	1.48	0.42	1.42	Peat	7.59E-05	
SFM000162	1.23	-0.13	0.87	Peat/Till	4.10E-06	
SFM000163	2.54	1.75	2.75	Unknown	2.12E-04	
SFM000167	1.80	3.62	4.62	Unknown	5.58E-05	
SFM000168	4.65	3.01	4.01	Unknown	3.17E-06	
SFM000169	1.73	1.40	2.40	Silty-sandy till	2.40E-05	
SFM000171	0.74	1.50	2.5	Silty till/Bedrock	1.17E-06	
SFM000174	2.99	0.42	1.42	Silty-sandy till, sandy till	7.55E-08	
SFM000176	4.68	4.40	5.40	Till	7.54E-06	
SFM000177	3.82	3.00	4.00	Clay	6.28E-07	
SFM000179	6.09	3.20	4.20	”Friction soil”	1.68E-05	
SFM000180	6.25	3.30	4.30	Till	3.22E-07	
SFM000182	1.66	2.00	3.00	Silty-sandy till	4.19E-07	
SFM000183	1.50	4.10	5.10	Silty till/Boulder/Till	8.14E-08	
SFM000187	1.04	-0.10	0.90	Silty till	7.76E-05	
SFM000188	0.99	1.70	2.70	Till/Silty till	3.06E-05	
SFM000190	4.70	4.07	5.07	Silty-sandy till	1.97E-07	
SFM000191	3.40	6.11	7.11	Silty-sandy till	4.96E-07	
SFM000192	2.41	5.97	6.97	Silty-sandy till	2.01E-06	
SFM000193	5.00	2.05	3.05	Silty-sandy-stony till/Bedrock	1.01E-07	
SFM000194	3.40	1.10	2.10	”Friction soil”/Bedrock	8.62E-04	
SFM000195	2.88	4.10	5.10	”Friction soil”/Till	1.24E-06	
SFM000197	2.10	5.40	6.40	Till	7.62E-07	
SFM000198	2.13	3.97	4.97	Clay	3.04E-07	

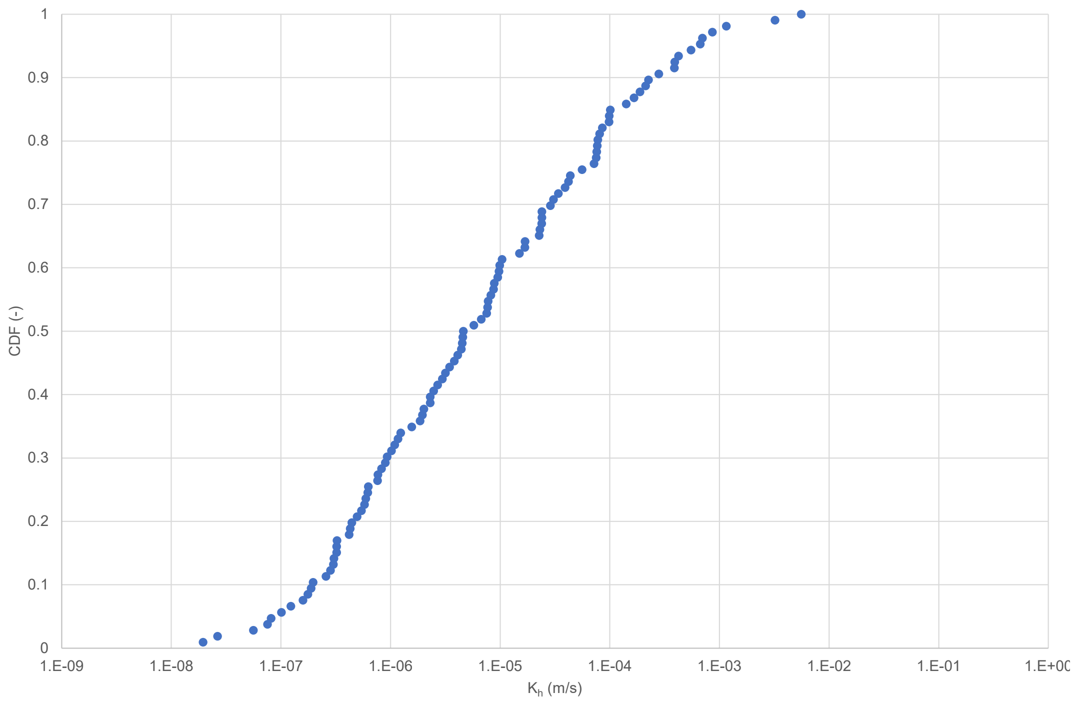

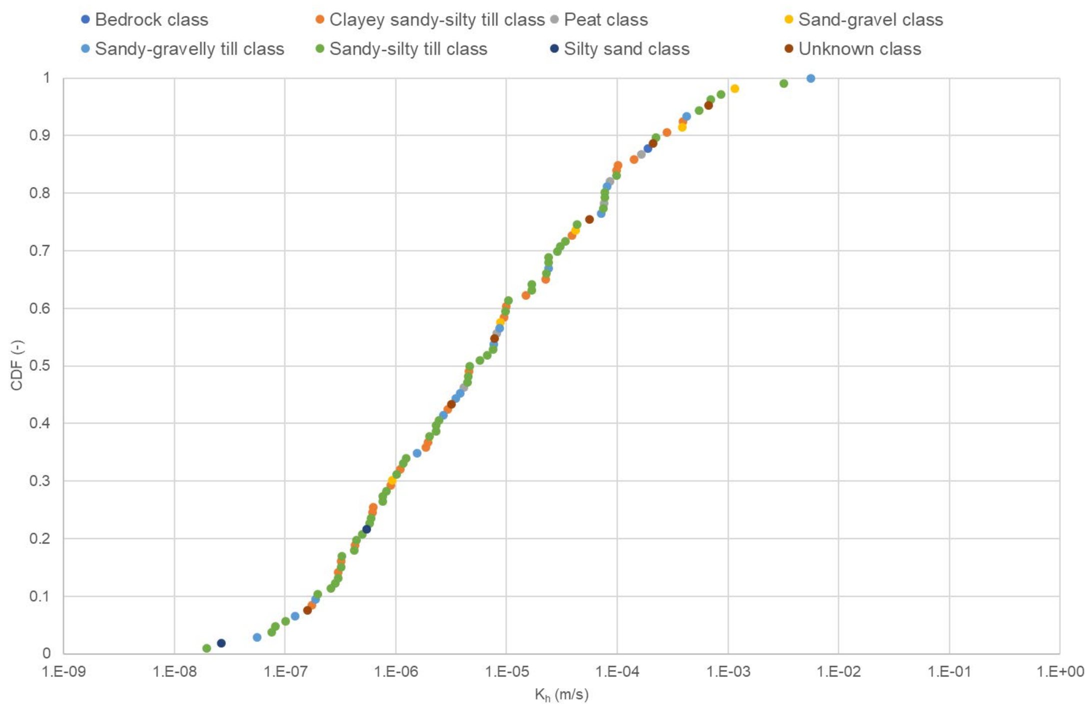

Figure 6-2. *Cumulative frequency distribution curve for horizontal hydraulic conductivity Kh (m/s) evaluated from slug tests. Upper plot: Cumulative frequency distribution curve for all slug tests of Table 6-1. Lower plot: Cumulative frequency distribution curve in which slug tests are classified into different classes of regolith types at well screen depth (cf. Table 6-1).*

6.2.2 Single hole (permeameter) tests: BAT filter tips (HY675)

This section summarizes results of single hole (permeameter) tests performed in so called BAT filter tips. The map of Figure 6-4 shows the locations of 10 wells equipped with such filter tips and in which permeameter tests have been performed (SFM0050, -52, -54, -82, -85, -88, -92, -96, -99, and -101). The tests are reported in Johansson (2004) and Alm et al. (2006). Note that the tests of Johansson (2004) are reported to Sicada, whereas those of Alm et al. (2006) are not. The results of the permeameter tests are summarized in Table 6-2

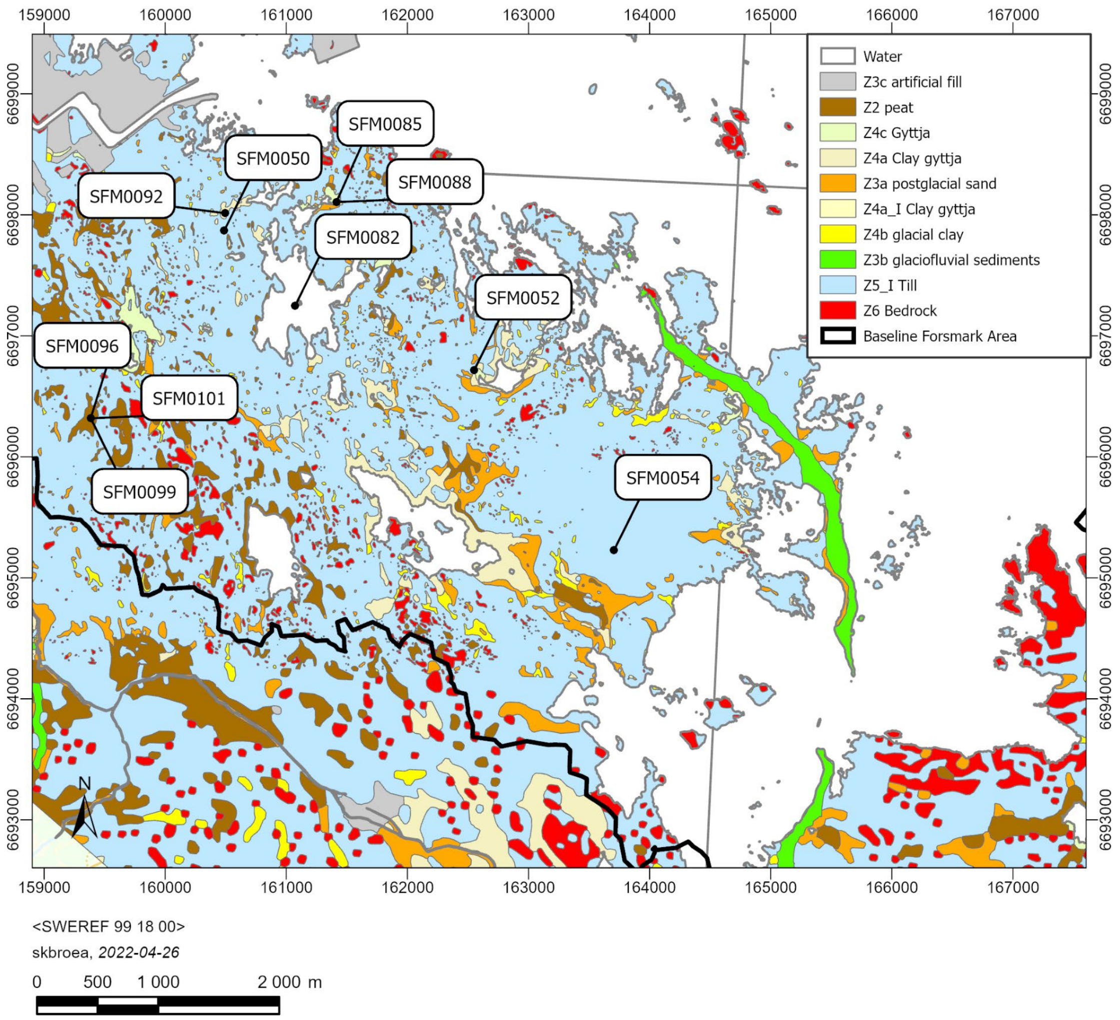

Figure 6-3. *Locations of BAT filter tips in which permeameter tests have been performed, displayed on the map of the surface distribution of regolith.*

Table 6-2. Summary of Kh (m/s) evaluated by permeameter tests in BAT filter tips.

Well id	Hydraulic conductivity K_h (m/s)	Regolith type at filter tip	Reference
SFM0050	4.44E-08	Sandy till	Johansson (2004)
SFM0052	3.80E-09	Clayey, sandy silty till	Johansson (2004)
SFM0054	1.03E-08	Boulder clay	Johansson (2004)
SFM0082	3.20E-07	Gyttja	Alm et al. (2006)
SFM0085	2.60E-07	Clay	Alm et al. (2006)
SFM0088	3.30E-07	Clayey gyttja	Alm et al. (2006)
SFM0092	3.40E-07	Gyttja	Alm et al. (2006)
SFM0096	2.90E-07	Clay	Alm et al. (2006)
SFM0099	3.20E-07	Gyttja	Alm et al. (2006)
SFM0101	3.30E-07	Peat	Alm et al. (2006)

6.2.3 Interference (pumping) tests (HY610, HY640 pumping holes, HY645 obs holes)

This section summarizes results of interference (pumping) tests performed in wells installed in regolith or across the regolith/bedrock interface in the Forsmark area. The map of Figure 6-4 shows the locations of the pumping and observation wells of these tests (Werner et al. 2004, Werner and Lundholm 2004, Alm et al. 2006), whereas the results are summarized in Table 6-3.

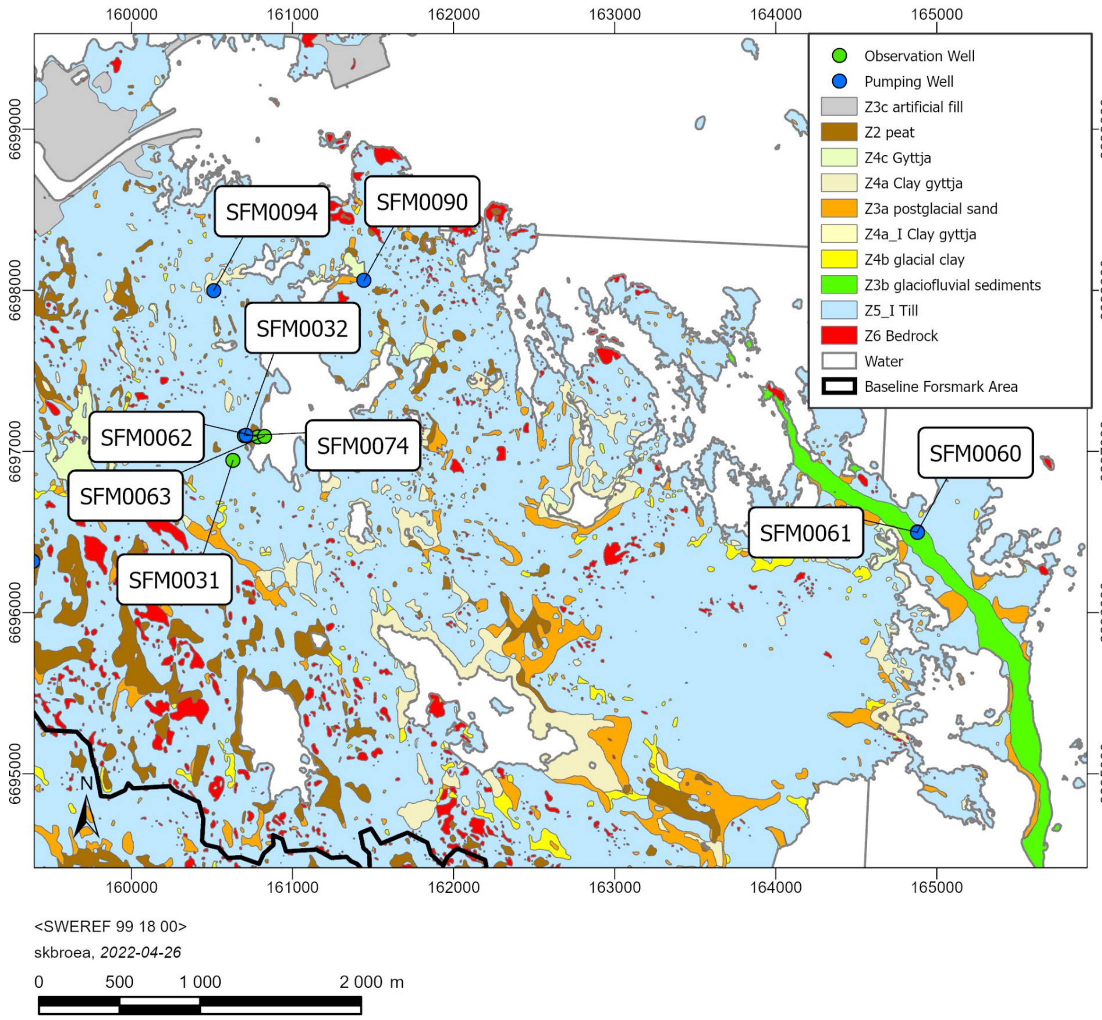

Figure 6-4. Locations of pumping and observation wells of interference tests performed in regolith and across the regolith/bedrock interface.

Table 6-3. Summary of results of interference tests in regolith and across the regolith/bedrock interface.

Pumping well (appr. regolith depth, m)	Regolith type	Observation well(s)	Distance from pumping well (m)	Regolith type	Hydraulic conductivity K_h (m/s)	Storage coeff. (-)	Reference
SFM0061 (6.5)	Glaciofluvial material				2.1E-04		Werner et al. (2004)
		SFM0060		Glaciofluvial material		4E-03	
SFM0074 (2.0)	Till/Bedrock						Werner and Lundholm (2004)
		SFM0031	175	Clayey-sandy till	5.6E-04	1E-03	
		SFM0032	12	Till	5.6E-05	2.5E-04	
		SFM0062	70	Sandy till	5.5E-05	1.8E-03	
		SFM0063	113	Sandy till	3.7E-04	1.6E-03	
SFM0090 (3.9)	Till/Bedrock				3.6E-06		Alm et al. (2006)
SFM0094 (2.7)	Till/Bedrock				6.7E-06		Alm et al. (2006)
SFM0103 (5.0)	Till/Bedrock				9.1E-05		Alm et al. (2006)
		SFM0095	12	Till	7.6 E-05	3.1E-04	

6.3 Laboratory tests

6.3.1 Permeameter (HY672) and CRS (GE017) tests

This section summarizes results of laboratory permeameter and CRS tests performed on regolith samples. Laboratory permeameter tests were performed on undisturbed regolith samples (∅ 7.2 cm, length 5 cm). In addition, CRS tests were performed on glacial clay samples (∅ 5 cm, length 2 cm). Due to the nature of the regolith sampling, these tests represent saturated vertical hydraulic conductivities (K_v, m/s). The data set comprises laboratory permeameter tests on 20 regolith samples sampled at different depths along four vertical profiles in trenches (Lundin et al. 2005).

Note that the PFM004459 tests are presented in the Lundin et al. (2005) report but not reported to Sicada. The sampling locations for samples subject to these tests are shown in Figure 6-5, whereas the results are summarized in Table 6-4. Further laboratory permeameter tests were made on regolith samples from investigations of sand and clay (PFM007855–7859). Data from these tests are available in Sicada but have not previously been reported.

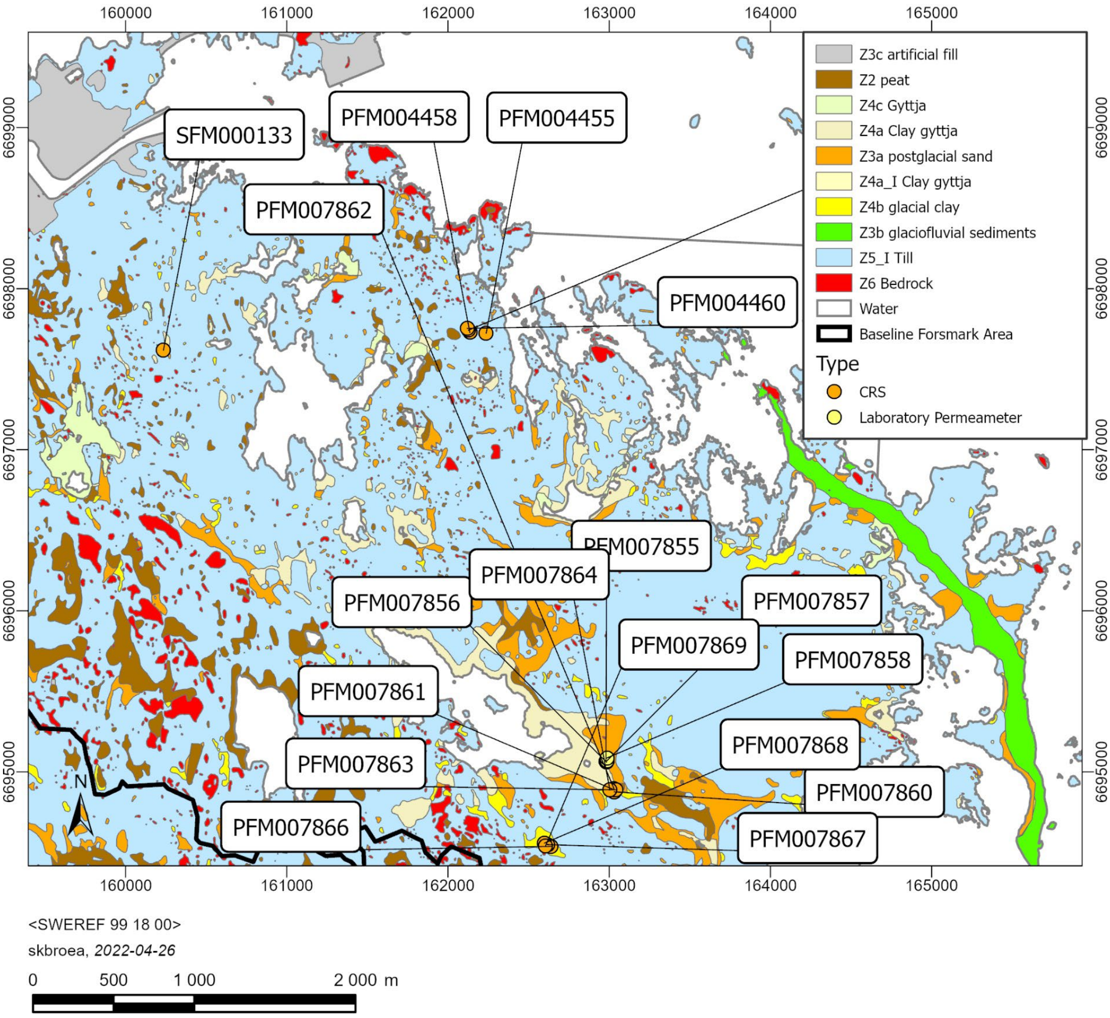

Figure 6-5. *Sampling locations for regolith samples subject to laboratory permeameter (orange) and CRS tests (yellow), displayed on the map of the surface distribution of regolith.*

Table 6-4. Results of laboratory permeameter and CRS* tests. NR = not reported.

Sampling point id	Depth (m b gs)	Regolith type	K_v (m/s)	Porosity (vol. %)	Reference
PFM004455	0.50–0.55	Sandy till	1.9E-07	31.0	Lundin et al. (2005)
	0.10–0.15	Gravelly sand	5.8E-05	37.9	
	0.20–0.25	Sandy till	3.7E-05	42.0	
	1.20–1.25	Sandy till	2.3E-08	27.1	
	0.80–0.85	Sandy till	1.2E-07	24.3	
	1.70–1.75	Sandy till	1.2E-07	29.8	
	2.50–2.55	Clayey sandy till	9.3E-08	23.0	
PFM004458	1.20–1.25	Gravelly till	2.3E-07	18.3	Lundin et al. (2005)
	2.50–2.55	Clayey sandy till	1.0E-07	17.0	
	1.70–1.75	Sandy till	2.3E-08	16.3	
	0.20–0.25	Sandy till	4.6E-07	27.3	
	0.50–0.55	Sandy till	6.9E-07	22.6	
	0.05–0.10	Sandy till	1.3E-06	26.0	
	0.80–0.85	Gravelly till	9.3E-07	22.2	
PFM004459	3.50–3.55	Clayey sandy-silty till	8.0E-09	19.8	Lundin et al. (2005)
PFM004460	0.50–0.55	Sandy till	3.5E-08	21.9	Lundin et al. (2005)
	0.05–0.10	Gravelly sand	3.0E-05	26.4	
	0.20–0.25	Till clay	4.6E-07	40.2	
	0.80–0.85	Sandy till	2.3E-08	20.7	
	1.20–1.25	Sandy till	1.2E-08	17.0	
	1.70–1.75	Sandy till	8.1E-09	16.0	
PFM007855	0.10–0.45	Sand	8.0E-06	35.2	NR
PFM007856	0.10–0.35	Sand	3.2E-05	50.0	NR
PFM007857	0.10–0.40	Sand	4.7E-05	43.8	NR
PFM007858	0.10–0.43	Sand	5.5E-05	40.9	NR
PFM007860*	1.00	Clay	7.2E-10	69.0	NR
PFM007861*	1.20	Clay	1.3 E-09	74.2	NR
PFM007862*	1.40	Clay	6.4E-11	71.3	NR
PFM007863*	1.00	Clay	3.1E-10	71.3	NR
PFM007864*	1.50	Clay	4.0E-10	74.7	NR
PFM007866*	1.40	Clay	1.3E-09	59.8	NR
PFM007867*	1.40	Clay	6.8E-10	65.5	NR
PFM007868*	1.60	Clay	5.3E-10	66.9	NR
PFM007869*	2.50	Clay	1.1 E-09	71.9	NR
	3.50	Clay	1.2E-09	73.4	-
SFM000133*	0.30–0.90	Glacial clay	1.1E-09	-	Werner at al. 2014

6.3.2 Sieve and sedimentation analyses: PSD curves (HY673 Grain size analysis, GE514 Sampling for sieving and sedimentation)

This section summarises hydraulic conductivity (K) estimated from PSD (particle size distribution curves) for regolith samples using the Hazen (1893), Fair-Hatch (Fair and Hatch 1933) and the Gustafson (Anderson et al. 1984) estimation methods. Table 6-5 lists all PSD estimations available in Sicada, whereas sampling locations are shown in Figure 6-6.

Note that the Sicada activity type HY673 Grain size analysis comprises hydraulic conductivity calculated using the methods mentioned above, whereas the Sicada activity type GE514 comprises PSD parameters (d_{10}, d_{60}) utilized to calculate hydraulic conductivity by the Hazen and Gustafson methods as part of the present work.

Figure 6-6 summarises the results of the PSD estimations in terms of cumulative frequency distribution curves for K (m/s). As can be seen in the figure, across all three estimations methods, estimated K values are in the approximate interval 5E-09–7E-02 m/s, i.e. spanning seven orders of magnitude, with a cumulative frequency of 50 % at K ≈ 5E-07 m/s.

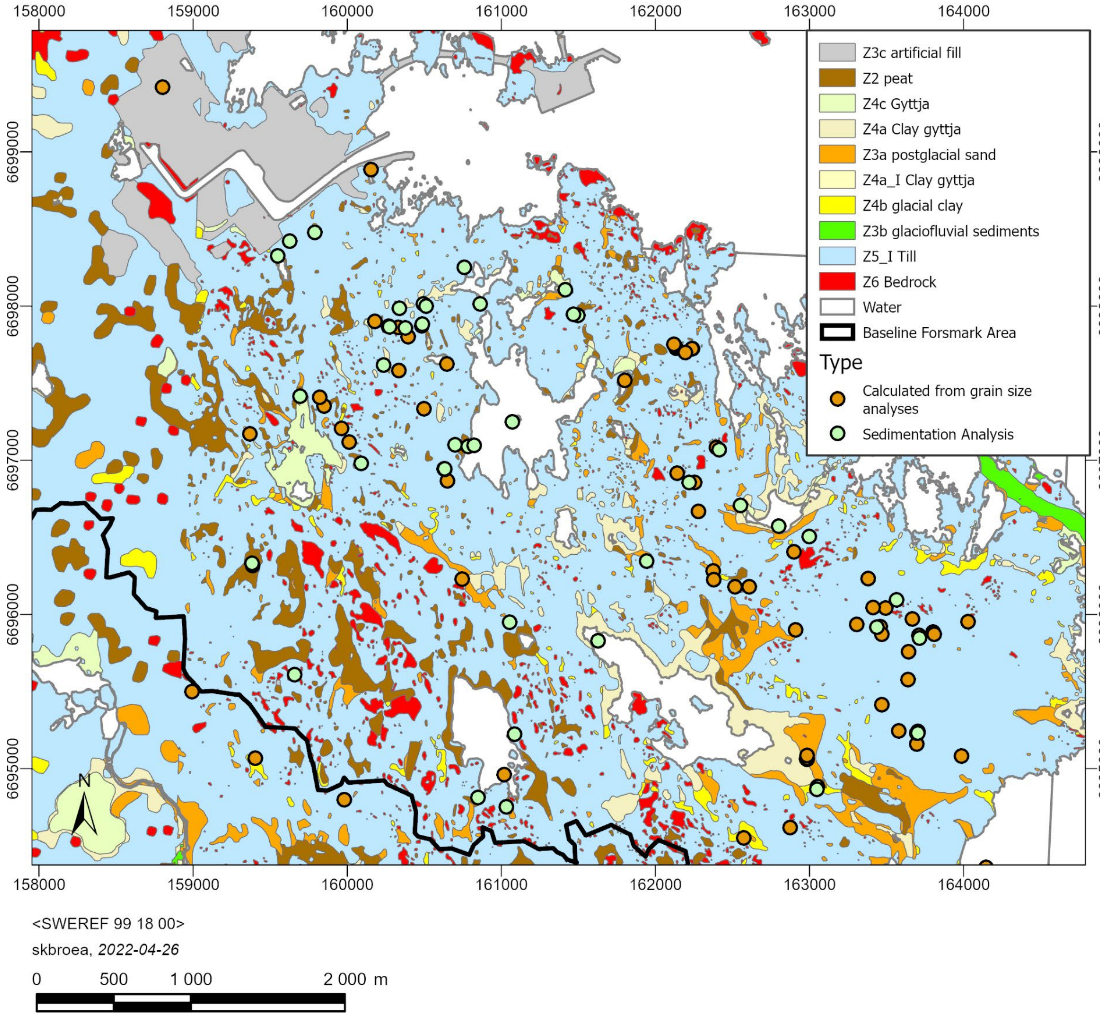

Figure 6-6. *Sampling locations for regolith samples subject to sieve and sedimentation analyses, displayed on the map of surface distribution of regolith.*

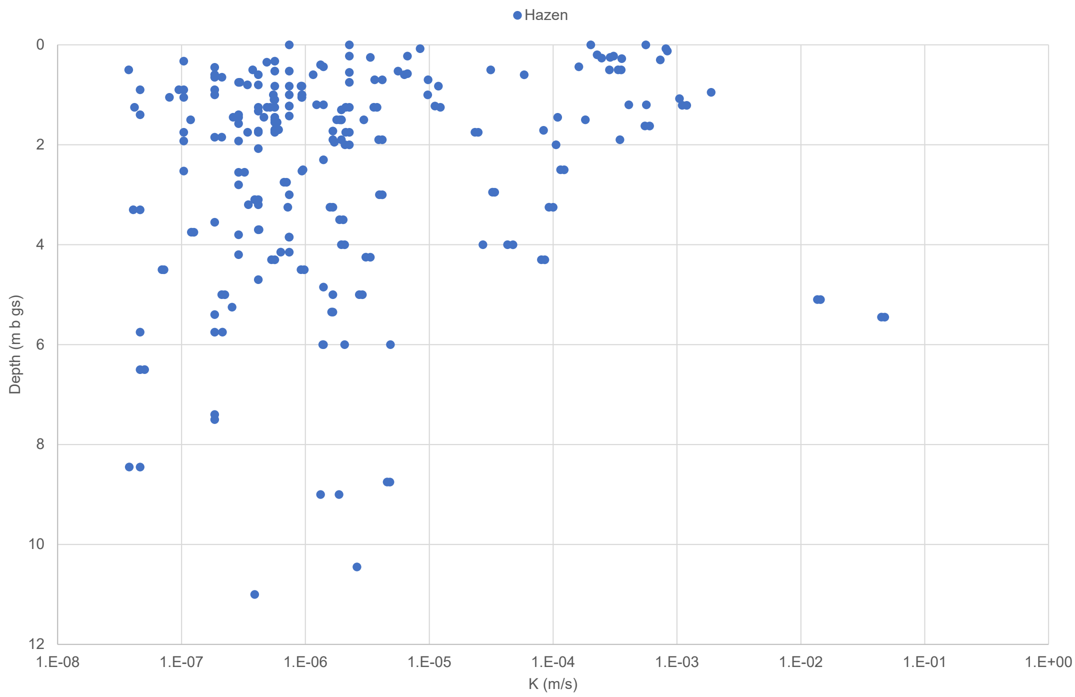
Hazen
Depth (m b gs)
K (m/s)
0
2
4
6
8
10
12
1.E-08
1.E-07
1.E-06
1.E-05
1.E-04
1.E-03
1.E-02
1.E-01
1.E+00

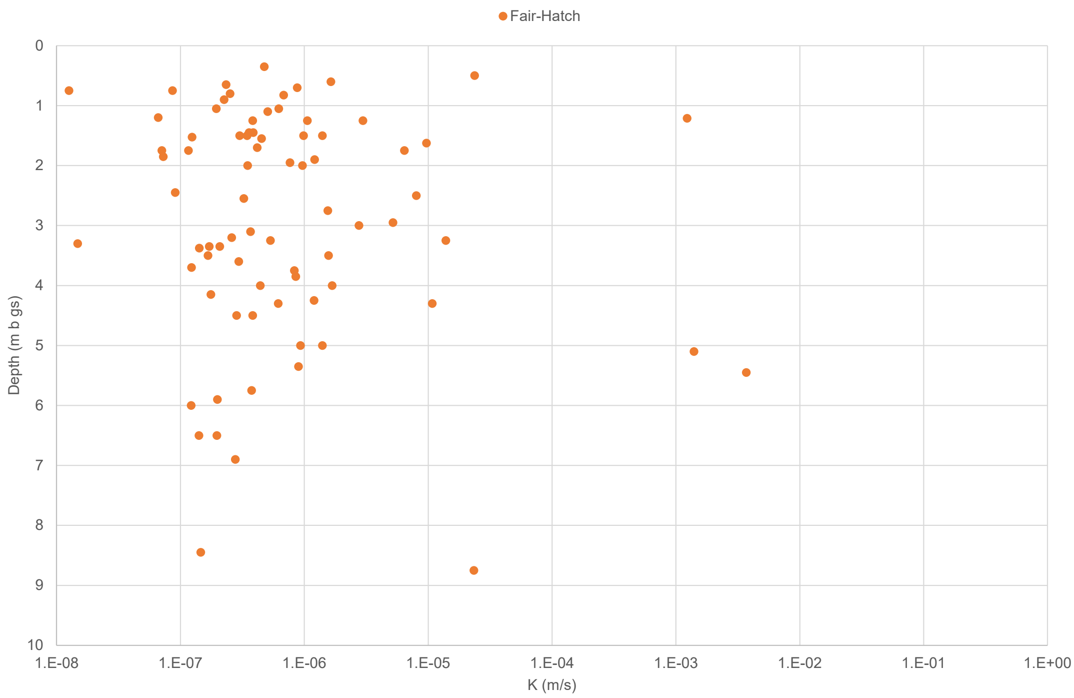
Fair-Hatch
Depth (m b gs)
K (m/s)
0
1
2
3
4
5
6
7
8
9
10
1.E-08
1.E-07
1.E-06
1.E-05
1.E-04
1.E-03
1.E-02
1.E-01
1.E+00

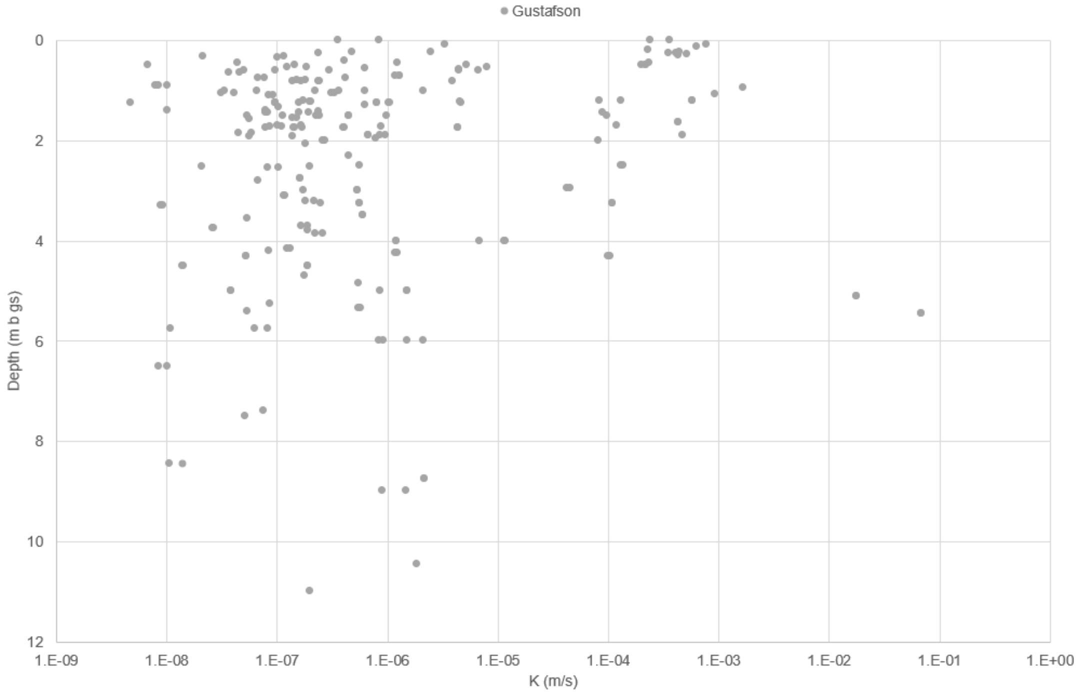

Figure 6-7. *Hydraulic conductivity K (m/s) estimated from particle size distribution curves for regolith sampled at different depths (m b gs) using the Hazen (upper plot), Fair-Hatch (middle plot) and Gustafson (lower plot) methods.*

Table 6-5. Summary of K (m/s) estimated from PSD. H = Hazen, F-H = Fair-Hatch, G = Gustafson.

Well	GSE (m, RH 2000)	Mid-sampling depth (m b gs)	Regolith type at sampling depth	K (m/s)		
				H	F-H	G
SFM0001	1.14	1.75	Gravelly till	2.34E-05	6.43E-06	4.35E-06
		3	Gravelly till	3.96E-06	2.76E-06	5.37E-07
		3.75	Clayey sandy-silty till	1.20E-07	8.31E-07	2.67E-08
SFM0002	1.80	1.5	Sandy till	1.79E-06	1.40E-06	4.48E-07
		3.5	Sandy till	1.89E-06	1.57E-06	6.03E-07
		5	Sandy till	2.72E-06	1.40E-06	1.53E-06
SFM0003	1.64	1.25	Sandy till	3.56E-06	2.97E-06	1.04E-06
		4	Sandy till	1.95E-06	1.68E-06	1.20E-06
		8.75	Sand	4.57E-06	2.34E-05	2.18E-06
SFM0004	3.71	2.75	Clayey sandy till	6.71E-07	1.55E-06	1.64E-07
SFM0005		1.25	Sandy till	4.90E-07	3.83E-07	9.72E-08
SFM0006	5.96	1.5	Clayey sandy-silty till		3.45E-07	
SFM0007	6.78	2	Clayey sandy-silty till		3.49E-07	
		4.5	Clayey sandy till	6.97E-08	3.83E-07	1.43E-08
SFM0008	3.54	1.5	Clay till		3.01E-07	
		4.5	Sandy till	9.23E-07	2.84E-07	1.89E-07
		5	Clayey sandy till	2.11E-07	9.32E-07	3.88E-08
SFM0010	13.42	1.05	Clayey sandy silty till	7.98E-08	1.95E-07	3.13E-08
SFM0011	2.19	0.9	Clayey sandy till	9.53E-08	2.25E-07	7.94E-09
		1.7	Sandy till	6.08E-07	4.17E-07	1.68E-07
		3.25	Sandy till	1.58E-06	5.32E-07	5.64E-07
SFM0013	1.47	5.1	Gravel (drill cuttings)	1.36E-02	1.40E-03	1.77E-02
		5.45	Gravel (drill cuttings)	4.48E-02	3.70E-03	6.92E-02
SFM0016	5.40	0.6	Sandy till	6.30E-06	1.64E-06	4.43E-06
		1.95	Sandy till	1.71E-06	7.65E-07	7.81E-07
		4.85	Sandy till	1.40E-06		5.50E-07
		5.9	Clayey sandy silty till		1.99E-07	
		6.9	Clayey sandy till		2.77E-07	
SFM0017	5.83	1.5	Gravelly till	1.95E-06	9.87E-07	2.43E-07
		1.9	Gravelly till	3.90E-06	1.21E-06	6.70E-07
		3.35	Clayey sandy silty till		2.08E-07	
SFM0018	5.96	3.2	Clayey sandy till	3.46E-07	2.59E-07	1.83E-07
		4.3	Clayey gravelly till	5.33E-07	6.15E-07	5.24E-08
SFM0019	3.86	1.25	Sandy till	2.12E-06	1.06E-06	8.00E-07
		4.25	Sandy till	3.08E-06	1.20E-06	1.19E-06
		5.35	Silty sand	1.63E-06	8.97E-07	5.74E-07
SFM0020	1.85	2.55	Clayey sandy till	3.23E-07	3.25E-07	1.04E-07
SFM0021	1.61	0.65	Clayey sandy till	2.12E-07	2.34E-07	4.64E-08
		1.45	Clayey sandy till	2.61E-07	3.58E-07	7.88E-08
SFM0022	1.16	4.3	Sandy till	8.03E-05	1.08E-05	1.00E-04
SFM0026	0.88	3.6	Clayey sandy till		2.96E-07	
		6.5	Clayey sandy silty till		1.41E-07	
SFM0027	1.09	3.5	Clayey sandy silty till		1.67E-007	
SFM0028	0.40	3.35	Clayey sandy till		1.71E-07	
		5.75	Clayey sandy silty till	2.14E-07	3.76E-07	8.32E-08
		6.5	Clayey sandy till	5.03E-08	1.97E-07	1.02E-08
SFM0030	1.85	0.825	Sandy till	9.23E-07	6.80E-07	2.44E-07
		1.55	Sandy till	5.92E-07	4.52E-07	1.54E-07

Well	GSE (m, RH 2000)	Mid-sampling depth (m b gs)	Regolith type at sampling depth	K (m/s)		
				H	F-H	G
		3.1	Clayey sandy till	4.17E-07		1.19E-07
SFM0031	1.93	3.1	Clayey sandy till	3.90E-07	3.68E-07	1.17E-07
SFM0032	0.75	1.05	Clayey sandy till	9.34E-07	6.22E-07	3.33E-07
SFM0034	0.85	0.35	Clayey sandy till	4.88E-07	4.75E-07	1.02E-07
		1.45	Sandy till	4.62E-07	3.87E-07	1.59E-007
SFM0036	0.80	0.8	Sandy till	3.41E-07	2.52E-07	1.52E-007
SFM0049	3.11	2	Gravelly till	2.09E-06	9.65E-07	2.63E-07
SFM0057	4.45	1.0	Gravelly till	9.73E-06		2.11E-06
		1.5	Clayey sandy till	5.67E-07		1.13E-07
SFM0062	0.86	2.95	Sandy till	3.24E-05	5.19E-06	4.27E-005
SFM0063	0.02	2.5	Sandy till	1.15E-04	8.02E-06	1.30E-004
SFM0065	0.21	3.85	Clayey sandy till	7.39E-07	8.52E-07	2.61E-007
SFM0069	2.06	0.5	Sandy gravel	3.35E-04	2.37E-05	2.19E-004
SFM0070	3.45	1.525	Clayey sandy silty till		1.24E-07	
SFM0071	3.48	3.375	Clay till		1.42E-07	
SFM0072	3.46	8.45	Clayey sandy silty till	3.79E-08	1.46E-07	1.07E-008
SFM0081	0.63	3.25	Till	9.26E-05	1.39E-05	1.10E-04
SFM0084	0.87	1.625	Sandy gravel	5.51E-04	9.67E-06	4.35E-04
		1.875				
SFM0091	0.80	1.21	Sandy gravel	1.10E-03	1.23E-03	5.85E-04
		1.285				
SFM0094	0.75	1.1	Clayey sandy till	5.59E-07	5.06E-07	9.30E-08
		1.75	Clayey sandy till	3.42E-07	1.16E-07	1.47E-07
		2.45	Clayey sandy till		9.09E-08	
SFM0095	11.28	2.26	Till			
		2.85				
SFM0103	11.22	4	No data	4.29E-05	4.42E-07	1.16E-05
SFM0104	3.13	6	Sandy till	1.38E-06	1.22E-07	9.26E-07
SFM0105	3.10	0.75	Sandy till	2.96E-07	8.64E-08	7.74E-08
		1.85	Sandy till	2.11E-07	7.26E-08	5.93E-08
SFM0106	4.48	0.75	Clayey sandy till		1.26E-08	
		3.3	Clayey sandy silty till	4.08E-08	1.48E-08	8.84E-09
SFM0107	2.68	3.7	Sandy till	4.22E-07	1.23E-07	1.89E-07
		4.15	Sandy till	6.33E-07	1.76E-07	1.23E-07
SFM0108	3.60	0.7	Sandy till	3.63E-06	8.76E-07	1.19E-06
SFM000133	2.73	1.2		1.23E-06	6.62E-08	
		1.75		2.12E-06	7.08E-08	4.12E-07
HFM01		6	Sandy till	4.86E-06		2.12E-06
		9	Sandy silty till	1.87E-06		1.49E-06
		1.25	Sandy till	1.23E-05		4.69E-06
HFM02		4	Gravelly till	2.71E-05		6.83E-06
		2	Gravelly till	1.06E-04		8.24E-05
		11	Sandy-silty till	3.89E-07		2.01E-07
HFM03		6	Sandy till	2.08E-06		1.50E-06
		1.5	Gravelly till	1.82E-04		9.69E-05
		9	Sandy-silty till	1.32E-06		9.12E-07
HFM04		0.7	Gravelly till	9.80E-06		1.30E-06
HFM05		3.25	Clayey sandy till	7.22E-07		2.49E-07
HFM06		1.25	Clayey sandy till	4.18E-08		4.73E-09
HFM09		1.75	Sandy silt	1.04E-07		7.98E-08

Well	GSE (m, RH 2000)	Mid-sampling depth (m b gs)	Regolith type at sampling depth	K (m/s)		
				H	F-H	G
		1	Sandy till	9.37E-07		3.65E-07
HFM10		0.75	Gravelly till	2.27E-06		4.17E-07
KFM01A		5.25	Clayey sandy silty till	2.56E-07		8.72E-08
		2.5	Silty sand	9.58E-07		5.66E-07
PFM002461		1.25	Clayey sandy till	4.17E-07		9.60E-08
PFM002462		2.3	Sandy till	1.40E-06		4.51E-07
PFM002462		0.2	Gravelly sand	2.27E-04		2.30E-04
PFM002463		10.45	Sandy till	2.60E-06		1.85E-06
PFM002463		7.5	Clayey sandy till	1.85E-07		5.16E-08
PFM002464		5.75	Clayey sandy silty till	4.63E-08		1.10E-08
PFM002464		7.4	Clayey sandy silty till	1.85E-07		7.56E-08
PFM002572		4.2	Clayey sandy till	2.89E-07		8.57E-08
PFM002572		5.4	Clayey sandy till	1.85E-07		5.42E-08
PFM002573		3.55	Clayey sandy till	1.85E-07		5.35E-08
PFM002576		5	Sandy till	1.67E-06		8.63E-07
PFM002576		1.9	Sandy till	1.67E-06		9.73E-07
PFM002577		0.6	Clayey sandy till	4.17E-07		9.75E-08
PFM002578		3.8	Clayey sandy silty till	2.89E-07		1.90E-07
PFM002581		1	Sandy silty till	9.37E-07		6.28E-07
PFM002582		0.6	Sandy till	1.16E-06		2.97E-07
PFM002582		1.7	Sandy till	5.67E-07		1.02E-07
PFM002586		0.6	Clayey sandy till	1.85E-07		5.01E-08
PFM002586		1.4	Sandy silty till	2.89E-07		7.88E-08
PFM002587		3	Sandy till	7.40E-07		1.76E-07
PFM002587		1	Gravelly till	7.40E-07		6.63E-08
PFM002589		4.7	Sandy till	4.17E-07		1.78E-07
PFM002591		0.9	Clayey gravelly till	1.85E-07		1.01E-08
PFM002594		1.4	Clayey sandy till	4.63E-08		1.01E-08
PFM002670		0.325	Clayey sandy till	1.04E-07		2.16E-08
PFM002687		1.5	Clayey sandy silt	1.18E-07		5.41E-08
PFM002687		0.5	Clayey sandy till	3.76E-07		1.44E-07
PFM002687		1	Sandy till	5.51E-07		2.21E-07
PFM002761		0.5	Clayey sandy till	3.75E-08		6.78E-09
PFM002768		1	Clayey sandy till	1.85E-07		3.35E-08
PFM002783		0.3	Sandy gravel	7.34E-04		4.35E-04
PFM002801		0.4	Sandy till	1.32E-06		4.15E-07
PFM002802		1.3	Sandy till	1.96E-06		6.35E-07
PFM003742		0	Sandy silty till	7.40E-07		3.58E-07
PFM004222		1.9	Sand	3.46E-04		4.77E-04
PFM004294		0	Gravelly sand	2.02E-04		2.39E-04
PFM004396		0.44	Clayey silty sand	1.40E-06		1.24E-06
PFM004454		1.425	Clayey sandy till	7.40E-07		2.37E-07
PFM004455		2.075	Clayey sandy silty till	4.17E-07		1.81E-07
PFM004455		0.125	Gravelly sand	8.37E-04		6.39E-04
PFM004455		1.725	Sandy till	1.67E-06		8.85E-07
PFM004455		0.825	Sandy till	7.40E-07		1.65E-07
PFM004455		0.225	Sandy till	2.27E-06		4.80E-07
PFM004455		2.525	Clayey sandy till	1.04E-07		2.08E-08
PFM004455		1.225	Sandy till	7.40E-07		1.98E-07
PFM004455		0.525	Sandy till	5.67E-07		1.25E-07

Well	GSE (m, RH 2000)	Mid-sampling depth (m b gs)	Regolith type at sampling depth	K (m/s)		
				H	F-H	G
PFM004456		1.925	Clayey sandy silty till	2.89E-07		1.38E-07
PFM004458		1.225	Gravelly till	1.11E-05		4.60E-06
PFM004458		1.725	Sandy till	5.67E-07		1.11E-07
PFM004458		0.225	Sandy till	6.66E-06		2.50E-06
PFM004458		2.525	Sandy till	9.37E-07		2.00E-07
PFM004458		0.525	Sandy till	5.60E-06		7.95E-06
PFM004458		0.825	Gravelly till	1.18E-05		3.94E-06
PFM004458		0.075	Sandy till	8.43E-06		3.36E-06
PFM004460		1.075	Gravelly sand	1.05E-03		9.33E-04
PFM004460		1.325	Clayey sandy till	4.17E-07		1.04E-07
PFM004460		1.575	Clayey sandy till	2.89E-07		5.67E-08
PFM004460		1.925	Clayey sandy silty till	1.04E-07		5.66E-08
PFM004460		1.225	Sandy till	7.40E-07		2.04E-07
PFM004460		0.075	Gravelly sand	8.13E-04		7.78E-04
PFM004460		0.525	Sandy till	7.40E-07		1.87E-07
PFM004460		0.825	Sandy till	5.67E-07		1.40E-07
PFM004460		1.725	Sandy till	4.17E-07		8.67E-08
PFM004514		0.9	Clayey sandy silty till	4.63E-08		8.58E-09
PFM004514		2.8	Clayey sandy till	2.89E-07		6.70E-08
PFM004514		1.5	Sandy till	2.96E-06		9.96E-07
PFM004531		0	Sandy gravel	5.60E-04		3.61E-04
PFM004752		0	Sandy till	2.27E-06		8.47E-07
PFM004760		1.25	Sandy till	5.67E-07		1.58E-07
PFM004761		0.55	Sandy till	2.27E-06		6.33E-07
PFM004762		0.45	Clayey sandy till	1.85E-07		4.38E-08
PFM006094		1.71	Sand	8.36E-05		1.20E-04
PFM006095		0.44	Sand	1.61E-04		2.35E-04
PFM007855		0.275	Sand	3.58E-04		5.16E-04
PFM007856		0.225	Sand	3.07E-04		4.41E-04
PFM007857		0.25	Sand	2.89E-04		4.17E-04
PFM007858		0.265	Sand	2.47E-04		3.58E-04
PFM007786		0.6	Silty till	5.83E-05		6.76E-06
PFM007786		0.95	Coarse sand/fine gravel	1.89E-03		1.67E-03
PFM007786		1.2	Sandy/gravelly till	4.09E-04		1.33E-04
SFM000191/ QFM000297		1.2	Gravelly stony till	5.65E-04		8.33E-05
SFM000192/ QFM000298		0.25	Sandy silty gravelly till	3.34E-06		2.37E-07
PFM002890		0.5		2.85E-04		1.99E-04
PFM002891		0.5		3.13E-05		5.22E-06

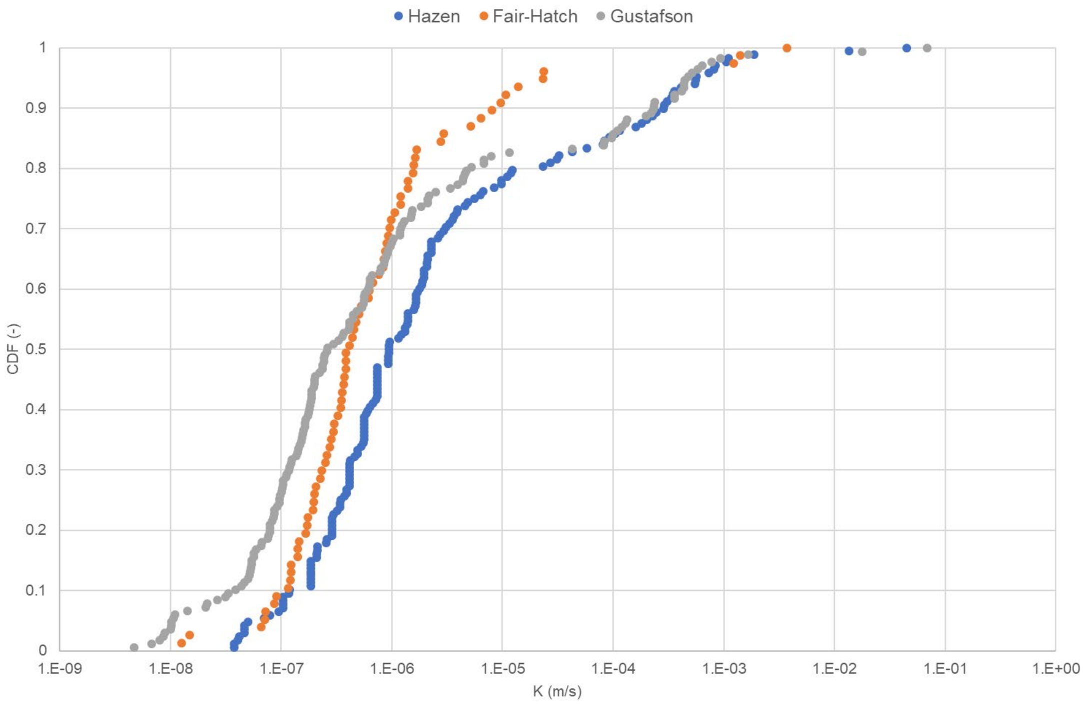

Figure 6-8. *Cumulative frequency distribution curves for hydraulic conductivity K (m/s) estimated from particle size distribution curves using the Hazen, Fair-Hatch and Gustafson methods.*

6.3.3 Properties related to water storage and retention in the unsaturated zone (HY672)

This section summarises properties related to water storage and retention in the unsaturated zone (Lundin et al. 2005). The sampling locations are shown in Figure 6-9. Figure 6-10 and Figure 6-11 summarise storage properties (total porosity and specific yield) as function of sampling depth (metres below ground surface), whereas Figure 6-12 to Figure 6-15 present soil water retention curves (for regolith types, see Table 6-5). According to these data, both the total porosity and the specific yield decrease with depth. The total porosity is 25–40 % down to a depth of c 0.25 m below ground surface, and 15–30 % below a depth of c 1 m. The specific yield decreases from c 15–30 % close to the ground surface to c 5 % below a depth of c 1 m. According to Figure 6-12 to Figure 6-15, the field capacity (by convention, the water content at a suction head of 100 cm) is relatively constant (c 15 %) irrespective of depth.

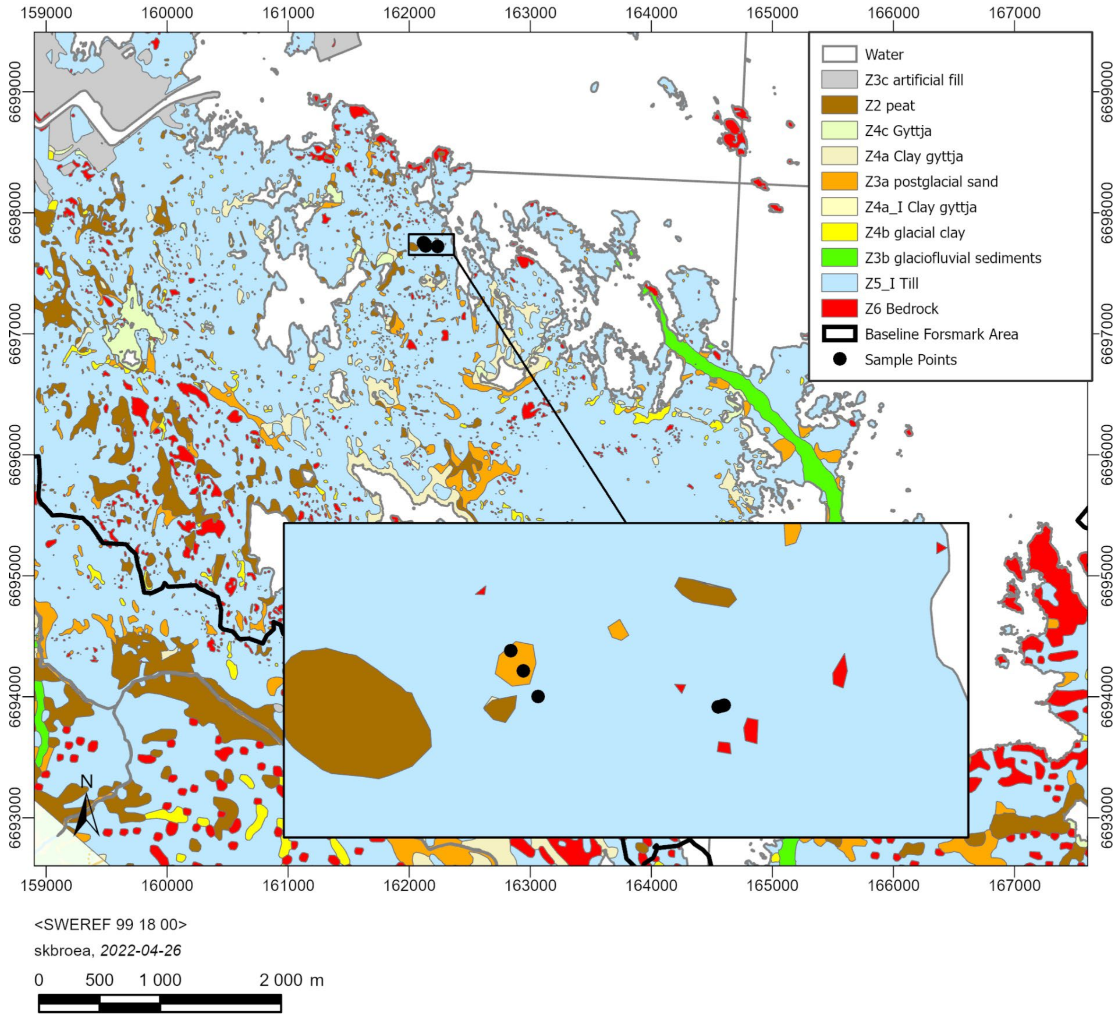

Figure 6-9. *Sampling locations for regolith samples subject to laboratory tests for estimation of water storage and retention properties in the unsaturated zone.*

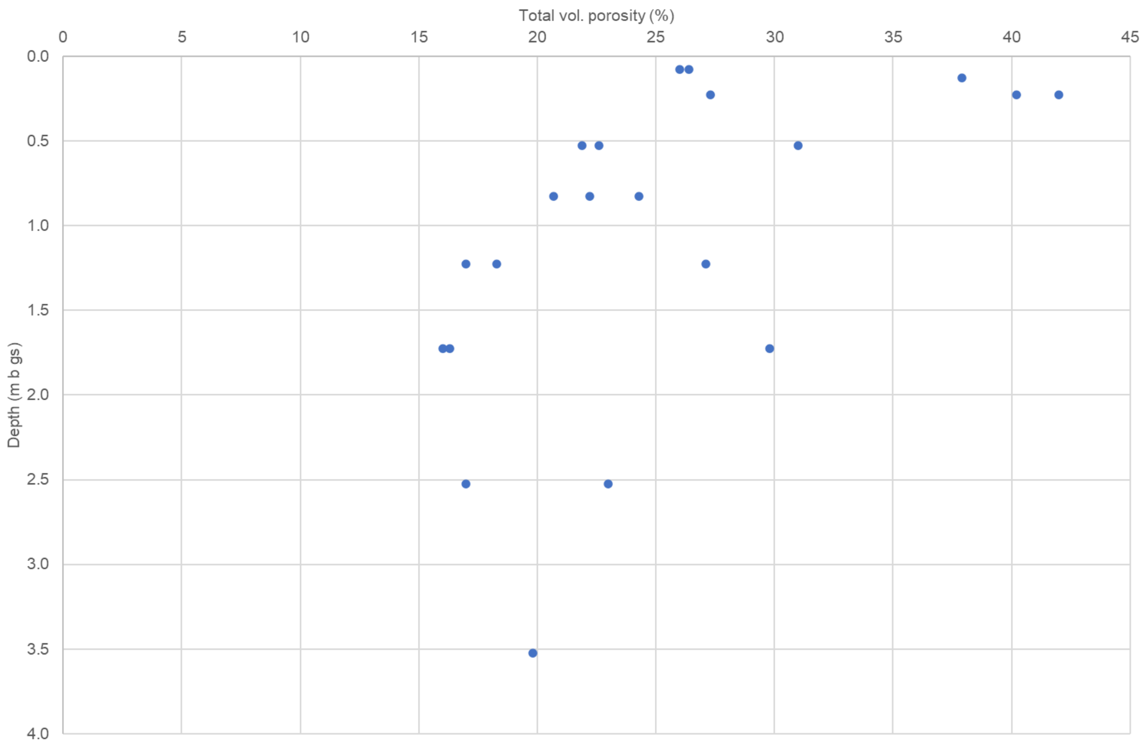

Figure 6-10. *Total porosity (% by volume) for regolith sampled at different depths (m b gs) at the PFM004455, -4458, -4459 and -4460 sampling locations.*

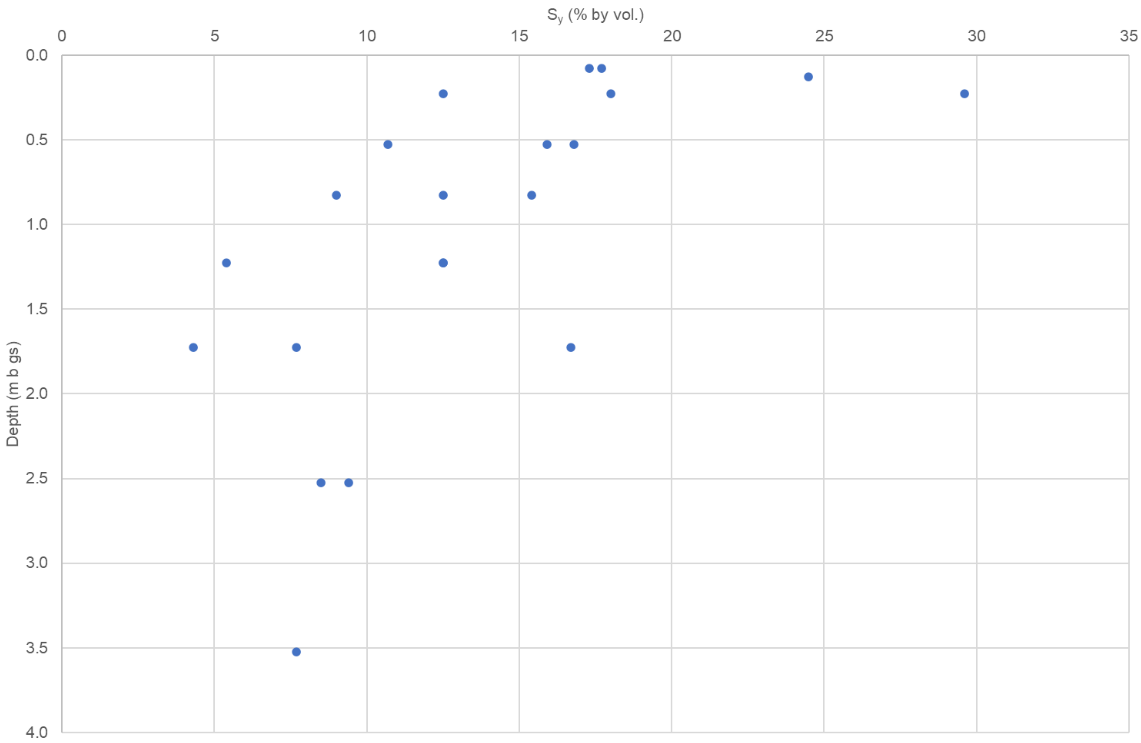

Figure 6-11. *Specific yield (% by volume) estimated from laboratory tests on regolith sampled at different depths (m b gs) at the PFM004455, -4458, -4459 and -4460 sampling locations.*

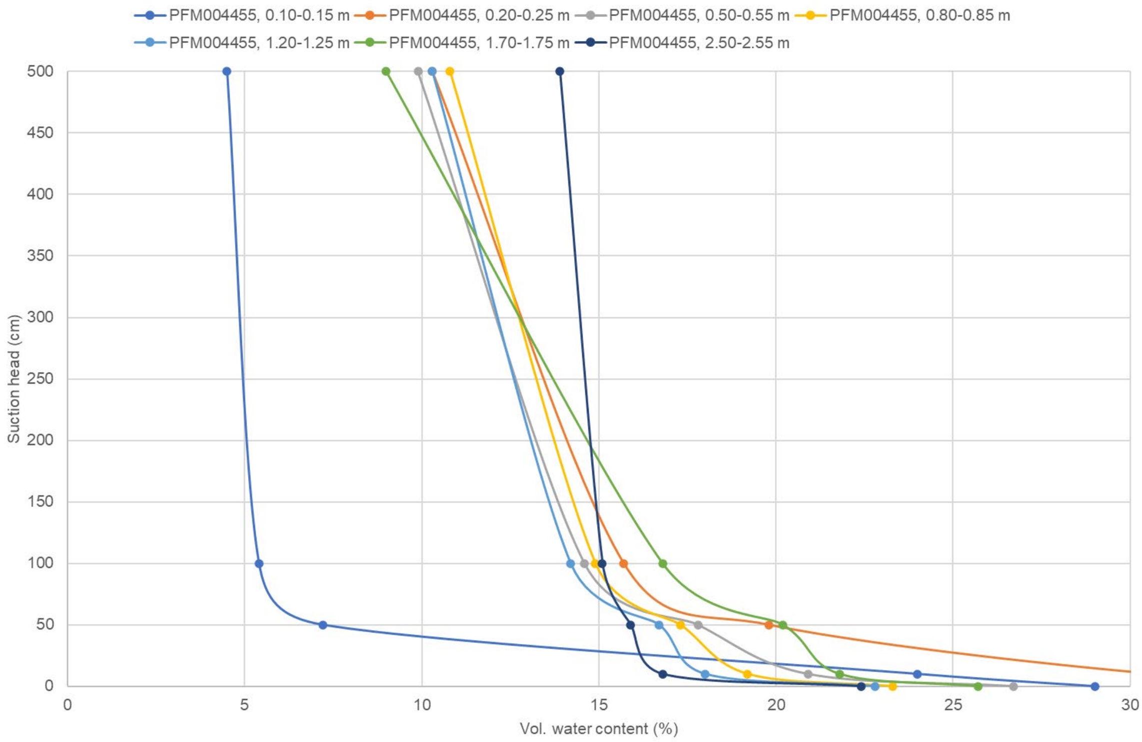

Figure 6-12. *Water retention curves for regolith sampled at different depths (m b gs) at the PFM004455 sampling location. By convention, field capacity corresponds to a suction head of 100 cm.*

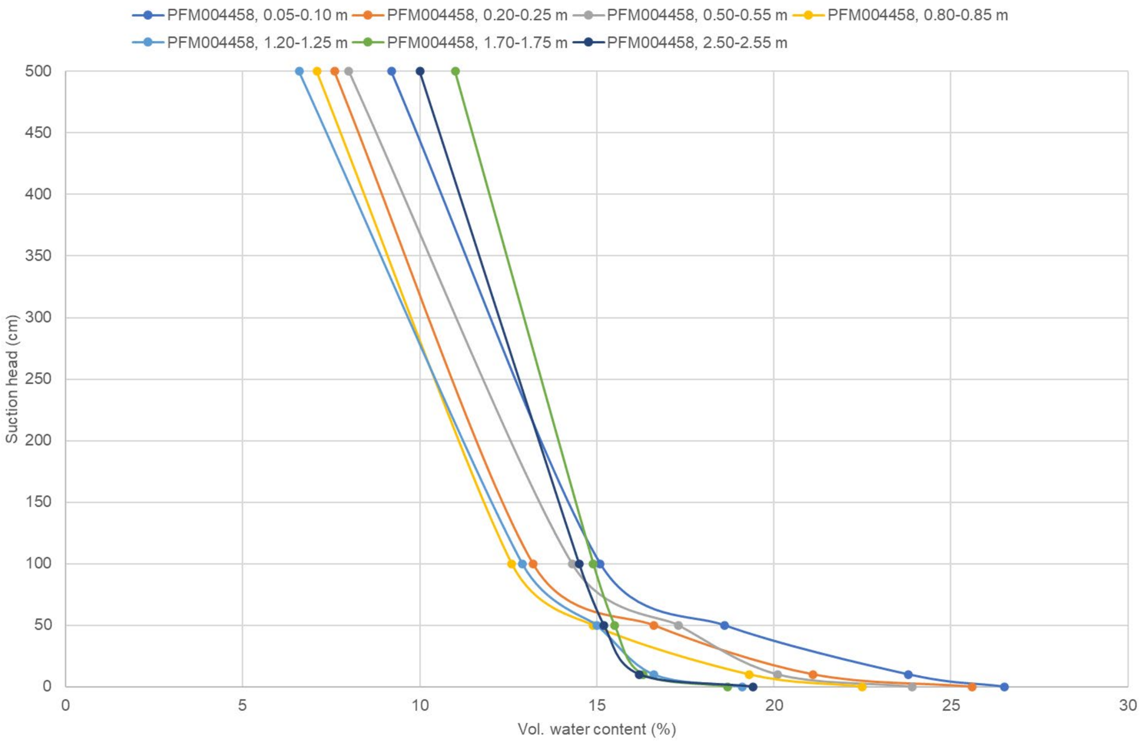

Figure 6-13. *Water retention curves for regolith sampled at different depths (m b gs) at the PFM004458 sampling location. By convention, field capacity corresponds to a suction head of 100 cm.*

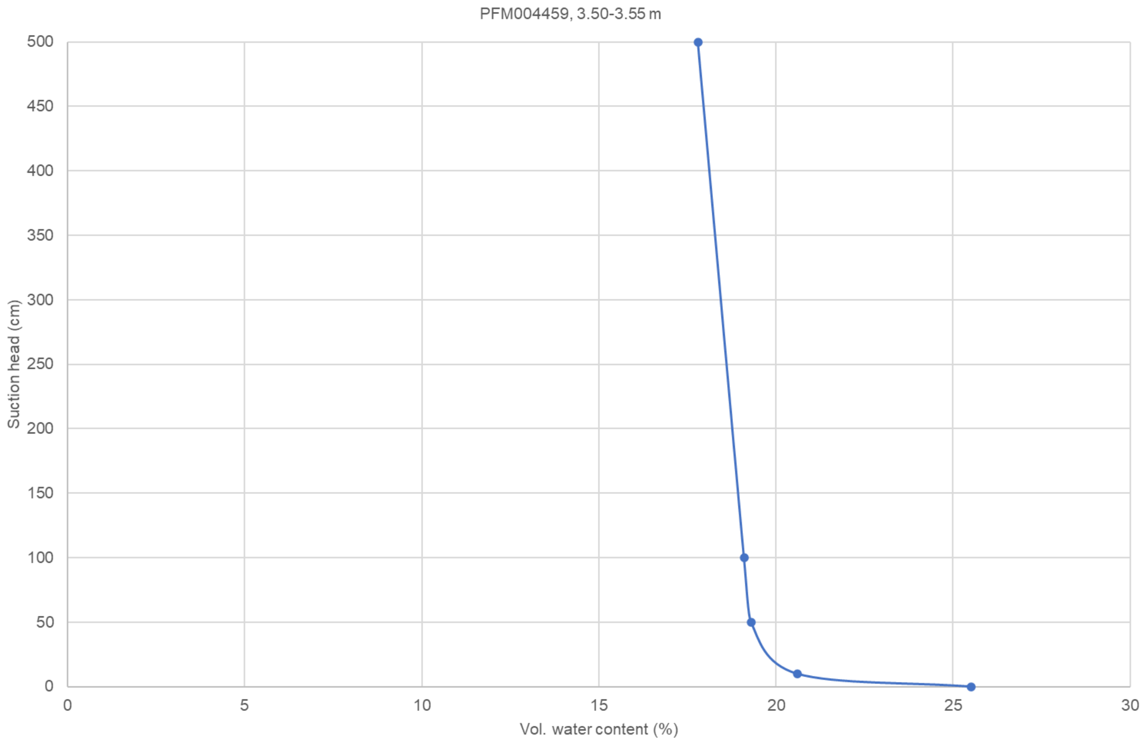

Figure 6-14. *Water retention curve for regolith sampled at a depth of 3.50–3.55 m b gs at the PFM004459 sampling location. By convention, field capacity corresponds to a suction head of 100 cm.*

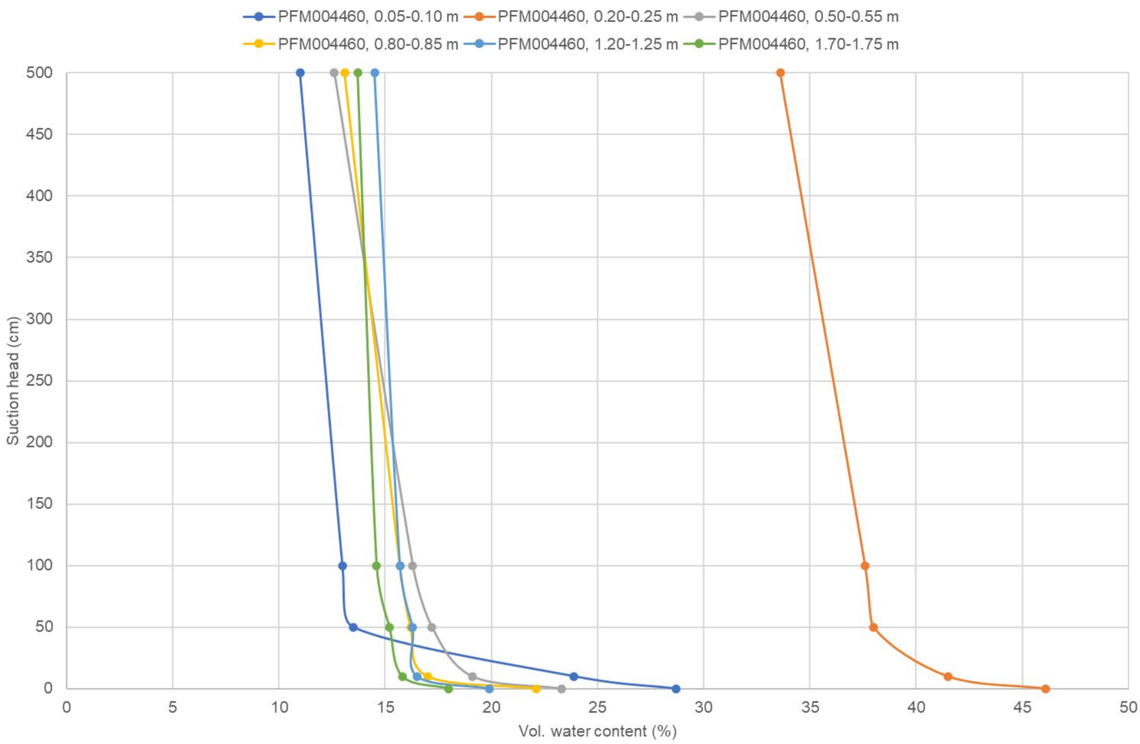

Figure 6-15. *Water retention curves for regolith sampled at different depths (m b gs) at the PFM004460 sampling location. By convention, field capacity corresponds to a suction head of 100 cm.*

7 Hydraulic characterisation of the near-surface bedrock

7.1 Hydraulic characterisation in SDM-Site and SDM-PSU

The uppermost bedrock in the Forsmark area contains transmissive sub-horizontal discrete features. Several of these are termed sheet joints (or sheeting joints) and typically occur in the uppermost tens of metres below the bedrock surface. However, sub horizontal features can occur as deep as 150 m below the bedrock surface. Hydraulically, the combination of transmissive sub horizontal discrete features at different depths and outcropping deformation zones, both gently dipping and steeply dipping, is believed to form a well-connected lattice of potential conduits for groundwater flow. Groundwater levels measured in percussion-drilled boreholes suggest that such conduits may short circuit both recharge from above and discharge from below (Figure 7-1).

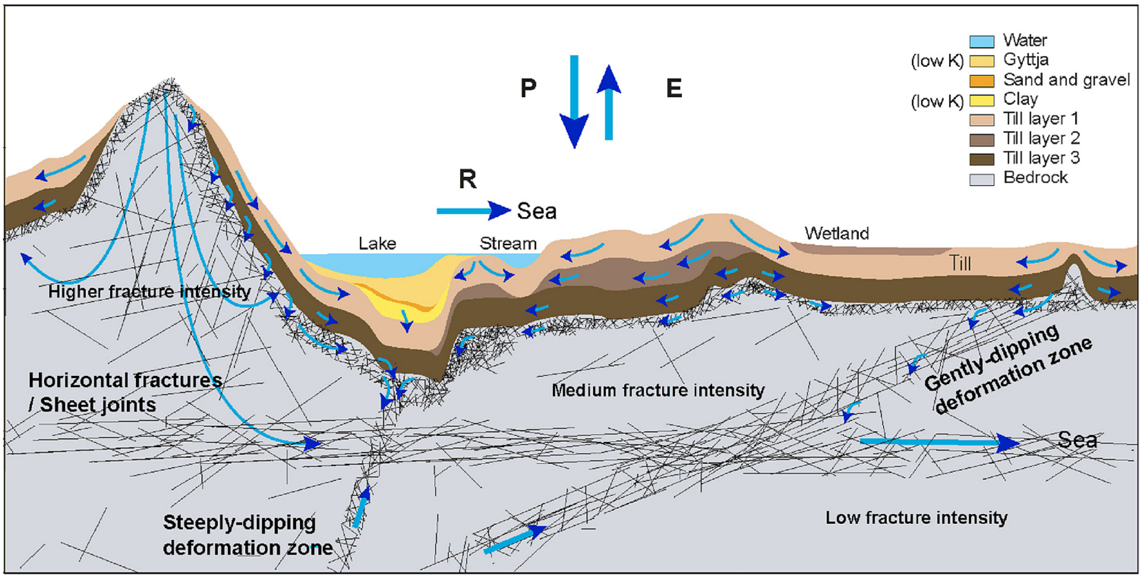

Figure 7-1. *Two-dimensional cartoon of the near-surface bedrock in Forsmark. The connectivity caused by horizontal sheet joints and outcropping deformation zones is envisaged to create a hydraulic cage in the north-western part of the tectonic lens. Strands of evidence that support the envisaged hydraulic interplay between the groundwater in the superficial bedrock and in the regolith are presented in Follin et al. (2007a).*

Examples of sub-horizontal features were documented during the construction of the cooling water canal, which runs between the Baltic Sea and the nuclear power plant (Figure 7-2); the trace lengths of these sheet joints were observed to be in the order of hundreds of metres. In addition to geo-structural evidence obtained during construction, there are three pieces of hydrogeological evidence that support the hydraulic importance of these structures (Follin et al. 2008):

1. Elevated groundwater yields. The median yield of the first 22 percussion-drilled boreholes (HFM01–HFM22)is approximately 12,000 L/h. This is roughly 20 times higher than the median yield of domestic water wells drilled outside but in close proximity to the candidate area, and which in turn is no different from the median yield of approximately 200,000 bedrock wells registered with the Geological Survey of Sweden (Gentzschein et al. 2007).
2. The near uniform groundwater level in the uppermost 150 m of bedrock observed among the percussion-drilled boreholes within the target area. This is on the average roughly 0.5 m above sea level. In contrast, the average groundwater level among the percussion-drilled boreholes outside the candidate area is roughly 2.8 m above the sea level (Gentzschein et al. 2007).
3. The extensive and rapid transmission of fluid pressure changes (drawdown) during the large-scale interference test, which was conducted over three weeks during the summer of year 2006 in borehole HFM14, located in the centre of the target area (Follin et al. 2007c).

Figure 7-2. Picture from the construction of the 13 m deep and more than one kilometre long canal between the Baltic Sea and the nuclear power plant. Horizontal fractures/sheet joints were encountered along the entire excavation. As seen in the picture, there are several "beds" of extensive sheet joints on top of each other. The picture is taken from the southern side of the canal where the current bridge crosses the canal between HFM20 and HFM22 (Carlsson and Christiansson 2007).

Based on the results obtained from the interference test in HFM14, the lateral extent of the horizontal fractures/sheet joints was hypothesised to correspond approximately to fracture domain FFM02, but stretching north all the way to the Singö deformation zone (ZFMWNW0001). The other hypothesised physical boundaries are deformation zone ZFMENE0062A to the southeast and the border of fracture domain FFM02 to the southwest and west, with the modification that the boundary passes between boreholes HFM20 and HFM28 (*Figure 3-2*). The core-drilled part of core-drilled boreholes in Forsmark generally starts at –100 m elevation, with the uppermost 100 m often being percussion-drilled and cased with a steel casing in order to allow for hydraulic testing with the PFL-f method and installation of groundwater monitoring equipment, which require a large-diameter borehole in order to host the equipment. This means that there are neither many cores collected nor fractures tested in detail with the PFL-f method in the uppermost part of the bedrock at the time of the site investigation for SDM-Site.

During the SDM-PSU site investigation phase (SKB 2011) it was observed that the hydraulic network within the uppermost bedrock within the SFR bedrock volume is dominated by transmissive, connected and sub-horizontal fractures, although these fractures were notably less transmissive and less extensive than similar structures observed within the tectonic lens. An additional deterministic modelling structure was developed, termed Shallow Bedrock Aquifer (SBA) structures (Öhman et al. 2012). These structures were interpreted from hydrogeological data during the SDM-PSU site investigation, wherein it was concluded that the upper 200 m of the bedrock is hydraulically dominated by a system of transmissive, connected, sub-horizontal fractures. The purpose of modelling these data separately was to honour deterministic data from single-hole and cross-hole hydraulic tests, and to avoid an over-representation of hydraulically transmissive fractures in the stochastic DFN model.

The orientations of the selected PFL-f data are sub-horizontal and, with one exception, had estimated transmissivity values in the order of $T > \approx 10^{-6}$ m^2/s. The selection of borehole intercepts data was supported by hydraulic head data, meaning that boreholes intersecting the same feature showed similar drilling responses and associated drawdown. In several cases the locations and orientations of the intercepts are supported by oriented radar reflectors and other geophysical data (Öhman et al. 2012). The features were subjectively terminated against deterministically modelled deformation zones and/or borehole feature intercepts lacking hydraulic responses.

It should be pointed out that in reality each SBA structure is envisaged to represent a network of connected sub-horizontal fractures, rather than a single fracture, and that the extension outside borehole coverage is highly uncertain. Also, the deterministically modelled features are probably only a sub-set of the total number of horizontal hydraulic conductors in the model area, since only features intercepted by boreholes are possible to observe.

7.2 Transmissivity data correlated to modelled sheet joint intercepts

Supporting single-hole hydraulic data correlated to deterministically modelled sheet joints (JFMxxx) as part of the DMS geological model include PFL tests, hydraulic injection tests or impeller flow logging (Table 7-1). As some of these structures have no modelled thickness, PFL-f anomalies within a set (±3 m) distance along the borehole from the upper and lower JFM-intercepts were summed and associated with to provide a representative conceptual understanding of hydraulic transmissivity in close proximity to each JFM structure. It was assumed that the sheet joints would account for the most transmissive structure within intercepts of injection test or impeller flow logging sections. In the absence of other data, the impeller flow logging transmissivity for the entire borehole was evaluated under the assumption that sheet joints would likely account for the most transmissive structures intercepted by the borehole.

Table 7-1. Summary of hydraulic data available for interpreting sheet joint intercepts in Forsmark boreholes. PFL-f anomaly transmissivity values were summed within three metres of the upper or lower intercept. No. PFL is the number of PFL anomalies within this borehole length interval. L_{PSS} and L_{HTHB} are the lengths of intercepting injection test sections and recorded impeller flow logging lengths, respectively. $\sum T_{PFL\text{-}f}$, $\sum T_{INJ}$ and $\sum T_{HTHB}$ are the sum of the included flow anomalies, injection test transmissivity or impeller flow logging transmissivity, respectively. Eval. meth. (or Data type) indicates whether Moye's transmissivity estimate (TM) or an estimate based on a 2D radial flow model (TT) was used. HTHB type indicates whether the transmissivity presented is that of an inferred flow anomaly (TFa) or is based on the entire borehole section (E.H.) considered representative for the flow logging.

SHEET JOINT	BH	TARGET INTERCEPT (BH length m)		No. PFL	$\sum T_{PFL\text{-}f}$	L_{PSS} (m)	$\sum T_{INJ}$	Eval. meth.	L_{HTHB} (m)	$\sum T_{HTHB}$	HTHB type
ID	ID	Upper	Lower	(-)	(m²/s)						
JFM002	KFM26	6.31	6.56	4	9E-07						
JFM003	KFM19	7.5	7.5						1.8	1E-05	TFa
JFM004	HFM39	7.07	7.07						14.0	3E-07	TFa
JFM004	KFM13	11.1	11.1						2.6	1E-04	TFa
JFM004	KFM14	6.79	6.79	1	1E-07				54.3	8E-05	E.H.
JFM004	KFM15	8.0	8.0	2	1E-08				2.0	3E-04	TFa
JFM004	KFM16	10.1	10.1	4	1E-06				55.9	2E-05	E.H.
JFM004	KFM17	6.3	6.3						54.5	2E-06	E.H.
JFM004	KFM18	10.5	10.5						5.1	1E-06	TFa
JFM004	KFM20	5.91	5.99	1	4E-06				6.7	3E-04	TFa
JFM004	KFM21	6.8	6.8	2	7E-05				3.2	1E-04	TFa
JFM004	KFM08B	10.77	10.77			5.0	2E-06	TT			
JFM005	KFM08B	21.36	21.39			5.0	1E-05	TT			
JFM005	KFM13	23.19	23.19						142.0	1E-04	E.H.
JFM005	KFM14	18.91	18.91	4	6E-06				1.3	3E-06	TFa
JFM005	KFM16	18.63	18.63	5	8E-06				6.5	2E-06	TFa
JFM006	HFM39	22.51	22.72						145.2	3E-07	E.H.
JFM006	KFM15	21.14	21.4	4	3E-07				54.8	3E-04	E.H.
JFM006	KFM18	20.62	21.08						51.6	3E-06	E.H.
JFM006	KFM20	20.05	20.19	4	2E-06				58.2	3E-04	E.H.
JFM007	KFM14	22.79	22.79	4	7E-06				54.3	8E-05	E.H.
JFM007	KFM13	27.06	27.23						142.0	1E-04	E.H.
JFM007	KFM21	23.7	23.7	5	1E-05				5.5	1E-05	TFa
JFM007	KFM23	23.5	23.5	2	1E-05				96.0	3E-04	E.H.
JFM007	KFM17	23.97	23.97						54.5	2E-06	E.H.
JFM007	KFM16	28.14	28.14	4	2E-06				3.4	1E-05	TFa
JFM007	HFM22	28.85	28.85						1.0	1E-05	TFa

SHEET JOINT ID	BH ID	TARGET INTERCEPT (BH length m) Upper	Lower	No. PFL (-)	$\sum T_{PFL\text{-}f}$ (m²/s)	L_{PSS} (m)	$\sum T_{INJ}$	Eval. meth.	L_{HTHB} (m)	$\sum T_{HTHB}$	HTHB type
JFM008	KFM08B	30.96	30.99			5.0	2E-05	TT			
JFM008	KFM14	24.17	24.17	4	7E-06				1.8	5E-06	TFa
JFM008	KFM16	28.14	28.14	4	2E-06				3.4	1E-05	TFa
JFM008	KFM21	26.99	26.99	5	2E-05				5.5	1E-05	TFa
JFM008	KFM23	27.1	27.1	4	2E-05				96.0	3E-04	E.H.
JFM008	HFM22	28.85	28.85						1.0	1E-05	TFa
JFM009	KFM08B	61.92	61.92			5.0	3E-08	TT			
JFM009	KFM14	53.3	53.3	2	4E-05				2.0	3E-05	TFa
JFM009	KFM23	54.5	54.5	4	3E-06				96.0	3E-04	E.H.
JFM009	KFM24	51.84	51.84	1	4E-08						
JFM009	HFM22	62.23	62.27						3.5	1E-04	TFa
JFM010	HFM42	12.37	12.42						195.0	7E-04	E.H.
JFM011	HFM21	27.21	27.21						175.0	7E-04	E.H.
JFM011	HFM42	23.3	23.3						195.0	7E-04	E.H.
JFM012	HFM21	48.08	48.08						175.0	7E-04	E.H.
JFM012	HFM42	41	41						195.0	7E-04	E.H.
JFM014	KFM07A	178.5	178.53	1	2E-05	5.0	2E-05	TT			
JFM014	KFM07C	156.3	156.38	1	5E-05						
JFM014	HFM42	157.86	157.86						1.0	2E-04	TFa
JFM015	KFM25	6.63	6.63	1	4E-06						
JFM016	KFR117	11.8	11.8			6.0	1E-04	TM			
JFM016	KFR119	11.4	11.4	3	7E-06	6.0	6E-04	TM			

7.3 Transmissivity data correlated to modelled SBA structure intercepts

Hydraulic intercept data, obtained during the SDM-PSU site investigations (Table 7-2), were used to deterministically model the geometries of the SBA-Structures. Five boreholes that were later established in the SFR area (KFR117-KFR121) intercept the modelled geometries of the modelled SBA structures (Table 7-3).

Table 7-2. PFL-f and HTHB flow anomalies used for parameterisation of the deterministically modelled SBA structures, adapted from Öhman et al. (2012).

SBA-struct.	BH	PFL-f ID	Length along BH (m)	Elev. (m)	Orientation [1)] Strike	Dip	T (m²/s)	PFL head [2)] (m)	Head BH Sect.[3)] (m)
SBA1	HFR102	–	55.04	–44.1	–	–	2.8E–06	–	–0.8
SBA1	KFR27	–[4)]	50.17	–48.1	322	13	1.8E–06	–	–0.5
SBA1	KFR27	–[4)]	54.74	–51.1	14	31	1.8E–06	–	–0.5
SBA2	KFR102A	KFR102A_001	72	–63.1	–	–	8.6E–08	–	–1.4
SBA2	KFR103	KFR103_031	84.58	–66.1	357	15	1.2E–06	–0.20	–0.5
SBA2	KFR103	KFR103_032	85.67	–67.0	223	2	9.5E–06	–0.20	–0.5
SBA2	KFR103	KFR103_033	86.61	–67.7	157	9	4.7E–06	–0.10	–0.5
SBA2	KFR103	KFR103_034	89.15	–69.8	318	32	3.3E–07	–0.10	–0.5
SBA2	KFR103	KFR103_035	89.69	–70.2	321	18	2.8E–08	–	–0.5
SBA2	KFR103	KFR103_036	91.83	–71.9	327	16	1.5E–08	–	–0.5
SBA2	KFR27	–[4)]	98.5	–96.1	84	9	1.1E–06	–	–0.5
SBA3	HFR106	HFR106_001	39	–31.9	233	7	3.1E–05	–	–0.2
SBA3	KFR103	KFR103_031	84.58	–66.1	357	15	1.2E–06	–0.20	–0.5
SBA3	KFR103	KFR103_032	85.67	–67.0	223	2	9.5E–06	–0.20	–0.5
SBA3	KFR103	KFR103_033	86.61	–67.7	157	9	4.7E–06	–0.10	–0.5
SBA3	KFR103	KFR103_034	89.15	–69.8	318	32	3.3E–07	–0.10	–0.5
SBA3	KFR103	KFR103_035	89.69	–70.2	321	18	2.8E–08	–	–0.5
SBA3	KFR103	KFR103_036	91.83	–71.9	327	16	1.5E–08	–	–0.5
SBA4	KFR103	KFR103_041	180.69	–143.1	268	33	6.8E–08	–	–0.6

SBA-struct.	BH	PFL-f ID	Length along BH (m)	Elev. (m)	Orientation [1] Strike	Dip	T (m^2/s)	PFL head [2] (m)	Head BH Sect.[3] (m)
SBA4	KFR103	KFR103_042	181.23	–143.5	120	11	2.1E–07	–	–0.6
SBA4	KFR103	KFR103_043	181.89	–144.0	130	6	4.8E–06	0.3	–0.6
SBA4	KFR106	KFR106_015	67.22	–62.1	307	22	2.2E–07	–	–0.3
SBA4	KFR106	KFR106_016	68.24	–63.0	286	19	1.3E–05	–	–0.3
SBA4	KFR106	KFR106_017	69.38	–64.1	255	40	1.0E–07	–	–0.3
SBA4	KFR106	KFR106_018	71.5	–66.1	284	37	6.3E–06	–	–0.3
SBA4	KFR106	KFR106_019	73.02	–67.5	206	26	4.6E–06	0.2	–0.3
SBA5	KFR103	KFR103_041	180.69	–143.1	268	33	6.8E–08	–	–0.6
SBA5	KFR103	KFR103_042	181.23	–143.5	120	11	2.1E–07	–	–0.6
SBA5	KFR103	KFR103_043	181.89	–144.0	130	6	4.8E–06	0.3	–0.6
SBA5	KFR106	KFR106_047	154.36	–143.7	98	38	2.3E–06	–	–0.6
SBA5	KFR106	KFR106_048	154.58	–143.9	100	32	4.0E–06	–	–0.6
SBA5	KFR106	KFR106_049	156.08	–145.3	116	7	1.8E–05	0.8	–0.6
SBA6	KFR101	KFR101_026	180.95	–143.6	124	18	1.3E–05	–1.80	–2.5
SBA6	KFR102A	KFR102A_034	188.3	–169.0	109	9	2.6E–06	–1.10	–0.9
SBA6	KFR102A	KFR102A_035	188.77	–169.5	345	9	5.4E–07	–	–0.9
SBA6	KFR102A	KFR102A_036	190.35	–170.9	196	23	6.0E–07	–1.10	–0.9
SBA6	KFR102A	KFR102A_037	192.01	–172.4	205	30	2.3E–08	–	–0.9
SBA6	KFR102A	KFR102A_039	196.32	–176.3	208	16	5.9E–09	–	–0.9
SBA6	KFR102A	KFR102A_040	196.89	–176.8	246	14	3.0E–08	–	–0.9
SBA6	KFR102A	KFR102A_041	197.45	–177.3	125	40	3.1E–08	–	–0.9
SBA6	KFR102A	KFR102A_042	200.81	–180.4	147	20	2.2E–06	–1.00	–0.9
SBA6	KFR102A	KFR102A_043	201.52	–181.0	146	12	7.0E–07	–	–0.9
SBA6	KFR102A	KFR102A_044	202.01	–181.5	201	39	4.1E–07	–	–0.9
SBA6	KFR102A	KFR102A_045	202.38	–181.8	205	9	3.5E–07	–	–0.9
SBA6	KFR102A	KFR102A_046	203.32	–182.7	163	18	4.8E–08	–	–0.9
SBA6	KFR102A	KFR102A_047	204.5	–183.8	195	20	5.3E–07	–	–0.9
SBA6	KFR102A	KFR102A_048	205.89	–185.0	166	16	3.4E–06	–0.60	–0.9
SBA6	KFR102B	KFR102B_086	171.95	–136.4	214	6	8.7E–07	–0.80	–2.5
SBA6	KFR102B	KFR102B_087	172.6	–136.9	216	13	2.0E–07	–	–2.5
SBA6	KFR102B	KFR102B_088	173.15	–137.3	161	10	2.3E–07	–	–2.5
SBA6	KFR102B	KFR102B_089	173.57	–137.7	115	41	3.6E–07	–	–2.5
SBA6	KFR27	KFR27_013	192.51	–189.6	63	23	6.8E–06	–1.80	–3.0
SBA6	KFR27	KFR27_014	193.01	–190.1	33	19	1.0E–08	–	–3.0

1) Orientation of associated fracture. [2] Calculated freshwater head for PFL-f. [3] Monitored point water head for the borehole section containing the flow anomaly. [4] No detailed flow logging, flow anomaly evaluated from 5-m measurement.

Table 7-3. Modelled intercepts of KFR117–121 with SBA structures and corresponding transmissivity from either nearest injection-test section (KFR117, KFR118, KFR119) or summed PFL-f anomaly transmissivity (KFR119, KFR121).

	Intercept (borehole length, m)				
	KFR117	**KFR118**	**KFR119**	**KFR120**	**KFR121**
SBA1	38.26	52.95	57.92	48.72	-
SBA2	-	-	-	90.26	102.21
SBA6	-	-	-	-	321.9-327.5[4]
	Transmissivity (m^2/s)				
	KFR117	**KFR118**	**KFR119**	**KFR120**	**KFR121**
SBA1	3E-07	1E-06	3E-06[1]	2E-07	-
SBA2	-	-	-	2E-07	2E-07[2]
SBA6	-	-	-	-	8E-06[4]

[1]Summed transmissivity from 3 PFL-f ±3 m (BH length) from SBA intercept. [2]Summed transmissivity from 5 PFL-f ±3 m (BH length) from SBA intercept. [3]Summed transmissivity from 1 PFL-f ±3 m (BH length) from SBA intercept. 4) Geometrical intercept adjusted from original modelled values based on PFL measurements and subsequent analyses in KFR121 (Earon et al. 2022)

8 Summary

This report presents and summarises geo-structural information related to the Baseline Forsmark modelling stage, and cross-references this information to available single-hole hydraulic test data. Similar work was carried out for 21 core-drilled and 32 percussion-drilled boreholes during the site investigation period for SDM-Site (Follin et al. 2007b), whereas the present report contains information from 52 core-drilled and 57 percussion-drilled boreholes. Additionally, in order to characterize the uppermost bedrock both from a geo-structural and hydrogeological perspective, an update of previous work includes the addition of gently dipping and sub-horizontal structures.

A set of field and laboratory methods is also presented in this report to assess the hydraulic properties of the regolith and the regolith/bedrock interface. Field methods include single-hole slug tests, single-hole permeameter tests, and multi-hole interference tests. Laboratory methods include permeameter and CRS tests, sieve and sedimentation analyses, as well as methods to assess water storage and retention properties of the unsaturated zone.

Hydraulic test methods vary in terms of theoretical basis, spatial resolution, duration and support scale. In addition, there are various methodologies available for analysis of hydraulic test data. Such methodologies are associated to different underlying assumptions, affecting interpretations in terms of hydraulic properties of bedrock and regolith. In the report, a hierarchical order of test methods is used to propose most representative hydraulic properties for each geo-structural unit.

References

SKB's (Svensk Kärnbränslehantering AB) publications can be found at www.skb.com/publications. SKBdoc documents will be submitted upon request to document@skb.se.

Alm P, Gebrezghi M, Werner K, 2006. Forsmark site investigation. Supplementary hydraulic tests in Quaternary deposits. SKB P-06-224, Svensk Kärnbränslehantering AB.

Andersson O, Gustafson G, 1984. Brunnar. Undersökning – Dimensionering– Drift. BFR Report R42:1984. Byggforskningsrådet (BFR). (In Swedish.)

Bosson E, Gustafsson, L-G, Sassner M, 2008. Numerical modelling of surface hydrology and near-surface hydrogeology at Forsmark. Site descriptive modelling SDMSite Forsmark. R-08-09, Svensk Kärnbränslehantering AB.

Bosson E, Sassner, Sabel U, Gustafsson L-G, 2010. Modelling of present and future hydrology and solute transport at Forsmark. SR-Site Biosphere. SKB R-10-02, Svensk Kärnbränslehantering AB.

Brooks R H, Corey AT, 1964. Hydraulic properties of porous media. Hydrology papers, Colorado state university, March 1964.

Butler J J Jr, 1998. The design, performance, and analysis of slug tests. Boca Raton, FL: CRC Press.

Campbell G S, 1974. A Simple Method for Determining Unsaturated Conductivity from Moisture Retention Data. Soil Science, 117, 311-314.

Carlsson A, Christiansson R, 2007. Construction experiences from underground works at Forsmark. Compilation Report. SKB R-07-10, Svensk Kärnbränslehantering AB.

Earon R, Rasul H, Ohman J, 2022. Utredning angående förekomst av Flacka Strukturer med underlag från KFR117, KFR118, KFR119, KFR120 och KFR121. SKBdoc 1966551 ver 1.0, Svensk Kärnbränslehantering AB.

Fair GM, Hatch LP, 1933. Fundamental factors governing the streamline flow of water through sand. J. Am. Water Works Ass. 25, 1551–1563.

Follin S, 2008. Bedrock hydrogeology Forsmark. Site descriptive modelling SDM-Site Forsmark. SKB R-08-95, Svensk Kärnbränslehantering AB.

Follin S, Johansson P-O, Levén J, Hartley L, Holton D, McCarthy R, Roberts D, 2007a. Updated strategy and test of new concepts for groundwater flow modelling in Forsmark in preparation of site descriptive modelling stage 2.2. SKB R-07-20, Svensk Kärnbränslehantering AB.

Follin S, Levén J, Hartley L, Jackson P, Joyce S, Roberts D, Swift B, 2007b. Hydrogeological characterisation and modelling of deformation zones and fracture domains, Forsmark modelling stage 2.2. SKB R-07-48, Svensk Kärnbränslehantering AB.

Follin S, Johansson P-O, Hartley L, Jackson P, Roberts D, Marsic N, 2007c. Hydrogeological conceptual model development and numerical modelling using CONNECTFLOW, Forsmark modelling stage 2.2. SKB R-07-49, Svensk Kärnbränslehantering AB.

Follin S, Hartley L, Jackson P, Roberts D, Marsic N, 2008. Hydrogeological conceptual development and numerical modelling using CONNECTFLOW, Forsmark modelling stage 2.3. SKB R-08-23, Svensk Kärnbränslehantering AB.

Gentzschein B, Levén J, Follin S, 2007. A comparison between well yield data from the site investigation in Forsmark and domestic wells in northern Uppland**.** SKB P-06-53, Svensk Kärnbränslehantering AB.

Hazen A, 1893. Some physical properties of sands and gravels with special reference to their use in filtration. Mass. State Board of Health, 24th Ann. Rep. 541–556, Boston, Mass., USA.

Hermansson J, Petersson J, 2022. Methodology for deterministic geological modelling of the Forsmark site. Application to the development of the final repository for spent nuclear fuel. SKB R-20-10, Svensk Kärnbränslehantering AB.

Johansson P-O, 2004. Forsmark site investigation. Undisturbed pore water sampling and permeability measurements with BAT filter tips. Soil sampling for pore water analyses. SKB P-04-136, Svensk Kärnbränslehantering AB.

Johansson P-O, 2008. Description of surface hydrology and near-surface hydrogeology at Forsmark. Site descriptive modelling SDM-Site Forsmark. R-08-08, Svensk Kärnbränslehantering AB

Jönsson S, 2013. Flödesloggningar i projekt SFK byggundersökningar. Geosigma. SKBdoc 1321424 ver 1.0, Svensk Kärnbränslehantering AB. (In Swedish.)

Lundin L, Stendahl J, Lode E, 2005. Forsmark site investigation. Soils in two large trenches. SKB P-05-166, Svensk Kärnbränslehantering AB.

Odén M, Follin S, Werner K, 2025. Methodology for hydrological-hydrogeological modelling of the Forsmark site. SKB R-20-14, Svensk Kärnbränslehantering AB.

Petrone J, Strömgren M, 2020. Baseline Forsmark – Digital elevation model. SKB R-17- 06, Svensk Kärnbränslehantering AB.

Petrone J, Sohlenius G, Ising J, 2020. Baseline Forsmark – Depth and stratigraphy of regolith. SKB R-17-07, Svensk Kärnbränslehantering AB.

Posiva SKB, 2017. Safety functions, performance targets and technical design requirements for a KBS-3V repository. Conclusions and recommendations from a joint SKB and Posiva working group. Posiva SKB Report 01, Posiva Oy, Svensk Kärnbränslehantering AB.

Rasul H, 2022. SFM-Grundvattenrör ritningar_2002 till 2022 (Bilaga C: Drawings of groundwater wells in regolith and across regolith/bedrock interface). SKBdoc 1982312 ver. 1.0, Svensk Kärnbränslehantering AB.

Rasul H, Earon R, Atmosudirdjo A, Werner K, 2023. Slug tests in groundwater monitoring wells in Forsmark in 2021. SKB P-22-26, Svensk Kärnbränslehantering AB.

Rhén I, Follin S, Hermanson J, 2003. Hydrological Site Descriptive Model – a strategy for its development during Site Investigations. SKB R-03-08, Svensk Kärnbränslehantering AB.

Selroos, J-O, Mas Ivars D, Munier R, Hartley L, Libby S, Davy P, Darcel C, Trinchero P, 2022. Methodology for discrete fracture network modelling of the Forsmark site. Part 1 – concepts, data and interpretation methods. SKB R-20-11, Svensk Kärnbränslehantering AB.

SKB, 2008. Site description of Forsmark at completion of the site investigation phase. SDM-Site Forsmark. SKB TR-08-05, Svensk Kärnbränslehantering AB.

SKB, 2010. Platsval – lokalisering av slutförvaret för använt kärnbränsle. SKB R-10-42, Svensk Kärnbränslehantering AB.

SKB, 2011. Long-term safety for the final repository for spent nuclear fuel at Forsmark. Main report of the SR-Site project. SKB TR-11-01, Svensk Kärnbränslehantering AB.

SKB, 2013. Site description of the SFR area at Forsmark at completion of the site investigation phase. SDM-PSU Forsmark. SKB TR-11-04, Svensk Kärnbränslehantering AB.

Smith A, 2017. Slugtester i utvalda grundvattenrör i Forsmark sommaren 2016. Genomförande och resultat. SKBdoc 1562216 ver. 1.0, Svensk Kärnbränslehantering AB. (In Swedish.)

Sohlenius G, Svensson M, 2021. Regolith in wetlands with high nature values. Additional studies. SKB P-21-09, Svensk Kärnbränslehantering AB.

Sohlenius G, Wilin L, Hedenström A, Karlsson C, 2019. Quaternary deposits in the drainage area of Gunnarsboträsket in Forsmark. Stratigraphical and surficial distribution of Quaternary deposits. SKB P-19-15, Svensk Kärnbränslehantering AB.

SSM, 2018. Strålsäkerhet efter slutförvarets förslutning. SSM 2018:07, Strålsäkerhetsmyndigheten. (In Swedish.)

Van Genuchten M T, 1980. A Closed Form Equation for Predicting the Hydraulic Conductivity of Unsaturated Soils. Soil Science Society of America Journal, 44, 892-898.

Werner K, 2004. Forsmark site investigation. Supplementary slug tests in groundwater monitoring wells in soil. SKB P-04-140, Svensk Kärnbränslehantering AB.

Werner K, 2018a. Bilaga till PM slugtester i grundvattenrör sommaren 2017. SKBdoc 1617130 ver. 1.0, Svensk Kärnbränslehantering AB. (In Swedish.)

Werner K, 2018b. Data compilation and analysis for the description of the access area of the planned spent fuel repository in Forsmark – meteorology, hydrology and near-surface hydrogeology. SKB P-17-19, Svensk Kärnbränslehantering AB.

Werner K, Johansson P-O, 2003. Forsmark site investigation. Slug tests in groundwater monitoring wells in soil. SKB P-03-65, Svensk Kärnbränslehantering AB.

Werner K, Lundholm K, 2004. Forsmark site investigation. Pumping tests in well SFM0074. SKB P-04-142, Svensk Kärnbränslehantering AB.

Werner K, Lundholm L, Johansson P-O, 2004. Forsmark site investigation. Drilling and pumping test of wells at Börstilåsen. SKB P-04-138, Svensk Kärnbränslehantering AB.

Werner K, Sassner M, Johansson E, 2013. Hydrology and near-surface hydrogeology at Forsmark – synthesis for the SR-PSU project. SR-PSU Biosphere. SKB R-13-19, Svensk Kärnbränslehantering AB.

Werner, K, Mårtensson E, Nordén S, 2014. Kärnbränsleförvaret i Forsmark. Pilotförsök med vattentillförsel till en våtmark. SKB R-14-23, Svensk Kärnbränslehantering AB.

Öhman J, Bockgård N, Follin S, 2012. Site investigation SFR. Bedrock Hydrogeology. SKB R-11-03, Svensk Kärnbränslehantering AB.

A Appendix

A1 Figures representing all single-hole test data

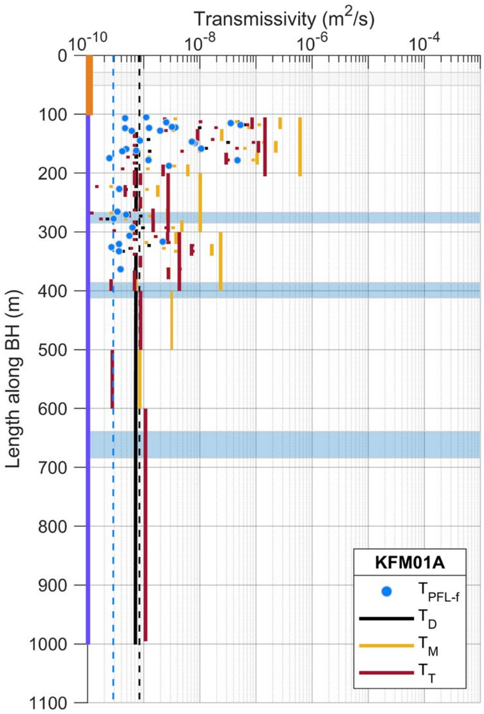

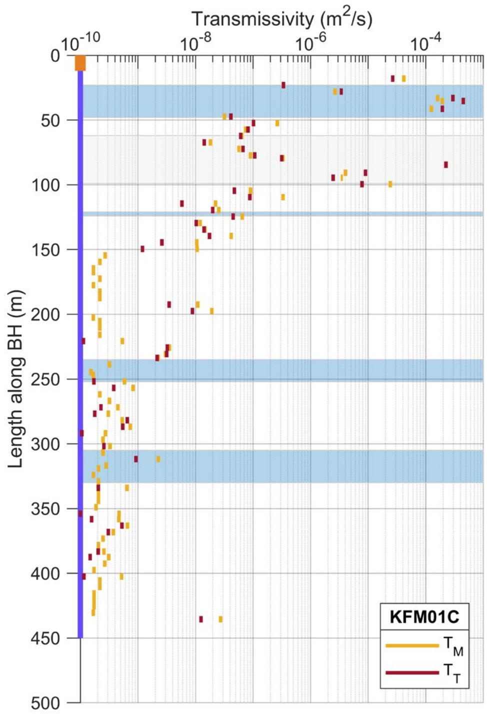

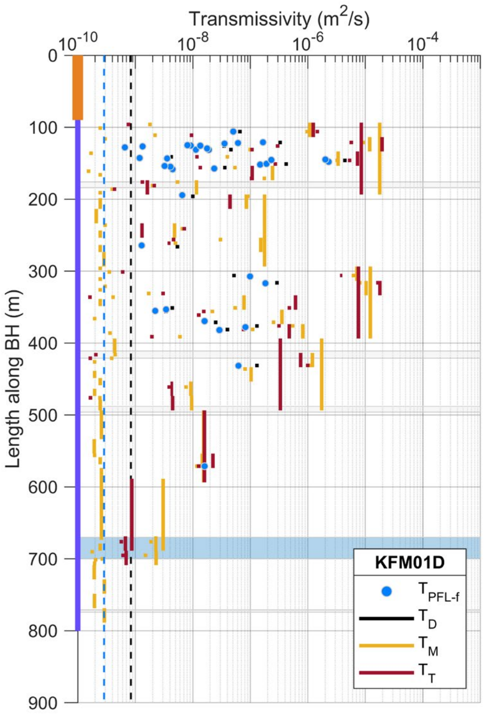

Figure A-1. *Single hole hydraulic (PFL and injection) test data from core-drilled boreholes at Drill Site 1. Shaded areas indicate interpreted intercepts with deterministic modelled deformation zones, with colouring scheme taken from Chapter 4.*

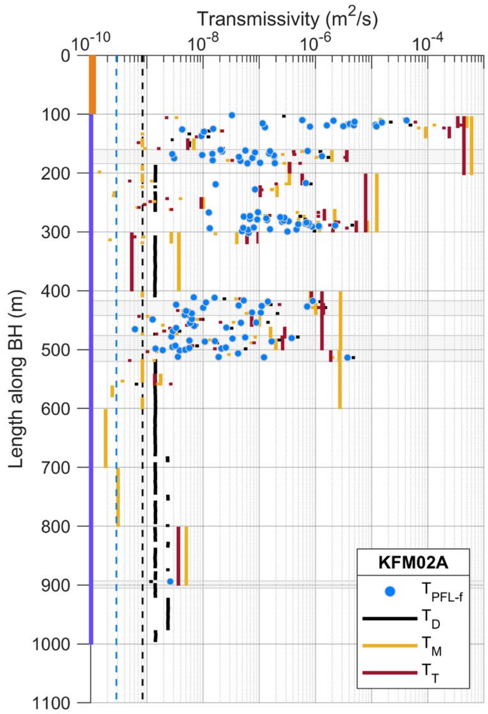

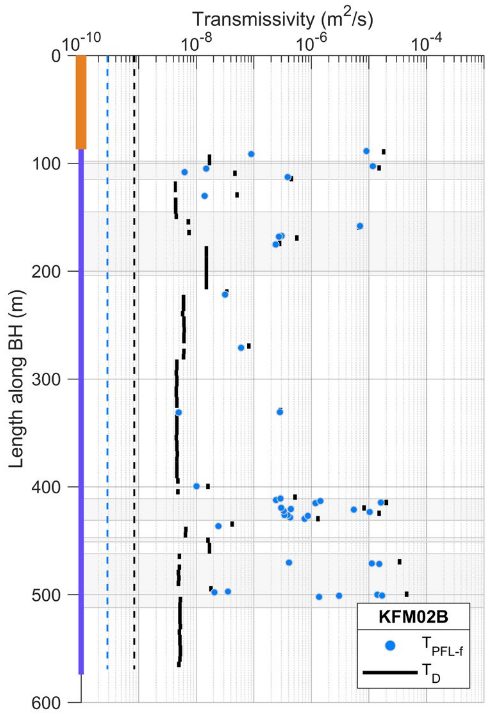

Figure A-2. *Single hole hydraulic (PFL and injection) test data from core-drilled boreholes at Drill Site 2. Shaded areas indicate interpreted intercept with deterministic modelled deformation zones, with colouring scheme taken from Chapter 4.*

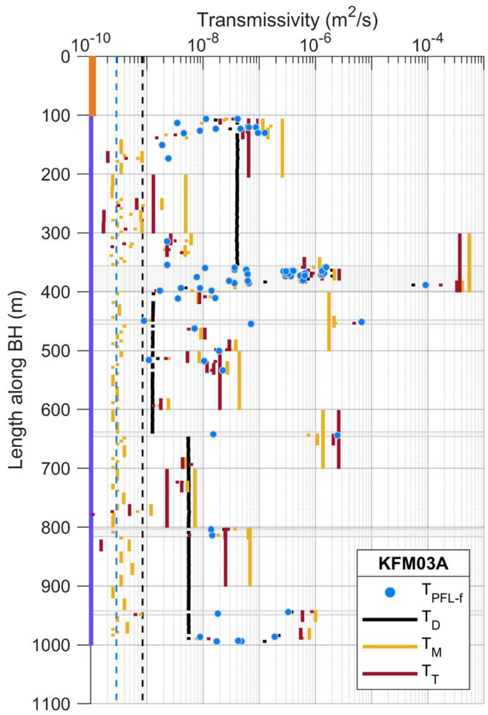

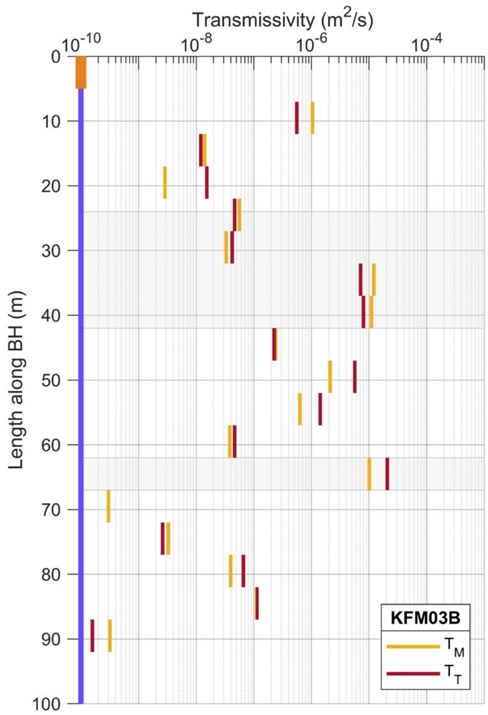

Figure A-3. *Single hole hydraulic (PFL and injection) test data from Drill Site 3. Shaded areas indicate interpreted intercept with deterministic modelled deformation zones, with colouring scheme taken from Chapter 4.*

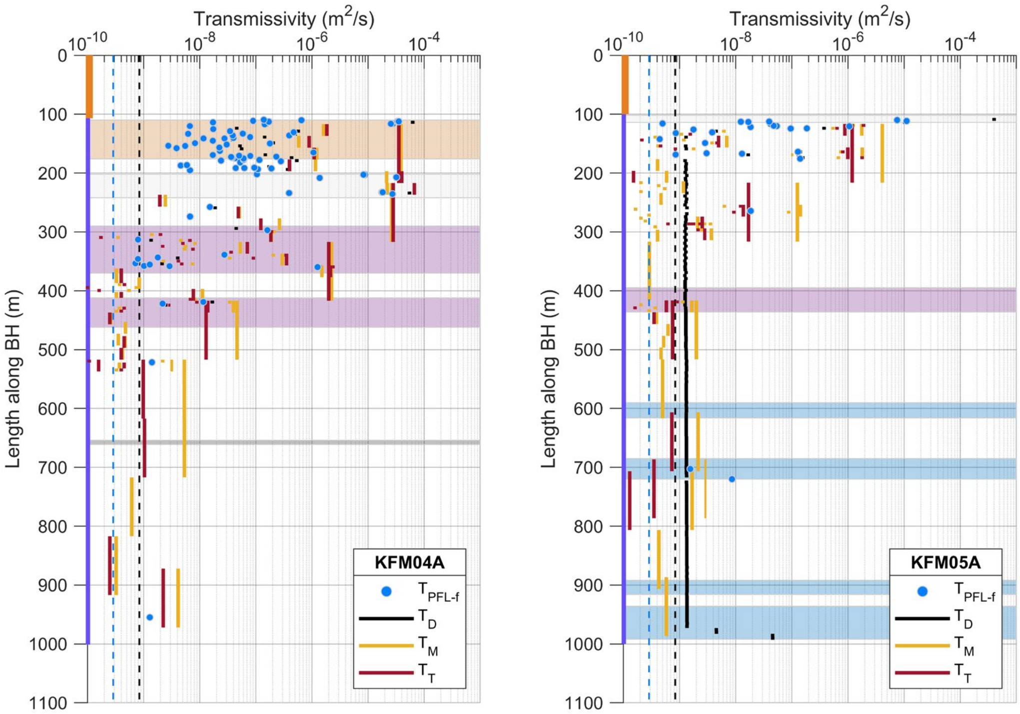

Figure A-4. *Single hole hydraulic (PFL and injection) test data from Drill Sites 4 and 5. Shaded areas indicate interpreted intercept with deterministic modelled deformation zones, with colouring scheme taken from Chapter 4.*

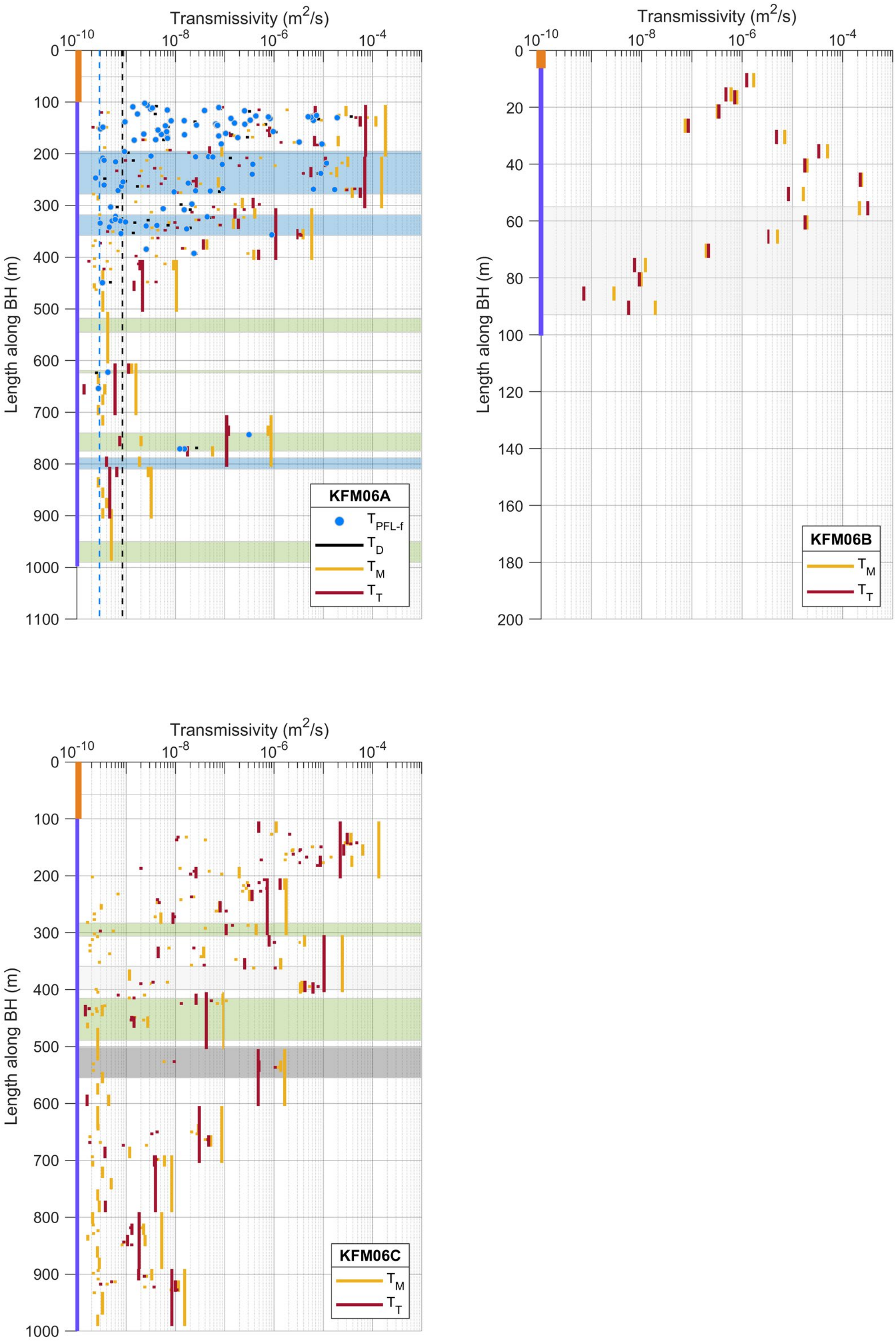

Figure A-5. *Single hole hydraulic (PFL and injection) test data from Drill Site 6. Shaded areas indicate interpreted intercept with deterministic modelled deformation zones, with colouring scheme taken from Chapter 4.*

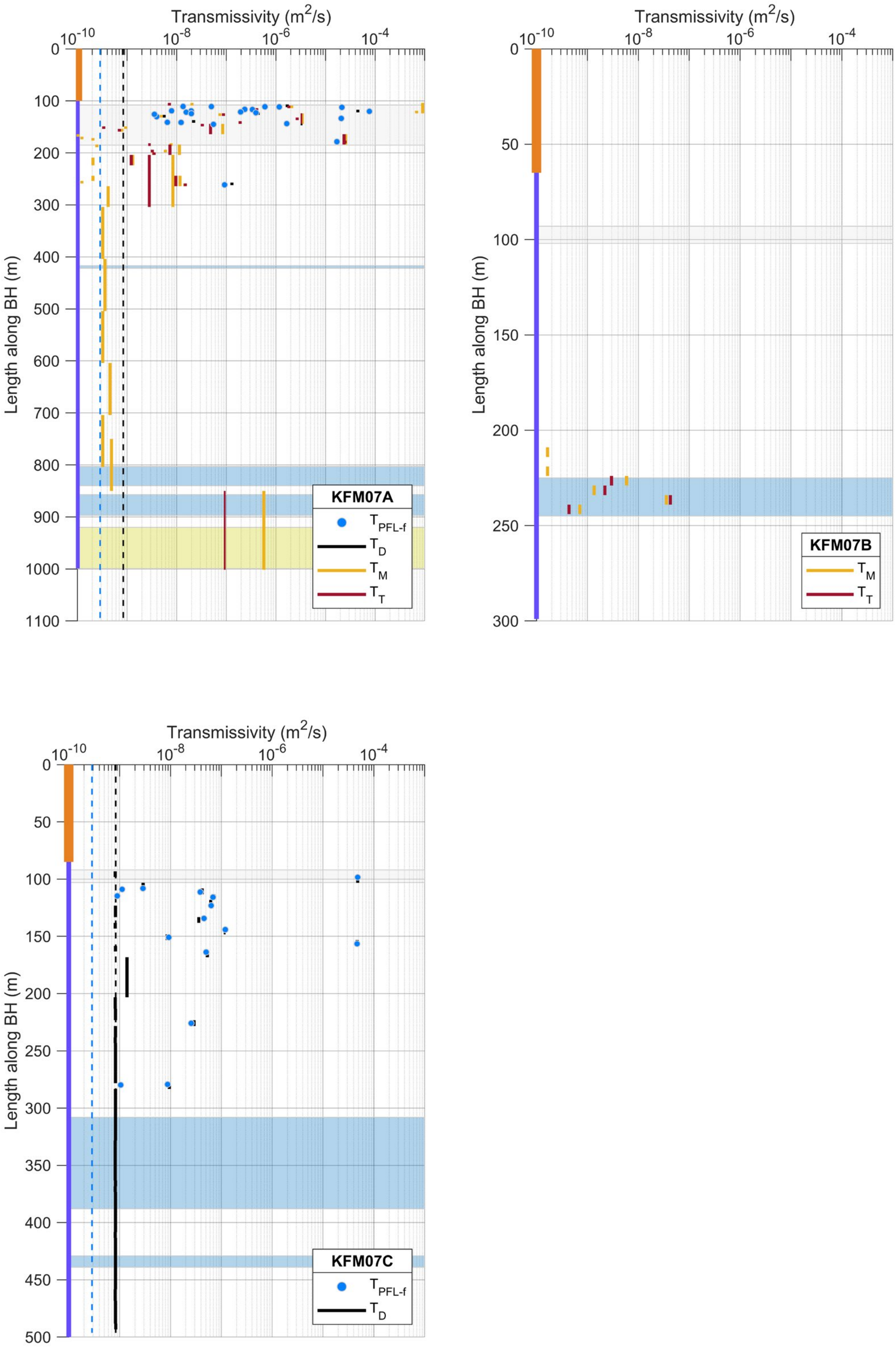

Figure A-6. *Single hole hydraulic (PFL and injection) test data from Drill Site 7. Shaded areas indicate interpreted intercept with deterministic modelled deformation zones, with colouring scheme taken from Chapter 4.*

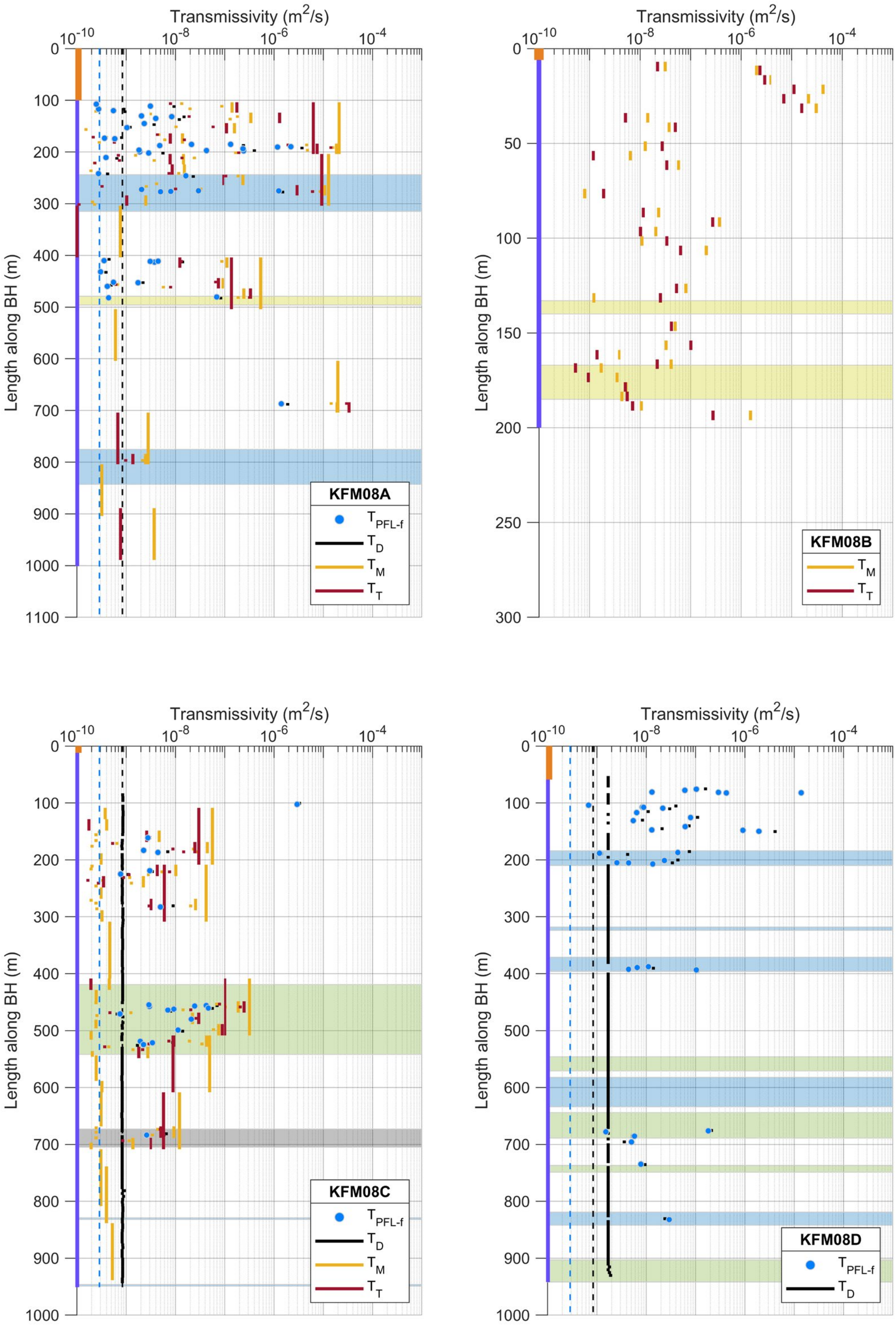

Figure A-7. *Single hole hydraulic (PFL and injection) test data from Drill Site 8. Shaded areas indicate interpreted intercept with deterministic modelled deformation zones, with colouring scheme taken from Chapter 4.*

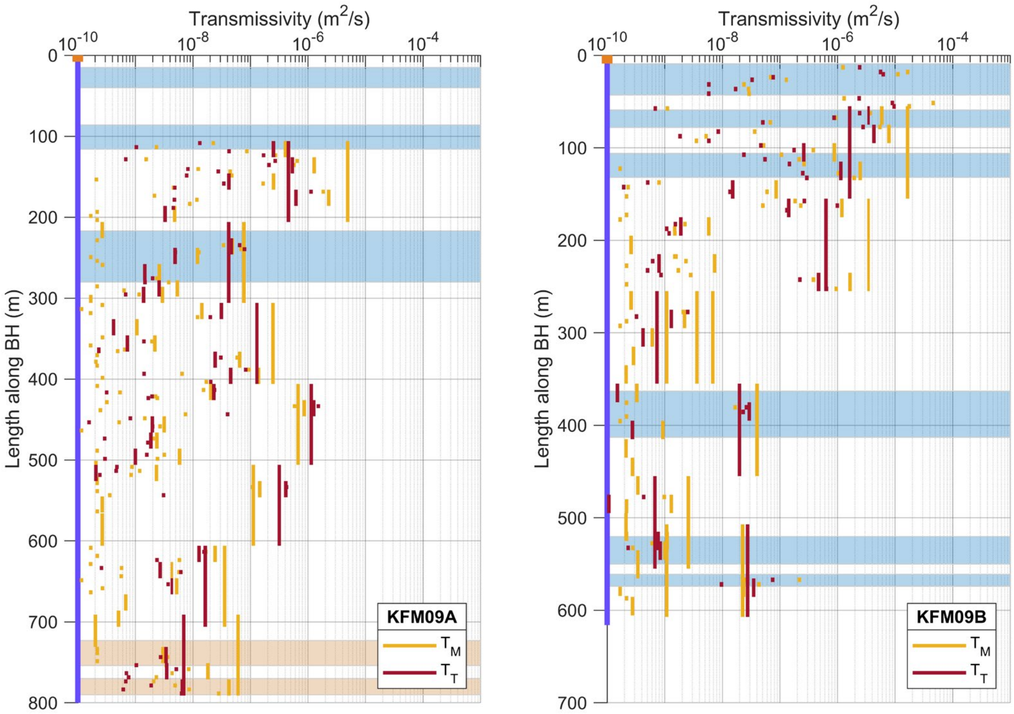

Figure A-8. *Single hole hydraulic (PFL and injection) test data from Drill Site 9. Shaded areas indicate interpreted intercept with deterministic modelled deformation zones, with colouring scheme taken from Chapter 4.*

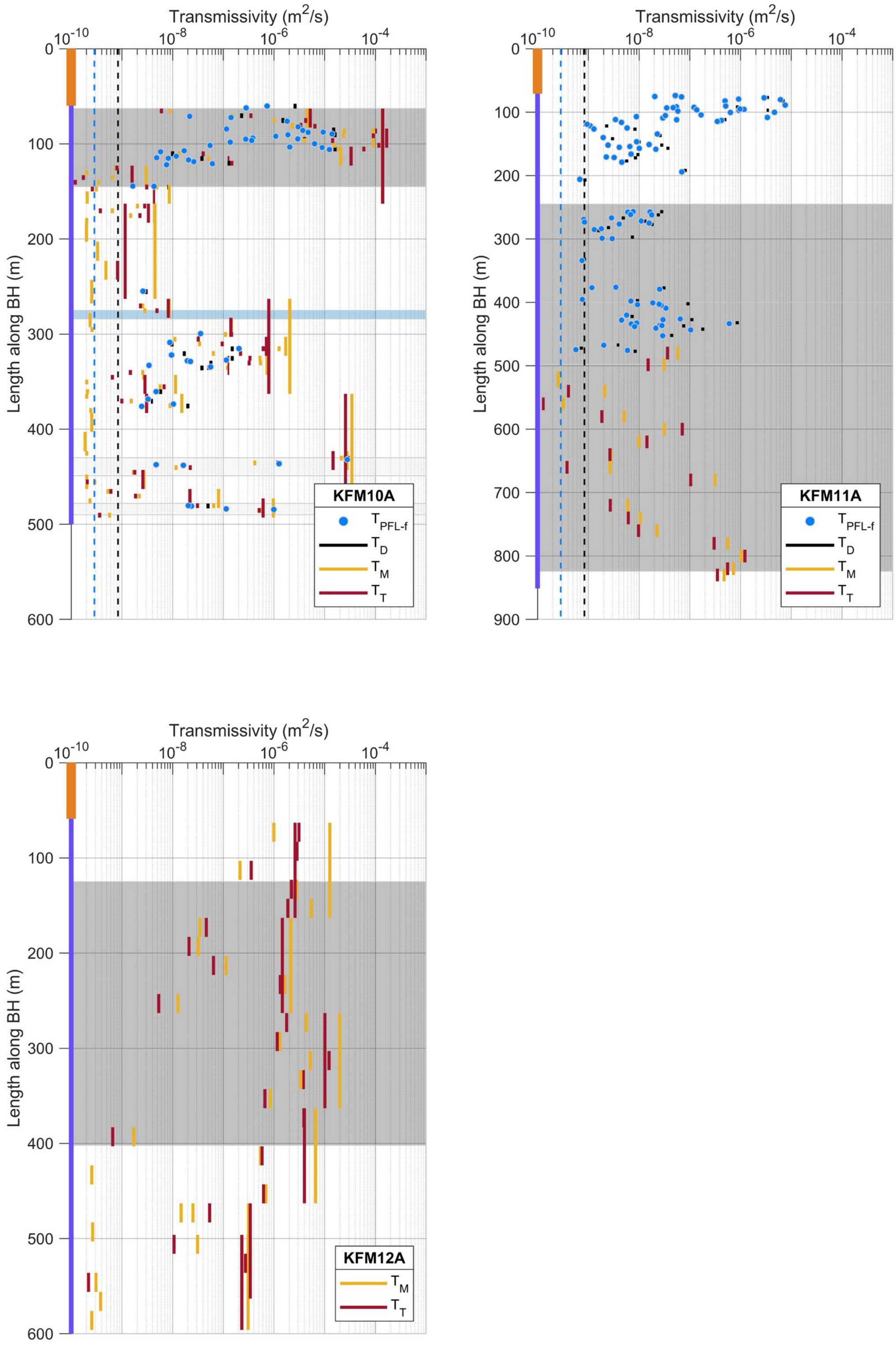

Figure A-9. *Single hole hydraulic (PFL and injection) test data from Drill Site 10, 11 and 12. Shaded areas indicate interpreted intercept with deterministic modelled deformation zones, with colouring scheme taken from Chapter 4.*

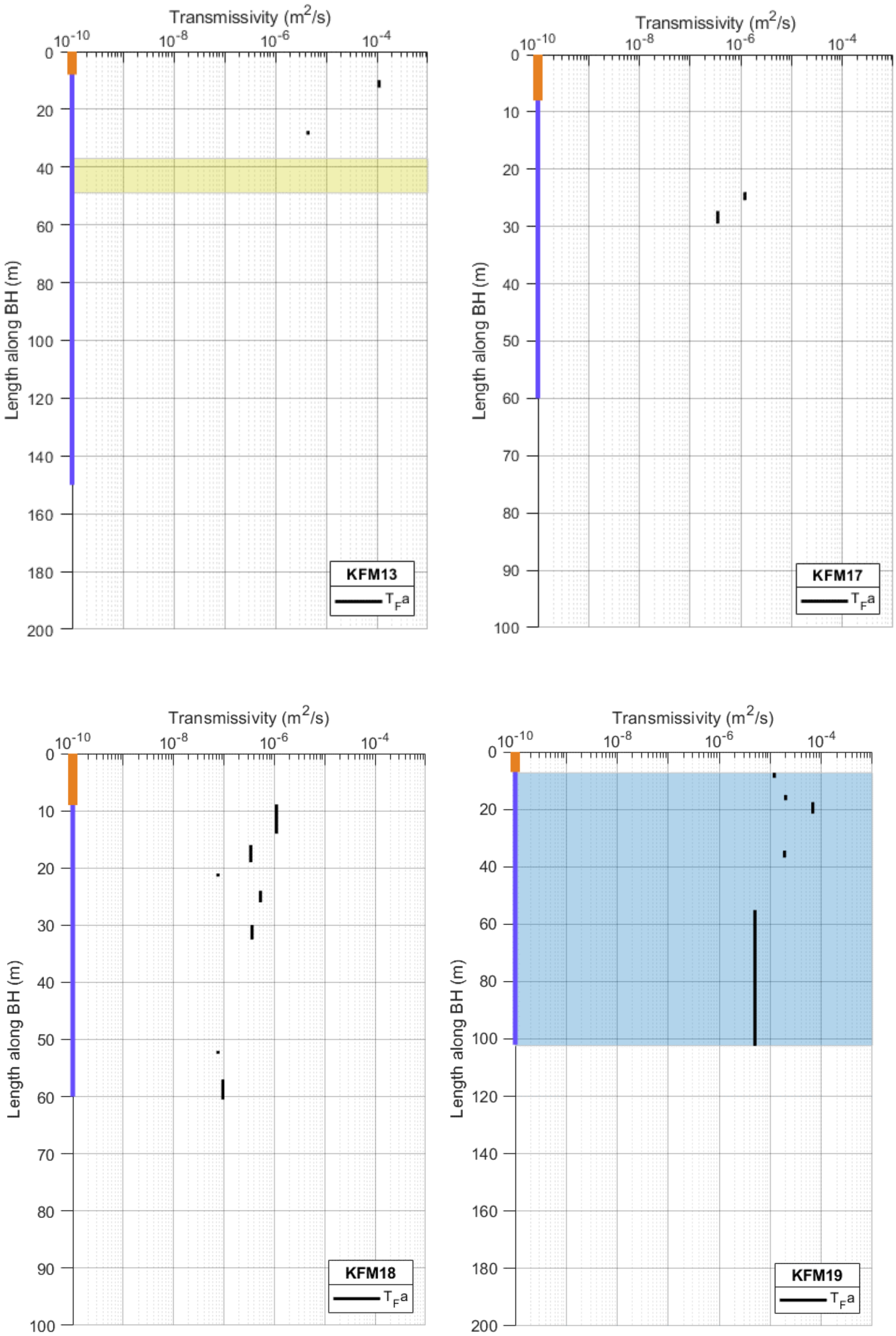

Figure A-10. *Single hole hydraulic, impeller flow logging (TFa), data gathered through hydraulic testing in core-drilled boreholes KFM13, KFM17, KFM18 and KFM19 (Jönsson 2013). Shaded areas indicate interpreted intercept with deterministic modelled deformation zones, with colouring scheme taken from Chapter 4.*

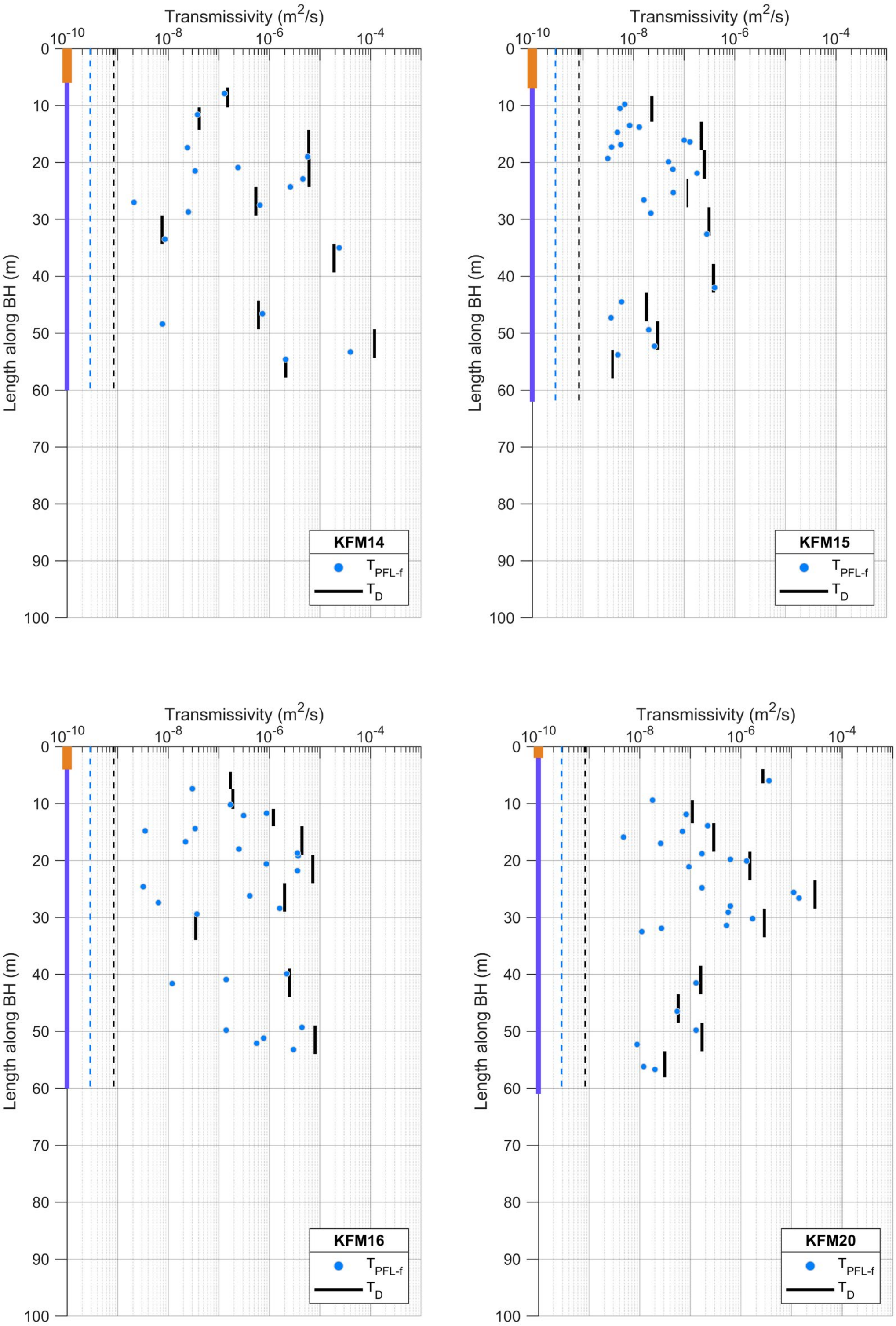

Figure A-11. *Single hole hydraulic (PFL and injection) test data from boreholes KFM14, KFM15, KFM16 and KFM20. Shaded areas indicate interpreted intercept with deterministic modelled deformation zones, with colouring scheme taken from Chapter 4.*

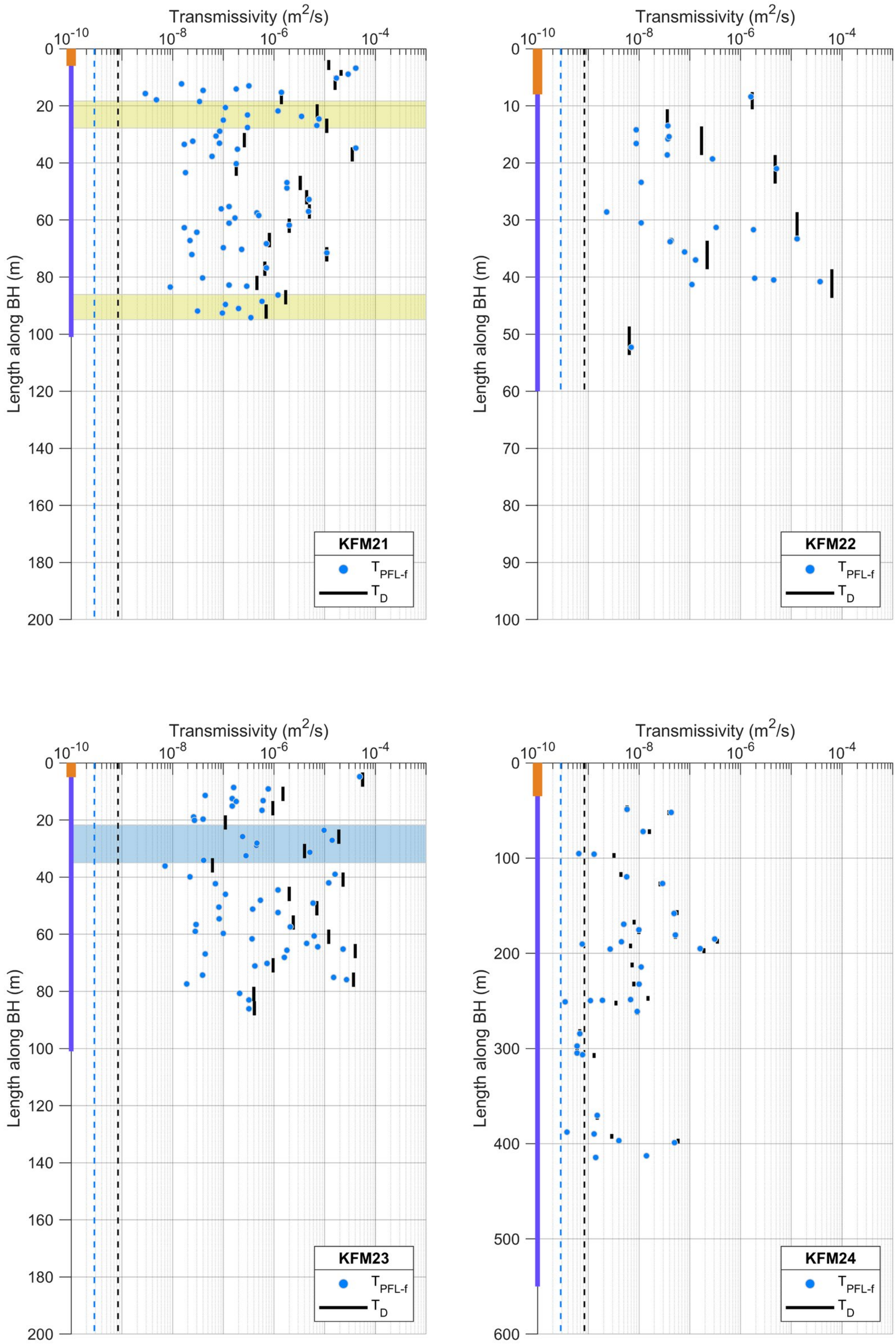

***Figure A-12.** Single hole hydraulic (PFL and injection) test data from boreholes KFM21, KFM22, KFM23 and KFM24. Shaded areas indicate interpreted intercept with deterministic modelled deformation zones, with colouring scheme taken from Chapter 4.*

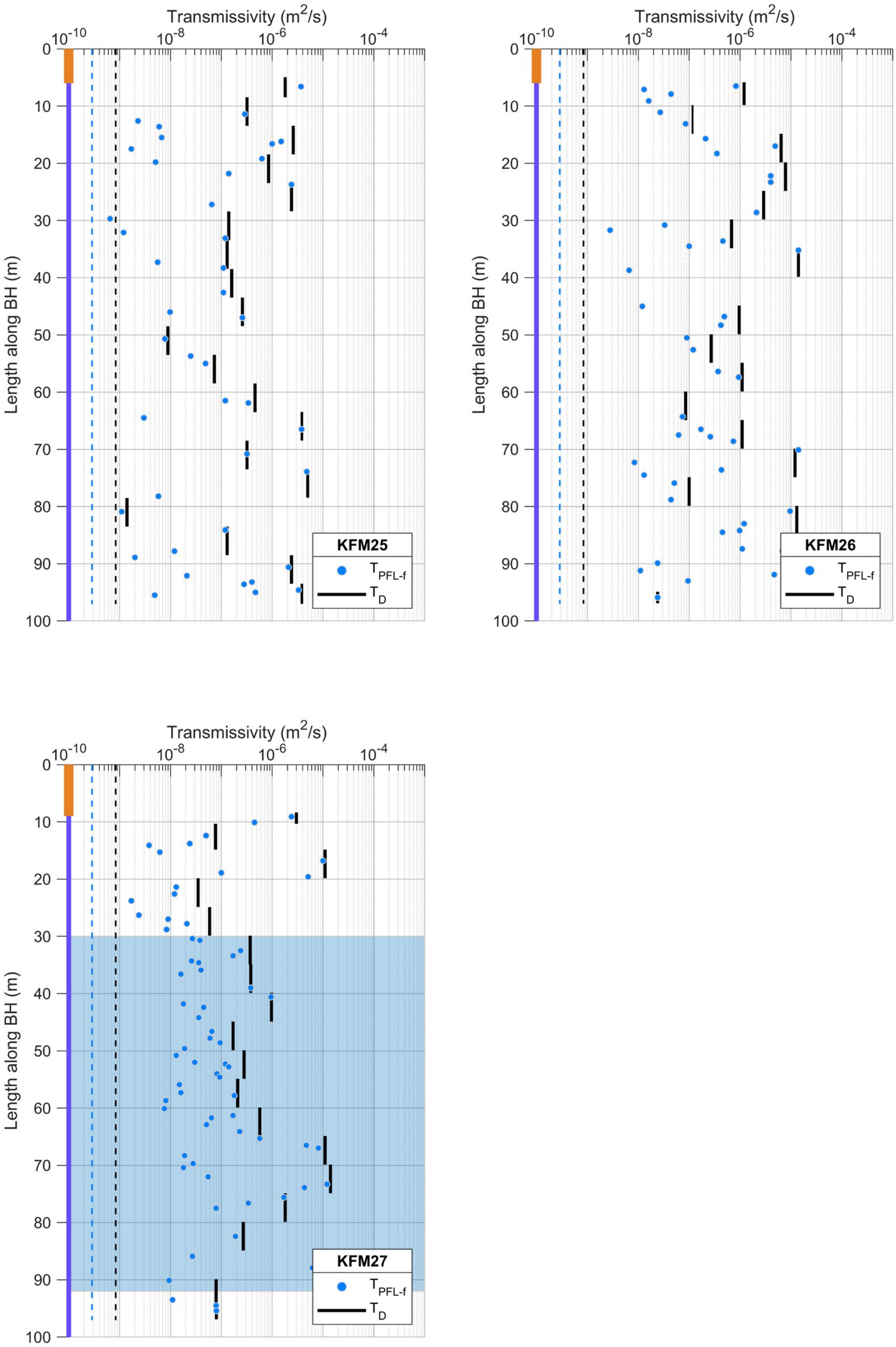

Figure A-13. *Single hole hydraulic (PFL and injection) test data from boreholes KFM25, KFM26 and KFM27. Shaded areas indicate interpreted intercept with deterministic modelled deformation zones, with colouring scheme taken from Chapter 4.*

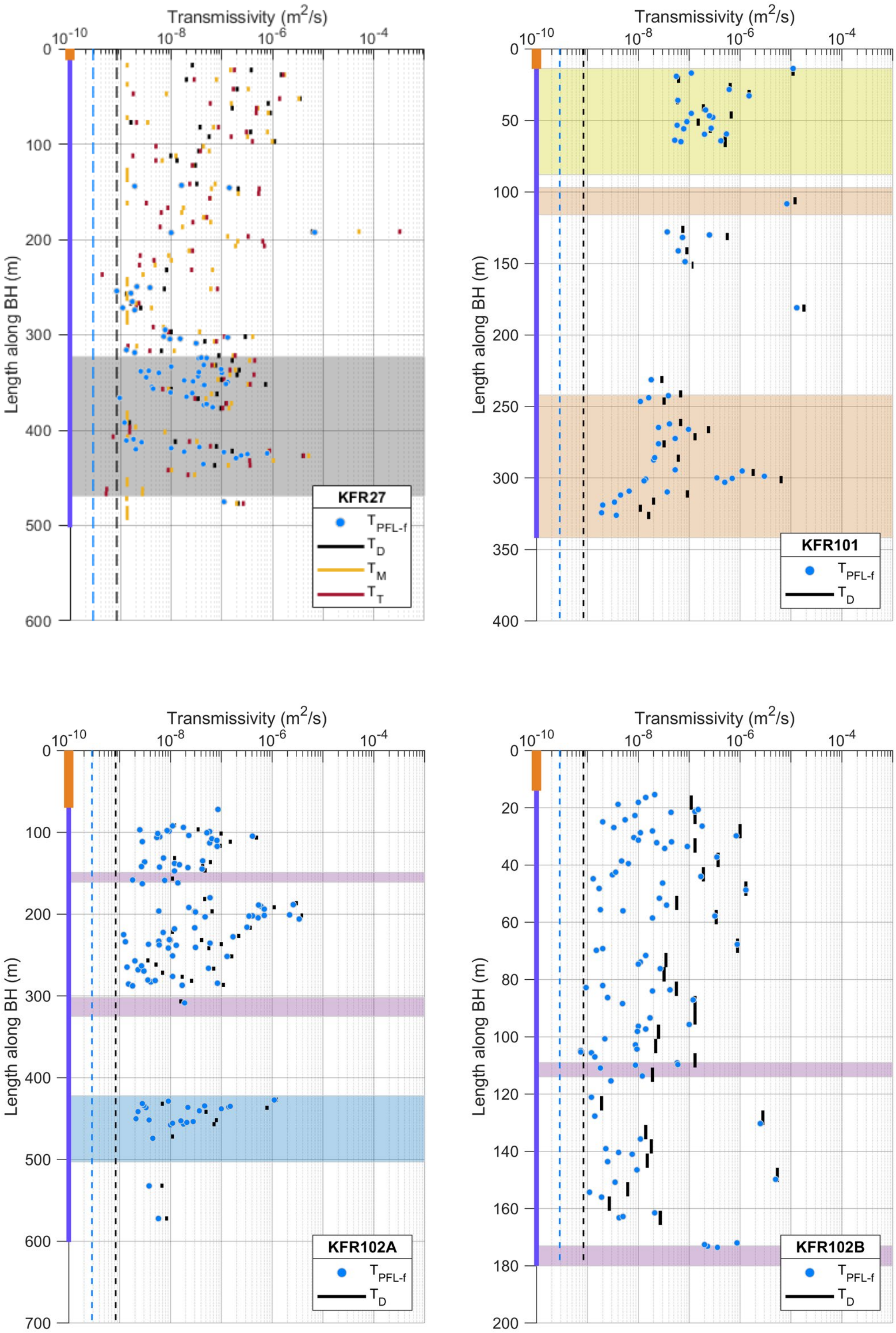

Figure A-14. *Single hole hydraulic (PFL and injection) test data from boreholes KFR27, KFR101, KFR102A and KFR102B. Shaded areas indicate interpreted intercept with deterministic modelled deformation zones, with colouring scheme taken from Chapter 4.*

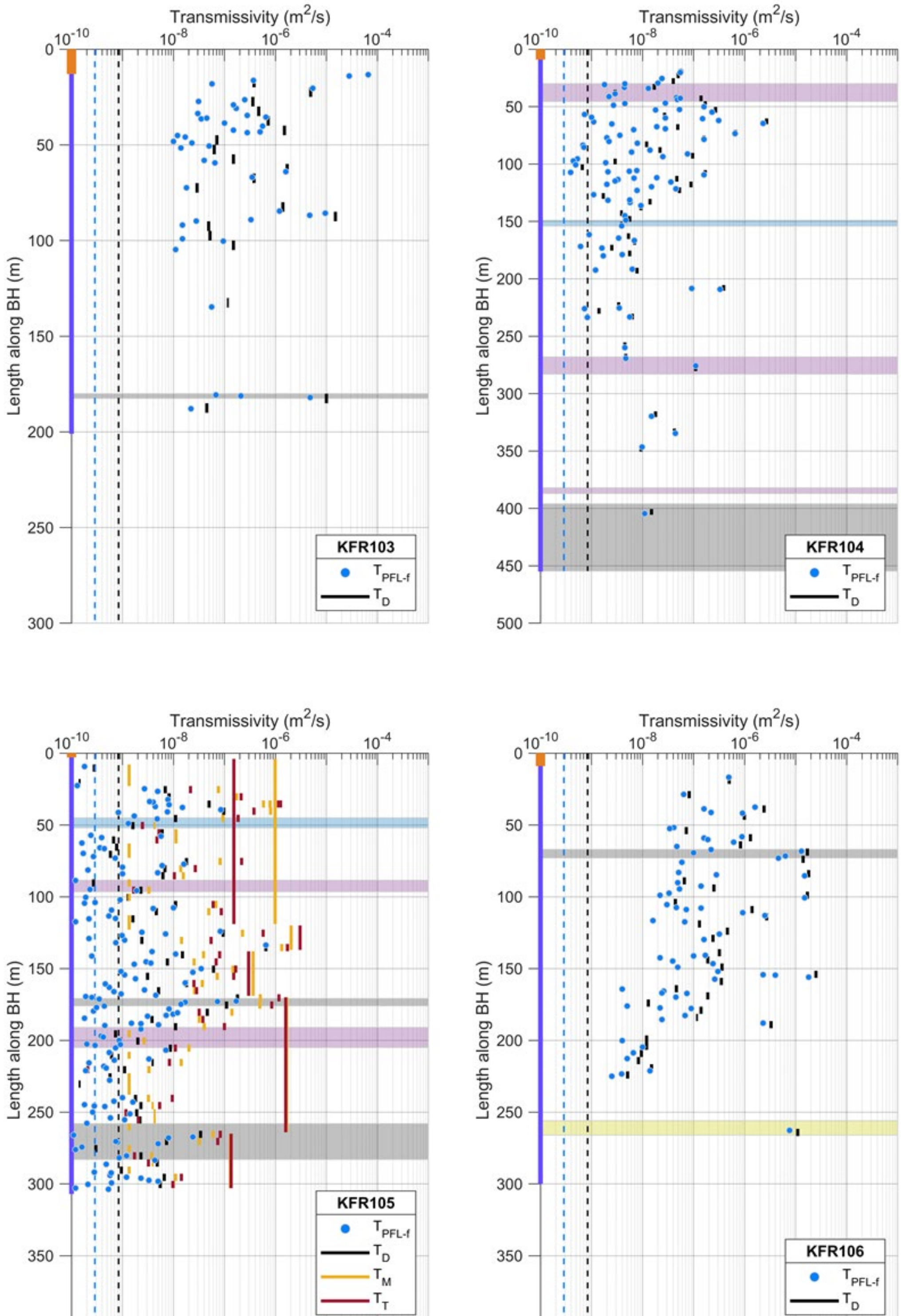

Figure A-15. *Single hole hydraulic (PFL and injection) test data from boreholes KFR103, KFR104, KFR105, and KFR106. Shaded areas indicate interpreted intercept with deterministic modelled deformation zones, with colouring scheme taken from Chapter 4.*

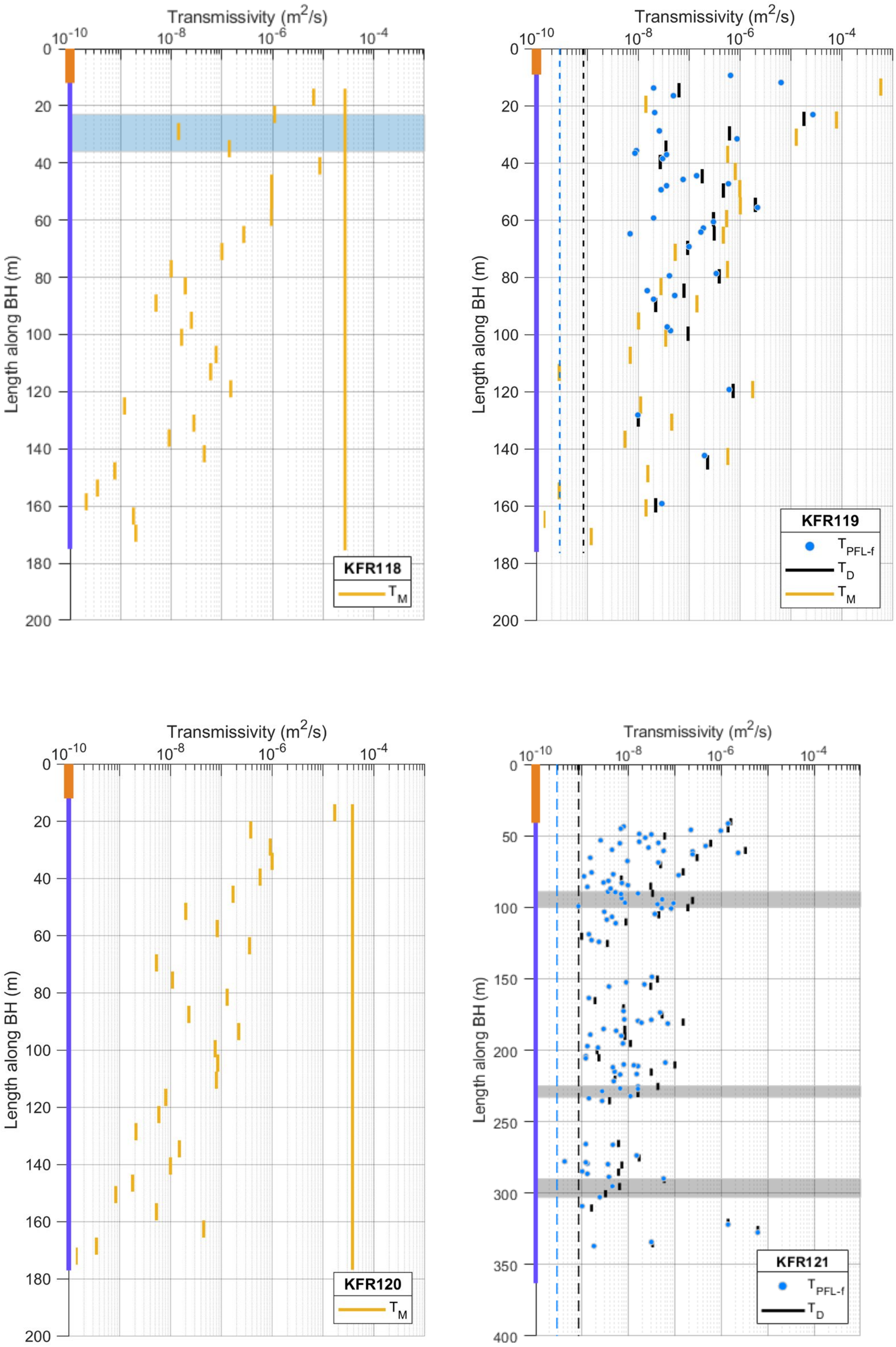

Figure A-16. *Single hole hydraulic (PFL and injection) test data from boreholes KFR118, KFR119, KFR120 and KFR121. Shaded areas indicate interpreted intercept with deterministic modelled deformation zones, with colouring scheme taken from Chapter 4.*

B Appendix

B1 Catalogue of reports containing data presented

Table B-1. List of reports corresponding to the information available from core-drilled boreholes presented in this report. SHI = single-hole interpretation. P refers to SKB's P report series, whereas 7-digit numbers refer to doc-id in SKB's document handling system SKBdoc.

IDCODE	Start date of drilling	Drilling	SHI	PFL	Injection test
KFM01A	2002-10-28	P-03-32	P-04-116	P-04-193	P-04-95
KFM01B	2004-01-15	P-04-302	P-04-116		
KFM01C	2017-01-12	P-06-173	P-06-135		P-06-165
KFM01D	2006-02-18	P-06-173	P-06-210	P-06-161	P-06-195
KFM02A	2003-03-12	P-03-52	P-04-117	P-04-188, P-05-37	P-05-145, P-04-100
KFM02B	2007-02-13	P-07-44	P-07-107	P-07-128, P-07-83	
KFM03A	2003-06-23	P-03-59	P-04-118	P-04-189	P-04-194
KFM03B	2003-07-02	P-03-59	P-04-118		P-04-278
KFM04A	2003-11-19	P-03-82	P-04-119	P-04-190	P-04-293
KFM04B	2003-06-30	P-03-82			
KFM05A	2004-05-05	P-04-222	P-04-296	P-04-191	P-05-56
KFM06A	2004-09-21	P-05-50	P-05-132	P-05-15	P-05-165
KFM06B	2005-02-08	P-05-50	P-05-132		P-05-165
KFM06C	2006-06-05	P-05-277	P-06-83		P-06-23
KFM07A	2006-12-05	P-05-142	P-06-134, P-05-157	P-05-63	P-05-133
KFM07B	2005-10-18	P-06-170			P-06-86
KFM07C	2006-08-08	P-06-170	P-06-208	P-06-247	
KFM08A	2005-01-25	P-05-172	P-05-262	P-05-43	P-06-194
KFM08B	2005-01-26	P-05-172	P-05-262	P-07-85	P-05-235
KFM08C	2006-05-09	P-06-171	P-06-207	P-06-189	P-07-06
KFM08D	2007-02-10	P-06-171	P-07-108	P-07-128	
KFM09A	2005-10-27	P-06-169	P-06-134		P-06-52
KFM09B	2005-12-19	P-06-169	P-06-135		P-06-122
KFM10A	2006-06-01	P-06-172	P-06-207		P-07-31
KFM11A	2006-11-20	P-07-45	P-07-109	P-07-85	
KFM12A	2007-03-12	P-07-46	P-07-110		P-07-121
KFM13	2011-06-27			P-06-190	
KFM14	2011-05-31			P-19-19	
KFM15	2011-06-16			P-19-19	
KFM16	2011-05-25			P-19-19	
KFM20	2011-05-17			P-19-19	
KFM21	2011-06-09			P-19-19	
KFM22	2011-07-01			P-19-19	
KFM23	2011-07-07			P-19-19	
KFM24	2016-06-13	P-16-32	P-16-29	P-16-27	
KFM25	2019-09-19	P-19-25	P-20-13	P-20-17	
KFM26	2019-10-03	P-19-25	P-20-13	P-20-17	
KFM27	2019-10-09	P-09-12, P-19-25	P-20-13	P-20-17	
KFR101	2008-07-02	P-09-13	P-09-34	P-08-98	
KFR102A	2008-12-12	P-09-19	P-09-60	P-09-21	
KFR102B	2008-08-13	P-09-13	P-09-33	P-08-99	
KFR103	2008-08-26	P-09-13	P-09-33	P-08-99	
KFR104	2008-09-29	P-09-13	P-09-35	P-09-20	
KFR105	2009-06-02		P-10-06	P-09-09	P-17-24
KFR106	2009-09-03		P-10-08	P-09-73	
KFR117	2020-05-04	P-20-32			
KFR118	2020-05-07	P-20-32			
KFR119	2020-05-17	P-20-32			
KFR120	2020-07-24	P-20-32			
KFR121	2020-06-16	P-20-32			
KFR27	1981-09-10		P-09-35	P-09-20, P-08-98	P-17-24

Table B-2. List of reports corresponding to the information available from percussion-drilled boreholes presented in this report. SHI = single-hole interpretation.

IDCODE	Start date of drilling	Drilling	SHI	Pumping test and/or impeller flow logging
HFM01	2002-05-03	**P-03-30**	**P-04-116**	**P-03-33**
HFM02	2002-05-21	**P-03-30**	**P-04-116**	**P-03-33**
HFM03	2002-05-28	**P-03-30**	**P-04-116**	**P-03-33**
HFM04	2002-12-03	**P-03-51**	**P-04-117**	**P-03-34**
HFM05	2002-12-16	**P-03-51**	**P-04-117**	**P-03-34**
HFM06	2003-01-14	**P-03-58**	**P-04-118**	**P-03-36**
HFM07	2003-01-28	**P-03-58**	**P-04-118**	**P-03-36**
HFM08	2003-02-12	**P-03-58**	**P-04-118**	**P-03-36**
HFM09	2003-06-30	**P-04-76**	**P-04-119**	**P-04-74**
HFM10	2003-08-19	**P-04-76**	**P-04-119**	**P-04-74**
HFM11	2003-09-01	**P-04-106**	**P-04-120**	**P-04-64**
HFM12	2003-09-16	**P-04-106**	**P-04-120**	**P-04-64**
HFM13	2003-10-02	**P-04-85**	**P-04-120**	**P-04-71**
HFM14	2003-10-09	**P-04-85**	**P-04-296**	**P-04-71**
HFM14B	2003-11-26			
HFM15	2003-10-15	**P-04-85**	**P-04-296**	**P-04-71**
HFM16	2003-11-11	**P-04-94**	**P-04-120**	**P-04-65**
HFM17	2003-12-08	**P-04-106**	**P-04-120**	**P-04-72**
HFM18	2003-12-16	**P-04-106**	**P-04-120**	**P-04-72**
HFM19	2003-12-18	**P-04-106**	**P-04-296**	**P-04-72**
HFM20	2004-06-01	**P-04-245**	**P-05-157**	**P-05-14**
HFM21	2004-06-07	**P-04-245**	**P-05-157**	**P-05-14**
HFM22	2004-09-10	**P-04-245**	**P-05-262**	**P-05-14**
HFM23	2005-09-01	**P-05-278**	**P-06-207**	**P-06-191**
HFM24	2005-11-29	**P-05-278**	**P-06-210**	**P-06-96**
HFM25	2005-09-08	**P-06-166**	**P-06-210**	**P-06-139**
HFM26	2005-11-18	**P-06-166**	**P-06-208**	**P-06-139**
HFM27	2005-11-10	**P-06-166**	**P-06-210**	**P-06-191**
HFM28	2005-09-14	**P-05-278**	**P-06-207**	**P-06-191**
HFM29	2005-12-19	**P-06-166**	**P-06-210**	**P-06-192**
HFM30	2006-05-11	**P-06-166**	**P-06-207**	**P-06-192**
HFM31	2006-05-19	**P-06-166**	**P-06-207**	
HFM32	2006-01-14	**P-06-166**	**P-06-207**	**P-06-96**
HFM33	2006-05-03	**P-07-11**	**P-07-109**	**P-06-193**
HFM34	2006-06-02	**P-07-11**	**P-07-109**	**P-06-193**
HFM35	2006-06-14	**P-07-11**	**P-07-109**	**P-06-193**
HFM36	2006-09-04	**P-07-43**	**P-07-110**	**P-07-22**
HFM37	2006-08-16	**P-07-43**	**P-07-110**	
HFM38	2006-06-22	**P-06-166**	**P-06-207**	
HFM39	2011-05-09			
HFM40	2011-05-19			
HFM41	2011-05-28			
HFM42	2018-04-11	**P-18-09**		
HFM43	2018-04-23	**P-18-09**		
HFM44	2018-04-26	**P-18-09**		
HFM45	2018-05-04	**P-18-09**		
HFM46	2018-05-09	**P-18-09**		
HFM47	2019-09-05	**P-19-25 (1860464)**		
HFR101	2008-05-15	**P-08-95**	**P-09-34**	
HFR102	2008-05-05	**P-08-95**	**P-09-34**	
HFR105	2008-04-22	**P-08-95**	**P-09-34**	
HFR106	2009-07-02	**P-09-47**		**P-09-54**

Table B-3. List of reports corresponding to the information available from field tests in groundwater wells presented in this report. P refers to SKB's P report series, whereas 7-digit numbers refer to doc-id in SKB's document handling system SKBdoc.

IDCODE	Date of drilling/ well installation	Drilling/well installation	Slug test	Pumping test	In situ permeameter test
SFM0001	2002-05-23	P-03-13	P-03-65		
SFM0002	2002-05-30	P-03-13	P-03-65		
SFM0003	2002-05-30	P-03-13	P-03-65		
SFM0004	2002-12-03	P-03-50	P-03-65		
SFM0005	2002-12-10	P-03-50	P-03-65		
SFM0006	2003-01-10	P-03-57	P-03-65		
SFM0007	2003-02-13	P-03-57	P-03-65		
SFM0008	2003-02-17	P-03-57	P-03-65		
SFM0009	2003-03-25	P-03-64	P-03-65		
SFM0010	2003-03-27	P-03-64	P-03-65		
SFM0011	2003-03-26	P-03-64	P-03-65		
SFM0012	2003-02-24	P-03-64	P-03-65		
SFM0013	2003-03-26	P-03-64	P-03-65		
SFM0014	2003-02-18	P-03-64	P-03-65		
SFM0015	2003-02-20	P-03-64	P-03-65		
SFM0016	2003-02-19	P-03-64	P-03-65		
SFM0017	2003-02-20	P-03-64	P-03-65		
SFM0018	2003-02-26	P-03-64	P-03-65		
SFM0019	2003-03-20	P-03-64	P-03-65		
SFM0020	2003-03-12	P-03-64	P-03-65		
SFM0021	2003-03-24	P-03-64	P-03-65		
SFM0022	2004-02-05	P-04-139	P-04-140		
SFM0023	2003-02-21	P-03-64	P-03-65		
SFM0024	2003-02-26	P-03-64	P-03-65		
SFM0025	2003-02-25	P-03-64	P-03-65		
SFM0026	2003-03-18	P-03-64	P-03-65		
SFM0027	2003-04-09	P-03-64	P-03-65		
SFM0028	2003-03-12	P-03-64	P-03-65		
SFM0029	2003-03-14	P-03-64	P-03-65		
SFM0030	2003-03-04	P-03-64	P-03-65		
SFM0031	2003-03-06	P-03-64	P-03-65	P-04-142	
SFM0032	2003-03-03	P-03-64	P-03-65	P-04-142	
SFM0033	2003-03-04	P-03-64	P-03-65		
SFM0034	2003-03-10	P-03-64	P-03-65		
SFM0035	2003-03-07	P-03-64	P-03-65		
SFM0036	2003-03-11	P-03-64	P-03-65		
SFM0037	2003-03-11	P-03-64	P-03-65		
SFM0049	2003-03-28	P-03-64	P-03-65		
SFM0050	2003-04-14	P-04-136			P-04-136
SFM0051	2003-04-11	P-04-136			
SFM0052	2003-04-16	P-04-136			P-04-136
SFM0053	2003-04-16	P-04-136			
SFM0054	2003-04-15	P-04-136			P-04-136
SFM0055	2003-04-15	P-04-136			
SFM0056	2003-05-21	P-04-136			
SFM0057	2003-08-06	P-04-76	1617130		
SFM0058	2003-11-26	P-04-85	1617130		
SFM0059	2003-11-19	P-04-138		P-04-138	
SFM0060	2003-11-13	P-04-138		P-04-138	
SFM0061	2003-11-17	P-04-138	1617130	P-04-138	
SFM0062	2004-02-05	P-04-139	P-04-140	P-04-142	
SFM0063	2004-02-05	P-04-139	P-04-140	P-04-142	
SFM0064	2004-02-12	P-04-139			
SFM0065	2004-02-06	P-04-139			
SFM0066	2004-02-06	P-04-139			
SFM0067	2004-03-24	P-04-139	P-04-140		
SFM0068	2004-03-23	P-04-139	P-04-140		
SFM0069	2004-03-29	P-04-139	P-04-140		
SFM0070	2004-03-25	P-04-139	P-04-140		
SFM0071	2004-03-29	P-04-139	P-04-140		
SFM0072	2004-03-25	P-04-139	P-04-140		
SFM0073	2004-03-24	P-04-139	P-04-140		
SFM0074	2004-03-30	P-04-139		P-04-142	
SFM0075	2004-03-26	P-04-139	P-04-140		
SFM0076	2004-06-16	P-04-245			
SFM0077	2005-06-20	P-06-89	P-17-19		
SFM0078	2005-06-21	P-06-89	P-17-19		
SFM0079	2005-06-22	P-06-89	P-17-19		
SFM0080	2005-11-30	P-05-278	P-06-224		

IDCODE	Date of drilling/ well installation	Drilling/well installation	Slug test	Pumping test	In situ permeameter test
SFM0081	2006-01-25	P-06-89	P-06-224		
SFM0082	2006-01-25	P-06-89			P-06-224
SFM0083	2006-01-25	P-06-89			
SFM0084	2006-02-28	P-06-89	P-06-224	P-06-224	
SFM0085	2006-03-07	P-06-89		P-06-224	P-06-224
SFM0086	2006-03-07	P-06-89			
SFM0087	2006-03-07	P-06-89	P-06-224	P-06-224	
SFM0088	2006-03-07	P-06-89		P-06-224	P-06-224
SFM0089	2006-03-07	P-06-89			
SFM0090	2006-02-23	P-06-89		P-06-224	
SFM0091	2006-02-28	P-06-89	P-06-224	P-06-224	
SFM0092	2006-03-07	P-06-89		P-06-224	P-06-224
SFM0093	2006-03-07	P-06-89			
SFM0094	2006-02-14	P-06-89			
SFM0095	2006-02-15	P-06-89	P-06-224	P-06-224	
SFM0096	2006-02-17	P-06-89		P-06-224	P-06-224
SFM0097	2006-02-17	P-06-89		P-06-224	
SFM0099	2006-02-17	P-06-89		P-06-224	P-06-224
SFM0100	2006-02-17	P-06-89			
SFM0101	2006-02-17	P-06-89		P-06-224	P-06-224
SFM0102	2006-02-17	P-06-89			
SFM0103	2006-02-16	P-06-89		P-06-224	
SFM0104	2006-02-24	P-06-89	P-06-224		
SFM0105	2006-02-23	P-06-89	P-06-224		
SFM0106	2006-02-22	P-06-89	P-06-224		
SFM0107	2006-02-21	P-06-89	P-06-224		
SFM0108	2006-02-21	P-06-89	P-06-224		
SFM0109	2006-08-21	P-07-43			
SFM000110	2009-02-12	P-09-17	1562216		
SFM000111	2009-02-12	P-09-17			
SFM000112	2009-02-09	P-09-17	1562216		
SFM000113	2009-02-09	P-09-17			
SFM000114	2009-02-12	P-09-17	1562216		
SFM000115	2009-02-12	P-09-17			
SFM000116	2009-02-10	P-09-17	1562216		
SFM000117	2009-02-10	P-09-17			
SFM000118	2009-02-10	P-09-17	1562216		
SFM000119	2009-02-09	P-09-17			
SFM000121	2011-04-14	1325128			
SFM000122	2011-04-14	1325128	P-17-19		
SFM000123	2011-04-14	1325128			
SFM000124	2011-04-14	1325128			
SFM000125	2011-04-14	1325128			
SFM000126	2011-03-01	1385889	1562216		
SFM000127	2011-03-03	1385889			
SFM000132	2012-09-17	1366471	1700798		
SFM000133	2012-09-18	1366471	1700798		
SFM000134	2012-09-18	1366471	1700798		
SFM000135	2012-09-18	1366471	1700798		
SFM000138	2014-06-23	1449026	1617130		
SFM000139	2014-06-23	1449026	P-17-19		
SFM000140	2014-06-23	1449026			
SFM000141	2014-06-23	1449026			
SFM000142	2014-06-23	1449026			
SFM000143	2016-03-08		P-17-19		
SFM000144	2016-03-09		P-17-19		
SFM000145	2016-03-09		P-17-19		
SFM000146	2016-04-12		P-17-19		
SFM000147	2016-04-26		P-17-19		
SFM000149	2016-04-04		P-17-19		
SFM000153	2016-04-26		P-17-19		
SFM000154	2016-04-11				
SFM000156	2016-03-07				
SFM000157	2016-03-04				
SFM000160	2016-03-18		1617130		
SFM000161	2016-03-18		1617130		
SFM000162	2016-03-18		1617130		
SFM000163	2017-04-26		1617130		
SFM000167	2017-04-20		1617130		
SFM000168	2017-04-20		1617130		
SFM000169	2019-03-11	1877396			
SFM000170	2019-02-13	1877396			
SFM000171	2019-02-13	1877396			
SFM000172	2019-02-01	1877396			

IDCODE	Date of drilling/ well installation	Drilling/well installation	Slug test	Pumping test	In situ permeameter test
SFM000173	2019-01-30	1877396			
SFM000174	2019-03-12	1877396			
SFM000175	2019-03-05	1877396			
SFM000176	2019-03-07	1877396			
SFM000177	2019-03-08	1877396			
SFM000178	2019-03-08	1877396			
SFM000179	2019-02-14	1877396			
SFM000180	2019-02-25	1877396			
SFM000181	2019-02-26	1877396			
SFM000182	2018-12-05	1877396			
SFM000183	2018-12-05	1877396			
SFM000184	2019-01-31	1877396			
SFM000186	2019-02-01	1877396			
SFM000187	2019-02-20	1877396			
SFM000188	2018-12-04	1877396			
SFM000190	2019-03-19	1877396			
SFM000191	2018-12-06	1877396			
SFM000192	2019-02-27	1877396			
SFM000193	2018-12-05	1877396			
SFM000194	2019-02-28	1877396			
SFM000195	2019-02-28	1877396			
SFM000196	2019-05-10	1877396			
SFM000197	2019-05-14	1877396			
SFM000198	2019-05-16	1877396			

Table B-4. List of reports corresponding to the information available from laboratory tests on regolith samples presented in this report. P and R refer to SKB's P and R report series, respectively whereas 7-digit numbers refer to doc-id in SKB's document handling system SKBdoc. 1Sampling is presented in the report, whereas PSD analyses were performed subsequent to the report. PSD = particle-size distribution, CRS = constant-rate of strain, UZ = unsaturated-zone properties.

IDCODE	PSD	Lab. permeameter test	CRS test	UZ
SFM0001	P-03-14			
SFM0002	P-03-14			
SFM0003	P-03-14			
SFM0004	P-03-14			
SFM0005	P-03-14			
SFM0006	P-03-14			
SFM0007	P-03-14			
SFM0008	P-03-14			
SFM0010	R-08-04			
SFM0011	R-08-04			
SFM0013	R-08-04			
SFM0016	R-08-04			
SFM0017	R-08-04			
SFM0018	R-08-04			
SFM0019	R-08-04			
SFM0020	R-08-04			
SFM0021	R-08-04			
SFM0022	R-08-04			
SFM0026	R-08-04			
SFM0027	R-08-04			
SFM0028	R-08-04			
SFM0030	R-08-04			
SFM0031	R-08-04			
SFM0032	R-08-04			
SFM0034	R-08-04			
SFM0036	R-08-04			
SFM0049	R-08-04			
SFM0057	R-08-04			
SFM0062	R-08-04			
SFM0063	R-08-04			
SFM0065	R-08-04			
SFM0069	R-08-04			
SFM0070	R-08-04			
SFM0071	R-08-04			
SFM0072	R-08-04			
SFM0081	R-08-04			
SFM0084	R-08-04			
SFM0091	R-08-04			
SFM0094	R-08-04			

IDCODE	PSD	Lab. permeameter test	CRS test	UZ
SFM0095	R-08-04			
SFM0103	R-08-04			
SFM0104	R-08-04			
SFM0105	R-08-04			
SFM0106	R-08-04			
SFM0107	R-08-04			
SFM0108	R-08-04			
SFM000133	R-14-23		R-14-23	
SFM000191[1]	1877396			
SFM000192[1]	1877396			
SFM000194[1]	1877396			
HFM01	P-03-14			
HFM02	P-03-14			
HFM03	P-03-14			
HFM04	P-03-14			
HFM05	P-03-14			
HFM06	P-03-14			
HFM07	P-03-14			
HFM08	P-03-14			
HFM09	P-04-111			
HFM10	P-04-111			
KFM01A	P-03-14			
PFM002461	R-08-04			
PFM002462	R-08-04			
PFM002463	R-08-04			
PFM002464	R-08-04			
PFM002572	R-08-04			
PFM002573	R-08-04			
PFM002574	R-08-04			
PFM002576	R-08-04			
PFM002577	R-08-04			
PFM002578	R-08-04			
PFM002581	R-08-04			
PFM002582	R-08-04			
PFM002586	R-08-04			
PFM002587	R-08-04			
PFM002588	R-08-04			
PFM002589	R-08-04			
PFM002590	R-08-04			
PFM002591	R-08-04			
PFM002592	R-08-04			
PFM002594	R-08-04			
PFM002670	R-08-04			
PFM002687	R-08-04			
PFM002760	R-08-04			
PFM002761	R-08-04			
PFM002762	R-08-04			
PFM002767	R-08-04			
PFM002768	R-08-04			
PFM002783	R-08-04			
PFM002801	R-08-04			
PFM002802	R-08-04			
PFM002890	R-08-04			
PFM002891	R-08-04			
PFM003742	R-08-04			
PFM004193	R-08-04			
PFM004204	R-08-04			
PFM004205	R-08-04			
PFM004216	R-08-04			
PFM004222	R-08-04			
PFM004294	R-08-04			
PFM004396	R-08-04			
PFM004454	R-08-04			
PFM004455	R-08-04	P-05-166		R-08-04
PFM004456	R-08-04			
PFM004458	R-08-04	P-05-166		R-08-04
PFM004459	R-08-04	P-05-166		R-08-04
PFM004460	R-08-04	P-05-166		R-08-04
PFM004514	R-08-04			
PFM004531	R-08-04			
PFM004752	R-08-04			
PFM004760	R-08-04			
PFM004761	R-08-04			
PFM004762	P-04-111			
PFM006073	P-06-88			

IDCODE	PSD	Lab. permeameter test	CRS test	UZ
PFM006094	P-06-88			
PFM006095	P-06-88			
PFM006097	P-06-88			
PFM007786	1564669			
PFM007855	1562492	1562492		
PFM007856	1562492	1562492		
PFM007857	1562492	1562492		
PFM007858	1562492	1562492		
PFM007860	1562492		1562492	
PFM007861	1562492		1562492	
PFM007862	1562492		1562492	
PFM007863	1562492		1562492	
PFM007864	1562492		1562492	
PFM007866	1562492		1562492	
PFM007867	1562492		1562492	
PFM007868	1562492		1562492	
PFM007869	1562492		1562492	
PFM008290	R-14-23			
PFM008291	R-14-23			

C Compilation of old single-hole hydraulic test data for geological model domains in the SFR bedrock volume

Table C-1. Single-hole hydraulic test data from core-drilled boreholes at SFR. Blue shaded cells indicate that overlapping transmissivities have been subtracted. Note strategies and methods for collection of the data in the table differ significantly from those for other data presented in the report (cf. Öhman et al. (2012)). PBT = pressure buildup test, TI = transient injection test, FH = falling head test.

Zup (m)	Zlow (m)	Secup(m)	Seclow(m)	Deformation zone (ZFM)	ΣT (m^2/s)	Borehole length (m)	Data type
KFR01							
		0	**62**				
		0	62	ZFMWNW0001	1.4E-06	50	PBT
KFR02							
		0	**170**				
		0	33		8.4E-09	10	TI
		33	38	ZFMNE0870	1.1E-06	20	TI
		38	99		1.4E-07	74	PBT
		99	100	PDZ2	5.5E-08	10	TI
		100	115		1.0E-07	10	TI
		115	124	ZFM871	6.5E-08	17	PBT
		124	170		1.2E-07	33	PBT
KFR03							
		0	**102**				
		0	6				
		6	12	PDZ1	1.0E-06	39	PBT
		12	48				
		48	96	ZFMNE0870	3.6E-07	34	PBT
		96	82				
		82	96	ZFM871	2.2E-08	21	PBT
		96	102				
KFR04							
		0	**101**				
		0	3	PDZ1			
		3	14				
		14	63	ZFMNE0870	9.1E-07	76	PBT
		63	91				
		91	100	ZFM871	2.6E-07	17	PBT
		100	101				
KFR05							
		0	**131**				
		0	85		1.1E-07	18	TI
		85	88	ZFM871			
		88	103				
		103	131	ZFMNE0870			
KFR05							
		0	**39**				
		0	39		7.1E-06	34	TI
KFR08							
		0	**104**				
		0	3				
		3	19	ZFMNW0805B	6.1E-07	29	PBT
		19	41				
		41	104	ZFMNW0805A	1.9E-05	67	PBT
KFR09							

Zup (m)	Zlow (m)	Secup(m)	Seclow(m)	Deformation zone (ZFM)	ΣT (m^2/s)	Borehole length (m)	Data type
		0	**80**				
		0	59	ZFMNNE0869	4.3E-05	53	PBT
		59	69				
		69	74	PDZ2	2.8E-06	17	PBT
		74	80				
KFR10							
		0	**107**				
		0	5	ZFMNNE0869			
		5	96		3.1E-06	79	PBT
		96	107	PDZ2	2.9E-05	20	PBT
KFR11							
		0	**98**				
		0	19	ZFMNW0805B	9.2E-06	17	PBT
		19	41		1.1E-07	14	PBT
		41	96	ZFMNW0805A	5.8E-05	57	PBT
		96	98				
KFR12							
		0	**50**				
		0	21				
		21	32	ZFM871	2.6E-06	13	PBT
		32	50		1.8E-08	16	PBT
KFR13							
		0	**77**				
		0	20				
		20	30	PDZ1	2.9E-09	29	PBT
		30	35				
		35	41	PDZ2	7.6E-09	19	PBT
		41	48				
		48	61	ZFMNE3118	1.4E-06	20	TI
		61	61				
		61	68	ZFM871	1.6E-06	10	TI
		68	77				
KFR19							
		0	**110**				
		0	39				
		39	49	PDZ1			
		49	110		1.3E-08	46	PBT
KFR20							
		0	**110**				
		0	49		3.4E-08	8	PBT
		49	52	PDZ1	1.0E-06	14	PBT
		52	109		3.9E-08	34	PBT
		109	110	ZFMNE0870			
KFR21							
		0	**251**				
		0	109		1.6E-06	66	FH
		109	129	ZFM871	1.2E-05	12	FH
		129	251		4.7E-07	63	FH
KFR22							
		0	**160**				
		0	140		1.2E-05	114	PSS/FH
		140	160	ZFM871	3.3E-06	12	FH
KFR23							
		0	**160**				

Zup (m)	Zlow (m)	Secup(m)	Seclow(m)	Deformation zone (ZFM)	ΣT (m^2/s)	Borehole length (m)	Data type
		0	10				
		10	11	ZFMNW0805A			
		11	83		1.1E-04	56	PSS/FH
		83	106	ZFM871	3.8E-05	21	FH
		106	160		6.0E-07	45	FH
KFR24							
		0	**159**				
		0	8				
		8	41	ZFMNW0805B	8.9E-06	27	PSS
		41	49		1.2E-06	3	PSS
		49	157	ZFMNW0805A	2.0E-05	39	PSS/FH
		157	157				
		157	159	ZFMWNW0836			
KFR25							
		0	**197**				
		0	9				
		9	51	ZFMNW0805B	2.4E-05	39	PSS
		51	51				
		51	197	ZFMNW0805A	3.2E-05	105	PSS/FH
KFR31							
		0	**242**				
		0	82		1.4E-06	3	PSS
		82	98	PDZ1	7.5E-07	3	PSS
		98	229		9.0E-06	123	PSS
		229	232	ZFM871	2.5E-06	47	PSS
		232	229				
		229	232	ZFMNE0870			
		232	242				
KFR32							
		0	**210**				
		0	156		1.3E-05	15	PSS
		156	159	PDZ1			
		159	163				
		163	186	ZFM871	4.0E-05	24	PSS
		186	210				
KFR33							
		0	**167**				
		0	46				
		46	115	ZFMNNW1209	9.08E-06	105	PSS
		115	158		6.2E-06	20	PSS
		158	167	ZFM871	3.9E-06	3	PSS
KFR34							
		0	**142**				
		0	142		9.8E-06	91	PSS
KFR35							
		0	**140**				
		0	33				
		33	70	ZFMNNW1209	1.2E-05	12	PSS
		70	140		2.1E-06	65	PSS
KFR36							
		0	**124**				
		0	45		9.5E-06	9	PSS
		45	116	ZFMNNE0869	4.1E-05	69	PSS

Zup (m)	Zlow (m)	Secup(m)	Seclow(m)	Deformation zone (ZFM)	ΣT (m^2/s)	Borehole length (m)	Data type
		116	124		1.6E-06	9	PSS
KFR37							
		0	**205**				
		0	37		2.8E-06	12	PSS
		37	46	PDZ1	8.9E-07	9	PSS
		46	183		2.8E-05	117	PSS
		183	194	ZFM871	4.2E-05	9	PSS
		194	205				
KFR38							
		0	**185**				
		0	154		2.2E-05	57	PSS
		154	182	ZFMNW0805B	4.3E-05	17	PSS
		182	185				
KFR52							
		0	**30**				
		0	20				
		20	22	PDZ1			
		22	30				
KFR53							
		0	**41**				
		0	6	ZFMNE3118			
		6	19		8.4E-09	10	PBT
		19	37	ZFMNE0870	2.3E-08	16	PBT
		37	41		4.6E-10	7	PBT
KFR54							
		0	**53**				
		0	3	ZFMNE3118			
		3	27		5.3E-08	24	PBT
		27	40	ZFMNE0870			
		40	53		1.2E-07	9	PBT
KFR55							
		0	**62**				
		0	3	PDZ1			
		3	8				
		8	17	ZFMNE3118			
		17	17				
		17	38	ZFMNE0870	1.7E-07	17	PBT
		38	62		1.2E-07	8	PBT
KFR56							
		0	**82**				
		0	4				
		4	45	ZFMNW0805B			
		45	57				
		57	82	ZFMNW0805A	5.5E-07	14	PBT
KFR57							
		0	**25**				
		0	16				
		16	25	ZFM871			
KFR61							
		0	**71**				
		0	1				
		1	71	ZFMWNW0001	1.8E-04	24	PSS

Zup (m)	Zlow (m)	Secup(m)	Seclow(m)	Deformation zone (ZFM)	ΣT (m^2/s)	Borehole length (m)	Data type
KFR62							
		0	**83**				
		0	46		7.8E-05	8	PSS
		46	83	ZFMWNW0001	8.6E-05	19	PSS
KFR63							
		0	**15**				
		0	15		5.3E-05	2	PSS
KFR64							
		0	**54**				
		0	13				
		13	54	ZFMWNW0001	3.2E-05	16	PSS
KFR65							
		0	**40**				
		0	18		3.4E-07	2	PSS
		18	40	ZFMWNW0001	1.6E-05	6	PSS
KFR66							
		0	**29**				
		0	15				
		15	29	ZFMWNW0001	3.8E-05	10	PSS
KFR67							
		0	**49**				
		0	14				
		14	49	ZFMWNW0001	1.4E-05	21	PSS
KFR68							
		0	**128**				
		0	72		1.4E-03	36	PSS
		72	105	ZFMNNE0869, ZFMNE0870	4.1E-06	9	PSS
		105	128				
KFR69							
		0	**201**				
		0	52		2.1E-07	6	PSS
		52	79	PDZ1	2.3E-07	6	PSS
		79	122				
		122	146	PDZ2	1.2E-05	9	PSS
		146	201		6.9E-07	69	PSS
KFR70							
		0	**173**				
		0	35				
		35	103	ZFMNE0870	5.6E-06	18	PSS
		103	173		1.4E-06	70	PSS
KFR71							
		0	**121**				
		0	66		3.7E-05	50	TI
		66	70	ZFMWNW0001	2.9E-06	10	TI
		70	72				
		72	121	ZFMWNW0001	7.8E-04	51	TI
0							

Zup (m)	Zlow (m)	Secup(m)	Seclow(m)	Deformation zone (ZFM)	ΣT (m^2/s)	Borehole length (m)	Data type
KFR72							
		0					
		0	13	PDZ1			
		13	24				
		24	153	PDZ2			
KFR7A							
		0	**75**				
		0	4				
		4	43	ZFMNW0805B, ZFM871	1.4E-05	44	PBT
		43	74	ZFMNW0805A, ZFM871	9.1E-05	27	PBT
		74	75				
KFR7B							
		0	**21**				
		0	17	ZFM871	2.6E-05	13	PBT
		17	21				
KFR7C							
		0	**34**				
		0	6				
		6	7	ZFMNE0870			
		7	6				
		6	32	ZFM871	6.7E-07	28	PBT
		32	34				
KFR80							
		0	**20**				
		0	13	ZFM871			
		13	20				
KFR83							
		0	**20**				
		0	6				
		6	20	ZFM871			
KFR84							
		0	**30**				
		0	30	ZFMWNW0001			
KFR85							
		0	**12**				
		0	12	ZFMWNW0001			
KFR86							
		0	**15**				
		0	15	ZFMWNW0001			
KFR87							
		0	**15**				
		0	15	ZFM871			
KFR88							
		0	**30**				
		0	30	ZFM871			

Zup (m)	Zlow (m)	Secup(m)	Seclow(m)	Deformation zone (ZFM)	ΣT (m^2/s)	Borehole length (m)	Data type
KFR89							
		0					
		0	11				
		11	14	PDZ1			

D Digital appendices

D1 Digital Appendix D1: KFM and KFR boreholes

Additional data can be found in a supplementary Excel file:
(2087698 - Appendix D1_KFM KFR R-22-07.zip)

Can be downloaded from: http://www.skb.com/publication/2519851/

D2 Digital Appendix D2: HFM and HFR boreholes

Additional data can be found in a supplementary Excel file:
(2087699 - Appendix D2_HFM HFR R-22-07.zip)

Can be downloaded from: http://www.skb.com/publication/2519851/

E Supplementary data: Borehole casing

Table E-1. Casing lengths for all bedrock boreholes presented in the report. Casing lengths are not reported per se in Sicada, and the data presented in the table are obtained from Sicada (SKBdata_24_004), drilling reports (Appendix B) and BIPS (Borehole Image Processing System) images.

IDCODE	CASING LENGTH (m)	IDCODE	CASING LENGTH (m)
KFM01A	100	HFM01	32
KFM01B	16	HFM02	25
KFM01C	12	HFM03	13
KFM01D*	91	HFM04	12
KFM02A*	102	HFM05	12
KFM02B*	89	HFM06	12
KFM03A*	102	HFM07	18
KFM03B	5	HFM08	18
KFM04A*	109	HFM09	17
KFM04B	12	HFM10	12
KFM05A*	110	HFM11	12
KFM06A*	102	HFM12	15
KFM06B	5	HFM13	15
KFM06C*	102	HFM14**	3
KFM07A*	102	HFM15	6
KFM07B	66	HFM16	12
KFM07C*	98	HFM17	8
KFM08A*	102	HFM18	9
KFM08B	6	HFM19	12
KFM08C*	102	HFM20	12
KFM08D*	60	HFM21	12
KFM09A	8	HFM22	12
KFM09B	9	HFM23	21
KFM09C	9	HFM24	18
KFM10A	63	HFM25	9
KFM11A*	73	HFM26	12
KFM12A*	61	HFM27	12
KFM13	8	HFM28	12
KFM14	6	HFM29	9
KFM15**	8	HFM30	18
KFM16	4	HFM31	9
KFM17	6	HFM32	6
KFM18	9	HFM33	12
KFM19	7	HFM34	12
KFM20	2	HFM35	12
KFM21	6	HFM36	12
KFM22**	8	HFM37	9
KFM23	5	HFM38**	9
KFM24**	37	HFM39	6
KFM25	6	HFM40	6
KFM26	6	HFM41	6
KFM27	9	HFM42	6
KFR101	14	HFM43	6
KFR102A*	72	HFM44	9
KFR102B	14	HFM45	6
KFR103	13	HFM46	6
KFR104*	9	HFM47	12
KFR105	3	HFR101	8
KFR106*	9	HFR102	9
KFR117	9	HFR105	21
KFR118	12	HFR106	9
KFR119	9		
KFR120	12		
KFR121*	41		
KFR27	12		

* The stated length is equal to the total length, encompassing the transition cone and other casing pieces or casing shoes.

** The stated length is based on a BIPS image.